



THE HONG KONG
POLYTECHNIC UNIVERSITY

香港理工大學

Pao Yue-kong Library

包玉剛圖書館

Copyright Undertaking

This thesis is protected by copyright, with all rights reserved.

By reading and using the thesis, the reader understands and agrees to the following terms:

1. The reader will abide by the rules and legal ordinances governing copyright regarding the use of the thesis.
2. The reader will use the thesis for the purpose of research or private study only and not for distribution or further reproduction or any other purpose.
3. The reader agrees to indemnify and hold the University harmless from and against any loss, damage, cost, liability or expenses arising from copyright infringement or unauthorized usage.

If you have reasons to believe that any materials in this thesis are deemed not suitable to be distributed in this form, or a copyright owner having difficulty with the material being included in our database, please contact lbsys@polyu.edu.hk providing details. The Library will look into your claim and consider taking remedial action upon receipt of the written requests.

Hydrogen Bond Mediated Reactions Using Ruthenium Complexes

A Thesis

forwarded to

Department of Applied Biology & Chemical Technology

in

Partial Fulfilment of the Requirements

for

the Degree of Doctor of Philosophy

at

The Hong Kong Polytechnic University

by

FUNG WAI KIT

December, 2004



Declaration

I hereby declare that this thesis summarized my own work carried out since my registration for the Degree of Doctor of Philosophy in September, 2000; and that has not been previously included in a thesis, dissertation or report submitted to this or any other institution for a degree, diploma or other qualifications.

Wai-Kit FUNG

Dec, 2004

Acknowledgements

I would like to express my deepest gratitude to my supervisor Prof. C. P. Lau for his valuable advice and patience throughout the course of my study. His guidance, encouragement and devoted attitude in research have made my study a truly rewarding experience.

Thanks are also expressed to Prof. Z. Y. Lin and his research group in the Department of Chemistry, The Hong Kong University of Science and Technology, for their support on the study of mechanism via theoretical calculations.

I would like to thank my postgraduate colleagues and the undergraduate students in Prof. Lau's research group, Dr. H. S. Chu, Miss M. Y. Hung, Mr. C. C. Mak, Miss W. N. Sit, Mr. D. X. Wang, Mr. C. Q. Yin, Dr. K. W. Ma, Mr. C. H. Ng and Miss P. Y. Chan, all of whom have made my study more pleasant. Special thanks are expressed to Dr. M. L. Man, Dr. K. C. Cheung, Mr. S. M. Ng, Mr. Y. F. Lam, Mr. T. C. Chan, Mr. Y. Y. Yip, and Dr. B. Brendan, for their valuable discussions, assistance and encouragement.

I am obliged to the staff and the technical service crew of the Chemical Technology Section of the Department of Applied Biology and Chemical Technology, The Hong Kong Polytechnic University for their assistance throughout my postgraduate study, especially to Miss P. S. Chan, Mr. Y. K. Au and Mr. W. K. Kwan for their assistance in recording the MS and NMR spectra, respectively.

I would like to thank my family and friends for their love and continual support in various ways, especially thanks to Miss Nissa Yuen for her support, patience and concern.

Finally, I would like to acknowledge the Research Degree Committee of The Hong Kong Polytechnic University for the award of a studentship, and for a grant supporting my conference presentation in the XXTH International Conference on Organometallic Chemistry held in Corfu, Greece in July, 2002.

Abstract of thesis entitled "Hydrogen Bond Mediated Reactions Using Ruthenium Complexes."

Submitted by Wai-Kit FUNG

for the degree of Doctor of Philosophy

at The Hong Kong Polytechnic University

in Dec, 2004.

Abstract

The indenyl ruthenium hydride complex $(\eta^5\text{-C}_9\text{H}_7)\text{Ru}(\text{dppm})\text{H}$ was found to be active in catalyzing the hydration of nitriles to amides. The chloro analogue $(\eta^5\text{-C}_9\text{H}_7)\text{Ru}(\text{dppm})\text{Cl}$ was, however, found to be inactive. Density functional theory calculations at the B3LYP level provide explanations for the effectiveness of the hydride complex and the ineffectiveness of the chloro complex in the catalysis. The result shows that the presence of Ru-H \cdots H-OH dihydrogen-bonding interaction in the transition state lowers the reaction barrier in the case of $(\eta^5\text{-C}_9\text{H}_7)\text{Ru}(\text{dppm})\text{H}$, but in the chloro system, the corresponding transition state does not contain such interaction and the reaction barrier is much higher. Similar dihydrogen bond-mediated effect is believed to be responsible for the catalytic activity of the hydrotris(pyrazolyl)borato (Tp) ruthenium complex $\text{TpRu}(\text{PPh}_3)(\text{CH}_3\text{CN})\text{H}$ in nitrile hydration. The chloro analogue $\text{TpRu}(\text{PPh}_3)(\text{CH}_3\text{CN})\text{Cl}$ shows no catalytic activity.

In our previous studies of the reactivity of some aminocyclopentadienyl ruthenium complexes, we learned that the amino sidearms of these complexes are able to heterolytically cleave the $\eta^2\text{-H}_2$ ligands to generate intramolecularly dihydrogen-bonded Ru-H \cdots H-N species. To further our investigation on the activities of the aminocyclopentadienyl ruthenium complexes in chemical reactions such as hydrogenation of CO_2 and hydration of nitriles, we synthesized the aminoindenylruthenium complexes, $(\eta^5\text{-C}_9\text{H}_6(\text{CH}_2)_2\text{NMe}_2)\text{Ru}(\text{dppm})\text{H}$ and $[\eta^5\text{:}\eta^1\text{-C}_9\text{H}_6(\text{CH}_2)_2\text{NMe}_2]\text{Ru}(\text{dppm})\text{]BF}_4$, and compared their activities with those of the corresponding aminocyclopentadienyl ruthenium complexes in these reactions. We

have found that the aminoindenylruthenium complexes are in general more active than the aminocyclopentadienyl ruthenium complexes.

Furthermore, we have found that the aminoindenylruthenium hydride complex $(\eta^5\text{-C}_9\text{H}_6(\text{CH}_2)_2\text{NMe}_2)\text{Ru}(\text{dppm})\text{H}$ is more active in catalyzing the hydration of nitriles than the indenyl ruthenium hydride complex, which has no amino side arm on its indenyl ligand. We believe that the amino side arm on the indenyl ligand might play an important role in the catalysis.

To understand the preponderance of the catalytic activity of $(\eta^5\text{-C}_9\text{H}_6(\text{CH}_2)_2\text{NMe}_2)\text{Ru}(\text{dppm})\text{H}$ in nitrile hydration over that of $(\eta^5\text{-C}_9\text{H}_7)\text{Ru}(\text{dppm})\text{H}$, density function calculations at the B3LYP level to establish a plausible catalytic pathway were carried out. It is learned that the presence of $\text{Ru-H}\cdots\text{H-OH}$ dihydrogen bonding and additional $\text{InN}\cdots\text{H-N}=(\text{OH})\text{Me}$ hydrogen bond interaction in the transition states lower the reaction barriers in the case of $(\eta^5\text{-C}_9\text{H}_6(\text{CH}_2)_2\text{NMe}_2)\text{Ru}(\text{dppm})\text{H}$, but in the $(\eta^5\text{-C}_9\text{H}_7)\text{Ru}(\text{dppm})\text{H}$ -catalyzed reaction, the transition states do not involve additional hydrogen bonding and thus the reaction barriers are much higher.

In addition to the hydration reaction, the aminoindenylruthenium hydride complex is also capable of catalyzing the hydrogenation of alkenes and selectively reducing the C=C bond in an α,β -unsaturated ketone; the reactivities of the $(\eta^5\text{-C}_9\text{H}_6(\text{CH}_2)_2\text{NMe}_2)\text{Ru}(\text{dppm})\text{H}$ and $(\eta^5\text{-C}_9\text{H}_7)\text{Ru}(\text{dppm})\text{H}$ in these reactions have been studied and compared. The complex $(\eta^5\text{-C}_9\text{H}_6(\text{CH}_2)_2\text{NMe}_2)\text{Ru}(\text{dppm})\text{H}$ shows higher catalytic activity in the hydrogenation of the C=C bond of α,β -unsaturated ketones

than $(\eta^5\text{-C}_9\text{H}_7)\text{Ru}(\text{dppm})\text{H}$. Presence of the amino side arm appears to facilitate the hydrogenation reaction, and we propose that the hydrogen bonding-interaction in the transition state lowers the reaction barrier in this case.

Table of Contents

	Abstract	i
	Table of content	iv
	List of Figures	ix
	List of Tables	xi
	List of Schemes	xii
	Abbreviations	xiv
Chapter One		
	Introduction	1
1.1	Review of hydrogen bonding in organometallic complexes and hydrogen bonding-mediated reactions	1
1.2	Hydration of nitriles	15
1.3	Homogeneous hydrogenation of unsaturated hydrocarbon	17
1.4	Introduction of cyclopentadienyl and indenyl ligands and their potential in catalysis	22
1.5	Introduction of indenyl and cyclopentadienyl complexes containing amino side-arms	26
Chapter Two		
	Dihydrogen-Bond-Promoted Catalysis: Catalytic Hydration of Nitriles with Ruthenium Hydride Complexes	
2.1	Introduction	34
2.2	Experimental	36
2.2.1	Materials and instrumentation	36
2.2.2	Syntheses and Reactions	38
2.2.2.1	Catalytic hydration of neat nitriles with IndRu(dppm)H	38

	(3)	
2.2.2.2	Catalytic hydration of nitriles with IndRu(dppm)H (3) in 1-pentanol	38
2.2.2.3	NMR study of nitriles hydration	39
2.2.2.4	H/D exchange experiment between complex 3 and D ₂ O	39
2.2.2.5	Acetamide control reaction	40
2.2.2.6	Acetamide Inhibition of acetonitrile Hydration	40
2.2.2.7	Recycling of catalyst	41
2.2.2.8	Typical procedure for reaction of the indenylruthenium hydride complex with water in dihydrogen-bonding interaction study	41
2.3	Results and discussion	42
2.3.1	Catalytic hydration of acetonitriles with 3-14	42
2.3.2	Hydration of nitriles by 3 & 5	45
2.3.3	Possible mechanism for hydration of nitriles catalyzed by 3	50
2.3.4	Reaction of IndRu(dppm)H (3) with H ₂ O	53
2.3.5	H/D exchange between IndRu(dppm)H (3) and D ₂ O	53
2.3.6	Theoretical study	56
2.3.7	Recycling of catalyst	63
2.3.8	Effects of amide on rate of hydration	64
2.3.9	Effect of diphosphine ligands on the rates of the hydration reactions	65
2.3.10	Reactivity of IndRu(dppm)H (3) towards terminal alkyne hydration	66
2.3.11	Reactivity of IndRu(dppm)H (3) towards alkene hydration	69
2.3.12	Reactivity of IndRu(dppm)H (3) towards hydroamination of phenylacetylene with aniline	73
2.3.13	Reactivity of IndRu(dppm)H (3) towards alcoholysis of nitriles	76

Chapter Three

Syntheses and Characterization of Aminoindenyl Ruthenium Complexes and Comparison of Their Reactivities Toward Some Reactions with those of Aminocyclopentadienyl Ruthenium Complexes.

3.1	Introduction	79
3.2	Experimental	80
3.2.1	Materials and instrumentation	80
3.2.2	Syntheses and Reactions	81
3.2.2.1	Synthesis of $(\eta^5\text{-C}_9\text{H}_6\text{CH}_2\text{CH}_2\text{NMe}_2)\text{Ru}(\text{PPh}_3)_2\text{Cl}$ (17)	82
3.2.2.2	Synthesis of $(\eta^5\text{-C}_9\text{H}_6\text{CH}_2\text{CH}_2\text{NMe}_2)\text{Ru}(\text{dppm})\text{Cl}$ (18)	82
3.2.2.3	Synthesis of $(\eta^5\text{-C}_9\text{H}_6\text{CH}_2\text{CH}_2\text{NMe}_2)\text{Ru}(\text{dppm})\text{H}$ (19)	83
3.2.2.4	Synthesis of $(\eta^5\text{-C}_9\text{H}_6\text{CH}_2\text{CH}_2\text{NMe}_2)\text{Ru}(\text{PPh}_3)_2\text{H}$ (20)	84
3.2.2.5	In <i>situ</i> preparation of $[(\eta^5\text{-C}_9\text{H}_6\text{CH}_2\text{CH}_2\text{NMe}_2\text{H}^+)\text{Ru}(\text{dppm})\text{H}]\text{BF}_4$ (21)	85
3.2.2.6	Synthesis of $[(\eta^5:\eta^1\text{-C}_9\text{H}_6\text{CH}_2\text{CH}_2\text{NMe}_2)\text{Ru}(\text{dppm})]\text{BF}_4$ (22)	85
3.2.2.7	Catalytic hydration of neat nitriles with $[(\eta^5:\eta^1\text{-C}_9\text{H}_6\text{CH}_2\text{CH}_2\text{NMe}_2)\text{Ru}(\text{dppm})]\text{BF}_4$ (22)	86
3.2.2.8	CO_2 reduction with $(\eta^5:\eta^1\text{-C}_5\text{H}_4\text{CH}_2\text{CH}_2\text{NMe}_2)\text{Ru}(\text{dppm})]\text{BF}_4$ (2) and $(\eta^5:\eta^1\text{-C}_9\text{H}_6\text{CH}_2\text{CH}_2\text{NMe}_2)\text{Ru}(\text{dppm})]\text{BF}_4$ (22)	87
3.2.2.9	Reaction of 22 with H_2	87
3.3	Results and discussion	88
3.3.1	Synthesis of $(\eta^5\text{-C}_9\text{H}_6\text{CH}_2\text{CH}_2\text{NMe}_2)\text{Ru}(\text{PPh}_3)_2\text{Cl}$ (17)	88
3.3.2	Synthesis of $(\eta^5\text{-C}_9\text{H}_6\text{CH}_2\text{CH}_2\text{NMe}_2)\text{Ru}(\text{dppm})\text{Cl}$ (18)	89
3.3.3	Synthesis of $(\eta^5\text{-C}_9\text{H}_6\text{CH}_2\text{CH}_2\text{NMe}_2)\text{Ru}(\text{dppm})\text{H}$ (19) and $(\eta^5\text{-C}_9\text{H}_6\text{CH}_2\text{CH}_2\text{NMe}_2)\text{Ru}(\text{PPh}_3)_2\text{H}$ (21)	91
3.3.4	Acidification of $(\eta^5\text{-C}_9\text{H}_6\text{CH}_2\text{CH}_2\text{NMe}_2)\text{Ru}(\text{dppm})\text{H}$ (19)	92
3.3.5	Synthesis of $[(\eta^5:\eta^1\text{-C}_9\text{H}_6\text{CH}_2\text{CH}_2\text{NMe}_2)\text{Ru}(\text{dppm})]\text{BF}_4$ (22)	96
3.3.6	Reactivity of $[(\eta^5:\eta^1\text{-C}_9\text{H}_6\text{CH}_2\text{CH}_2\text{NMe}_2)\text{Ru}(\text{dppm})]\text{BF}_4$	97

	(22) towards H ₂	
3.3.7	Reactivity of $[(\eta^5:\eta^1\text{-C}_5\text{H}_4\text{CH}_2\text{CH}_2\text{NMe}_2)\text{Ru}(\text{dppm})]\text{BF}_4$ (2) and $[(\eta^5:\eta^1\text{-C}_9\text{H}_6\text{CH}_2\text{CH}_2\text{NMe}_2)\text{Ru}(\text{dppm})]\text{BF}_4$ (22) in nitriles hydration	98
3.3.8	Reactivity of $[(\eta^5:\eta^1\text{-C}_5\text{H}_4\text{CH}_2\text{CH}_2\text{NMe}_2)\text{Ru}(\text{dppm})]\text{BF}_4$ (2) and $[(\eta^5:\eta^1\text{-C}_9\text{H}_6\text{CH}_2\text{CH}_2\text{NMe}_2)\text{Ru}(\text{dppm})]\text{BF}_4$ (22) in alkene and alkyne hydration	100
3.3.9	Reactivity of $[(\eta^5:\eta^1\text{-C}_5\text{H}_4\text{CH}_2\text{CH}_2\text{NMe}_2)\text{Ru}(\text{dppm})]\text{BF}_4$ (2) and $[(\eta^5:\eta^1\text{-C}_9\text{H}_6\text{CH}_2\text{CH}_2\text{NMe}_2)\text{Ru}(\text{dppm})]\text{BF}_4$ (22) towards H ₂ /CO ₂ , formic acid and sodium formate	102

Chapter four

Dihydrogen-Bond-Promoted Catalysis: Catalytic Hydration of Nitriles and Hydrogenation of Unsaturated Hydrocarbon with the Aminoindenyl Ruthenium Complexes

4.1	Introduction	109
4.2	Experimental	111
4.2.1	Materials and instrumentation	111
4.2.2	Reactions	112
4.2.2.1	Catalytic hydration of neat nitriles with $\text{InNRu}(\text{dppm})\text{H}$ (19)	112
4.2.2.2	Catalytic hydration of nitriles with $\text{InNRu}(\text{dppm})\text{H}$ (19) in 1-pentanol	112
4.2.2.3	NMR study of hydration of acetonitrile with 19	113
4.2.2.4	H/D exchange experiment between complex 19 and D ₂ O	113
4.2.2.5	Typical procedure for the catalytic hydrogenation reactions with 3 and 19	114
4.2.2.6	Recovery of catalyst (hydration of nitriles)	115
4.2.2.7	Recovery of catalyst (hydrogenation of unsaturated hydrocarbons)	115
4.3	Results and discussion	116

4.3.1	Catalytic hydration of nitriles with indenyl and aminoindenyl ruthenium complexes	116
4.3.2	Effects of acid on the rates of nitrile hydration by complex 19	119
4.3.3	Reaction of InNRu(dppm)H and IndRu(dppm)H with D ₂ O	121
4.3.4	Possible mechanism for hydration of nitriles catalyzed by 19	124
4.3.5	Theoretical study on the possible mechanism for the hydration of nitrile catalyzed by 19	127
4.3.6	Effect of the monodentate ligands on the rates of nitriles hydration	135
4.3.7	Reactivity of InNRu(dppm)H (19) towards alkene and alkyne hydration	137
4.3.8	Hydrogenation of unsaturated hydrocarbons	138
4.3.9	Possible mechanism for hydrogenation of α,β -unsaturated ketone catalyzed by 19	143
Chapter five		
	Conclusion	145
	References	148
	Appendix	188

List of Figures

Figure 1.1		28
Figure 1.2		28
Figure 2.1	Schematic illustration of the mechanism for Complex 3 together with calculated free energies (kcal/mol) for species involved in the reactions	57
Figure 2.2	Schematic illustration of the mechanism for Complex 4 together with calculated free energies (kcal/mol) for species involved in the reactions	57
Figure 2.3	B3LYP optimized structures for those species shown in Figure 2.1.	59
Figure 2.4	B3LYP optimized structures for those species shown in Figure 2.2.	60
Figure 2.5	B3LYP optimized structures of intermediates and transition states for a hydration process that involves the ring slippage of the indenyl ligand.	62
Figure 3.1	400 MHz ^1H -NMR spectrum of $(\eta^5\text{-C}_9\text{H}_6\text{CH}_2\text{CH}_2\text{NMe}_2)\text{Ru}(\text{PPh}_3)_2\text{Cl}$ (17)	189
Figure 3.2	162 MHz $^{31}\text{P}\{^1\text{H}\}$ -NMR spectrum of $(\eta^5\text{-C}_9\text{H}_6\text{CH}_2\text{CH}_2\text{NMe}_2)\text{Ru}(\text{PPh}_3)_2\text{Cl}$ (17)	190
Figure 3.3	Mass spectrum of $(\eta^5\text{-C}_9\text{H}_6\text{CH}_2\text{CH}_2\text{NMe}_2)\text{Ru}(\text{PPh}_3)_2\text{Cl}$ (17)	191
Figure 3.4	400 MHz ^1H -NMR spectrum of $(\eta^5\text{-C}_9\text{H}_6\text{CH}_2\text{CH}_2\text{NMe}_2)\text{Ru}(\text{dppm})\text{Cl}$ (18)	192
Figure 3.5	162 MHz $^{31}\text{P}\{^1\text{H}\}$ -NMR spectrum of $(\eta^5\text{-C}_9\text{H}_6\text{CH}_2\text{CH}_2\text{NMe}_2)\text{Ru}(\text{dppm})\text{Cl}$ (18)	193
Figure 3.6	Mass spectrum of $(\eta^5\text{-C}_9\text{H}_6\text{CH}_2\text{CH}_2\text{NMe}_2)\text{Ru}(\text{dppm})\text{Cl}$ (18)	194
Figure 3.7	400 MHz ^1H -NMR spectrum of $(\eta^5\text{-C}_9\text{H}_6\text{CH}_2\text{CH}_2\text{NMe}_2)\text{Ru}(\text{dppm})\text{H}$ (19)	195

Figure 3.8.	162 MHz $^{31}\text{P}\{^1\text{H}\}$ -NMR spectrum of $(\eta^5\text{-C}_9\text{H}_6\text{CH}_2\text{CH}_2\text{NMe}_2)\text{Ru}(\text{dppm})\text{H}$ (19)	196
Figure 3.9	Mass spectrum of $(\eta^5\text{-C}_9\text{H}_6\text{CH}_2\text{CH}_2\text{NMe}_2)\text{Ru}(\text{dppm})\text{H}$ (19)	197
Figure 3.10	400 MHz ^1H -NMR spectrum of $(\eta^5\text{-C}_9\text{H}_6\text{CH}_2\text{CH}_2\text{NMe}_2)\text{Ru}(\text{PPh}_3)_2\text{H}$ (20)	198
Figure 3.11	162 MHz $^{31}\text{P}\{^1\text{H}\}$ -NMR spectrum of $(\eta^5\text{-C}_9\text{H}_6\text{CH}_2\text{CH}_2\text{NMe}_2)\text{Ru}(\text{PPh}_3)_2\text{H}$ (20)	199
Figure 3.12	Mass spectrum of $(\eta^5\text{-C}_9\text{H}_6\text{CH}_2\text{CH}_2\text{NMe}_2)\text{Ru}(\text{PPh}_3)_2\text{H}$ (20)	200
Figure 3.13	400 MHz ^1H -NMR spectrum of $[(\eta^5\text{-C}_9\text{H}_6\text{CH}_2\text{CH}_2\text{NMe}_2\text{H}^+)\text{Ru}(\text{dppm})\text{H}]\text{BF}_4$ (21)	201
Figure 3.14	162 MHz $^{31}\text{P}\{^1\text{H}\}$ -NMR spectrum of $[(\eta^5\text{-C}_9\text{H}_6\text{CH}_2\text{CH}_2\text{NMe}_2\text{H}^+)\text{Ru}(\text{dppm})\text{H}]\text{BF}_4$ (21)	202
Figure 3.15	400 MHz ^1H -NMR spectrum of $[(\eta^5:\eta^1\text{-C}_9\text{H}_6\text{CH}_2\text{CH}_2\text{NMe}_2)\text{Ru}(\text{dppm})]\text{BF}_4$ (22)	203
Figure 3.16	162 MHz $^{31}\text{P}\{^1\text{H}\}$ -NMR spectrum of $[(\eta^5:\eta^1\text{-C}_9\text{H}_6\text{CH}_2\text{CH}_2\text{NMe}_2)\text{Ru}(\text{dppm})]\text{BF}_4$ (22)	204
Figure 3.17	Mass spectrum of $[(\eta^5:\eta^1\text{-C}_9\text{H}_6\text{CH}_2\text{CH}_2\text{NMe}_2)\text{Ru}(\text{dppm})]\text{BF}_4$ (22)	205
Figure 4.1	Calculated free energy profile of 19-catalyzed hydration of acetonitriles. The energies are in kcal/mol	128
Figure 4.2	B3LYP optimized structures for those species shown in Figure 4.1	129
Figure 4.3	Calculated free energy profile of 3-catalyzed hydration of acetonitriles. The energies are in kcal/mol	133
Figure 4.4	B3LYP optimized structures for those species shown in Figure 4.3	134

List of Tables

Table 2.1	Hydration of acetonitrile with ruthenium complexes	44
Table 2.2	Catalytic hydration of aromatic nitriles with 3 & 5	47
Table 2.3	Catalytic hydration of aliphatic nitriles with 3 & 5	49
Table 2.4	H/D exchange between Ru-H & D ₂ O	54
Table 2.5	Hydration of nitriles with 3 and recycled catalyst 3	64
Table 2.6	Hydration of acetonitrile with/without added acetamide	65
Table 2.7	Hydration of acetonitrile with complexes containing different diphosphines	66
Table 3.1	CO ₂ reduction with 2 & 22	105
Table 4.1	Hydration of nitriles with 3 & 19	117
Table 4.2	19 -catalyzed hydration of nitriles with/without acid	120
Table 4.3	Percentage of deuteration of Ru-H of 3 and 19 by D ₂ O	122
Table 4.4	Hydration of nitriles with 20 & 23	136
Table 4.5	Catalytic hydrogenation of alkenes with 3 and 19	139
Table 4.6	Catalytic hydrogenation of α,β -unsaturated ketones with 3 and 19	141

List of Schemes

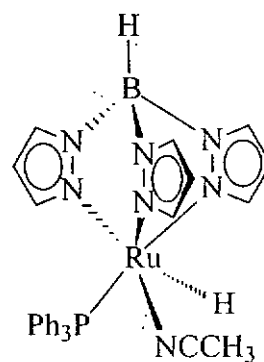
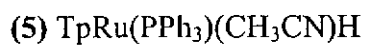
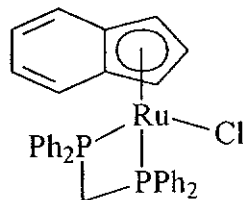
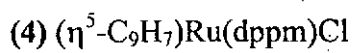
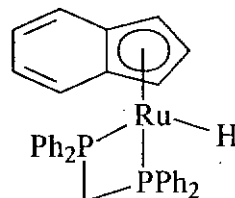
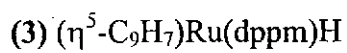
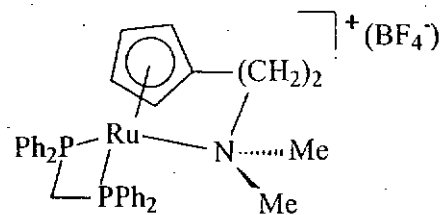
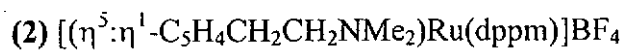
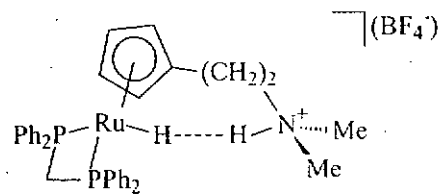
Scheme 1.1		2
Scheme 1.2		3
Scheme 1.3		4
Scheme 1.4		5
Scheme 1.5	Intramolecular N-H...H-Ru Dihydrogen Bond Mediating Proton Transfer	7
Scheme 1.6	2-catalyzed CO ₂ hydrogenation to formic acid	8
Scheme 1.7	Dihydrogen-Bond-Controlled Diastereoselective Borohydride Reduction of α -Hydrocycloalkanones	9
Scheme 1.8		10
Scheme 1.9		12
Scheme 1.10	Hydrogen bonding mediated aldehyde imination	13
Scheme 1.11	Hydrogen Bonding mediated aminolysis of 6-chloropurine	14
Scheme 1.12		17
Scheme 1.13		18
Scheme 1.14		19
Scheme 1.15		21
Scheme 1.16		22
Scheme 1.17	Mechanisms of methyl migration in [Mo(η^5 -C ₉ H ₇)(Me)(CO) ₃]	24
Scheme 1.18	Amino-indenyl ruthenium catalyzed hydration of alkynes	32
Scheme 2.1		51
Scheme 2.2	Proposed mechanism of 3-catalyzed Hydration of Nitriles	52
Scheme 2.3	Proposed mechanism of H/D exchange of the hydride of 3 with D ₂ O	55
Scheme 2.4	3-catalyzed hydration of terminal alkynes	68
Scheme 2.5	3-catalyzed hydration of alkenes	72

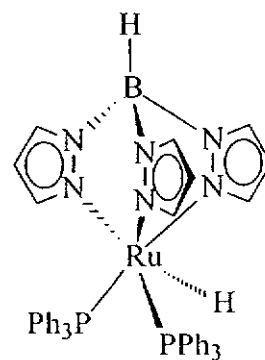
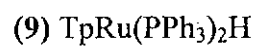
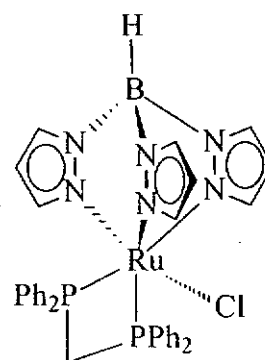
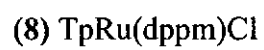
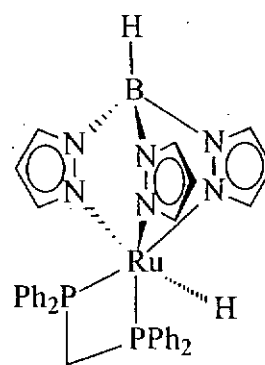
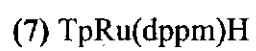
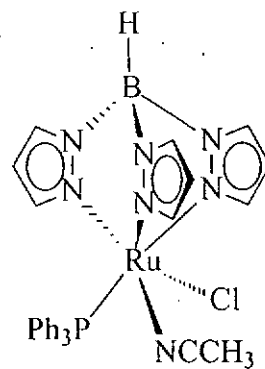
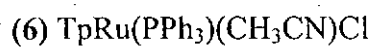
Scheme 2.6		74
Scheme 2.7		74
Scheme 2.8	3-catalyzed hydroamination of alkynes	75
Scheme 2.9	3-catalyzed alcoholysis of nitriles	77
Scheme 3.1	Synthetic pathways of 17	88
Scheme 3.2	Proposed mechanism of H/D exchange of the hydride ligand of 21 with D ₂ O	96
Scheme 3.3		98
Scheme 3.4	Proposed mechanism of 22 -catalyzed hydration of acetonitriles	99
Scheme 3.5	Proposed mechanism of 2 - & 22 -catalyzed hydration of alkynes	101
Scheme 3.6		104
Scheme 3.7	Proposed mechanism of 22 -catalyzed CO ₂ hydrogenation	107
Scheme 3.8		108
Scheme 3.9		108
Scheme 4.1	Intramolecular N-H...H-Ru Dihydrogen-Bond-Mediated Proton Transfer	109
Scheme 4.2	Proposed mechanism for H/D exchange of the hydride of 19 with D ₂ O	123
Scheme 4.3	Proposed mechanism of 19 -catalyzed hydration of nitriles	126
Scheme 4.4	Proposed mechanism of 19 -catalyzed hydration of nitriles (derived by theoretical calculations)	131
Scheme 4.5	Proposed mechanism of 19 -catalyzed hydrogenation of alkene	140
Scheme 4.6	Proposed mechanism of 19 -catalyzed hydrogenation of α,β -unsaturated ketone	144

Abbreviations

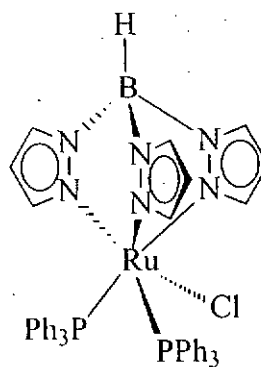
δ	Chemical shift (NMR)
η	Descriptor for hapticity
μ	Descriptor for bridging
L	Generalized ligand, in particular a $2e^-$ ligand
[M]	Generalized metal fragment with n ligands
ESI-MS	Electro-spray ionization mass spectroscopy
FAB-MS	Fast atom bombardment mass spectroscopy
IR	Infra-red
NMR	Nuclear magnetic resonance spectroscopy
THF	Tetrahydrofuran
TMS	Tetramethylsilane
MeOH	Methanol
EtOH	Ethanol
Et ₂ O	Diethyl ether
DMSO	Dimethylsulphoxide
DMF	N,N-dimethylformamide
CH ₃ CN	Acetonitrile
Tp	Hydrotris(1-pyrazolyl) borate
Pz	Pyrazolate ion
Cp	Cyclopentadienyl
Cp*	Pentamethylcyclopentadienyl
Ind	Indenyl

CpN	(2-(Dimethylamino)ethyl) cyclopentadienyl
InN	(2-(Dimethylamino)ethyl) indenyl
¹ PPr ₃	Triisopropylphosphine
PPh ₃	Triphenylphosphine
dppm	Bis(diphenylphosphino)methane
BF ₄	Tetrafluoroborate
R	Generalized alkyl group
Me	Methyl
Et	Ethyl
¹ Pr	Isopropyl
¹ Bu	t-butyl
Ph	Phenyl
e ⁻	Electron
br	Broad
s	Singlet
d	Doublet
t	Triplet
q	Quartet
m	Multiplet
T ₁	Spin-lattice relaxation time
NOE	Nuclear Overhauser Effect

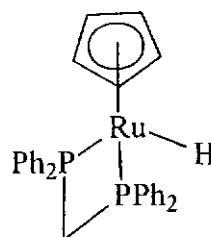




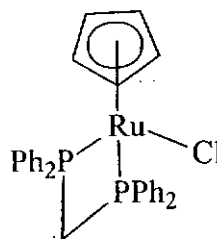
(10) $\text{TpRu}(\text{PPh}_3)_2\text{Cl}$



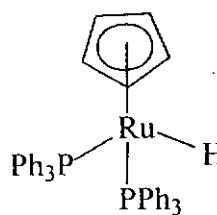
(11) $\text{CpRu}(\text{dppm})\text{H}$



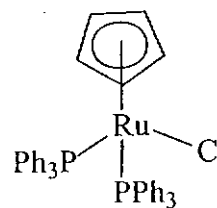
(12) $\text{CpRu}(\text{dppm})\text{Cl}$



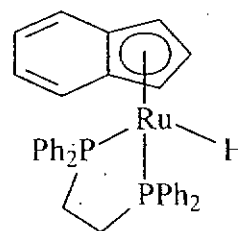
(13) $\text{CpRu}(\text{PPh}_3)_2\text{H}$



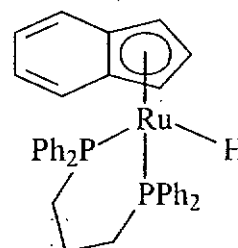
(14) $\text{CpRu}(\text{PPh}_3)_2\text{Cl}$



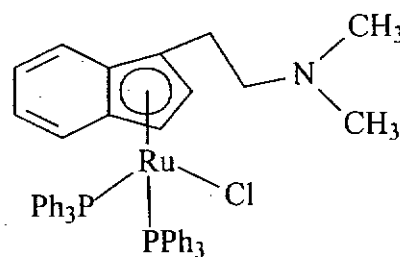
(15) $(\eta^5\text{-C}_9\text{H}_7)\text{Ru}(\text{dppe})\text{H}$



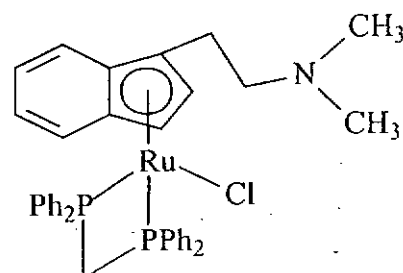
(16) $(\eta^5\text{-C}_9\text{H}_7)\text{Ru}(\text{dppp})\text{H}$



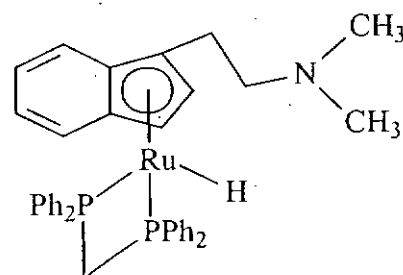
(17) $(\eta^5\text{-C}_9\text{H}_6\text{CH}_2\text{CH}_2\text{NMe}_2)\text{Ru}(\text{PPh}_3)_2\text{Cl}$

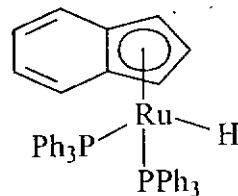
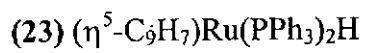
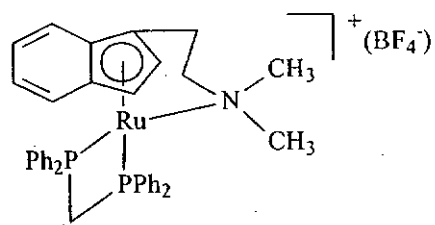
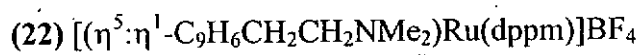
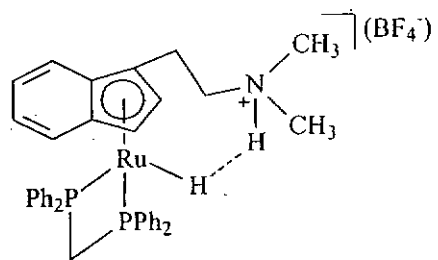
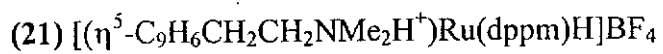
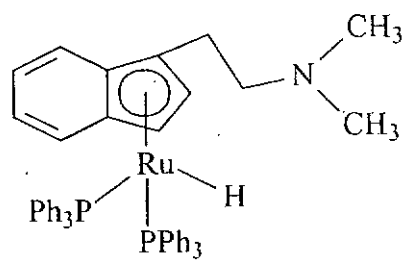
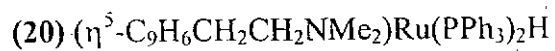


(18) $(\eta^5\text{-C}_9\text{H}_6\text{CH}_2\text{CH}_2\text{NMe}_2)\text{Ru}(\text{dppm})\text{Cl}$



(19) $(\eta^5\text{-C}_9\text{H}_6\text{CH}_2\text{CH}_2\text{NMe}_2)\text{Ru}(\text{dppm})\text{H}$





Chapter 1 Introduction

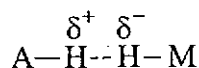
1.1 Review of hydrogen bonding in organometallic complexes and hydrogen bonding-mediated reactions

Hydrogen bonding is an important but generally weak (2-10 kcal/mole) chemical bonding phenomenon[1]. It can occur in an intra- or intermolecular manner between a proton donor group and proton acceptor such as the lone pair of a heteroatom, the π -electrons of an aromatic ring, or a multiple bond.

Recently, an unusual type of hydrogen bond, in which a σ M-H bond (where M is a transition metal or B) acts as proton acceptor, has attracted considerable attention.

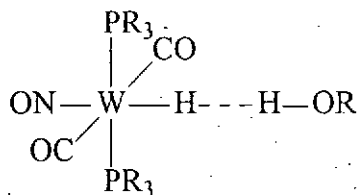
(Chart 1.1)[2-9]

Chart 1.1

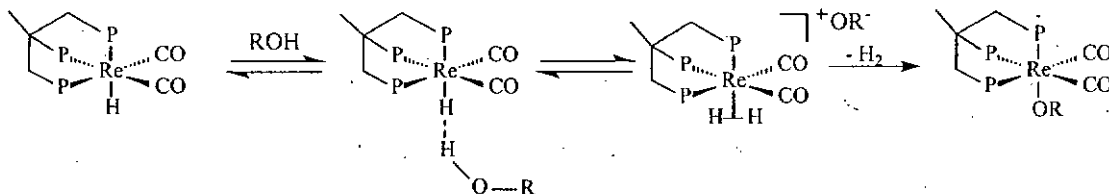


This hydridic-protonic interaction, also called dihydrogen bonding, has strength and directionality comparable with those found in conventional hydrogen bonding.

Chart 1.2



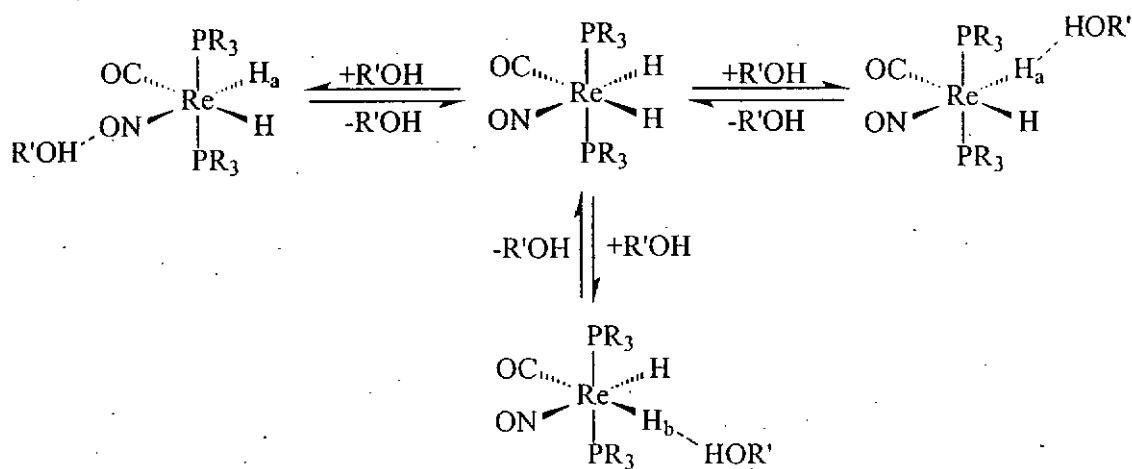
Using in situ IR and NMR spectroscopies, Epstein *et al.*[11] have shown that the terminal hydride ligand in $[(\text{triphos})\text{Re}(\text{CO})_2\text{H}]$ forms $\text{Re-H}\cdots\text{HOR}$ adducts by reaction with an acidic alcohol such as phenol.(Scheme 1.2) The hydrogen-bonded adduct $\text{Re-H}\cdots\text{HOR}$ may be considered as the first stage of the proton-transfer which ultimately yields the dihydrogen complex $[(\text{triphos})\text{Re}(\text{CO})_2(\eta^2\text{-H}_2)]^+$. Finally, it has been found that the equilibrium between the H-bonded complex $[(\text{triphos})\text{Re}(\text{CO})_2\text{H}\cdots\text{HOR}]$ and the dihydrogen complex $[(\text{triphos})\text{Re}(\text{CO})_2(\eta^2\text{-H}_2)]^+$ is reversible. At temperatures higher than 260 K, H_2 elimination occurs with formation of the $[(\text{triphos})\text{Re}(\text{CO})_2(\eta^1\text{-OR})]$.



$\text{ROH} = \text{PhOH}$, hexafluoro-2-propanol (HFIP), fluoro-2-methyl-2-propanol (PFTB)

Scheme 1.2

Berke *et al.* have demonstrated that $\text{Re}(\text{PR}_3)_2(\text{NO})(\text{CO})\text{H}_2$ possess not only chemically different hydride positions, but also the O_{NO} atom as competing sites for hydrogen bonding. The phosphine ligand appears to have an important influence over the regioselectivity of the H-bonding formation. Thus, in $\text{Re}(\text{PMe}_3)_2(\text{NO})(\text{CO})\text{H}_2$ interaction with one of the hydridic hydrogens is preferred, but the NO group competes more and more effectively for the proton donors as the bulkiness of R group increase, to the point where only $\text{O}-\text{H}\cdots\text{ON}$ hydrogen bonds are observed for $\text{Re}(\text{P}^i\text{Pr}_3)_2(\text{NO})(\text{CO})\text{H}_2$. [12] (Scheme 1.3)



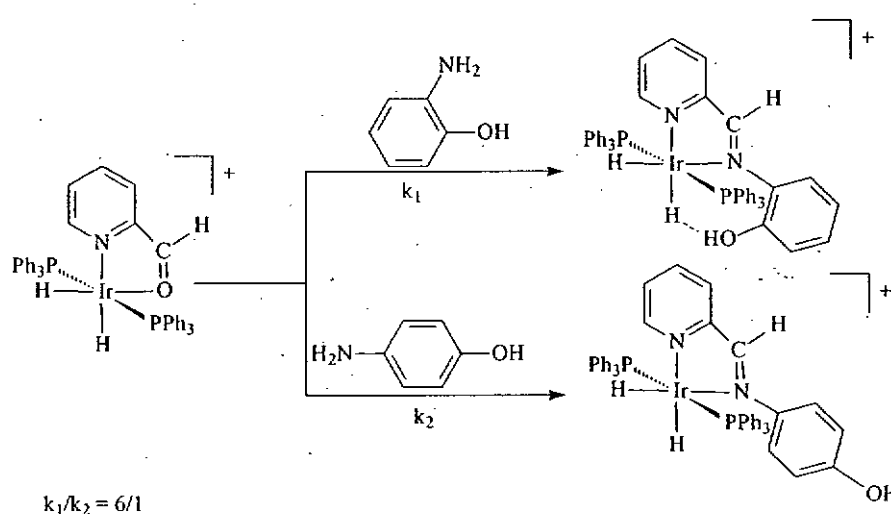
where $\text{R} = \text{Me}, \text{Et}, {}^i\text{Pr}$
 $\text{R}' = \text{CH}(\text{CF}_3)_2, \text{C}(\text{CF}_3)_3$

Scheme 1.3

More interestingly, dihydrogen bond can also influence the structures of the complexes and their reactivity and selectivity both in solution and in the solid state, thus finding potential use in catalysis, crystal engineering, and materials chemistry.[13]

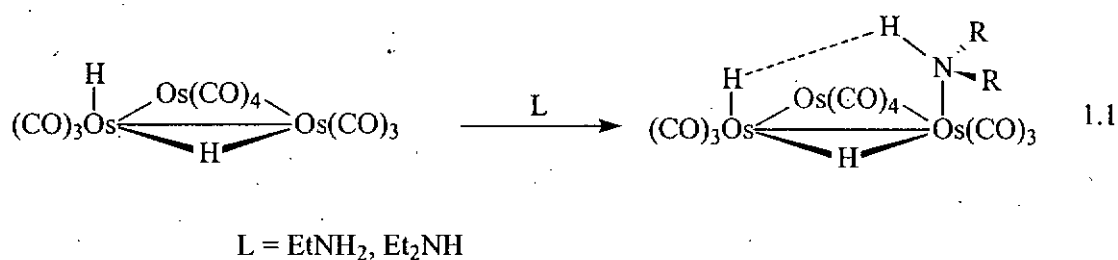
Examples showing dihydrogen bonds playing important roles in controlling reactivity and regioselectivity of chemical reactions have been documented.[14-19]

It has been found that the (η^2 -2-pyridinecarboxaldehyde-*N,O*) iridium complex $[\text{IrH}_2(\eta^2\text{-2-C}_5\text{H}_4\text{NCHO-}N,O)(\text{PPh}_3)_2]^+$ undergoes selective imination with an equimolar mixture of 2-aminophenol and 4-aminophenol, favoring the 2-aminophenol-derived product, the outcome appears to be the result of its stabilization by intramolecular Ir-H \cdots H-O dihydrogen bonding and presumably the stabilization of the transition state leading to it.[18] (Scheme 1.4)

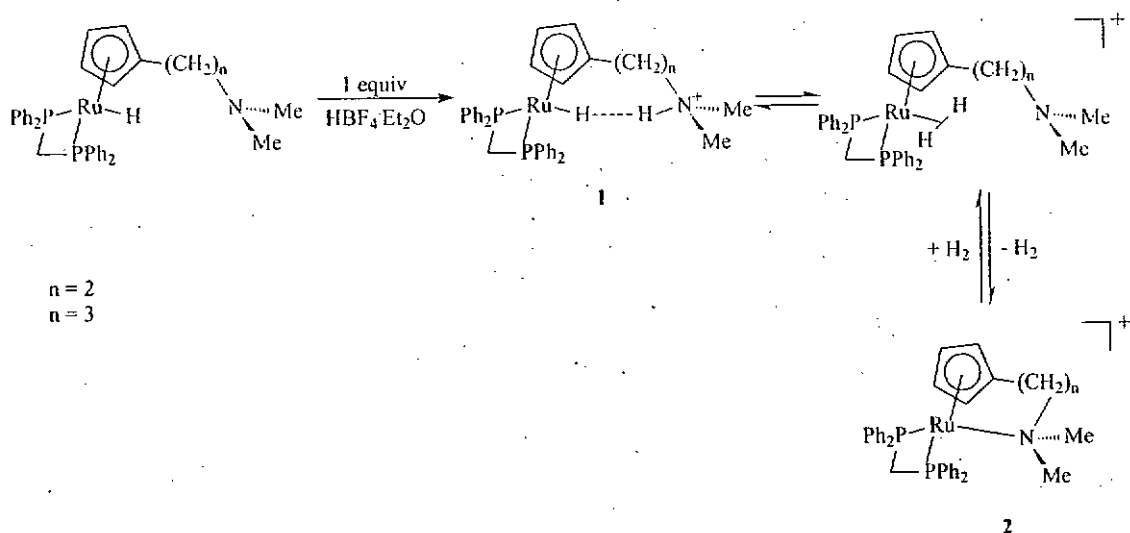


Scheme 1.4

Aime *et al.* have suggested that dihydrogen-bonding interaction may be even more important in transition-metal cluster chemistry in directing the stereochemistry of ligand attachment to the clusters and in determining the regioselectivity of reactions in these systems. Thus, reaction of the electronically unsaturated osmium cluster $\text{H}_2\text{Os}_3(\text{CO})_{10}$ with EtNH_2 and Et_2NH yields exclusively the syn product, stabilized by an intramolecular $\text{N-H}\cdots\text{H-Os}$ interaction, which would not be possible in the anti isomer.[16, 17] (eq 1.1)

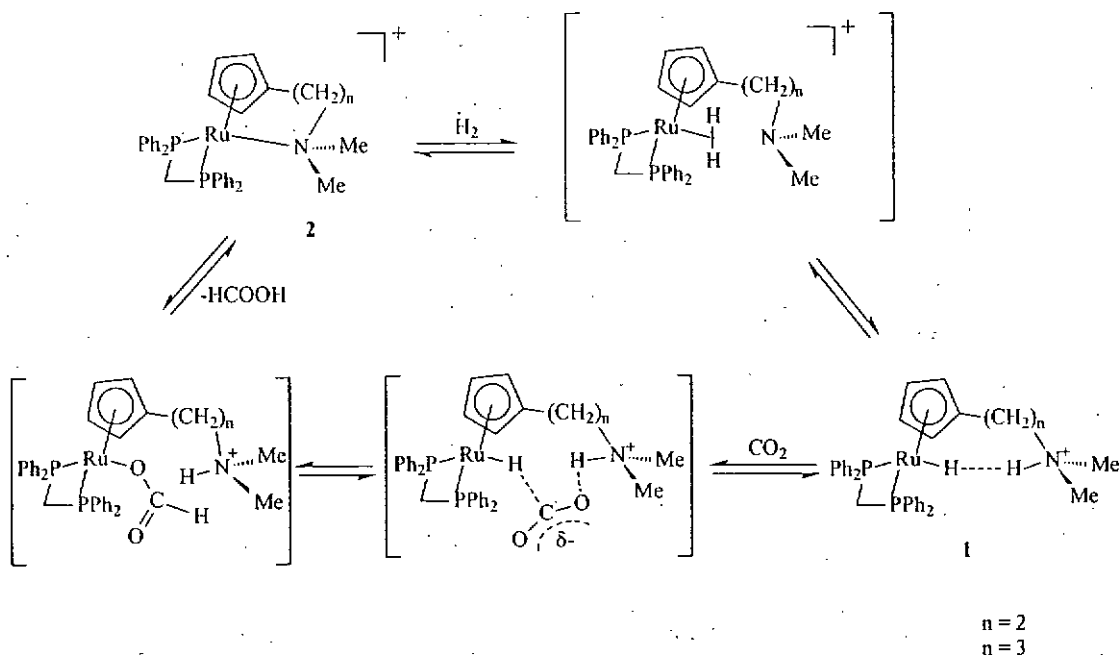


Our research group have synthesized the aminocyclopentadienyl ruthenium hydride complex **1** and demonstrated that intramolecular $\text{N-H}\cdots\text{H-Ru}$ dihydrogen bond plays an important role in mediating proton transfer and subsequent formation of Ru-N bonds (complex **2**, Scheme 1.5).



Scheme 1.5 Intramolecular N-H...H-Ru Dihydrogen Bond Mediating Proton Transfer

It is suggested that **1** is in equilibrium with the η^2 -dihydrogen intermediate, H_2 loss from which results in the formation of the Ru–N bonded chelated structure **2**. The reversed Ru–N bond hydrogenolysis can be achieved at 60 °C under 60 atm of H_2 . Complex **2** was found to be able to catalyze CO_2 hydrogenation to formic acid, although in low yields.

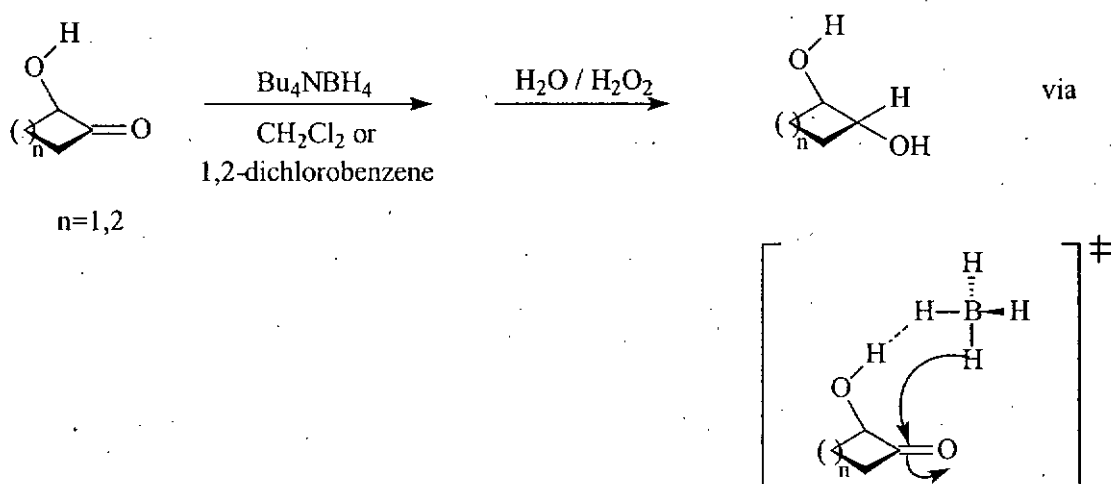


Scheme 1.6 2-catalyzed CO₂ hydrogenation to formic acid

The crucial step in the catalysis is proposed to be the heterolytic cleavage of H₂ to generate 1.[20] Theoretical investigations indicate that H-bonding of the amine-bound proton in 1 to the oxygen atom of an incoming CO₂, which is not coordinated to the metal center, enhances the electrophilicity at the carbon of the molecule, enabling it to abstract the hydride from the metal to form the transient metal-formate intermediate.[21, 22] (Scheme 1.6)

Jackson *et al.* have unequivocally demonstrated the control of the regioselectivity, *via* dihydrogen bonding, of the diastereoselective borohydride reduction of α -hydroxycycloalkanones to give the trans-diols (Scheme 1.7). The

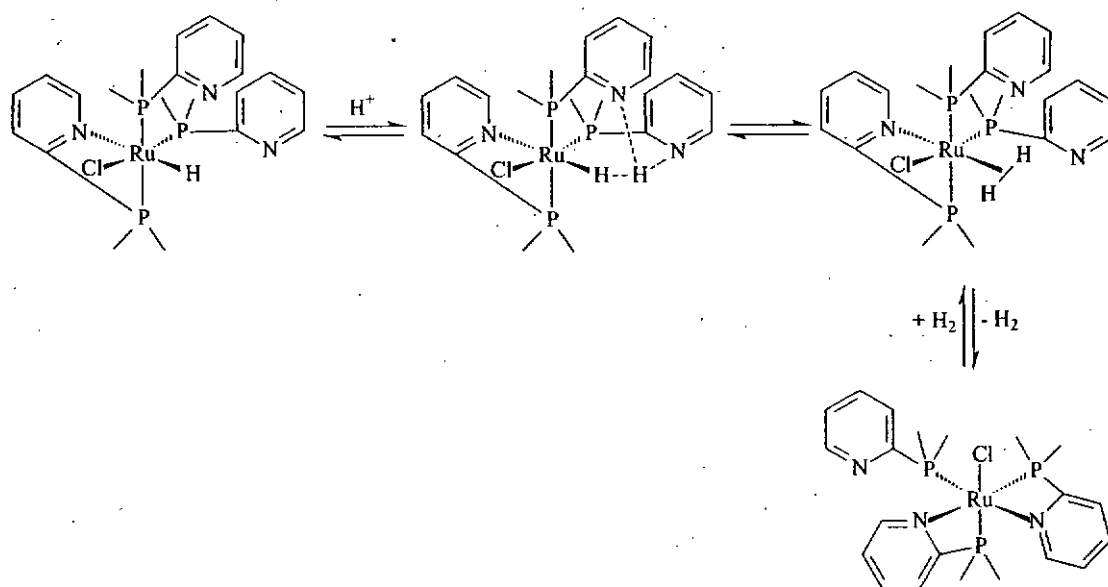
OH...BH₄⁻ dihydrogen-bonding interaction guides the hydride delivery to produce the trans diol product. The reduction reactions with tetrabutylammonium borohydride in non-hydrogen bonding solvents CH₂Cl₂, ClCH₂CH₂Cl, or *o*-dichlorobenzene are accelerated about 150 times relative to the reductions of the corresponding unsubstituted cycloalkanones. These effects are greatly reduced in the presence of competing hydrogen bonding alcohols or anions such as F⁻, Cl⁻, or Br⁻. This was the first recognized instance of a directing effect specifically mediated by dihydrogen bonding.[23]



Scheme 1.7 Dihydrogen-Bond-Controlled Diastereoselective Borohydride Reduction of α -Hydroxycycloalkanones

A very interesting dihydrogen-bonded system and its hydrogen exchange dynamics was described by Jalón *et al.*[24] They found that addition of a proton to the ruthenium monohydrides formed a complex with a three-centered dihydrogen bond

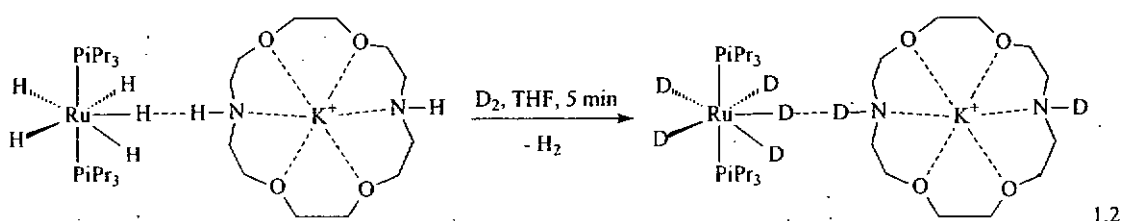
(Ru-H...H-Py₂) and this system showed a fast exchange between the proton and hydride moieties. (Scheme 1.8). Moreover, this system proved to be a very active catalyst for D⁺/H₂ exchange. Thus, when a solution of it in CD₃OD, which acts as a deuteron source and provides D⁺ ions for the exchange of H₂, was exposed to a dihydrogen atmosphere at room temperature and 1 atm, more than 90% of H₂ was exchanged for D₂ in about half an hour.



Scheme 1.8

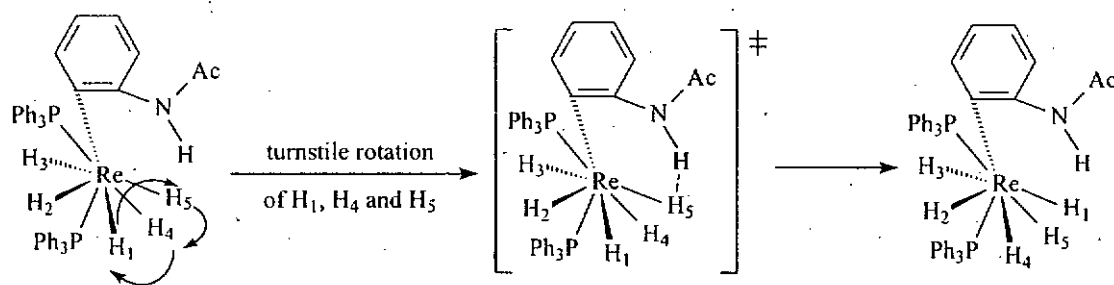
A similar H/D exchange was reported by Morris *et al.* with the ruthenium polyhydride complex [RuH₅(PⁱPr₃)₂][K(1,10-diaza-18-crown-6)]. [25] (eq. 1.2) This salt containing a N-H...H-Ru dihydrogen bonding interaction, enhances the rate of H/D exchange of the metal hydride and the NH with D₂ gas. Upon exposure to D₂ gas

at 1 atm and room temperature for 5 min, the intensities of the NH and RuH ^1H NMR (THF- d_8) signals were depleted by 100% and 90%, respectively. It implies that there are close proton-hydride contacts between the hydrides and NH in solutions of these complexes. For comparison, only 13% decrease in the hydride resonance was observed after 10 days when the much less acidic 18-crown-6 ether was used for complexation. The exchange is also significantly slower if the ruthenium hydride is replaced by the less basic analogous osmium hydride. While the conjugate acid of $\text{RuH}_5(\text{P}^i\text{Pr}_3)_2$, the known $\text{RuH}_2(\text{H}_2)_2(\text{P}^i\text{Pr}_3)_2$ dihydrogen complex, could reasonably play the role of the intermediate in the exchange process depicted in eq 1.2, its involvement in this transformation was ruled out by control experiments, implying efficient activation of the M-H bonds by $\text{N-H}\cdots\text{H-Ru}$ dihydrogen bonding.



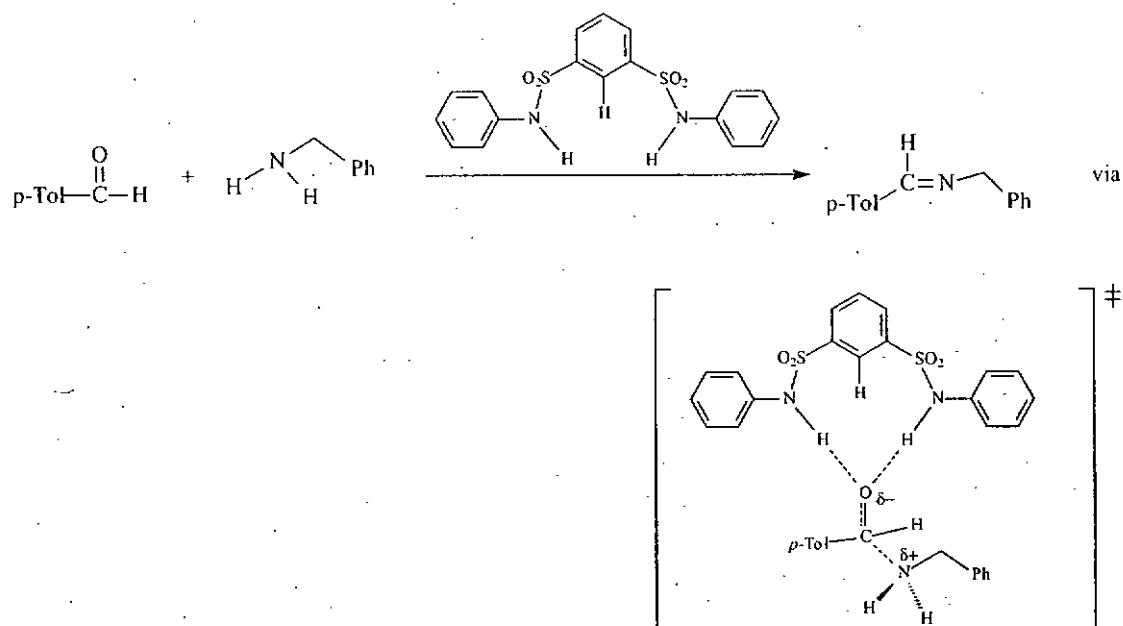
Crabtree *et al.* have found that intramolecular $\text{N-H}\cdots\text{H-Re}$ interactions can affect the hydride fluxionality in $\text{ReH}_5(\text{PPh}_3)_2\text{L}$ ($\text{L} = \text{N-acetyl-2-aminopyridine}$).^[26] (Scheme 1.9) The free energy of activation for the turnstile rotation involving the H_1 , H_4 , H_5 atoms in this complex is 0.7 kcal/mol smaller than for the analogous complex

with the NHAc group in the *para* position of the pyridine ring. Stabilization of the transition state by strong N-H...H-Re dihydrogen bonding, which is only possible in the *ortho*-NHAc isomer, seems to be responsible for the observed difference.



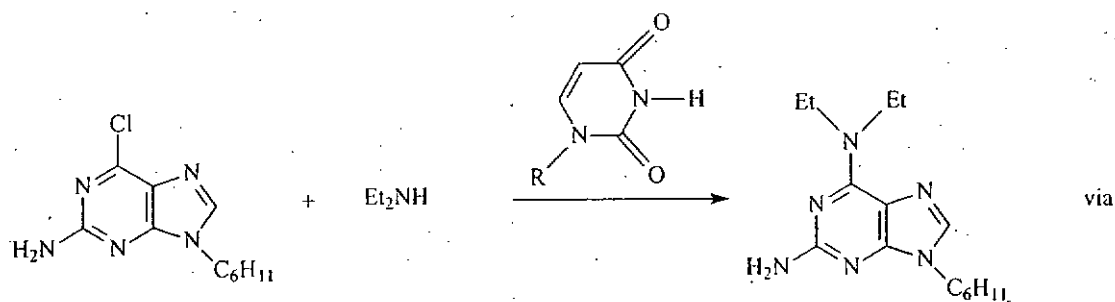
Scheme 1.9

Kavallieratos and Crabtree suggested that a favorable two-point hydrogen-bonding interaction of the two convergent sulfonamide groups with the anionic oxygen in the transition-state is responsible for the catalysis of aldehyde imination with the organic disulfonamide receptor.[27] (**Scheme 1.10**)

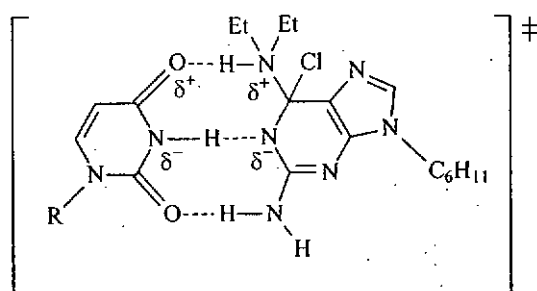


Scheme 1.10 Hydrogen bonding mediated aldehyde imination

Konishi *et al.* reported that the aminolysis of 2-amino-6-chloropurine was catalyzed by derivatives of uracil. (Scheme 1.11) The catalytic behavior was proposed to be resulting from the multiple hydrogen-bonding interactions between the uracils and 6-chloropurine derivative. The interactions assist the formation of a reactive intermediate and stabilize the transition state, giving rise to catalytic enhancement in the observed rate of aminolysis.[28] Computation study, employing density functional theory, of model reactions – aminolysis of 6-chloropyrimidine and 2-amino-6-chloropyrimidine, have been carried out to provide rationalizations for the role of the hydrogen-bonding interactions in the catalytic processes.[29, 30]



[R = (tBuMe₂Si)₃-ribose]

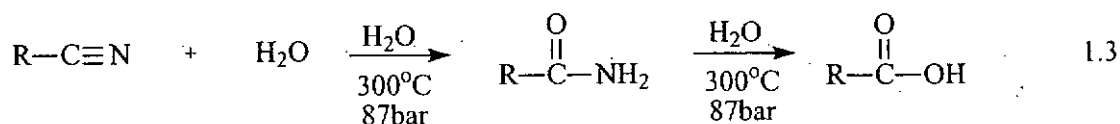


Scheme 1.11 Hydrogen Bonding mediated aminolysis of 6-chloropurine

Although it is now established that dihydrogen bonds can be utilized to control reactivity and selectivity of chemical reactions, well recognized cases of dihydrogen bonds playing an essential role in promoting catalytic reactions are still rare. We are here going to demonstrate the principle of promoting catalytic chemical reactions with H-bonding. We will focus on the hydration of nitriles and homogeneous hydrogenation of unsaturated hydrocarbons[31-44]. These reactions are not only good model reactions to demonstrate the principle, but are useful and important ones both in the laboratory and in industry.

1.2 Hydration of nitriles

Hydration of nitriles to their corresponding carboxamides is an attractive and important reaction both in industry and laboratory studies. Traditionally, stoichiometric hydration reactions of nitriles have been achieved by using a variety of acids and bases. However, many of these classical methods require harsh conditions and result in low yields.[45, 46] High yields can only be obtained by using extremely high temperature and pressure. However, under these conditions, the corresponding carboxylic acids inevitably form as hydrolysis of amides occurs readily, and sometimes this reaction even predominates.[47] (eq 1.3)



Nevertheless, harsh reaction conditions and the use of strong acids and bases can be potentially avoided by employing transition-metal complexes as catalysts for the hydration reaction.

To date, a variety of different transition metal complexes have been used as catalysts in the hydration of nitriles. For example, $\text{Pt}(\text{C}_6\text{H}_8)(\text{dppe})$, [2] and

substitutionally inert metals such as $[\text{Co}(\text{cyclen})(\text{OH}_2)_2]^{3+}$ (cyclen = 1,4,7,11-tetraazacyclododecane) [48, 49], $[(\text{NH}_3)_5\text{Rh}(\text{CH}_3\text{CN})]^{3+}$ [50] and $[(\text{NH}_3)_5\text{Ir}(\text{CH}_3\text{CN})]^{3+}$ [50].

However, in the last few decades, only one example of a nitrile hydration reaction involving ruthenium complexes has been reported in the literature.[51] A major limitation of the reactions is that the amide product chelates onto the metal center and therefore the amide product cannot be easily isolated.[51] It has also been pointed out that Co(III) complexes are substitutionally inert, and therefore catalytic hydration using Co(III) complexes tends to give little or no catalytic turnover.[48]

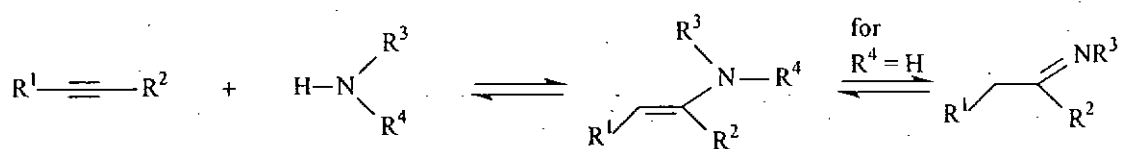
In addition to the hydration of nitriles with transition metal complexes, addition of other protic nucleophiles such as alcohols to metal-bound nitriles will also be attempted. Metal-imino-ether ($\text{M-NH}=\text{C}(\text{OR}')\text{R}$) complexes have been prepared from reactions of $\text{M-N}\equiv\text{CR}$ with $\text{R}'\text{OH}$, [52] but alcoholysis of nitriles catalyzed by metal complexes are still rare.[53, 54] (eq 1.4)



1.4

Moreover, it is interesting to study the role of hydrogen bond in the hydration of other substrates (e.g. activated olefins and alkynes) [55-62] with the ruthenium complexes.

We believe that it is also interesting to study H-bond mediated hydroamination of alkynes.[63-77] (Scheme 1.12)

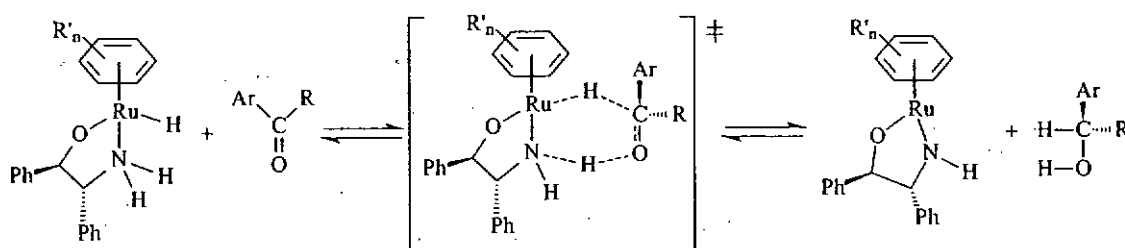


Scheme 1.12

1.3 Homogeneous hydrogenation of unsaturated hydrocarbon

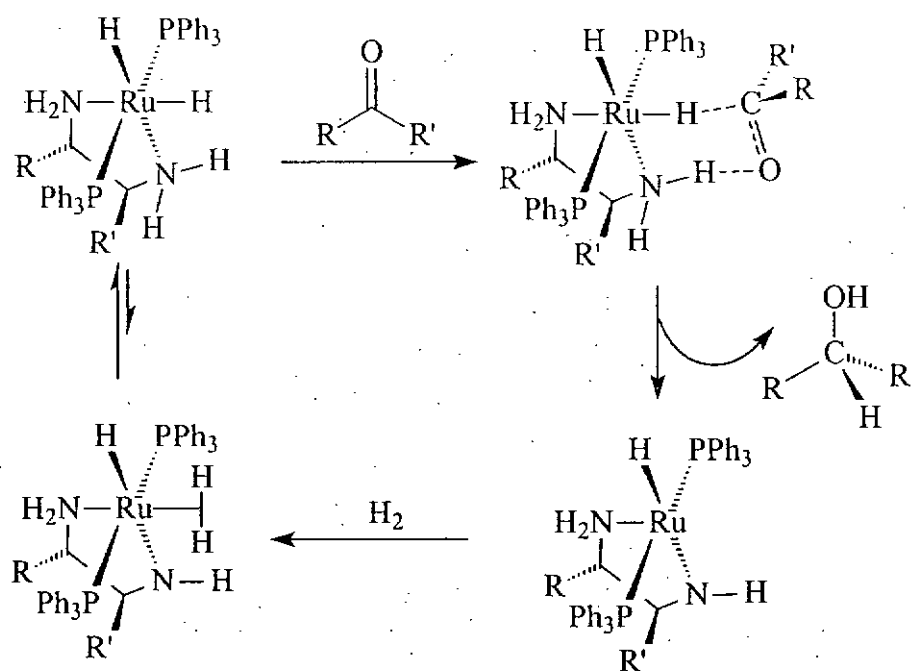
Homogeneous catalytic reduction of polar functional groups mediated by transition-metal complexes has emerged as an alternative to stoichiometric reduction by metal hydrides such as $LiAlH_4$ and $NaBH_4$. [42] Interest in this area has been spurred by development of highly efficient catalysts for the selective hydrogenation of ketones and imines.[78] The design of the catalysts with a “metal/NH bifunctionality”, [79-84] in which an amino proton and a metal hydride are concertedly transferred to C=O or C=N doubles via pericyclic transition states, [38, 85-91] has attracted much attention.

Recently, Noyori and co-worker have proposed a concerted mechanism in the study of Ru(II)-catalyzed hydrogen transfer between alcohols and carbonyl compounds.[81] Most significantly, this concerted mechanism does not require the formation of metal alkoxides in the catalytic cycle.(Scheme 1.13) Instead, the hydrogenative transformation of C=O linkages with a coordinatively saturated Ru-hydride intermediate and its reverse process occur in an outer coordination sphere of the transition metal with the aid of ligand-substrate hydrogen bonding.



Scheme 1.13

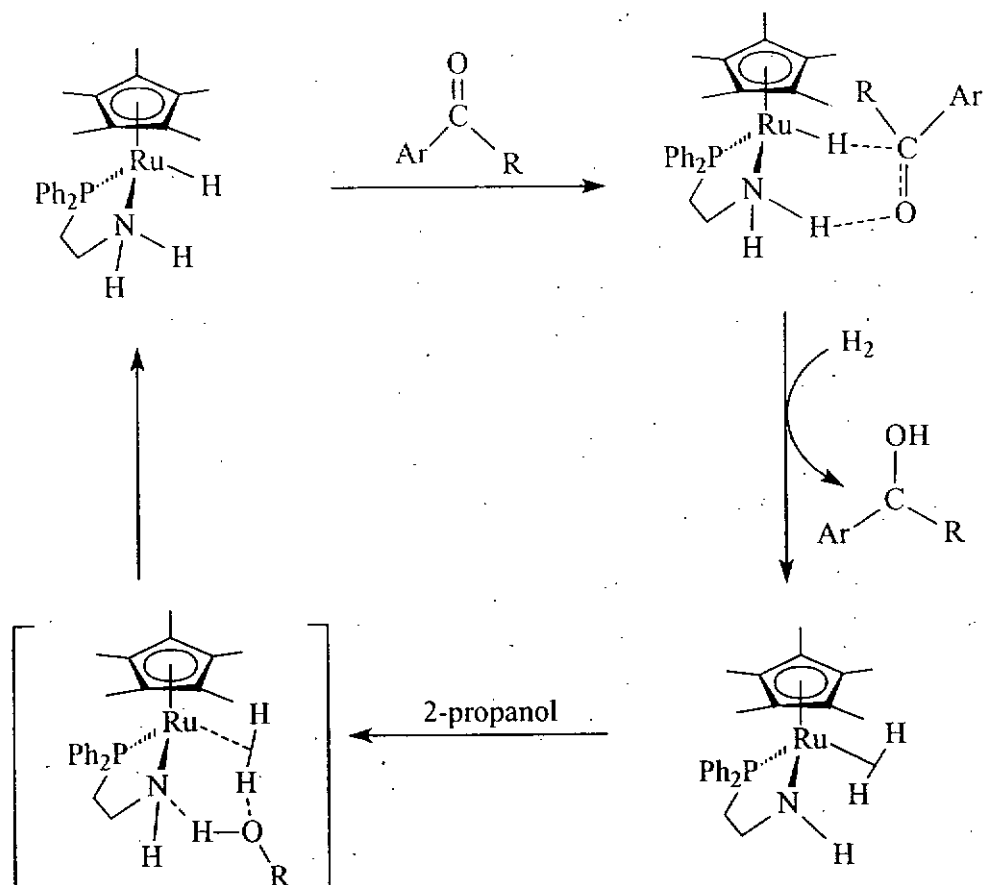
Morris *et al.* have reported similar concerted dihydrogen transfer from *cis* hydride and N-H groups of a ruthenium complex to the ketone or imine substrate, heterolytic dihydrogen splitting then regenerates the active complex.[82](Scheme 1.14) This scheme demonstrates the importance of the *cis*-Ru-H \cdots H-N to provide nascent, polarized dihydrogen(H $^{\delta-}$ \cdots H $^{\delta+}$) for the catalytic hydrogenation of polar bonds.



Scheme 1.14

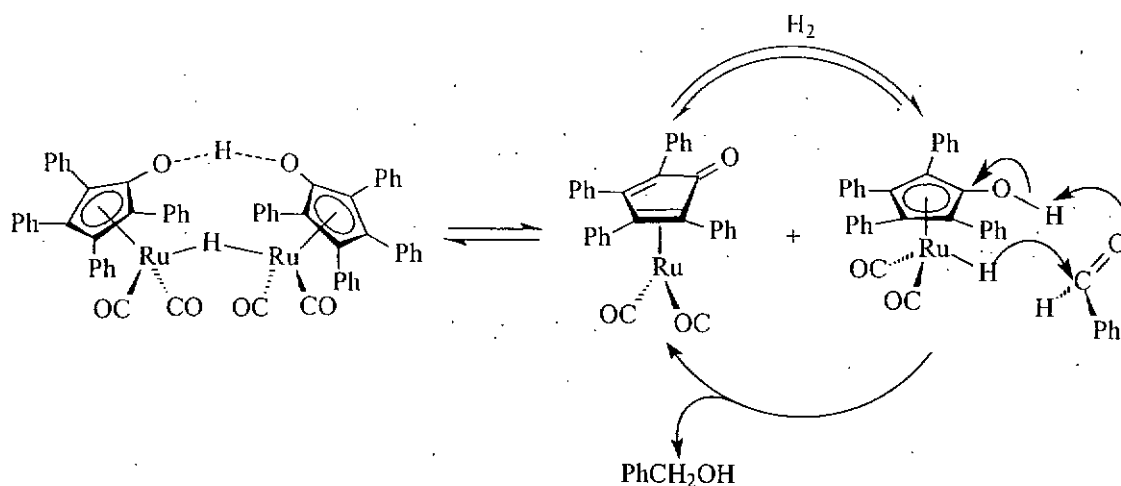
Ikariya and co-workers have reported that the rapid hydrogenation of ketones is accomplished by using a combination of Cp^{*}Ru complexes and primary amines as a catalyst in 2-propanol.[92](Scheme 1.15) They have studied the effect of hydrogenation of acetophenones with Cp^{*}Ru complexes by varying of amines. The results showed that N,N-dimethylethylenediamine gives the highest yield alcohol while the amines without NH group (e.g. N,N,N-trimethylethylenediamine and N,N,N,N,-tetramethylethylenediamine) were found to be ineffective in catalyzing the reaction. Thus, it implies that the amino NH group plays a crucial role for the catalysis.

In addition, they have also found that 2-propanol is the best solvent for those hydrogenation reactions, while use of aprotic solvents such as DMF, THF, acetonitrile and CH_2Cl_2 results in moderate to low yield. It can be explained by the reaction of $\text{Cp}^*\text{Ru}(\text{cod})\text{Cl}$ with D_2 in $(\text{CH}_3)_2\text{CHOD}$, in which provided an alcoholic product with greater than 90% deuterium content at the benzylic carbon. These results clearly show that a rapid exchange of hydrogen atoms between H_2 and ROH occurs reversibly prior to the reduction of the ketones. This scrambling caused by the catalyst in 2-propanol proceeds possibly via interconversion of $\text{Cp}^*\text{Ru}(\text{amido})(\eta^2\text{-H}_2)$ [93-98] and $\text{Cp}^*\text{Ru}(\text{amine})\text{H}$, in which 2-propanol participates in the H_2 activation through the formation of a hydrogen-bonding network,[3, 4, 7, 15, 99] as shown in **Scheme 1.15**.



Scheme 1.15

Casey *et al.* have also proposed the concerted mechanism for the reduction of carbonyl compounds, which involves concerted transfer of proton and hydride to the aldehyde outside the coordination sphere of the metal.[100](Scheme 1.16) In the proposed mechanism, the simultaneous transfer of H⁺ from CpOH and H⁻ from RuH occur outside the coordination sphere of the metal, in which can be supported by the kinetic studies.



Scheme 1.16

1.4 Introduction of cyclopentadienyl and indenyl ligands and their potential in catalysis

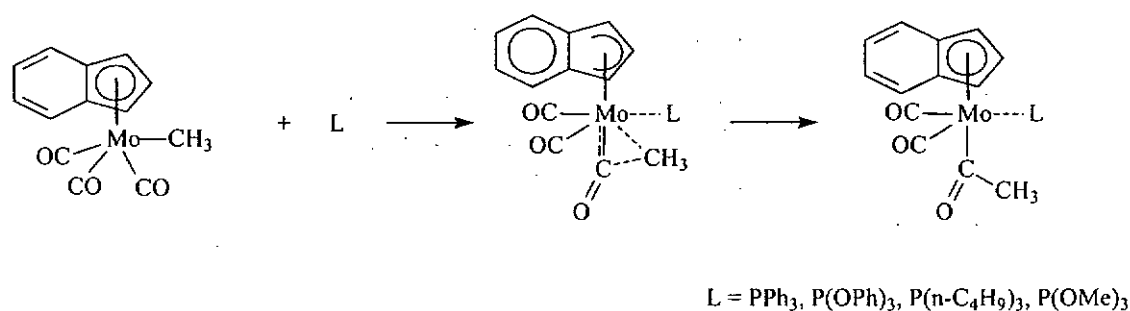
The cyclopentadienyl group, C_5H_5^- (Cp) and derivatives, are one of the most important class of ligands in organometallic chemistry. Their key roles in this field can be judged from the vast number of cyclopentadienyl complexes (σ - or π -bonded to the central atom) of virtually every element[101-104] and more than 80% of all known organotransition metal compounds contain the Cp system or a derivative thereof.[105] Cyclopentadienyl ligands stabilize metals in both high and low oxidation states and can bind to a metal through one to five of the ring carbon atoms. The easy change of hapticity allows flexible adjustment of the cyclopentadienyl ligand to the electronic and steric requirements of the central atom, resulting in

extensively complex chemistry.

Interest in using indenyl C_9H_7 (Ind) as a substitute for cyclopentadienyl has become widespread because it has been shown that indenyl transition metal complexes often show higher reactivity with respect to their cyclopentadienyl analogues, either in stoichiometric or in catalytic processes. Substitution of the η^5 -indenyl ligand for the η^5 -cyclopentadienyl ligand in transition-metal complex has been shown to promote associative reactions between nucleophilic substrates and metal centers. Green and co-workers reported the greater reactivity of $(\eta^5-C_9H_7)Rh(C_2H_4)_2$ toward substitution of the bound ethylenes by other alkenes, dienes, and alkynes.[106, 107] Similarly, Basolo and co-workers have observed a 3×10^8 -fold enhancement in the rate of CO substitution by triphenylphosphine for $(\eta^5-C_9H_7)Rh(CO)_2$ over $(\eta^5-C_5H_5)Rh(CO)_2$. [108, 109] Several new routes to group 9 indenyl complexes have been developed and these have been used to explore some structural and reactivity aspects of this class of complexes.[110-117]

The indenyl ligand facilitates migratory insertion reactions. The first observation of a rate acceleration in bimolecular reaction of a η^5 -indenyl complex relative to that of a η^5 -cyclopentadienyl complex was that of Hart-Davis and Mawby for the reaction

of $(\eta^5\text{-C}_9\text{H}_7)\text{Mo}(\text{CO})_3\text{CH}_3$ with PPh_3 to yield $(\eta^5\text{-C}_9\text{H}_7)\text{Mo}(\text{CO})_2(\text{PPh}_3)\text{COCH}_3$, the result of CO insertion into the Mo-CH₃ bond.[118] To explain the rate acceleration and the observed first-order dependence on both the metal complex and PPh_3 , an η^3 -indenyl intermediate (Scheme 1.17) has been proposed. The indenyl ligand behaves as a π -allyl ligand to accommodate the electrons of the incoming PPh_3 , with this binding mode being more accessible for the indenyl ligand because of the resulting aromatization of the fused benzene ring.[119] Basolo and co-workers have referred to this phenomenon as the "indenyl ligand effect".[108]



Scheme 1.17 Mechanisms of methyl migration in $[\text{Mo}(\eta^5\text{-C}_9\text{H}_7)(\text{Me})(\text{CO})_3]$

However, experimental data based on calorimetric studies of Cp and Ind Mo and W complexes,[120] as well as theoretical studies focused on the indenyl effect,[121, 122] hinted that the more facile η^5 -to- η^3 ring slippage of indenyl, relative to cyclopentadienyl, might be related to the η^5 -Cp ligand's binding more strongly than

the η^5 -Ind, and η^3 -coordination is more favorable for the indenyl.[123]

For instances, Romao has studied addition reactions with the 18-electron complex $[(\eta^5\text{-C}_9\text{H}_7)\text{W}(\text{CO})_2(\text{NCMe})_2]\text{BF}_4$ in order to ascertain the conditions most favorable for "ring slippage," and has isolated a η^3 -indenyl species $[(\eta^3\text{-C}_9\text{H}_7)\text{W}(\text{CO})_2(\text{NCMe})_3]\text{BF}_4$, which is stable enough to be characterized by crystallographic spectroscopy.[124] It implies that ring slippage of indenyl ligand is facile during the addition reactions.

Fu *et al.* have demonstrated the utilization of the indenyl effect in designing a specific catalytic hydroboration reaction.[125] They have found that $(\eta^5\text{-C}_9\text{H}_7)\text{Rh}(\text{C}_2\text{H}_4)_2$ -catalyzed hydroboration of 4-(benzyloxy)cyclohexene shows higher rate of reaction than the cyclopentadienyl analogues. It is suggested that the ring-slippage strategy is in fact viable.

1.5 Introduction of indenyl and cyclopentadienyl complexes containing amino side-arms

Recently, an increasing number of new ring-substituted cyclopentadienes have been reported. In principle, all five hydrogen atoms of the C_5H_5 fragment can be substituted in any fashion. Variations in the Cp ligand sphere often results in significant changes in chemical reactivity, stability, sensitivity to oxidation and many other properties.[126-129]

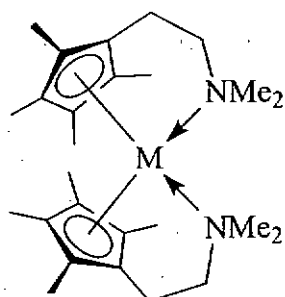
In ring substituted cyclopentadienyl complexes of transition metals, the effect of an additional donor group strongly depends on the nature of the metal and of the donor group. The strength of the coordination of the tethered donor fragment to the metal center can be estimated on the basis of Pearson's HSAB concept of 'hard' and 'soft' acids and bases.[130] 'Hard' ligands combine preferentially with 'hard' centers, and 'soft' ligands favor the interaction with 'soft' metal centers. On the other hand, otherwise unfavored 'hard-soft' combination are stabilized to a certain extent by the chelate effect; this unusual binding situation leads to interesting electronic effects at the respective metal center with consequences for the chemical reactivity. Of course, the side-chain donor can be easily substituted in such types of complexes. This results

in a hemilabile behaviour,[131, 132] where the side-chain functionality can either act as a donor or as a spectator ligand.

The hemilabile situation is expected in compounds where a 'hard' donor, such as an amino or alkoxy group, coordinates to a 'soft' metal center, as present in complexes with a late transition metal in low oxidation states. Vice versa, hemilability is anticipated when a 'soft' donor, such as a phosphino, thio, or alkenyl group, interacts with a 'hard' center, as present in complexes with early transition metals in high oxidation states. Of course, there exist many 'borderline' bonding situations, where the donor-acceptor interaction is difficult to predict. A substitutionally labile group is capable of temporarily blocking a coordination site and therefore allows tuning of the reactivity of the metal center. The fluxional 'opening and closing' character provides interesting perspectives in terms of stabilization of reactive, unsaturated species, of substrate activation, of chemical sensing, and of homogeneous catalysis.

Many examples of dialkylaminoalkyl-substituted Cp complexes with s-, p-, d-, and f-block elements have been described in the literature.[127-129]

Jutzi *et al.* have synthesized the calcocene and samarocene monomers with the amino side arms coordinated to the metal centers. (Figure 1.1). The coordination of the amino side arms prevents an association to oligomers. [133] The monomeric lanthanum complex (Figure 1.2), reported by Herrmann and co-workers, contains three dimethylaminoethylsubstituted cyclopentadienyl groups; two amino groups coordinate to the metal center and thus prevent the usual formation of oligomers. [134]



M = Ca, Sm

Figure 1.1

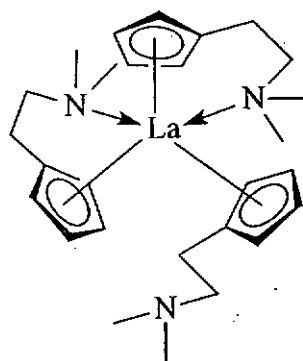


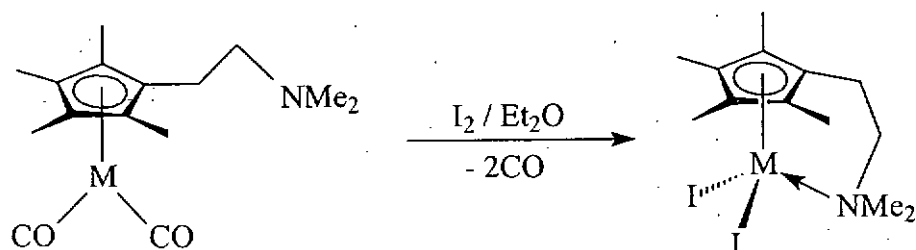
Figure 1.2

The influence of the alkyl substituents at the amino group has been studied in $(\eta^5:\eta^1-(C_5H_4CH_2CH_2NMe_2)TiCl_3)$ and $(\eta^5:\eta^1-(C_5H_4CH_2CH_2N^iPr_2)MCl_3)$ (M = Ti, Zr). Raush and co-workers have described the reactivity of the the titanium half-sandwich complex, which is monomeric in the solid state and in solution, [135] analogous to the parent compound $CpTiCl_3$. [136] In combination with methylaluminoxane (MAO), $(\eta^5:\eta^1-(C_5H_4CH_2CH_2NMe_2)TiCl_3)$ is a very active catalyst for the polymerization of

ethylene; the role of the dimethylamino group in the polymerization has not been elucidated yet.

The bonding characteristics of the $C_5H_4(CH_2CH_2)NMe_2$ ligand in late transition-metal compounds have been extensively studied in Jutzi's group.[137, 138]

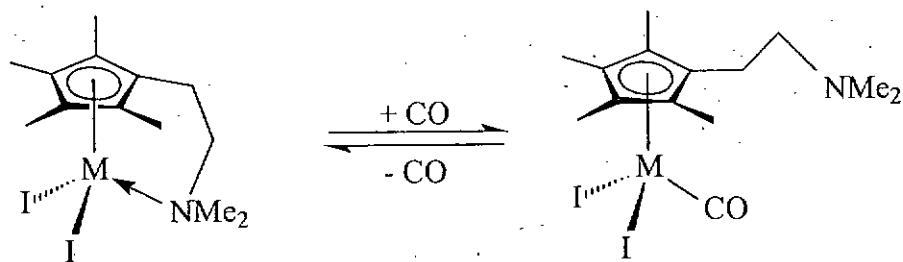
The amino side-chain does not coordinate in complexes of the type $(\eta^5-C_5H_4CH_2CH_2NMe_2)L_2M$, ($L=CO, C_2H_4$; $M = Co, Rh, Ir$) (eq 1.5). On the other hand, coordination takes place in $(\eta^5-C_5H_4CH_2CH_2NMe_2)I_2M$ ($M = Co, Rh, Ir$) with the metal center in the +3 oxidation state.



$M = Co, Rh, Ir$

1.5

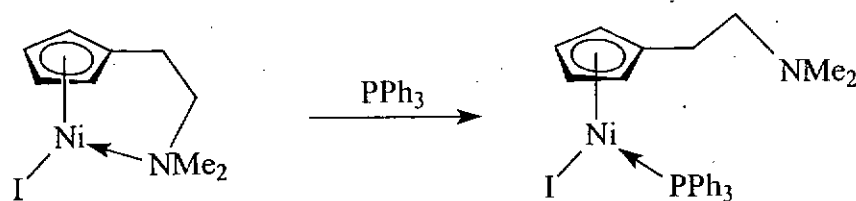
Interestingly, a hemilabile situation has been observed in the application of CO pressure to $(\eta^5-C_5H_4CH_2CH_2NMe_2)I_2M$ ($M = Co, Rh, Ir$), where the amino group can be reversibly displaced.[137] (eq 1.6)



M = Co, Rh, Ir

1.6

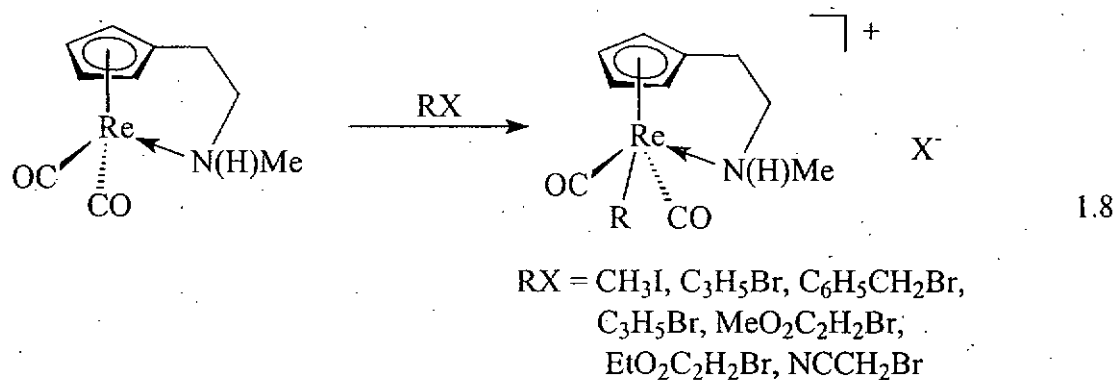
Fischer and co-workers[139] have also reported the intramolecular coordination of amino sidearm to a Group 10 element. The labile dimethylaminoethyl group in the nickel(II) complex can easily be displaced by a triphenylphosphine ligand.(eq 1.7)



1.7

Wang *et al.* have contributed significantly to the area of amino-substituted Cp ligands,[140-143] for example, they have synthesized $(\eta^5:\eta^1-(C_5H_4CH_2CH_2N(H)Me)ReCO_2)$, in which the 'hard' amino group is coordinated to a 'soft' Re(I) center. The enhanced nucleophilicity of the metal now enables alkylation with substrates RX.[144] (eq 1.8) The same group have also presented the complex $(\eta^5:\eta^1-(C_5H_4CH_2CH_2N(H)Me)MnCO_2)$, in which the

coordination of an N-donor to a monovalent metal center is supported by the chelate effect.[145]



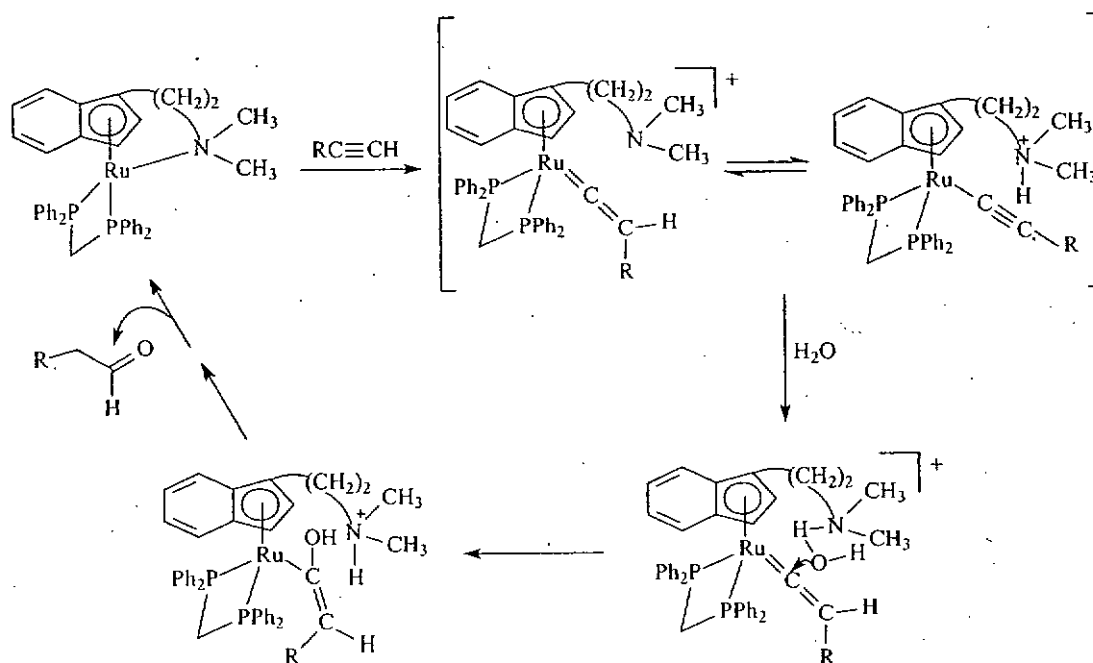
It is well-known that transition metal indenyl complexes display higher reactivity in stoichiometric and catalytic reactions than their cyclopentadienyl analogues.[119, 146, 147] However, apart from the parent ligand C_9H_7 , very few substituted indenyl complexes are known, most of them being alkyl-, aryl-, [112, 146, 148-156] halo-, [157, 158] or ferrocenyindenyl derivatives.[159] To date, no aminoindenylruthenium complexes have been reported in the literature and hence, there is impetus to synthesize complexes of this type in order to compare their reactivities with these of the unsubstituted indenyl complexes.

In this research program, an indenyl metal hydride complex $IndRu(dppm)H$ (3) was synthesized; the hydride ligand of the complex is able to hydrogen-bond the incoming nucleophile such as a water, an alcohol or amine molecule. The hydrogen-bonding interaction not only guides the course of nucleophilic attack on the

coordinated substrate, which is a nitrile or unsaturated hydrocarbon, but also increases the nucleophilicity of the water and thus the hydration reaction proceeds more readily.

Very few metal complexes are known to catalyze anti-Markovnikov's hydration of terminal alkynes to give aldehydes.[160-162] Functionalized indenyl and cyclopentadienyl complexes, $\text{InNRu}(\text{dppm})\text{BF}_4$ and $\text{CpNRu}(\text{dppm})\text{BF}_4$ respectively, might be used in such a way that an alkyne will probably displace the coordinated amine side arm, and the resulting pendant amino group can H-bond to the incoming H_2O molecule. Using aminoindenyl ruthenium complex as an example, H-bond mediated hydration of alkynes might proceed via the mechanism depicted in **Scheme 1.18**.

1.18.



Scheme 1.18 Amino-indenyl ruthenium catalyzed hydration of alkynes

We believe that it is interesting to study the effect of the amino side-arm of the indenyl ligand on the catalytic activity of the complexes in reactions such as hydration of nitrile and hydrogenation of unsaturated hydrocarbon. Therefore, we synthesized the complex InNRu(dppm)H (**19**) (InN = aminoindenyl ligand), which is a derivative of the indenyl hydride complex IndRu(dppm)H , the indenyl ligand of **19** has an amino side arm attached. The catalytic activities of **19** in nitrile hydration and hydrogenation of unsaturated hydrocarbon were studied and compared with those of **3**.

Chapter 2 Dihydrogen-Bond-Promoted Catalysis: Catalytic Hydration of Nitriles with Ruthenium Hydride Complexes

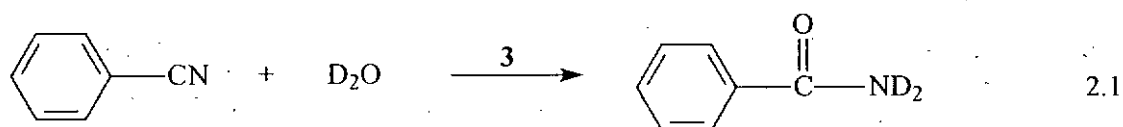
2.1 Introduction:

The unconventional hydrogen bond (dihydrogen bond) between a transition metal hydride and a common hydrogen bond donor containing an O-H or an N-H group is a hydride-proton interaction. Complexes containing this H...H interaction of the type M-H...H-O or M-H...H-N might be regarded as intermediates in hydride protonation to generate a η^2 -H₂ ligand and the reverse reaction, i.e., heterolytic splitting of dihydrogen. Dihydrogen bond is also recognized for activating the M-H bond for reactions such as H/D exchanges, proton transfer, and substitution.[10, 24, 25, 82, 92, 99, 163-165] It is also well demonstrated that dihydrogen bond plays an important role in controlling the reactivity and stereochemistry of organometallic hydride complexes.[13-19, 83]

Although it is now known that dihydrogen bonds can be utilized to control reactivity and selectivity of chemical reactions,[14-19] well-recognized cases of dihydrogen bonds playing an essential role in promoting catalytic reactions are still rare. Lau and co-workers have recently synthesized and characterized the

intramolecular Ru-H...H-N dihydrogen bonding in the aminocyclopentadienyl ruthenium hydride complexes and have also demonstrated that the Ru-H...H-N dihydrogen bond is a key feature in the catalytic hydrogenation of CO₂ to formic acid.[20]

One of the interests of our research group has been “the study of C-H bond activation with transition metal complexes”; a recent endeavor in this area is the deuteration of C-H bonds using D₂O as the isotopic source. This is an attractive reaction since D₂O is inexpensive and has low toxicity. In the course of this study, we have learned that the indenyl ruthenium hydride complex (η^5 -C₉H₇)Ru(dppm)H (3) is capable of promoting deuteration of some aromatic solvents such as benzene, toluene, xylene, and chlorobenzene with D₂O, under Argon or in the presence of H₂, which also undergoes H/D exchange with D₂O. It was, however, found that in the case of benzonitrile, deuteration of the compound did not occur, instead it was hydrated to give the deuterated benzamide (eq 2.1).



We are here to provide a novel example demonstrating that the catalytic hydration of nitriles to amides by an indenylruthenium hydride complex is in fact promoted by the Ru-H...H-OH dihydrogen bond.

2.2 Experimental

2.2.1 Materials and instrumentation

All reactions were carried out under a dry nitrogen atmosphere using standard Schlenk techniques. Ruthenium trichloride, $\text{RuCl}_3 \cdot 3\text{H}_2\text{O}$, indene, bis(diphenylphosphino)methane (dppm), sodium borohydride, 4-chlorobenzonitrile, 4-nitrobenzonitrile, 4-methoxybenzonitrile, iodoacetonitrile and pyrazole were purchased from Aldrich and were used as received. Malonitrile was purchased from Aldrich and was distilled from P_2O_5 . The complexes IndRu(dppm)H , [166] IndRu(dppm)Cl , [166] IndRu(dppp)H , [166] IndRu(dppe)H , [166] $\text{TpRu(PPh}_3\text{)(CH}_3\text{CN)H}$, [167] $\text{TpRu(PPh}_3\text{)(CH}_3\text{CN)Cl}$, [167] TpRu(dppm)H , [168] TpRu(dppm)Cl , [168] $\text{TpRu(PPh}_3\text{)}_2\text{H}$, [167] $\text{TpRu(PPh}_3\text{)}_2\text{Cl}$, [169] CpRu(dppm)H , [170] CpRu(dppm)Cl , [170], $\text{CpRu(PPh}_3\text{)}_2\text{H}$, [170] and $\text{CpRu(PPh}_3\text{)}_2\text{Cl}$, [170] were synthesized

according to literature methods. Solvents were distilled under a dry nitrogen atmosphere with appropriate drying agents (solvent/drying agent): methanol/Mg-I₂, ethanol/Mg-I₂, acetonitrile/CaH₂, tetrahydrofuran/Na-benzophenone, diethyl ether/Na, n-hexane/Na, 1-pentanol/K₂CO₃, benzonitrile/K₂CO₃. THF-*d*₈ and CDCl₃ were dried over P₂O₅ and CaH₂, respectively.

Proton NMR spectra were obtained from a Bruker DPX 400 spectrometer. Chemical shifts were reported relative to residual protons of the deuterated solvents. ³¹P{¹H} NMR spectra were recorded on a Bruker DPX 400 spectrometer at 162 MHz; chemical shifts were externally referenced to 85% H₃PO₄ in D₂O. Electrospray Ionization Mass spectrometry was carried out with a Finnigan MAT 95S mass spectrometer. Elemental analyses were performed by M-H-W Laboratories, Phoenix, AZ, USA.

2.2.2 Syntheses and Reactions

2.2.2.1 Catalytic hydration of neat nitriles with IndRu(dppm)H (3).

In a typical run, a sample of **3** (0.010 g, 0.017 mmol) was dissolved in a 1:1 mixture of nitrile (0.017 mol) and water (0.310 mL, 0.017 mol). The solution was heated at reflux for 72 h, after which the solution was cooled to room temperature, and the amide formed was dissolved by the addition of 1 mL of acetone. An 0.1 mL aliquot of the solution was removed and analyzed by ^1H NMR spectroscopy (in CDCl_3). Comparison of the integrations of the characteristic peaks of the amide and the unreacted nitrile gave the turnover number of the reaction.

2.2.2.2 Catalytic hydration of nitriles with IndRu(dppm)H (3) in 1-pentanol.

To a sample of **3** (0.010 g, 0.017 mmol) in 2 mL of 1-pentanol were added the nitrile (0.017 mol) and water (0.310 mL, 0.017 mol). The resulting solution was heated at 120°C for 72 h. At the end of the reaction time, the solution was cooled to room temperature, and an 0.1 mL aliquot of it was removed and analyzed by ^1H NMR spectroscopy (in CDCl_3). Comparison of the integrations of the characteristic peaks of the amide product and the unreacted nitrile yielded the turnover number of the reaction.

2.2.2.3 NMR study of nitriles hydration.

A sample of complex **3** (0.010 g, 0.017 mmol) was loaded into a 5 mm NMR tube which was then capped with a rubber septum. The tube was evacuated and filled with nitrogen gas for three cycles. Degassed THF-*d*₈ (0.4 mL) was added, via a syringe, to dissolve the sample. Ten equivalents of H₂O and acetonitrile each were added through microsyringes. The tube was loaded into the NMR probe preheated to 80°C, and the sample was analyzed by ¹H and ³¹P{¹H} NMR spectroscopies at 15 min intervals for the first 4 h. The sample was refluxed at 80°C in an oil bath overnight. The reaction was then monitored by taking ¹H NMR & ³¹P{¹H} NMR spectra of the sample in 4 h intervals for 48 h. It was found that the catalyst remained unchanged throughout the reaction. The yield of the hydration product was measured by ¹H NMR spectroscopy.

2.2.2.4 H/D exchange experiment between complex **3** and D₂O.

A sample of complex **3** (0.010 g, 0.017 mmol) was loaded into a 5 mm NMR tube which was then capped with a rubber septum. The tube was purged and filled with nitrogen for three cycles. Degassed THF-*d*₈ (0.4 mL) was syringed in to dissolve the sample. D₂O (20 μL) was then added to the mixture by using a micro-syringe. The ¹H NMR spectrum of the mixture was recorded immediately at room temperature.

The sample was then refluxed at 120°C (oil bath temperature). The H/D exchange reaction between Ru-H of **3** and D₂O was analyzed at room temperature by ¹H NMR & ³¹P{¹H} NMR spectroscopies in 1 h intervals for the first 12 h. After refluxing the solution at 120°C overnight, the sample was analyzed at room temperature by ¹H NMR & ³¹P{¹H} NMR spectroscopies in 24 h intervals for 96 h. The percentage of deuteration of the Ru-H signal was measured by ¹H NMR spectroscopy.

2.2.2.5 Acetamide control reaction.

A sample of complex **3** (0.010 g, 0.017 mmol) and 5 equiv of acetamide (5 mg, 0.085 mmol) were loaded into a 5 mm NMR tube which was then capped with rubber septum. The tube was evacuated and filled with nitrogen gas for three cycles. Degassed THF-*d*₈ (0.4 mL) was added, via a syringe, to dissolve the sample. Prior to heating, the ¹H NMR spectrum of the solution showed the resonance of acetamide at δ 1.98 (s, 3H of CH₃CONH₂). The tube was then heated at 80°C for 10 days in an oil bath. It was found that the catalyst remained unchanged.

2.2.2.6 Acetamide Inhibition of acetonitrile Hydration.

Samples of **3** (0.010 g, 0.017 mmol) and acetamide (0.470 g, 0.008 mol) were dissolved in a 1:1 mixture of acetonitrile (0.700 mL, 0.017 mol) and water (0.310 mL,

0.017 mol). The solution was reflux for 72 h, after which the solution was cooled to room temperature, and all amide was dissolved by the addition of 1 mL of acetone. An 0.1 mL aliquot of the solution was removed and analyzed by ^1H NMR spectroscopy (in CDCl_3). Comparison of the integrations of the characteristic peaks of the amide and the unreacted nitrile gave the turnover number of the reaction.

2.2.2.7 Recycling of catalyst.

After catalysis, the solvent of the resulting solution was removed by vacuum. The residue was extracted with toluene (10 mL); and after removal of the solvent under vacuum, the yellow solid obtained was washed with hexane (2 x 1 mL). It was dried in vacuum, 1000 equivalents of substrate and water were then added and the catalytic hydration reaction was repeated.

2.2.2.8 Typical procedure for reaction of the indenylruthenium hydride complex with water in dihydrogen-bonding interaction study.

Measurements of T_1 relaxation time: A sample of complex 3 (0.010 g, 0.017 mmol) was weighed into a 5mm NMR tube. The NMR tube was sealed with a rubber septum, purged and filled with nitrogen for three times before the addition of dried and

degassed deuterated toluene (0.4 mL). Relaxation time T_1 measurements on the Ru-*H* signal were carried out at 400 MHz by the inversion-recovery method using the standard 180° - τ - 90° pulse sequence. NMR measurements were carried out in the temperature range of 233K-293K at 10K intervals, the solution was allowed to equilibrate for 10 minutes before each measurement. Water (1.5 μ L, 0.083 mmol) was then added to the solution of the complex by use of a microsyringe, T_1 measurements on the Ru-*H* signal were repeated in the same temperature range.

2.3 Results and discussion

2.3.1 Catalytic hydration of acetonitriles with 3-14

In the light of the 3-catalyzed hydration of benzonitrile to give benzamide, other complexes are examined for their catalytic activities in the hydration reactions.

For comparison purposes, we have studied the activities of the complexes IndRu(dppm)Cl (4), TpRu(PPh₃)(CH₃CN)H (5), TpRu(PPh₃)(CH₃CN)Cl (6), TpRu(dppm)H (7), TpRu(dppm)Cl (8), TpRu(PPh₃)₂H (9), TpRu(PPh₃)₂Cl (10),

CpRu(dppm)H (11), CpRu(dppm)Cl (12), CpRu(PPh₃)₂H (13) and CpRu(PPh₃)₂Cl (14) in the catalytic hydration of nitriles. Taking the hydration of acetonitrile as an example, it was found that the hydride complexes were active in catalyzing the hydration of nitriles to amides; the chloro complexes were, however, found to be inactive. The results of acetonitrile hydration with the hydride complexes and their chloro analogues are shown in Table 2.1. We suggest that the presence of Ru-H...H-OH dihydrogen bonding interaction lowers the reaction barrier in the hydration of nitriles with the metal hydride complexes. The hydride ligand, by hydrogen-bonding the incoming water molecule, not only guides the course of attack of water at the co-ordinated nitrile, but also increases the nucleophilicity of the oxygen atom of water. On the other hand, in the chloro systems, the hydrogen-bonding interaction between Ru-Cl and the water molecule if present, is expected to be much weaker than that between Ru-H and H₂O in the hydride systems, therefore the water molecule is not sufficiently activated to undergo nucleophilic attack at the carbon of the nitrile. This hypothesis is supported by theoretical calculations (2.3.6).

Table 2.1 Hydration of acetonitrile with ruthenium complexes^a

Entry	Catalyst	Product	Turnover no. ^b
1	IndRu(dppm)H (3)	CH ₃ CONH ₂	865
2	IndRu(dppm)Cl (4)	CH ₃ CONH ₂	-----
3	TpRu(PPh ₃)(CH ₃ CN)H (5)	CH ₃ CONH ₂	200
4	TpRu(PPh ₃)(CH ₃ CN)Cl (6)	CH ₃ CONH ₂	-----
5	TpRu(dppm)H (7)	CH ₃ CONH ₂	19
6	TpRu(dppm)Cl (8)	CH ₃ CONH ₂	-----
7	TpRu(PPh ₃) ₂ H (9)	CH ₃ CONH ₂	26
8	TpRu(PPh ₃) ₂ Cl (10)	CH ₃ CONH ₂	-----
9	CpRu(dppm)H (11)	CH ₃ CONH ₂	25
10	CpRu(dppm)Cl (12)	CH ₃ CONH ₂	-----
11	CpRu(PPh ₃) ₂ H (13)	CH ₃ CONH ₂	38
12	CpRu(PPh ₃) ₂ Cl (14)	CH ₃ CONH ₂	-----

^aTypical reaction condition: catalyst, 0.017mmole; substrate : H₂O : catalyst = 1000 : 1000 : 1; reaction time, 72h; temperature, reflux temperature, ^bTurnover no. (TON) = mol of product/mol of catalyst.

The turnover number of **11**-catalyzed hydration of acetonitrile was found to be much lower than that of the **3**-catalyzed reaction. (Entries 1 and 9, Table 2.1) It has been suggested,[171] on the basis of kinetics and electrochemistry studies, that indenyl is more electron donating toward the metal fragment, with respect to cyclopentadienyl. The hydride of the indenyl ruthenium complex is expected to be more hydridic than the corresponding one in the analogous Cp complex, thus, hydrogen-bonding interaction between the Ru-H of complex **3** and the water molecule is stronger than that between the Ru-H of **11** and H₂O; hydrogen-bonding interaction between M-H and H₂O is by nature a hydride-proton interaction. It is therefore not surprising to find that complex **3** is more active than complex **11** in the catalytic nitrile hydration reactions.

2.3.2 Hydration of nitriles by **3** & **5**

Persual of Table 2.1 reveals that the complexes IndRu(dppm)H (**3**) & TpRu(PPh₃)(CH₃CN)H (**5**) are far more active than the other complexes in catalyzing the hydration reaction, we therefore studied in more detail their catalytic activities towards other nitriles.

The results of the 3- & 5-catalyzed hydration reactions are shown in Table 2.2. Since 4-nitrobenzotrile, 4-chlorobenzotrile and 4-methoxybenzotrile are water-insoluble solids, we therefore performed the hydration reactions of these substrates in 1-pentanol (entries 3-5, Table 2.2)

In carrying out the hydration of benzotrile in 1-pentanol (entry 2, Table 2.2), the turnover number was found to be much lower than the reaction performed in the neat substrate (entry 1, Table 2.2). It is probably due to the fact that 1-pentanol is capable of competing with Ru-H for H-bonding with H₂O. Decrease of turnover numbers in the cases of 4-nitrobenzotrile and 4-chlorobenzotrile (entries 3 & 4, Table 2.2) is probably due to the fact that the nitro group and the chloro group of the substrates can compete with Ru-H for H-bonding with H₂O. Substrates with NO₂ group or Cl group show higher rates of hydration than 4-methoxybenzotrile, these results are similar to those of Kaminskaia and Kostic[45], i.e. the rate of hydration increases with increasing electron withdrawing ability of the substituents on the nitriles. Thus, the electron withdrawing group (e.g. Cl and NO₂) increases the electrophilicity of the carbon atom of the cyano group, rendering it more susceptible to nucleophilic attack by the water molecule. On the other hand, the electron donating group (e.g. OMe) decreases the electrophilicity of the carbon atom of the cyano group

and thus making it less available for nucleophilic attack.

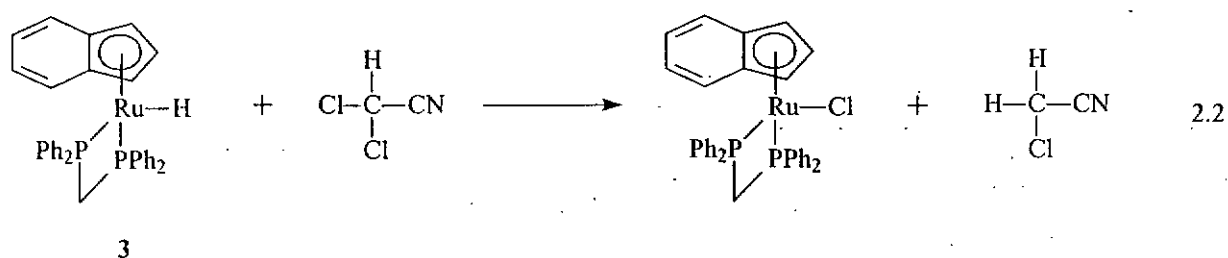
Table 2.2 Catalytic hydration of aromatic nitriles with 3 & 5^a

Entry	Substrate	Product	Turnover no. ^b	
			IndRu(dppm)H (3)	TpRu(PPh ₃)(CH ₃ CN)H (5)
1 ^c	C ₆ H ₅ CN	C ₆ H ₅ CONH ₂	800	190
2 ^d	C ₆ H ₅ CN	C ₆ H ₅ CONH ₂	300	90
3 ^d	4-NO ₂ -C ₆ H ₄ CN	4-NO ₂ -C ₆ H ₄ CONH ₂	210	80
4 ^d	4-Cl-C ₆ H ₄ -CN	4-Cl-C ₆ H ₄ -CONH ₂	110	40
5 ^d	4-CH ₃ O-C ₆ H ₄ -CN	4-CH ₃ O-C ₆ H ₄ -CONH ₂	40	20

^aTypical reaction condition: catalyst, 0.017mmole; substrate : H₂O : catalyst = 1000 : 1000 : 1; reaction time, 72h; temperature, 120°C, ^bTurnover no. (TON) = mol of product/mol of catalyst. ^cin neat substrate. ^dsolvent, 1-pentanol(2mL)

In some of the aliphatic nitriles (entries 2-4, Table 2.3), the hydration reactions did not seem to proceed; no amide was obtained, but side reactions between the complex and the substrate occurred. The reaction of 3 with 10 equivalents each of

dichloroacetonitrile and water in THF- d_8 at 80°C produced no hydration product. ^1H and $^{31}\text{P}\{^1\text{H}\}$ NMR spectroscopic studies confirmed that the hydride complex **3** was converted to the chloro complex $\text{IndRu}(\text{dppm})\text{Cl}$, which is inactive in catalytic nitriles hydration (eq 2.2).



Moreover, in carrying out the hydration of iodoacetonitrile (ICH_2CN) and malononitrile (CNCH_2CN) with **3** and **5**, no hydration product was observed. It is envisaged that ICH_2CN is decomposed under high temperature and the hydrogen atom of CNCH_2CN is so protonic, that it could protonate the hydride of **3** and **5**, and therefore the reaction failed.

Table 2.3 Catalytic hydration of aliphatic nitriles with 3 & 5^a

Entry	Substrate	Product	Turnover no. ^b	
			IndRu(dppm)H (3)	TpRu(PPh ₃)(CH ₃ CN)H (5)
1	CH ₃ CN	CH ₃ CONH ₂	865	200
2	ICH ₂ CN	----	----	----
3	CNCH ₂ CN	----	----	----
4	Cl ₂ CHCN	----	----	----

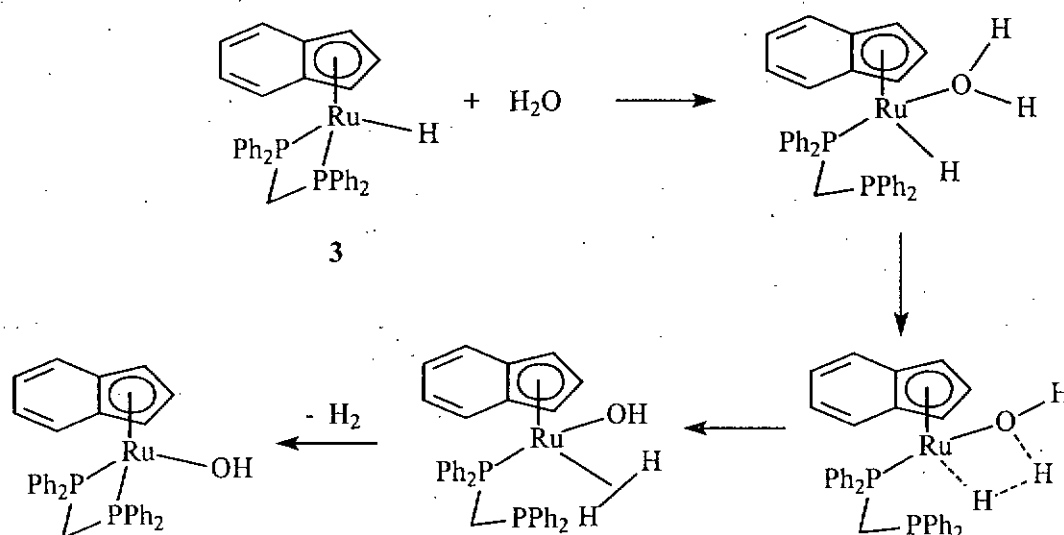
^aTypical reaction condition: catalyst, 0.017mmole; substrate : H₂O : catalyst = 1000 : 1000 : 1; reaction time, 72h; temperature, reflux temperature, ^bTurnover no. (TON) = mol of product/mol of catalyst.

Acetonitrile gives the highest yield among all the nitriles tested. It is believed that electronic factor is just one of the factors affecting the hydration reaction. The steric factor may also play a role in the hydration reactions. As the aromatic nitriles are more bulky than the aliphatic one, they coordinate to the metal center less readily and therefore their hydration reactions are less facile.

2.3.3 Possible mechanism for hydration of nitriles catalyzed by **3**

The complex IndRu(dppm)H (**3**) was found to be the most active complex in catalyzing the hydration of acetonitrile to the amide (entry 1, Table 2.1). The chloro analogue IndRu(dppm)Cl (**4**) was, however found to be inactive (entry 2, Table 2.1). Complexes **3** and **4** can provide the vacant site for the nitrile coordination by $\eta^5 \rightarrow \eta^3$ ring slippage, which is a well-known phenomenon for η^5 -indenyl transition-metal complexes,[108, 172, 173] or by unarming of the dppm ligand. If the crucial step of the hydration reaction is nucleophilic attack at the carbon atom of the bound nitrile to form the C–O bond, complex **4**, which contains a more electronegative chloro group would render the carbon of the bound nitrile more susceptible to nucleophilic attack, and therefore it is expected that **4** would be more active than **3** for the catalytic processes. One may argue that **3** but not **4** could react with water to form the hydroxo complex $(\eta^5\text{-C}_9\text{H}_7)\text{Ru}(\text{dppm})(\text{OH})$, which is the real active species.(Scheme 2.1) Previous theoretical calculations and experimental work have indicated that σ -bond metathesis reaction of water with a metal hydride to give metal hydroxo should be feasible.[174-176] This hypothesis, however, seems unlikely in our case, since in each of the catalytic reactions with **3** in Table 2.2 & 2.3, the complex was recovered unchanged after the catalysis. We also monitored the reaction of **3** with 10 equivalents

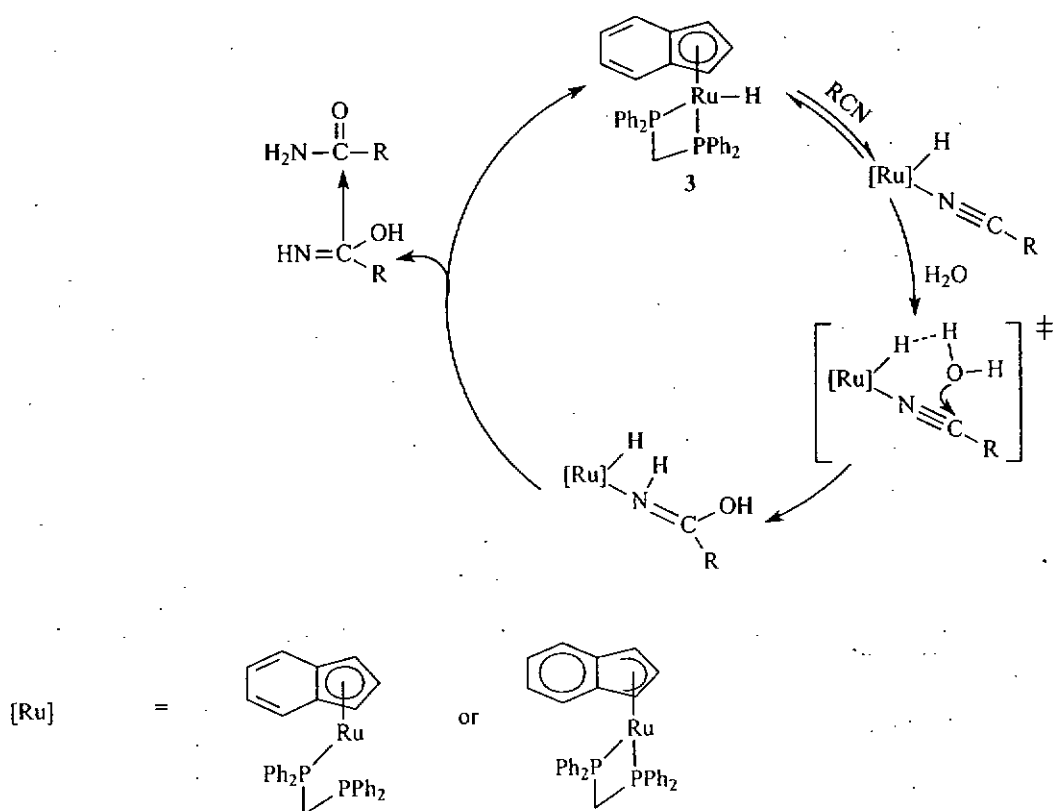
each of acetonitrile and water in THF- d_8 at 80°C by ^1H and $^{31}\text{P}\{^1\text{H}\}$ NMR spectroscopies at 4 and 8 h intervals for a period of 48 h, it was observed that while the nitrile was gradually converted to amide, complex **3** remained unchanged throughout the experiment. Furthermore, it was learned that after heating at 80°C a THF- d_8 solution of **3** containing 20 equivalents of H_2O for 4 days, ^1H and $^{31}\text{P}\{^1\text{H}\}$ NMR spectroscopies showed no sign of any new complex; **3** remained intact.



Scheme 2.1

Despite the fact that the hydride complex **3** is active while the choro analogue **4** is inactive in the catalytic nitrile hydration reactions, we still believe that during the catalysis with the former, nucleophilic attack at the carbon atom of the bound nitrile by H_2O is a crucial step of the process. A proposed reaction mechanism to account for

the effectiveness and ineffectiveness of **3** and **4**, respectively, is depicted in **Scheme 2.2**. We suggest that the **3**-catalyzed nitrile hydration reaction is a dihydrogen bond-promoted reaction, the dihydrogen-bonding interaction between the hydride ligand and the incoming water molecule might be crucial in lowering the activation energy of the C–O formation step of the hydration reaction. That the chloro complex **4** is not active is probably attributable to the fact that the chloro ligand is not as capable as the hydride ligand of **3** in playing an active role.



Scheme 2.2 Proposed mechanism of 3-catalyzed Hydration of Nitriles

2.3.4 Reaction of IndRu(dppm)H (3) with H₂O

As shown in Scheme 2.2, dihydrogen-bonding interaction between the hydride of complex 3 and H₂O is proposed to be important. We try to verify the existence of the dihydrogen-bonding interaction between the hydride of complex 3 and H₂O by comparing the T_1 relaxation time of the hydride ligand in the absence and in the presence of H₂O. Only slight decrease of the longitudinal relaxation time T_1 (min) of the hydride signal was observed when complex 3 and H₂O were mixed in toluene-*d*₈. After the addition of 5 equiv of H₂O, the T_1 (min) dropped from 929 ms(240K) to 909 ms(238 K). It seems to indicate that only weak dihydrogen-bonding interaction exists between the hydride of 3 and H₂O in the ground state. (vide infra)

2.3.5 H/D exchange between IndRu(dppm)H (3) and D₂O

In addition to the T_1 (min) measurements, we also investigate the interaction between 3 and water, by studying the reaction of 3 with D₂O. Table 2.4 shows that H/D exchange occurs between the Ru-H of 3 and D₂O.

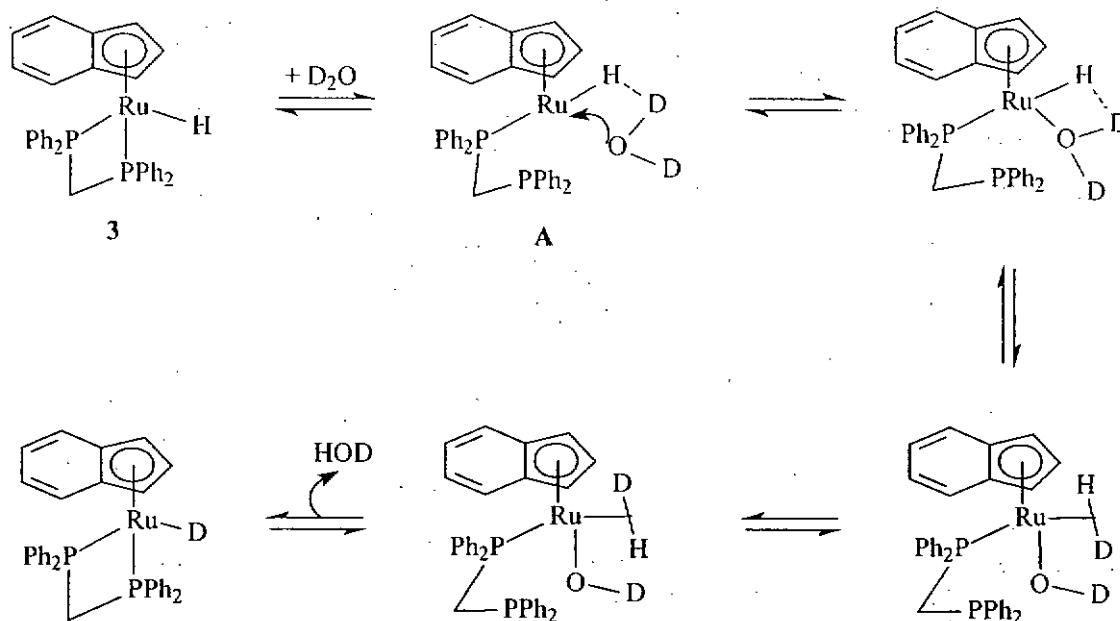
Table 2.4 H/D exchange between Ru-H & D₂O^a

Time	D ₂ O	Percentage of deuteration of Ru-H ^b
6 h	20 μL	9 %
12 h		16 %
24 h		30 %
48 h		45 %
72 h		66 %
96 h		67 %

^aReaction condition : 0.017mmol of 3 in 0.4 mL THF-*d*₈; reaction temperature: 120°C. ^bdetermined by

¹H NMR spectroscopy using H² of indenyl ligand as internal reference.

It was found that H/D exchange of Ru-H of 3 with D₂O occurred at 120°C. The H/D exchange probably proceeds via the sequence depicted in Scheme 2.3. Basically, it is the protonation of the Ru-H by the coordinated D₂O molecule. The acidity of the D₂O increases upon coordination to the Ru metal center and thus making it more capable of deuterating the Ru-H via the formation of η²-HD intermediate. Protonation of M-H by a coordinated H₂O to form a dihydrogen hydroxo species is a well-conceived process.[174, 175, 177]

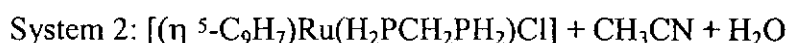
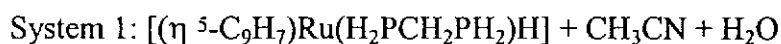


Scheme 2.3 Proposed mechanism of H/D exchange of the hydride of **3 with D_2O**

The invariance of the T_1 (min) of the hydride signal of **3** in the presence of water can be rationalized in terms of the notion that the equilibrium in Scheme 2.3 are fast so that the hydride ligand exchange with the water molecule very rapidly, and the dihydrogen-bonded species $[Ru]-H \cdots H-OH$ (the undeuterated form of **A**) is a very transient species.

2.3.6 Theoretical study

In-situ high pressure NMR spectroscopic studies did not enable us to gain information on the possible intermediates of the **3**-catalyzed hydration of acetonitrile because the only observable organometallic species throughout the catalysis was **3** itself. To study the feasibility of the proposed reaction mechanism, theoretical calculations at the B3LYP level of density function theory to study a more detailed catalytic pathway were carried out, the following two model systems have been calculated: System 1 is the model for the **3**-catalyzed acetonitrile hydration, and system 2 is that for the **4**-catalyzed reaction.



The calculations indicate that in the catalytic process the dissociation of one arm of the bidentate ligand from the metal center followed by the coordination of CH₃CN is the initial event. The dppm unarming requires only 15.2 kcal/mol. Figure 2.1 shows the possible reaction pathways together with the calculated free energies (kcal/mol, in parentheses) for species involved in the reactions. Figure 2.3 gives the optimized structures for species involved in the reaction paths shown in Figure 2.1.

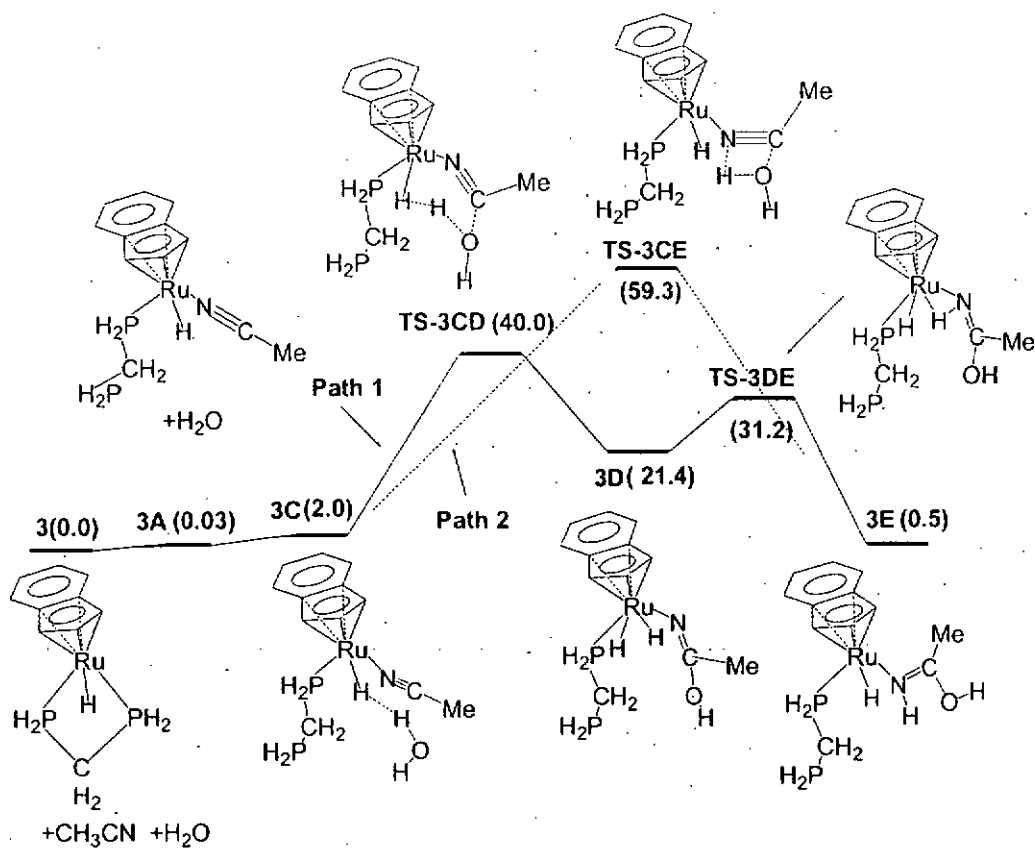


Figure 2.1 Schematic illustration of the mechanism for Complex 3 together with calculated free energies (kcal/mol) for species involved in the reactions

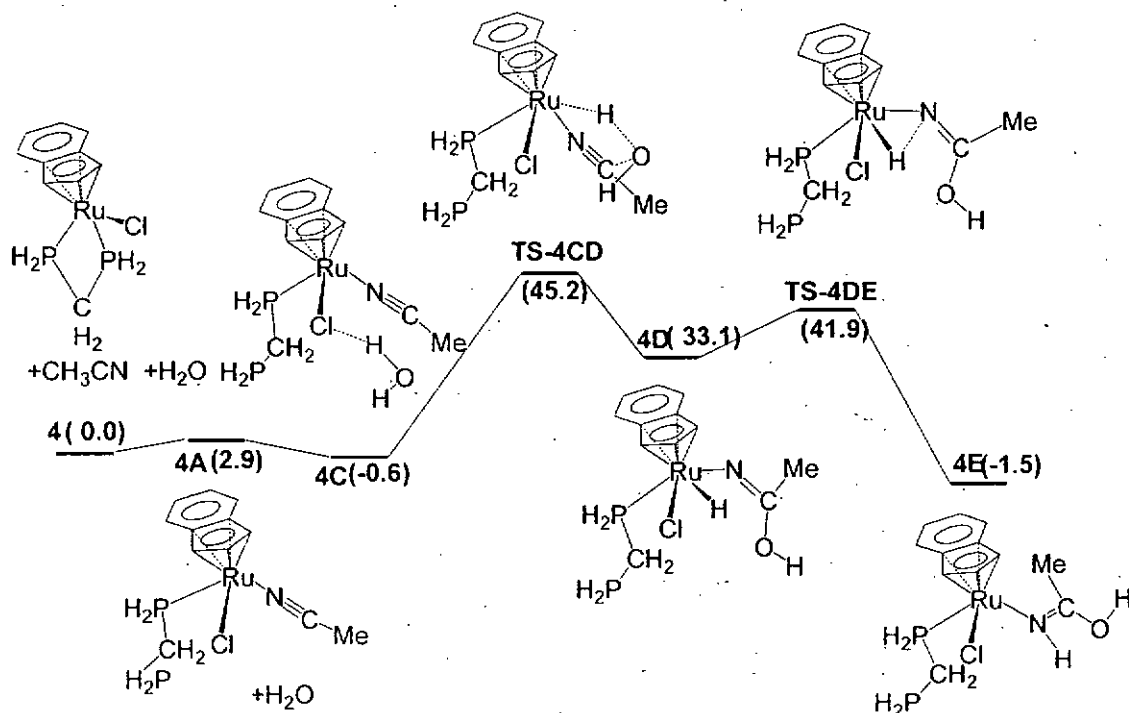


Figure 2.2. Schematic illustration of the mechanism for Complex 4 together with calculated free energies (kcal/mol) for species involved in the reactions

The acetonitrile-coordinated species **3C** is weakly dihydrogen-bonded to a water molecule, having an H---H distance of 2.123 Å, and in equilibrium with the hydride complex **3**. From **3C**, the concerted process (path 2 of Figure 2.1) has a substantially higher barrier than the stepwise pathway (path 1). For the stepwise pathway (path 1), the reaction overcomes a barrier of 38.0 kcal/mol through **TS-3CD**, which is the rate-determining step, forming a four-legged piano-stool *cis* dihydride intermediate **3D**. After the rate-determining barrier is surmounted, the reaction proceeds easily by having a proton transfer to form complex **3E**. The dissociation of the hydroxo imine (HN=C(OH)Me) requires only 11.6 kcal/mol, making the catalytic circle feasible.

Supporting the hypothesis discussed above, the calculations show that dihydrogen-bonding interaction exists from **3C** to the transition state **TS-3CD** in the rate-determining step. The selected structural parameters shown in Figure 2.3 indicate the strong H(water)---H(hydride) (1.071 Å) interaction in the transition state. The dihydrogen-bonding interaction makes **TS-3CD** an early transition state and lowers the reaction barrier. In contrast, the corresponding transition state **TS-4CD** for the chloro system (Figures 2.2 & 2.4) does not contain this type of interaction (H(water)---Cl: 2.582Å) and is a late transition state having a structure closer to the

four-legged piano-stool hydride intermediate **4D**. Therefore, for the chloro system the rate-determining step leading to the formation of a chloro-hydride intermediate has a much higher reaction barrier of 45.8 kcal/mol (Figure 2.2).

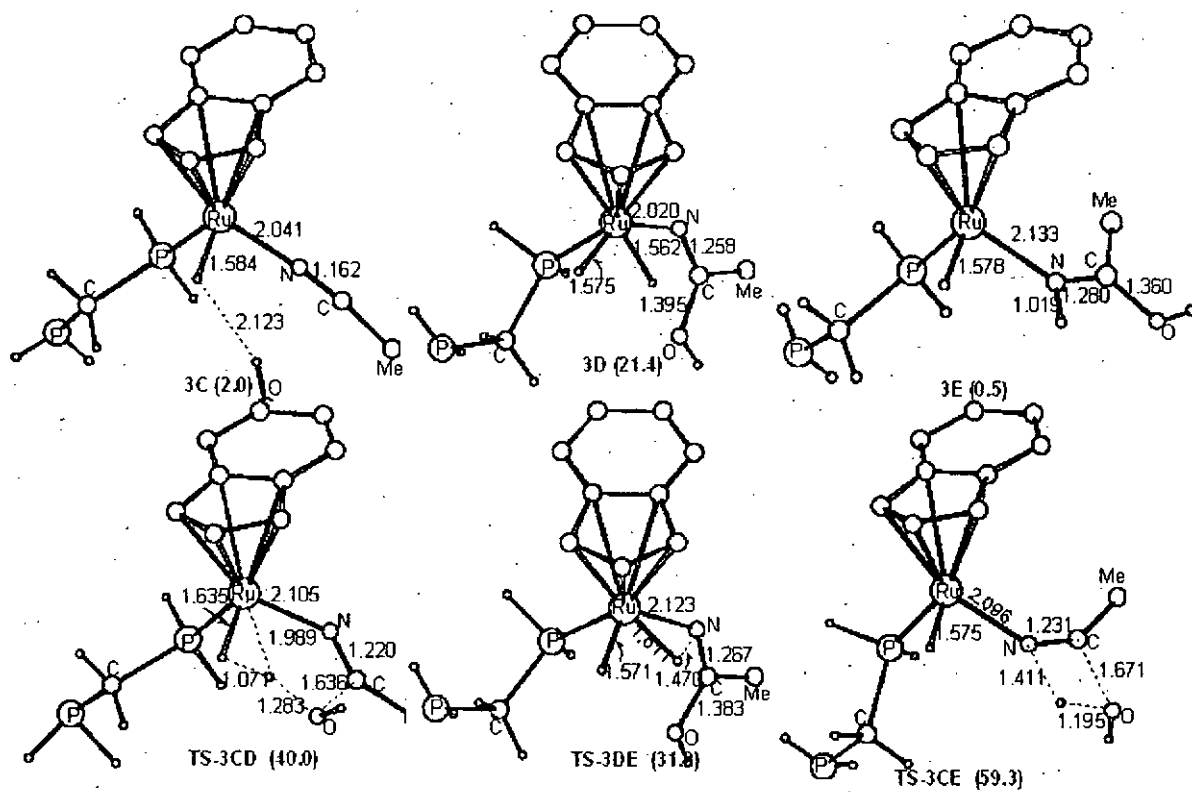


Figure 2.3. B3LYP optimized structures for those species shown in Figure 2.1. The free relative energies (kcal/mol) shown in parentheses take $3 + \text{MeCN} + \text{H}_2\text{O}$ as the reference. For the purpose of clarity, hydrogen atoms on the indenyl ligand and the methyl group of MeCN are omitted.

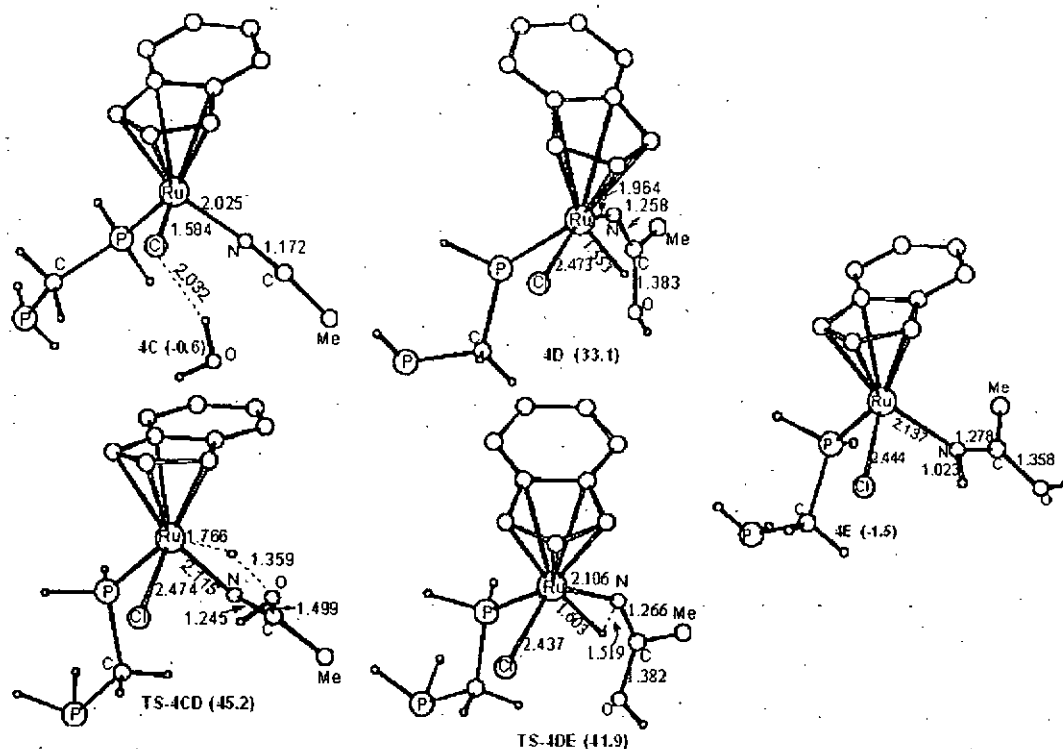


Figure 2.4. B3LYP optimized structures for those species shown in Figure 2.2. The free relative energies (kcal/mol) shown in parentheses take $4 + \text{MeCN} + \text{H}_2\text{O}$ as the reference. For the purpose of clarity, hydrogen atoms on the indenyl ligand and the methyl group of MeCN are omitted.

The possibility of having a hydration process that involves the ring slippage of the indenyl ligand was also investigated. Figure 2.5 gives the structural details for the intermediates and transition states together with their relative free energies in the corresponding hydration process involving the ring slippage of the indenyl ligand.

The results of calculations show that the energies of all the

intermediates/transition-states based on the ring-slipped structures are higher than the corresponding species shown in Figure 2.1 by more than 10 kcal/mol. Clearly, the ring slippage is much less favorable in comparison to the dppm unarming in the hydration process. Interestingly, all the ring-slipped structures calculated are η^1 -type instead of η^3 -type. This result is understandable in view of the fact that many 16-electron, five-coordinate Ru-complexes are stable, particularly when there is a strong trans-influencing ligand present.[178, 179] The dihydrogen-bonded species **3C'** and the hydroxo imine complex **3E'** (Figure 2.5) can be described as having square-pyramidal structures with a hydride ligand occupying the axial position. The dihydride intermediate **3D'** (Figure 2.5) is a capped square-pyramidal structure. First-order Jahn-Teller Distortion is always expected for 16-electron, six-coordinate complexes that are diamagnetic.[180-183] Therefore, **3D'** does not adopt an octahedral structure.

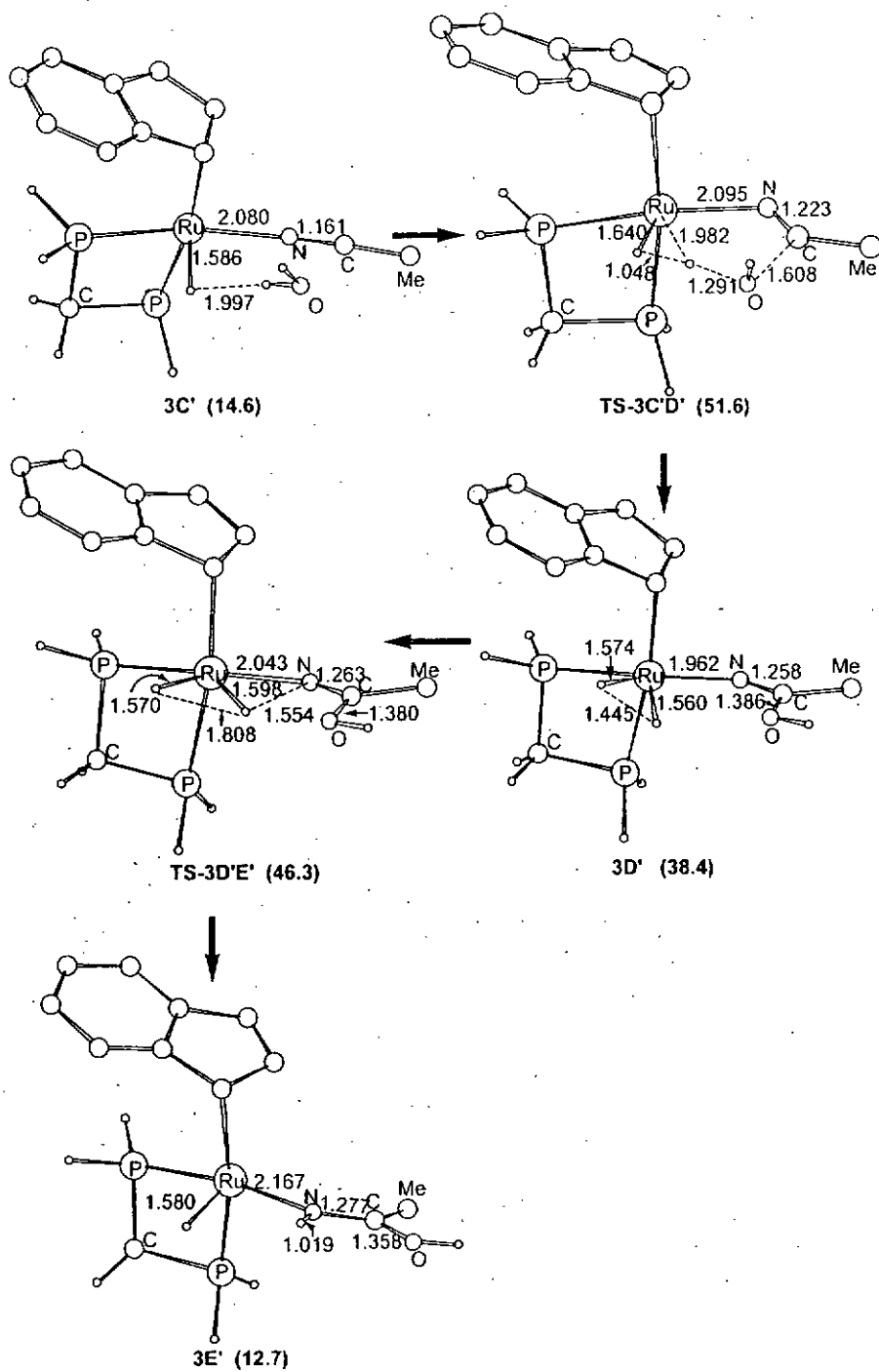


Figure 2.5. B3LYP optimized structures of intermediates and transition states for a hydration process that involves the ring slippage of the indenyl ligand. The free relative energies (kcal/mol) shown in parentheses take $3 + \text{MeCN} + \text{H}_2\text{O}$ as the reference. For the purpose of clarity, hydrogen atoms on the indenyl ligand and the methyl group of MeCN are omitted.

Therefore, instead of the ring slippage commonly observed in chemical reactions involving η^5 -indenyl systems,[108, 172, 173] our Ru indenyl hydride complex catalyzed-hydration reaction is initiated by dppm unarming. This is not too surprising because ligand dissociation in other indenyl complexes has also been found as the initial event for chemical reactions.[171]

2.3.7 Recycling of catalyst

The activity of the recycled catalyst **3** was studied. It was found that the catalyst remained active after it was recovered from the hydration reactions of benzonitrile and acetonitrile, although the turnover numbers were lower (Table 2.5). This decrease of turnover number of the recycled-**3** was probably due to partial loss of the catalyst in the course of recycling, and to its partial decomposition due to prolonged heating at relatively high temperatures.

Table 2.5 Hydration of nitriles with **3** and recycled catalyst **3**^a

Entry	Complex	Substrate	Product	Turnover no. ^b
1	IndRu(dppm)H	CH ₃ CN	CH ₃ CONH ₂	865
2 ^c	IndRu(dppm)H	CH ₃ CN	CH ₃ CONH ₂	302
3	IndRu(dppm)H	C ₆ H ₅ CN	C ₆ H ₅ CONH ₂	800
4 ^c	IndRu(dppm)H	C ₆ H ₅ CN	C ₆ H ₅ CONH ₂	655

^aTypical reaction condition: catalyst, 0.017mmole; substrate : H₂O : catalyst = 1000 : 1000 : 1; reaction time, 72h; temperature, reflux temperature, ^bTurnover no. (TON) = mol of product/mol of catalyst. ^cThe recycled run.

2.3.8 Effects of amide on rate of hydration

Tyler *et al.* showed that addition of acetamide decreased the rate of nitriles hydration with [Cp'₂Mo(μ-OH)₂MoCp'₂]²⁺ (Cp' = η⁵-CH₃C₅H₄). We have also learned that addition of acetamide exhibits detrimental effect on the **3**-catalyzed hydration of acetonitrile (Table 2.6). Apparently, the added acetamide molecules compete for the vacant site with the acetonitrile molecule. Thus, the **3**-catalyzed nitrile hydration reaction is a product-inhibited catalytic reaction.

Table 2.6 Hydration of acetonitrile with/without added acetamide^a

Entry	Substrate	Product	Turnover no. ^b
1	CH ₃ CN	CH ₃ CONH ₂	865
2	CH ₃ CN + CH ₃ CONH ₂	CH ₃ CONH ₂	412

^aTypical reaction condition: catalyst, 0.017mmole; substrate : H₂O : catalyst = 1000 : 1000 : 1; mole ratio of acetamide : catalyst = 500 : 1. reaction time, 72h; temperature, reflux temperature, ^bTurnover no. (TON) = mol of product/mol of catalyst.

2.3.9 Effect of diphosphine ligands on the rates of the hydration reactions

The dppe and dppp analogues of **3**, IndRu(dppe)H (**15**) and IndRu(dppp)H (**16**), respectively are also active in catalyzing nitrile hydration reactions. However, they are found to be less active than **3**.(Table 2.7)

Table 2.7 Hydration of acetonitrile with complexes containing different diphosphines^a

Entry	Complex	Substrate	Product	Turnover no. ^b
1	IndRu(dppm)H (3)	CH ₃ CN	CH ₃ CONH ₂	865
2	IndRu(dppe)H (15)	CH ₃ CN	CH ₃ CONH ₂	443
3	IndRu(dppp)H (16)	CH ₃ CN	CH ₃ CONH ₂	679

^aTypical reaction condition: catalyst, 0.0017mmole; substrate : H₂O : catalyst = 1000 : 1000 : 1; reaction time, 72h; temperature, reflux temperature , ^bTurnover no. (TON) = mol of product/mol of catalyst.

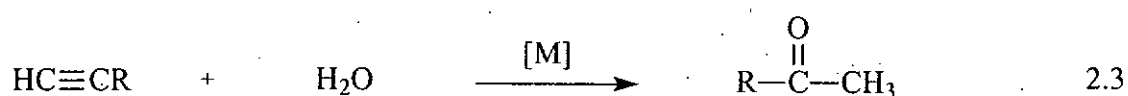
It is postulated that the dppm ligand has larger angle strain than the dppp and dppe, it undergoes arm-off to provide a vacant site for the nitrile more readily and is therefore more active than 15 and 16 in catalyzing the hydration of nitriles.

2.3.10 Reactivity of IndRu(dppm)H (3) towards terminal alkyne hydration

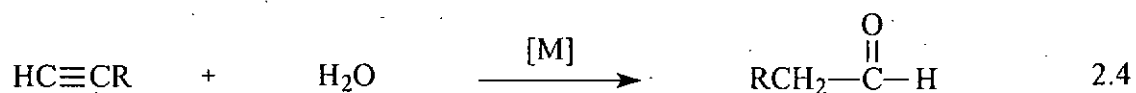
Hydration of alkynes catalyzed by metal complexes represents a convenient method for the preparation of carbonyl compounds. The reaction proceeds by addition of water to the metal π -alkyne complex, according to Markovnikov's rule, to form the corresponding ketone compound.[184] (eq. 2.3) In contrast, the hydration of terminal

alkynes can be regioselectively oriented to the formation of aldehydes in an anti-Markovnikov manner.(eq. 2.4) However, examples of hydration of alkynes which follow *anti*-Markovnikov's rule to furnish aldehydes are rare.

Markovnikov's addition

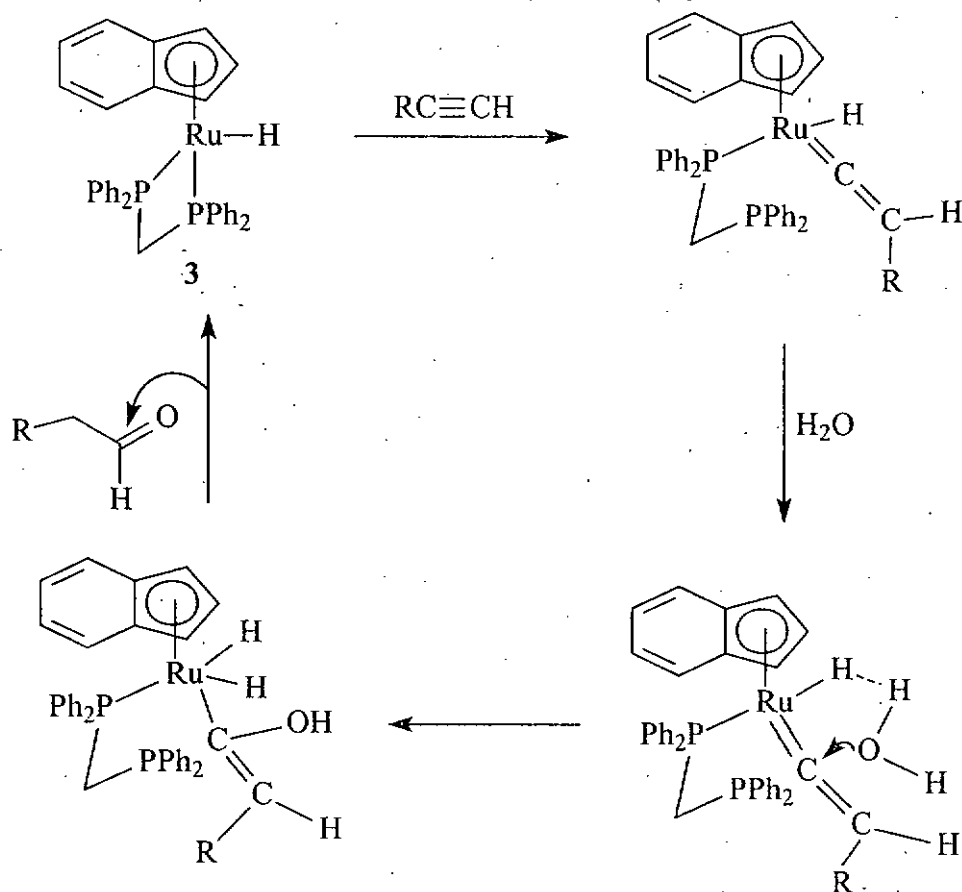


Anti-Markovnikov's addition



We are interested, in addition to nitrile hydration, in studying the activity of **3** in hydration reactions of terminal alkynes. The coordination of alkynes into the metal center is the initial event for the hydration of alkynes. After the coordination of alkynes, the reaction could proceed either via the formation of vinylidene complex or the insertion of alkynes into Ru-H. We hope that the formation of vinylidene complex could be faster than that of insertion of alkynes into Ru-H with our complex. Nucleophilic attack of the water molecule at the α -carbon atom of the vinylidene ligand then follows. The hydride ligand can H-bond the incoming water molecule and

the H-bond mediated hydration might therefore proceed via the mechanism depicted in Scheme 2.4.

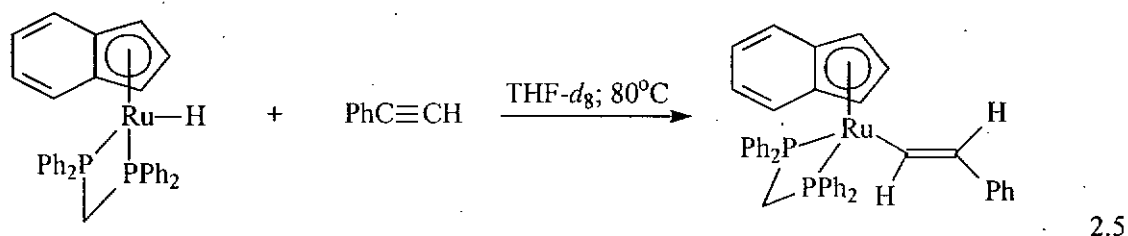


Scheme 2.4 3-catalyzed hydration of terminal alkynes

The reaction of complex **3** with 50 equivalents each of phenylacetylene and water, however, did not give hydration product but the color of the solution was changed. We then monitored the reaction of **3** with 10 equivalents each of phenylacetylene and water in THF-*d*₈ at 80°C by ¹H and ³¹P{¹H} NMR

spectroscopies at 2 and 4 h intervals for a period of 48 h; it was observed that the signals of phenylacetylene gradually decreased, the intensity of the hydride signal of complex **3** also diminished and finally disappeared. Furthermore, the complex shows the typical alkenyl resonances at δ 5.4 (d, 1H, $J(\text{HH}) = 17.1$ Hz, $\text{HC}=\text{CHPh}$) and δ 7.6 (dt, 1H, $J(\text{HH}) = 17.1$ Hz, $^3J(\text{PH}) = 5.3$ Hz, $\text{HC}=\text{CHPh}$) in the ^1H NMR spectrum. In the $^{31}\text{P}\{^1\text{H}\}$ NMR spectrum, a new singlet peak at δ 22.9 also observed. This is probably the result of insertion of the phenylacetylene into the Ru-H bond.(eq 2.5)

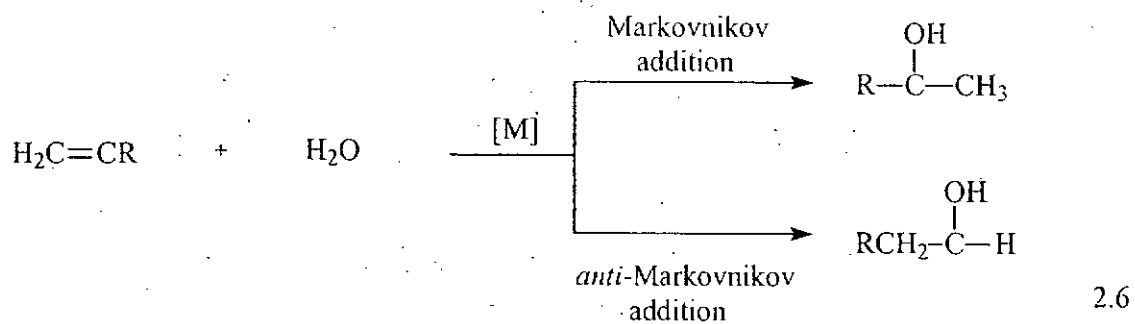
The resulting vinyl complex was inert to the water present. Apparently, the reaction of **3** with phenylacetylene did not proceed as what we expected.



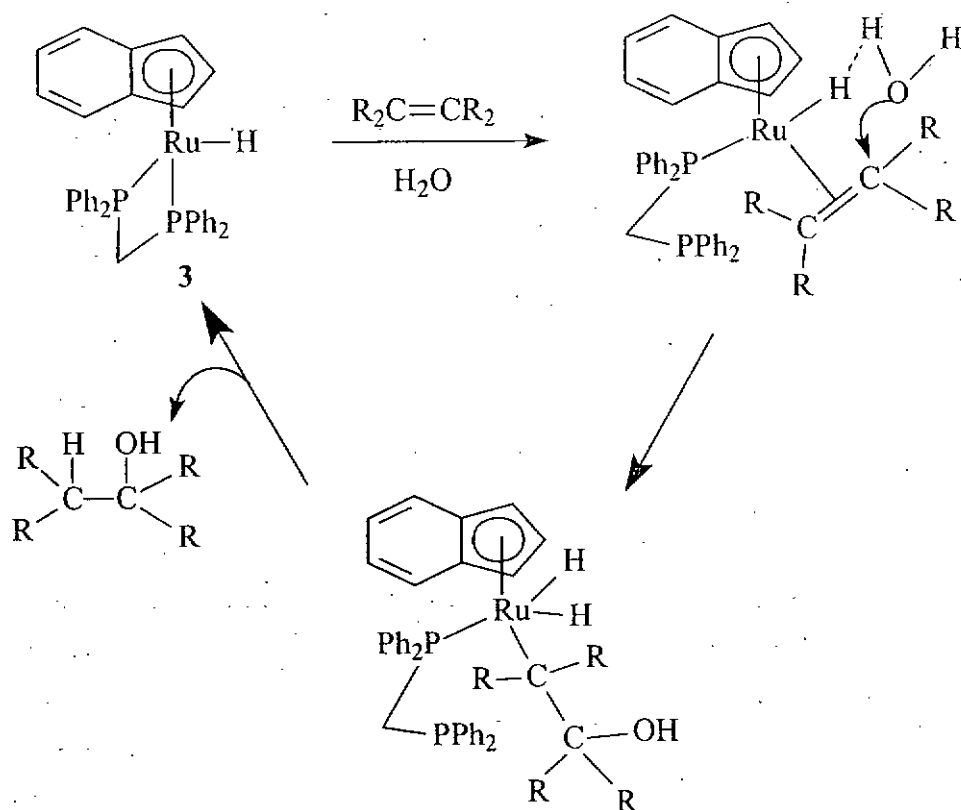
2.3.11 Reactivity of IndRu(dppm)H (**3**) towards alkene hydration

The addition of H_2O to a carbon-carbon double bond is a potentially useful route for the synthesis of alcohols from alkenes.(eq. 2.6) But very few metal complexes are known to catalyze this reaction.[185-187] The paucity of successful

alkene hydration with transition-metal complexes originated from the nature of coordination of the alkene to the metal center. If the alkene is strongly bound to the metal, the carbon-carbon double bond would be too nucleophilic due to abundant back-donation from the metal, for attack by the water molecule. On the other hand, although curtailed $d \rightarrow \pi^*$ back-donation would render the carbon-carbon more electrophilic and therefore more susceptible to nucleophilic attack by the water molecule, the alkene, which is now only weakly bound to the metal center, is very vulnerable to ligand substitution by the water. Commercially, catalysts for this transformation include phosphoric acid, transition metal oxides, zeolites, and clays. These catalysts require moderate to high operating temperatures and pressures. They are of limited use because addition of water obeys Markovnikov's rule and primary alcohols, which are used widely in surfactants, plasticizers, and detergent precursors, are not obtained. Although *anti*-Markovnikov hydration can be effected by stoichiometric reactions, such as hydroboration, catalytic processes for this transformation are lacking.



We hope that the insertion of alkenes into the Ru-H of **3** is slower than the nucleophilic attack of water molecule to coordinated alkenes. If so, the hydride ligand of complex **3** could H-bond the incoming water molecule and increases the nucleophilicity of the oxygen atom of water, thus, the hydration reaction might proceed more readily. The H-bond mediated hydration might proceed via the proposed mechanism depicted in Scheme 2.5.



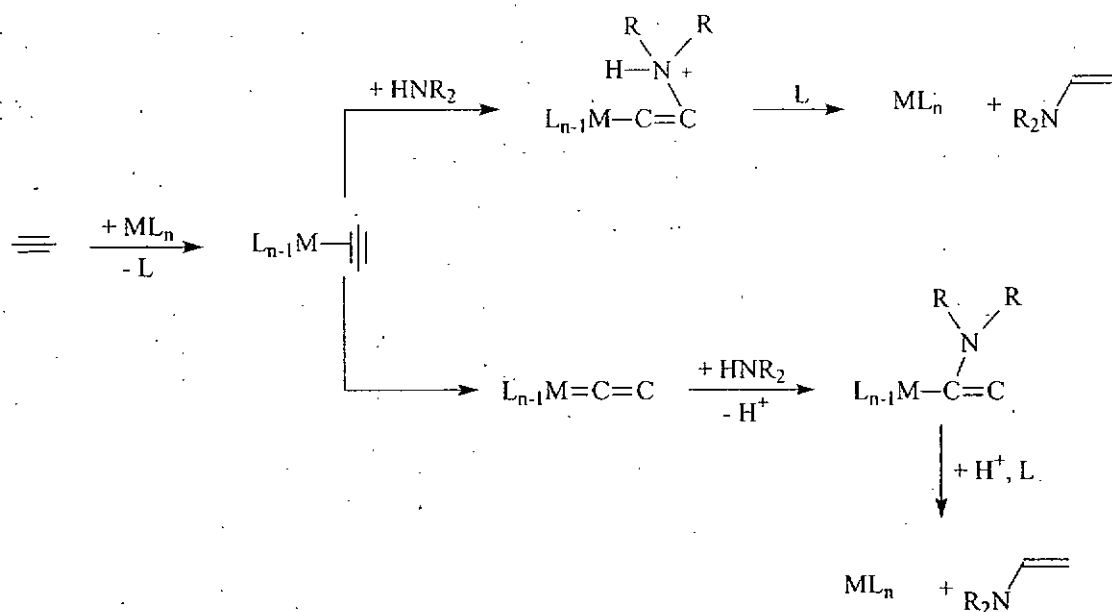
Scheme 2.5 3-catalyzed hydration of alkenes

Reaction of complex **3** with 50 equivalents each of methyl acrylate and water, however, did not give the hydration product. We tried to monitor the reaction of **3** with 10 equivalents each of methyl acrylate and H₂O in THF-*d*₈ at 80°C by ¹H and ³¹P{¹H} NMR spectroscopies at 2 and 4 h intervals for a period of 48 h; it was observed that complex **3** was unchanged and no methyl acrylate-bonded complex was observed. Therefore, we conclude that the alkene did not coordinate to the metal center and the reaction was not initiated. We did not proceed with the hydration reactions of the non-activated alkenes because we are of the opinion that these

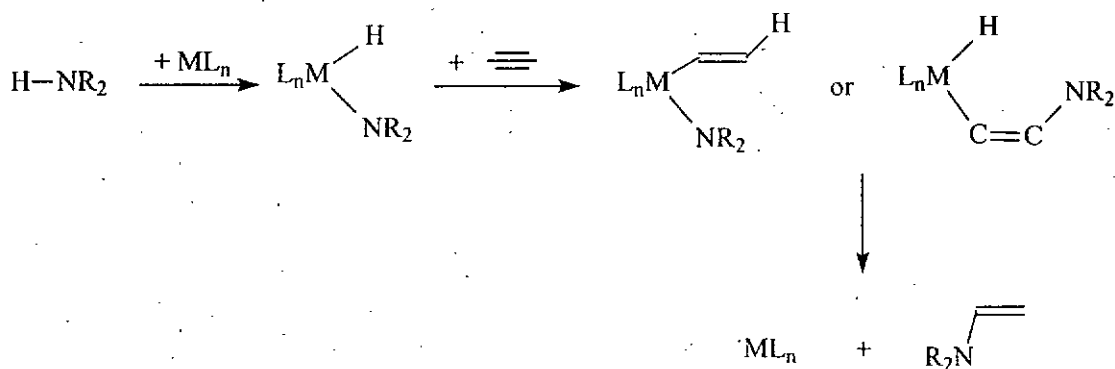
reactions would probably be non-productive in view of the failure of the hydration reaction with methyl acrylate, which is an activated alkene.

2.3.12 Reactivity of IndRu(dppm)H (3) towards hydroamination of phenylacetylene with aniline

Hydroamination of alkynes is one of the most efficient approaches for the synthesis of imines.[188-190] Although the condensation between carbonyl compounds and primary amines is a well-established standard method for synthesizing imines.[191] Imines are versatile building blocks for organic synthesis, as they are used to prepare substituted amines and can function as masked carbonyl substituents. Hydroamination of alkynes has attracted intense interest as an environmentally benign alternative route for it, 100% atom efficiency.[189, 190, 192-197] Two common mechanisms have been proposed for the hydroamination of alkynes, coordination of alkynes followed by the nucleophilic attack of amine molecule (Scheme 2.6) and oxidative addition of amine molecule to the metal center followed by the insertion of alkynes.(Scheme 2.7)



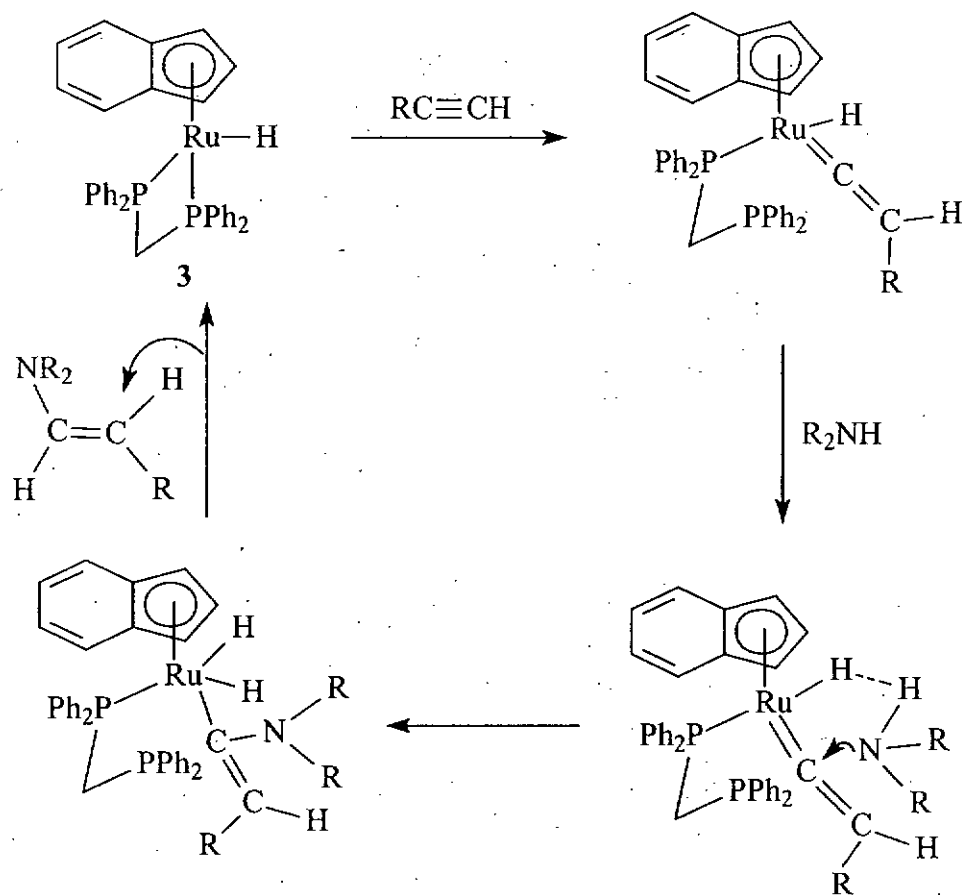
Scheme 2.6



Scheme 2.7

We hope that upon coordination of the alkyne to the metal center of **3**, tautomerization to yield the vinylidene complex is more facile than the insertion of the alkyne ligand into Ru-H to give the metal vinyl.(Scheme 2.8) The hydride ligand of **3** can H-bond the hydrogen atom of the amine molecule, enhancing the nucleophilicity of nitrogen atom of amine, making the nucleophilic attack of amine

molecule to the vinylidene more facile.



Scheme 2.8 3-catalyzed hydroamination of alkynes

Unfortunately, the reaction of complex 3 with 50 equivalents each of phenylacetylene and aniline did not give the corresponding imine. The failure of the reaction is again due to the insertion of phenylacetylene in the Ru-H bond to give the metal vinyl which is inert to the amine.

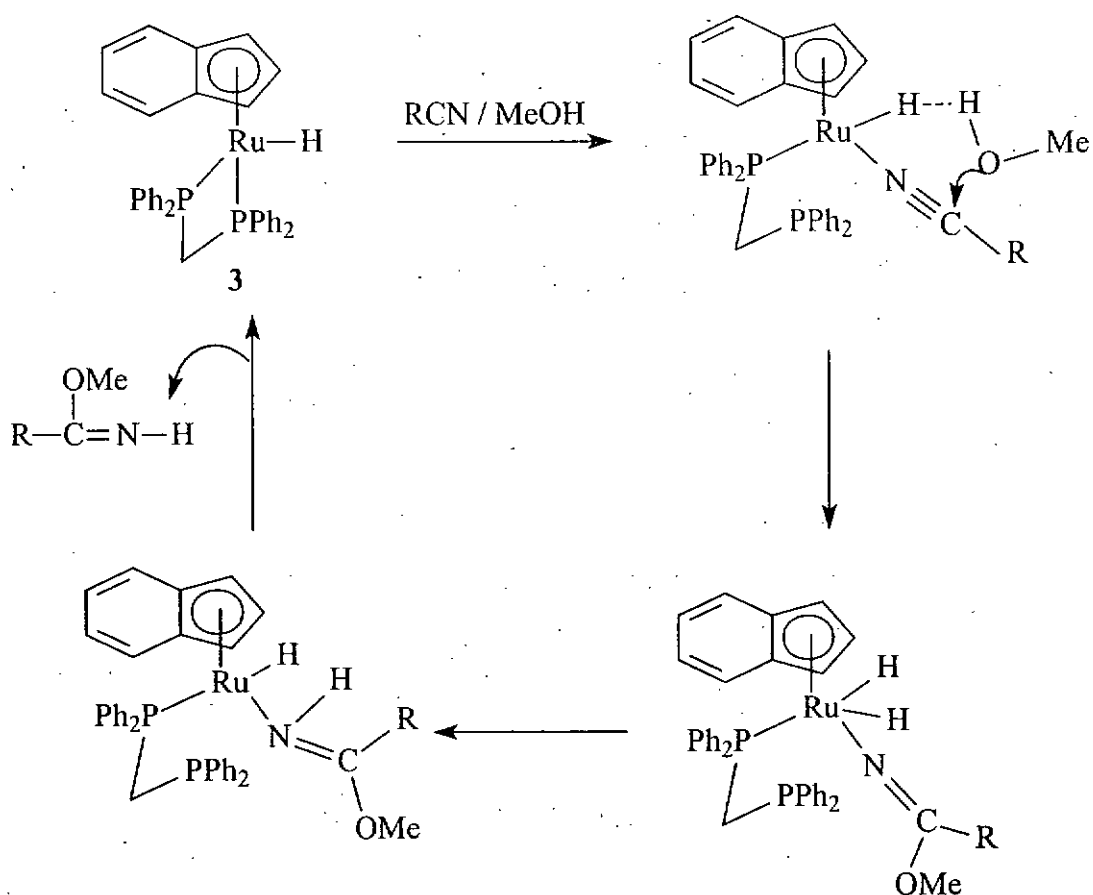
2.3.13 Reactivity of IndRu(dppm)H (3) towards alcoholysis of nitriles

In addition to the hydration of nitriles with complex 3, addition of other protic nucleophiles such as alcohol to metal-bound nitriles was attempted. (eq. 2.7)



2.7

Similar to the hydration of nitriles, the hydride ligand of complex 3 should be able to H-bond the methanol. (Scheme 2.9) The hydrogen-bonding interaction between the Ru-H of 3 and the hydrogen atom of methanol not only guides the course of nucleophilic attack of methanol on the coordinated nitrile, but also increases the nucleophilicity of the oxygen atom of methanol.



Scheme 2.9 3-catalyzed alcoholysis of nitriles

However, refluxing **3** in 50 equivalents each of MeOH and nitriles did not afford any imino ether. As metal-imino-ether (NH=C(OR')R) has a higher coordination power than the corresponding nitrile, the formation of the imino-ether ruthenium complex might impede the coordination of nitrile.[52] We then monitored the reaction of **3** with 10 equivalents each of MeOH and H₂O in THF-*d*₈ at 80°C by ¹H and ³¹P{¹H} NMR spectroscopies at 2 and 4 h intervals for a period of 48 h; it was, however, observed that the complex **3** remained unchanged and no metal-imino-ether

was formed. In this case, the hydrogen atom in MeOH may be not protonic enough to form dihydrogen bond with the metal hydride and thus the nucleophilicity of oxygen atom is not enhanced and the reaction did not proceed. Furthermore, the bulkiness of MeOH (relative to H₂O) might have prohibitive effect on the addition reaction.

Chapter 3 Syntheses and Characterization of Aminoindenyl Ruthenium Complexes and Comparison of Their Reactivities Toward Some Reactions with those of Aminocyclopentadienyl Ruthenium Complexes.

3.1 Introduction

Cyclopentadienyl is one of the most widely used classes of ligands in organometallic chemistry and homogeneous catalysis[198]. One attractive feature of the cyclopentadienyl is the ease with which its steric and electronic property can be modified by the judicious introduction of diverse substituents. Many studies concerning functionalized cyclopentadienyl ligands have been reported. Cyclopentadienyl with tethered amino groups(CpN) have been used for coordination with various transition metals[127-129] but ruthenium complexes containing these ligands are still rare. Our research group has studied the chemical properties of some aminocyclopentadienyl ruthenium systems and their reactions towards dihydrogen molecules.[20]

It is well known that transition metal indenyl complexes display higher reactivity in stoichiometric and catalytic reactions than their cyclopentadienyl analogues.[119, 146, 147] However, very few aminoindenyl complexes are known. In fact, no aminoindenyl(InN) ruthenium complex has been reported to date. Therefore, it is interesting to compare the chemical properties and reactivity of the InN ruthenium complexes with those of the CpN ruthenium complexes.

3.2 Experimental

3.2.1 Materials and instrumentation

All reactions were carried out under a dry nitrogen atmosphere using standard Schlenk techniques. Solvents were distilled under nitrogen from appropriate drying agents (solvent/drying agent): methanol/Mg-I₂, ethanol/Mg-I₂, acetonitrile/CaH₂, dichloromethane/CaH₂, tetrahydrofuran/Na-Benzophenone, diethylether/Na, n-hexane/Na.

Ruthenium trichloride (RuCl₃·3H₂O), triphenylphosphine, bis(diphenyl(phosphino)methane) (dppm), *tert*-butyllithium (1.7 M solution in pentane), 1-chloroethyldimethylamine hydrochloride and indene were purchased from

Aldrich.

The ligand $C_9H_7(CH_2)_2NMe_2$ [199], the complexes $(\eta^5:\eta^1-C_5H_4CH_2CH_2NMe_2)Ru(dppm)]BF_4$ (2)[20] and $Ru(PPh_3)_3Cl_2$ [200] were prepared according to published procedures.

Proton NMR spectra were obtained from a Bruker DPX 400 spectrometer. Chemical shifts were reported relative to residual protons of the deuterated solvents. $^{31}P\{^1H\}$ NMR spectra were recorded on a Bruker DPX 400 spectrometer at 162 MHz; chemical shifts were externally referenced to 85% H_3PO_4 in D_2O . Electrospray Ionization Mass spectrometry was carried out with a Finnigan MAT 95S mass spectrometer. Elemental analyses were performed by M-H-W Laboratories, Phoenix, AZ, USA.

3.2.2 Syntheses and Reactions

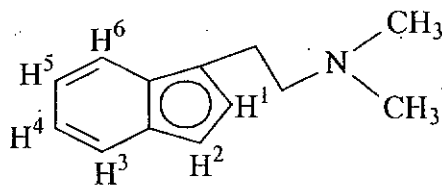


Chart 1

3.2.2.1 Synthesis of (η^5 -C₉H₆CH₂CH₂NMe₂)Ru(PPh₃)₂Cl (17)

A Schlenk flask was charged with (2-dimethylaminoethyl)indene (0.59 g, 3.14 mmol) and THF (20 mL). *tert*-BuLi (1.80 mL, 3.14 mmol, 1.7 M in pentane) was added dropwisely to the solution via a syringe at 0°C. The solution was stirred for 30 min, and it was then added slowly to a stirring suspension of Ru(PPh₃)₃Cl₂ (1.50 g, 1.57 mmol) in THF (20 mL) at 0°C. The color of the mixture gradually changed to dark red, and the resulting solution was stirred for another 15 min at room temperature. It was filtered, and the solvent was removed under vacuum. The residue was washed with hexane (2 x 20 mL), and the red solid was recrystallized from dichloromethane/hexane. Yield: 0.81 g (61%). Anal. Calcd for C₄₉H₄₆ClNP₂Ru: C, 69.45; H, 5.47; N, 1.65. Found: C, 69.62; H, 5.46; N, 1.64. ¹H NMR (CDCl₃, 400 MHz, 25°C) δ 7.50-6.90 (m, 30H of PPh₃ and 2H of H^{5&6})(see Chart 1), 6.59 (t, 1H, ³J(HH)= 7.5 Hz, H⁴), 6.18 (d, 1H, ³J(HH)= 8.3 Hz, H³), 4.65 (br s, 1H, H¹), 3.20 (br s, 1H, H²), 2.80 and 2.50 (m, 2H, -CH₂N-), 2.40 and 2.10 (m, 2H, -IndCH₂-), 2.07 (s, 6H, NCH₃). ³¹P{¹H} NMR (162 MHz, CDCl₃, 25°C) δ 44.9 [d, ²J(PP) = 45.3 Hz], δ 37.8 [d, ²J(PP) = 45.3 Hz]. ESI-MS (CH₂Cl₂-MeOH as solvent) m/z: 811 [M-Cl]⁺

3.2.2.2 Synthesis of (η^5 -C₉H₆CH₂CH₂NMe₂)Ru(dppm)Cl (18)

Complex 17 (0.30 g, 0.35 mmol) and dppm (0.15 g, 0.39 mmol) were

dissolved in 50 mL of toluene, and the solution was refluxed for 4 h. The solvent was then removed completely under vacuum; the residue was washed with diethyl ether (2x5 mL) and dried in vacuo. Yield: 0.2 g (80%). Anal. Calcd for $C_{38}H_{38}ClNP_2Ru$: C, 64.54; H, 5.42; N, 1.98. Found: C, 64.35; H, 5.44; N, 1.97. 1H NMR ($CDCl_3$, 400 MHz, 25°C) δ 7.50-6.90 (m, 20H of dppm and 4H of H^{3-6})(see Chart 1), 5.02 (br s, 1H, H^1), 4.12 (br s, 1H, H^2), 4.90 (m, 1H of PCH_2P), 4.30 (m, 1H of PCH_2P), 3.00 and 2.60 (m, 2H, $-CH_2N-$), 2.50 (m, 2H, $-IndCH_2-$), 2.24 (s, 6H, NCH_3). $^{31}P\{^1H\}$ NMR (162 MHz, $CDCl_3$, 25°C) δ 21.0 [d, $^2J(PP) = 102$ Hz], δ 5.7 [d, $^2J(PP) = 102$ Hz]. ESI-MS (CH_2Cl_2 -MeOH as solvent).m/z: 707 $[M-Cl]^+$

3.2.2.3 Synthesis of $(\eta^5-C_9H_6CH_2CH_2NMe_2)Ru(dppm)H$ (19)

A sample of 18 (0.20 g, 0.24 mmol) was added to 30 mL of NaOMe/MeOH (0.77M) solution. The resulting solution was refluxed for 24 h, and then the solvent was removed by vacuum. The residue was extracted with 30 mL of toluene; and after the removal of the solvent of the extract under vacuum, the yellow solid was washed with hexane (2x5 mL). Yield: 0.13 g (68%). Anal. Calcd for $C_{38}H_{39}NP_2Ru$: C, 67.84; H, 5.84; N, 2.08. Found: C, 68.05; H, 5.82; N, 2.08. 1H NMR (C_6D_6 , 400MHz, 25°C) δ 7.20-6.80 (m, 20H of dppm and 4H of H^{3-6})(see Chart 1), 5.48 (br s, 1H, H^1), 5.32 (br s, 1H, H^2), 4.30 (m, 1H of PCH_2P), 3.50 (m, 1H of PCH_2P), 3.00 and 2.70 (m, 2H,

-CH₂N-), 2.48 and 2.44 (m, 2H, -IndCH₂-), 2.08 (s, 6H, NCH₃), -13.13 (dt, 1H, ²J(PH) = 30.4 Hz, J(HH) = 4.0 Hz, Ru-H). ³¹P{¹H} NMR (162 MHz, C₆D₆, 25°C) δ 4.4 [d, ²J(PP) = 95.9 Hz], δ 1.3 [d, ²J(PP) = 95.9 Hz]. ESI-MS (CH₂Cl₂-MeOH as solvent) m/z: 672 [M]⁺.

Variable-temperature T₁ measurements on the Ru-H signal were carried out by the inversion-recovery method using standard 180°-τ-90° pulse sequences. T₁ (400MHz): 1498 ms (293K), 1356 ms (283K), 1145 ms (273K), 1036 ms (263K), 930 ms (253K), 869 ms (243K), 811 ms (233K), 845 ms (223K), 914 ms (213K)

T₁(min) (832 ms at 230K and 400MHz) was obtained from the lnT₁ vs 1000/T plot.

3.2.2.4 Synthesis of (η⁵-C₉H₆CH₂CH₂NMe₂)Ru(PPh₃)₂H (20)

This complex was prepared by using the same procedure as for the preparation of 19, except 17 was used instead of 18. Yield: 0.15 g (78%) Anal. Calcd for C₄₉H₄₇NP₂Ru: C, 72.40; H, 5.83; N, 1.72. Found: C, 72.65; H, 5.85; N, 1.73.

¹H NMR (C₆D₆, 400 MHz, 25°C) δ 6.90-7.30 (m, 30H of PPh₃ and 2H of H⁵⁻⁶) (see Chart 1), 6.22 (m, 1H, H⁴), 6.52 (m, 1H, H³), 5.77 (br s, 1H, H¹), 4.53 (br s, 1H, H²), 2.25 (m, 2H, -CH₂N-), 2.23 (m, 2H, -IndCH₂-), 1.99 (s, 6H, NCH₃), -14.90 (t, 1H, ²J(PH) = 31.2Hz, Ru-H). ³¹P{¹H} NMR (162 MHz, C₆D₆, 25°C) δ 60.9 (br s), δ 59.3 (br s)

ESI-MS: 812 [M]⁺

3.2.2.5 *In situ* preparation of $[(\eta^5\text{-C}_9\text{H}_6\text{CH}_2\text{CH}_2\text{NMe}_2\text{H}^+)\text{Ru}(\text{dppm})\text{H}]\text{BF}_4$ (21)

$\text{HBF}_4 \cdot \text{Et}_2\text{O}$ (2.0 μL , 0.015 mmol) was added to a solution of 19 (0.010 g, 0.015 mmol) in 0.4 mL of $\text{THF-}d_8$ in a 5mm NMR tube, and the NMR spectra were collected immediately:

^1H NMR ($\text{THF-}d_8$, 400 MHz, 25°C) δ 7.60-7.30 (m, 20H of dppm and 4H of H^{3-6}) (see Chart 1), 5.47 (br s, 1H, H^1), 5.39 (br s, 1H, H^2), 4.70 (m, 1H of PCH_2P), 3.80 (m, 1H of PCH_2P), 3.2-2.8 (m, 4H of $-\text{IndCH}_2-$ & $-\text{CH}_2\text{N}-$), 2.71 (s, 6H, NCH_3), -13.41 (t, 1H, $^2J(\text{PH}) = 30\text{Hz}$, Ru-H).

$^{31}\text{P}\{^1\text{H}\}$ NMR (162 MHz, $\text{THF-}d_8$, 25°C) δ 8.1 [d, $^2J(\text{PP}) = 76.1$ Hz], δ 3.4 [d, $^2J(\text{PP}) = 76.1$ Hz]

Variable-temperature T_1 measurements on the Ru-H signal were carried out by the inversion-recovery method using standard $180^\circ\text{-}\tau\text{-}90^\circ$ pulse sequences. T_1 (400MHz): 538 ms (293K), 489 ms (283K), 441 ms (273K), 500 ms (263K), 524 ms (253K), 580 ms (243K), 654 ms (233K), 767 ms (223K), 814 ms (213K)

$T_1(\text{min})$ (493 ms at 282K and 400MHz) was obtained from the $\ln T_1$ vs $1000/T$ plot.

3.2.2.6 Synthesis of $[(\eta^5\text{-}\eta^1\text{-C}_9\text{H}_6\text{CH}_2\text{CH}_2\text{NMe}_2)\text{Ru}(\text{dppm})]\text{BF}_4$ (22)

A mixture of 18 (0.50 g, 0.71 mmol) and NaBF_4 (0.08 g, 0.71 mmol) in 20 mL of THF was refluxed for 48 h. The solvent of the orange solution was removed by

vacuum and the solid was extracted with dichloromethane (2x10 mL), the orange solid was recrystallized from dichloromethane / hexane. Yield: 0.45 g (84%)

Anal. Calcd for $C_{38}H_{38}BF_4NP_2Ru$: C, 60.17; H, 5.05; N, 1.85. Found C, 60.35; H, 5.02; N, 1.87.

1H NMR (CD_2Cl_2 , 400MHz, 25°C) δ 7.50-7.10 (m, 20H of dppm and 1 H of H^6) (see Chart 1), 6.78 (m, 3H of H^{3-5}), 5.63 (br s, 1H, H^1), 4.19 (br s, 1H, H^2), 4.76 (m, 1H of PCH_2P), 4.37 (m, 1H of PCH_2P), 3.35 (m, 1H, $-CH_2N-$), 3.10 (m, 2H, $-IndCH_2-$), 2.90 (m, 1H, $-CH_2N-$), 2.34 (br s, 6H, NCH_3).

$^{31}P\{^1H\}$ NMR (CD_2Cl_2 , 162 MHz, 25°C) δ 15.6 [d, $^2J(PP) = 280$ Hz], δ 4.6 [d, $^2J(PP) = 280$ Hz]. ESI-MS (CH_2Cl_2 -MeOH as solvent) m/z: 707 $[M]^+$

3.2.2.7 Catalytic hydration of neat nitriles with $[(\eta^5:\eta^1-C_9H_6CH_2CH_2NMe_2)Ru(dppm)]BF_4$ (22).

In a typical run, a sample of 22 (0.010 g, 0.013 mmol) was dissolved in a 1:1 (molar ratio) mixture of nitrile and water. The solution was heated at 120°C (oil bath temperature) for 72 h, after which the solution was cooled to room temperature, and the amide formed was dissolved by addition of 1 mL of acetone. A 0.1 mL aliquot of the solution was removed and analyzed by 1H NMR spectroscopy (in $CDCl_3$). Comparison of the integrations of the characteristic peaks of the amide and the

unreacted nitrile gave the turnover number of the reaction.

3.2.2.8 CO₂ reduction with ($\eta^5:\eta^1$ -C₅H₄CH₂CH₂NMe₂)Ru(dppm)BF₄ (**2**) and ($\eta^5:\eta^1$ -C₉H₆CH₂CH₂NMe₂)Ru(dppm)BF₄ (**22**)

A solution of **2** (0.010 g, 0.014 mmol) or **22** (0.010 g, 0.013 mmol) in 10 mL of THF was heated under 60 bar of H₂/CO₂ (1/1) in a stainless steel autoclave for 16 h. The reactor was cooled rapidly and carefully vented. Formic acid formed was analyzed by ¹H NMR spectroscopy, with DMF (5 μ L) as an internal standard.

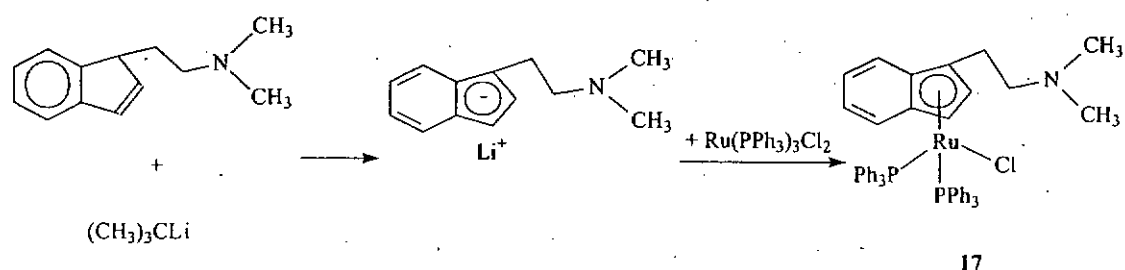
3.2.2.9 Reaction of **22** with H₂

A 0.4 mL DMSO-*d*₆ solution of **22** (0.010 g, 0.013 mmol) in a 5mm high pressure NMR tube was pressurized with 12 bar of H₂, and the tube was then heated to 100°C for 4 h. ¹H and ³¹P{¹H}-NMR spectra were recorded after the tube was cooled to room temperature.

3.3 Results and discussion

3.3.1 Synthesis of $(\eta^5\text{-C}_9\text{H}_6\text{CH}_2\text{CH}_2\text{NMe}_2)\text{Ru}(\text{PPh}_3)_2\text{Cl}$ (17)

Groux *et al.* have reported the preparation of $(\eta^3:\eta^0\text{-C}_9\text{H}_6(\text{CH}_2)_2\text{NMe}_2)\text{Ni}(\text{PPh}_3)_2\text{Cl}$ by reacting Li^+InN^- ($\text{InN}^- = \text{C}_9\text{H}_6(\text{CH}_2)_2\text{NMe}_2^-$) with $\text{Ni}(\text{PPh}_3)_2\text{Cl}_2$ in diethyl ether solution.[201] We generated the Li^+InN^- by reacting InN with *tert*-butyllithium in THF; treatment of Li^+InN^- with $\text{Ru}(\text{PPh}_3)_3\text{Cl}_2$ in THF gave the aminoindenyl complex $\text{InNRu}(\text{PPh}_3)_2\text{Cl}$ (17) (Scheme 3.1)



Scheme 3.1 Synthetic pathways of 17

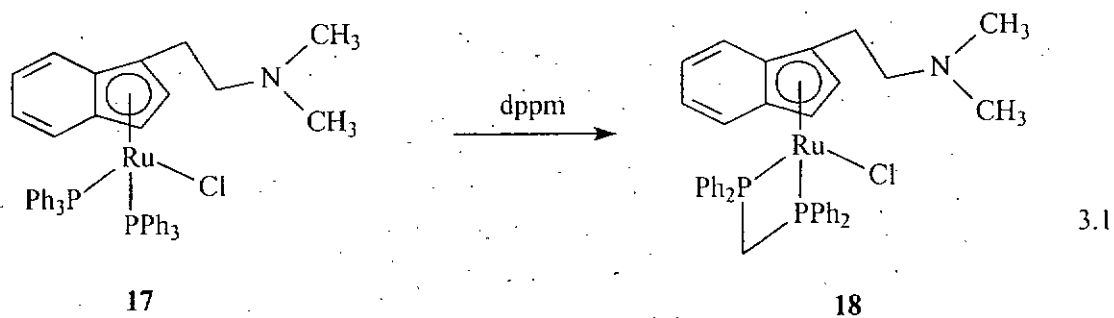
The amino side arm of 17 is not coordinated to the metal center, indicated by the similarity of the chemical shift of the aminomethyl protons of 17 to the chemical shift of those of the free ligands. The N-methyl protons of 17 appear as a singlet in the ¹H NMR spectrum at δ 2.07 ppm, and those of the free ligand InN are measured at δ

2.10 ppm.

The ^1H NMR spectrum of **17** shows the following pattern for the proton resonances of the $\eta^5\text{-InN}$ coordination; signals for the C_6 ring protons (H^{3-6}) are between δ 7.5 ppm and δ 6.2 ppm, and signal for H^1 is at δ 4.65 ppm. Groux *et al.*[201] showed that aminonickel complex has η^3 -coordination for the indenyl ligand; a remarkable downfield shift of the H^1 signal (at δ 6.7 ppm) was observed. Romao *et al.*[124] also showed that in the molybdenum complexes with the η^3 -indenyl ligands, downfield shift of the ^1H signal (at δ 6.5-7.3 ppm) is the feature of η^3 -coordination of indenyl ligand. In view of the chemical shift of the ^1H signal in **17**, it is probably true that the aminoindenyl ligand is η^5 -coordinated in the complex.

3.3.2 Synthesis of $(\eta^5\text{-C}_9\text{H}_6\text{CH}_2\text{CH}_2\text{NMe}_2)\text{Ru}(\text{dppm})\text{Cl}$ (**18**)

Similar to its non-substituted indenyl analog $(\eta^5\text{-C}_9\text{H}_7)\text{Ru}(\text{PPh}_3)_2\text{Cl}$, displacement of the PPh_3 ligands in **17** with dppm produced the corresponding dppm chloro complex **18**.(eq. 3.1)



The ^1H NMR spectrum of complex **18** show two separate signals for the two non-equivalent methylene protons of dppm, which are diastereotopic due to the lack of plane of symmetry passing through the P-C-P plane and the metal center.

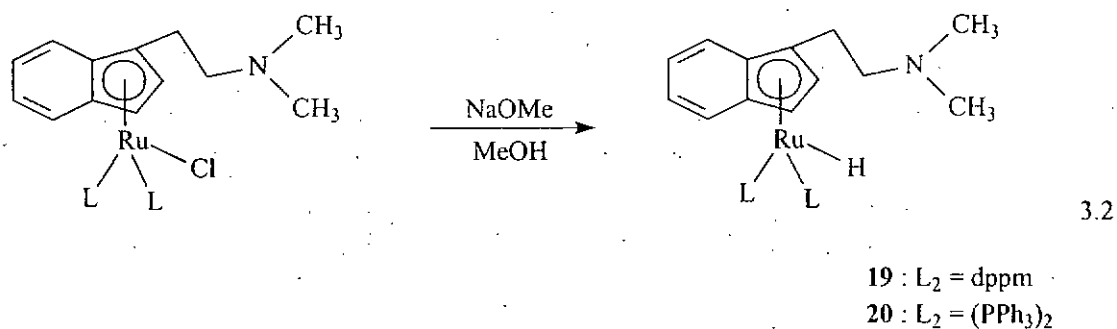
The $^{31}\text{P}\{^1\text{H}\}$ NMR spectrum of **18** showed two doublets corresponding to the two non-equivalent phosphorus atoms at δ 21 ppm and δ 5.7 ppm ($J(\text{PP}) = 102$ Hz). They are upfield shifted compared with the phosphorous signals of the bis-triphenylphosphine precursor. The upfield shift is in agreement with the general phenomenon reported by Garrou that the phosphorous atoms of the diphosphine forming a 4-membered ring with the metal center, are more shielded than those of the non-chelating phosphines and those of the chelating phosphine which form 5- or 6-membered ring with the metal center.[202]

The similarity of the chemical shift of the N-methyl protons of **18** (δ 2.24 ppm) to that of the free ligand (δ 2.10 ppm) is indicative of non-coordination of the amino

side arm of the aminoindenyl ligand. In addition, the amino indenyl ligand of **18** is also η^5 -coordinated instead of η^3 -coordinated, as revealed by the fact that the ^1H NMR spectrum of **18** shows the familiar pattern of the proton resonances for the η^5 -InN coordination (H^{3-6} , δ 6.9 – 7.5 ppm; H^1 , δ 5.02 ppm).

3.3.3 Synthesis of $(\eta^5\text{-C}_9\text{H}_6\text{CH}_2\text{CH}_2\text{NMe}_2)\text{Ru}(\text{dppm})\text{H}$ (**19**) and $(\eta^5\text{-C}_9\text{H}_6\text{CH}_2\text{CH}_2\text{NMe}_2)\text{Ru}(\text{PPh}_3)_2\text{H}$ (**21**)

There are quite a few synthetic routes for transition metal hydride complexes. The usage of LiAlH_4 [203], NaBH_4 [167] and NaOMe [204] as the hydride sources are well documented. It was reported by Oro *et al.* that the reaction of $(\eta^5\text{-C}_9\text{H}_7)\text{Ru}(\text{PPh}_3)_2\text{Cl}$ with sodium methoxide in methanol led to the formation of $(\eta^5\text{-C}_9\text{H}_7)\text{Ru}(\text{PPh}_3)_2\text{H}$ [166]. Similarly, the hydride complexes $(\eta^5\text{-C}_9\text{H}_6\text{CH}_2\text{CH}_2\text{NMe}_2)\text{Ru}(\text{L}_2)\text{H}$ (**19** : $\text{L}_2 = \text{dppm}$; **20** : $\text{L}_2 = (\text{PPh}_3)_2$) were prepared by heating the chloro precursors in refluxing methanol containing sodium methoxide (eq. 3.2).

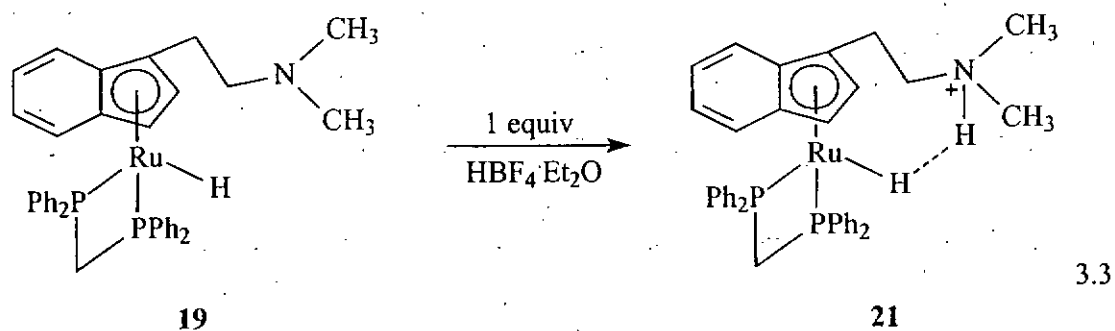


The ¹H NMR spectra of **19** and **20** showed the hydride signal at -13.13 ppm and -14.90 ppm, respectively. The hydride of **19** is coupled with one of the methylene protons of the dppm ligand, thus the ¹H NMR spectrum of **19** showed the hydride signal at -13.13 ppm as a triplet of doublets (²J(HP) = 30.4 Hz, J(HH) = 4.0 Hz). Coupling of the hydride ligand with one of the methylene protons of dppm has also been observed in IndRu(dppm)H.[166]

3.3.4 Acidification of (η⁵-C₉H₆CH₂CH₂NMe₂)Ru(dppm)H (**19**)

In the hydride complex **19** or **20**, there are 3 potential sites for electrophilic attack by a proton, the metal center, the hydride ligand, and the nitrogen atom of the amino side arm. It is therefore interesting to study the reaction of **19** or **20** with an acid. It was found that addition of 1 equiv of HBF₄·Et₂O to **19** resulted in the protonation of the pendant amine group to give [(η⁵-C₉H₆CH₂CH₂NH⁺Me₂)Ru(dppm)H]BF₄ (**21**). (eq. 3.3) The ¹H NMR spectrum of

21 in THF- d_8 revealed a downfield shift for the N-methyl signal at δ 2.71 ppm, vs the analogous signal in the parent complex **19** at δ 2.18 ppm. Similar downfield shifts of the N-methyl protons were observed upon protonation of the amino groups of the aminocyclopentadienyl ligands of the titanium,[135, 205] rhenium,[142] rhodium,[206] and ruthenium[20] complexes.

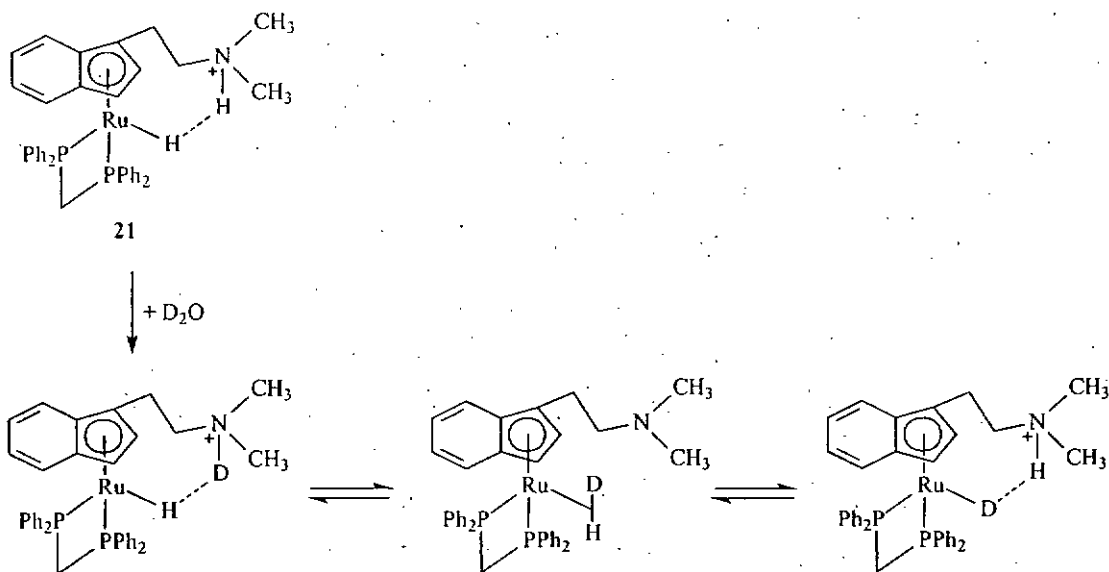


At room temperature, the hydride signal of **21**, which appears as a broad triplet ($^2J(\text{HP}) = 31.6 \text{ Hz}$) at -13.41 ppm in the ^1H NMR spectrum, is slightly upfield (by 26 ppb) from that of **19**. Unlike the hydride ligand of **19**, coupling of the hydride ligand in **21** to the methylene proton of the dppm ligand is not observed. At lower temperature (0°C or lower), the hydride signal of **21** sharpens slightly, but coupling with the methylene proton is still undetectable. Broadening of the hydride signal of **21** is probably due to its $\text{H}\cdots\text{H}$ interaction with the N-H on the pendant amine arm. It was reported that the hydride signal of $\text{WH}(\text{CO})_2(\text{NO})(\text{PMe}_3)_2$ broadened in the presence of acidic alcohol, due to the formation of intermolecular $\text{M-H}\cdots\text{H-OR}$

dihydrogen bonding.[1] Significant lowering of relaxation time T_1 for one of the hydride ligands in trans-[RuH₂(dppm)₂] was recorded in the presence of PhOH at room temperature, due to the existence of the dihydrogen-bonded species (dppm)₂HRu-H...H-OR; a dynamic equilibrium between (dppm)₂HRu-H...H-OR and [(dppm)₂HRu(H₂)]⁺(OR)⁻ was established at low temperature.[10] The presence of H...H interaction in **21** is supported by relaxation time T_1 measurement. The relaxation time (T_1) for the hydride signal of **19** measured in THF-*d*₈ at room temperature was found to be 1498 ms. Upon addition of 1 equiv of HBF₄·Et₂O, **19** was converted to **21**, and the T_1 value for the hydride signal of the latter was determined to be 538 ms, which was appreciably lower than that of the hydride signal of the former. When the same experiment was performed in chlorobenzene-*d*₅ instead of THF-*d*₈, the T_1 value dropped from 1276 ms for **19** to 195 ms for **21**. The T_1 (min) values of **19** and **21** in THF-*d*₈ were found to be 832 ms (230 K) and 493 ms (282 K), respectively. In chlorobenzene-*d*₅, the T_1 (min) of **19** was 865 ms (253 K), and that of the **21** was 180 ms (286 K). Lowering of the T_1 values nevertheless suggests some degree of hydrogen-bonding interaction between the hydride ligand and the N-bound proton complex in **21**. A smaller drop of T_1 and T_1 (min) value in THF-*d*₈ solution can be attributed to the THF-*d*₈'s competing with the Ru-H of **21** for hydrogen-bonding interaction with the amine proton **21**. This N-H...THF hydrogen bonding interaction is

maintained at the expense of N-H...H-Ru interaction. 'Switching on and off' of the intramolecular H...H interaction by using solvents of different hydrogen-bonding abilities have been reported.[207] Unfortunately, it is not possible to carry out the spin saturation transfer measurement on **21** in order to gain additional support for the presence of Ru-H...H-N interaction because the N-H signal is obscured by the other proton signals of the complex.

The H/D exchange of the hydride of **21** with D₂O however, provides additional support for the existence of Ru-H...H-N dihydrogen-bonding interaction. We found that the hydride signal of **21** disappeared within 20 min after the addition of D₂O to a THF-*d*₈ of the complex. It is believed that N-H first underwent H/D exchange with D₂O to give the N-D function, which then H/D exchanged with the metal-hydride via the intermediacy of the η²-HD species.(Scheme 3.2) In contrast, the hydride ligand and the proton on the pyridinium ring in [IrH(η¹-SC₅H₄NH)(η²-SC₅H₄N)(PPh₃)₂]BF₄ do not seem to undergo any significant exchange, although the presence of Ir-H...H-N interaction has been ascertained.[208]

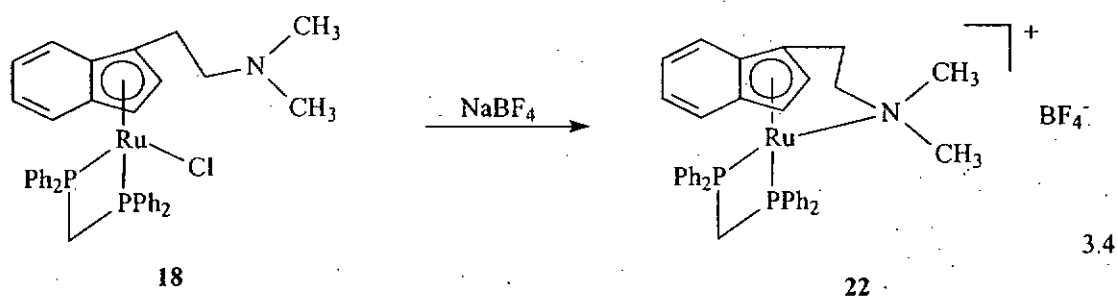


Scheme 3.2. Proposed mechanism of H/D exchange of the hydride ligand of 21 with D₂O

3.3.5 Synthesis of $[(\eta^5:\eta^1\text{-C}_9\text{H}_6\text{CH}_2\text{CH}_2\text{NMe}_2)\text{Ru}(\text{dppm})]\text{BF}_4$ (22)

Various methods can be used to abstract the chloro ligand of the ruthenium complexes. Santi *et al.* reported that the cationic $[(\eta^5\text{-C}_9\text{H}_7)\text{Ru}(\text{PPh}_3)_2]^+$ complex was generated in situ by chloride abstraction of $(\eta^5\text{-C}_9\text{H}_7)\text{Ru}(\text{PPh}_3)_2\text{Cl}$ with AgBF_4 or AgPF_6 in THF solution.[209] Gimeno *et al.* showed that the vinylidene complex $[\text{Ru}\{\text{=C=C}(\text{H})^t\text{Bu}\}(\eta^5\text{-C}_9\text{H}_7)\text{dppm}][\text{PF}_6]$ was obtained by treatment of $[(\eta^5\text{-C}_9\text{H}_7)\text{Ru}(\text{dppm})\text{Cl}]$ with an excess of 3,3-dimethyl-1-butyne and NaPF_6 in refluxing ethanol, the chloro ligand was removed with the help of the sodium ion.[210]

Heating the chloro complex **18** in THF in the presence of the NaBF_4 gave the amine-bonded cationic complex $[(\eta^5:\eta^1\text{-C}_9\text{H}_6\text{CH}_2\text{CH}_2\text{NMe}_2)\text{Ru}(\text{dppm})]\text{BF}_4$ (**22**) (eq. 3.4). Evidence for the presence of N-bounded side arm is provided by the ^1H NMR spectrum of **22**; it shows that the proton signal of the two N-methyl groups is downfield-shifted (by 0.1 ppm) from that of **18**. Similar downfield shifts of the N-methyl protons have been observed in $[(\eta^5:\eta^1\text{-C}_5\text{H}_4\text{CH}_2\text{CH}_2\text{NMe}_2)\text{Ru}(\text{dppm})]\text{BF}_4$ (**2**).

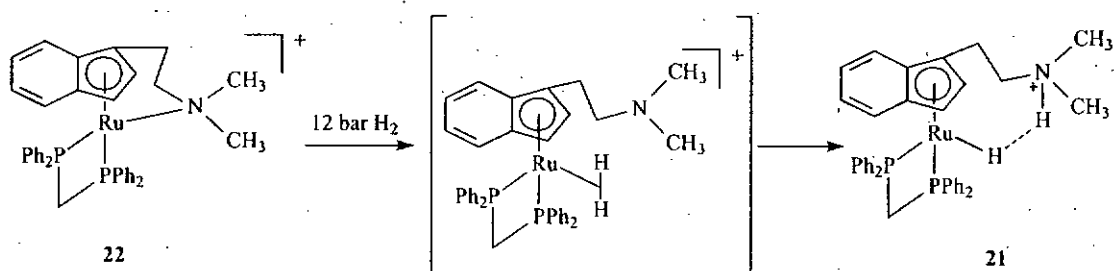


3.3.6 Reactivity of $[(\eta^5:\eta^1\text{-C}_9\text{H}_6\text{CH}_2\text{CH}_2\text{NMe}_2)\text{Ru}(\text{dppm})]\text{BF}_4$ (**22**) towards H_2

Reaction of $[(\eta^5:\eta^1\text{-C}_9\text{H}_6\text{CH}_2\text{CH}_2\text{NMe}_2)\text{Ru}(\text{dppm})]\text{BF}_4$ (**22**) with H_2 was studied. The reaction of **22** with H_2 (12 bar) in $\text{DMSO-}d_6$ in a 5 mm high pressure NMR tube at 80°C was monitored by ^1H and $^{31}\text{P}\{^1\text{H}\}$ NMR spectroscopies in 4 to 8 h intervals for a period of 120 h; it was found that **22** was gradually converted to **21** within five days. Probably, **22** first reacted with H_2 to form a dihydrogen complex intermediate,

the $\eta^2\text{-H}_2$ ligand of which was then deprotonated by the amino group to form 21.

(Scheme 3.3) Unfortunately, we were not able to detect the $\eta^2\text{-H}_2$ intermediate in the NMR studies. Our research group has also reported similar intramolecular heterolytic cleavage of $\eta^2\text{-H}_2$ ligand by the amino side arm of the Cp-N ligand of $[(\eta^5:\eta^1\text{-C}_5\text{H}_4\text{CH}_2\text{CH}_2\text{NMe}_2)\text{Ru}(\text{dppm})]\text{BF}_4$. [20] Moreover, Rettig *et al.* have found that the ruthenium amide complex $\text{RuCl}(\text{PPh}_3)[(\text{N}(\text{SiMe}_2\text{CH}_2\text{PPh}_2)_2)]$ cleaved H_2 heterolytically to form two isomeric amine-hydride derivatives of the formula $\text{RuHCl}(\text{PPh}_3)[(\text{NH}(\text{SiMe}_2\text{CH}_2\text{PPh}_2)_2)]$. [211]

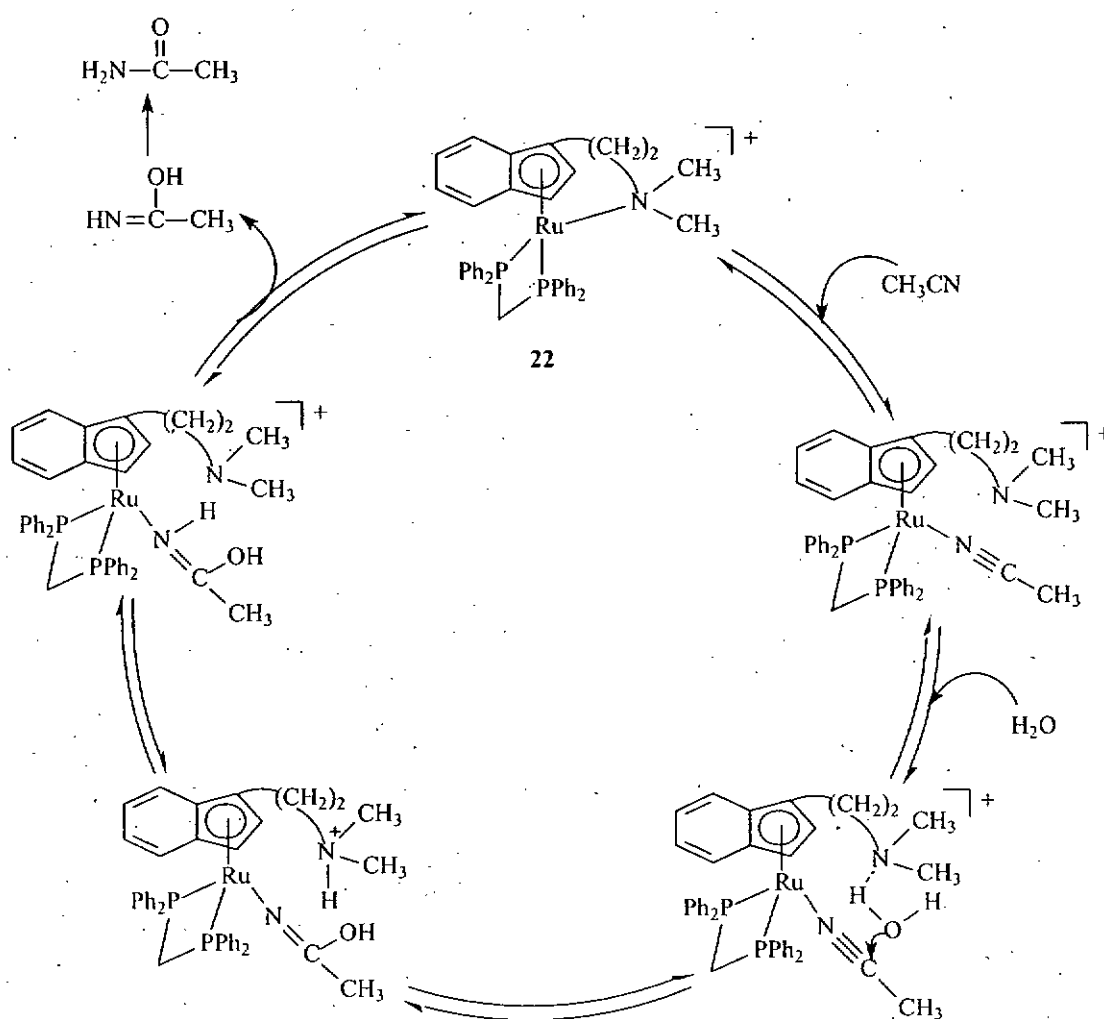


Scheme 3.3

3.3.7 Reactivity of $[(\eta^5:\eta^1\text{-C}_5\text{H}_4\text{CH}_2\text{CH}_2\text{NMe}_2)\text{Ru}(\text{dppm})]\text{BF}_4$ (2) and $[(\eta^5:\eta^1\text{-C}_9\text{H}_6\text{CH}_2\text{CH}_2\text{NMe}_2)\text{Ru}(\text{dppm})]\text{BF}_4$ (22) in nitriles hydration.

We have studied the dihydrogen bond-promoted catalytic hydration of nitriles in chapter 2, and have learned that the hydride complex $\text{IndRu}(\text{dppm})\text{H}$ (3) is capable

of catalyzing the hydration of nitriles to amides, but the chloro analogue of **3** is not. We believe that the presence of Ru-H...H-OH dihydrogen-bonding interaction plays a crucial role in the catalytic process. Against this backdrop, we anticipate that the amino side arms of **2** and **22** are potential sites to hydrogen-bond the water molecule during the catalysis of nitriles hydration; such hydrogen-bonding interaction would enhance the nucleophilicity of oxygen of the H₂O, thus enabling its attack at the cyano group of the attached nitrile. (Scheme 3.4)



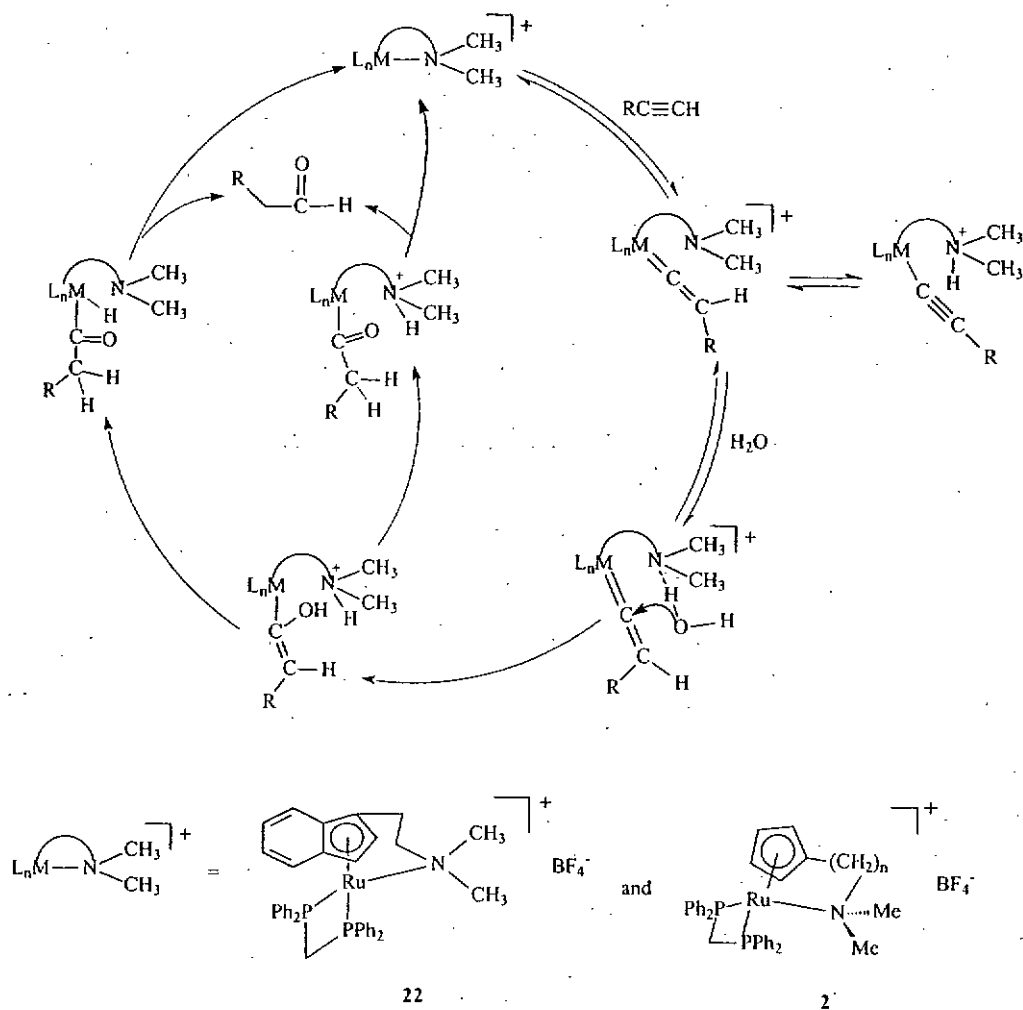
Scheme 3.4. Proposed mechanism of **22**-catalyzed hydration of acetonitriles

However, it was found that the catalytic hydration of acetonitrile with **22** did not proceed. After reacting a THF-*d*₈ solution of **22** with 10 equivalents each of CH₃CN and water at room temperature for 2 h in a 5 mm NMR tube, the reaction stopped upon the coordination of CH₃CN to the metal and forming the stable solvento complex [InNRu(dppm)(CH₃CN)]BF₄. This study seems to indicate that the hydride ligand in the indenyl complex is essential for the success of the catalytic hydration reactions of the nitriles.

3.3.8 Reactivity of $[(\eta^5:\eta^1\text{-C}_5\text{H}_4\text{CH}_2\text{CH}_2\text{NMe}_2)\text{Ru}(\text{dppm})]\text{BF}_4$ (**2**) and $[(\eta^5:\eta^1\text{-C}_9\text{H}_6\text{CH}_2\text{CH}_2\text{NMe}_2)\text{Ru}(\text{dppm})]\text{BF}_4$ (**22**) in alkene and alkyne hydration.

The addition of H₂O to a C=C bond and C≡C bond is a potentially useful route for the preparation of alcohols and carbonyl compounds, respectively. But very few metal complexes are known to catalyze these reactions.[185-187] We have learned that IndRu(dppm)H (**3**) is inactive in catalyzing these hydration reactions since the alkyne inserts into the Ru-H and alkene fails to coordinate to the metal center. We therefore investigated the catalytic activity of complexes **2** and **22** in the hydration reactions. For **2** or **22**, the alkene molecule will probably displace the coordinated amino side arm, and potentially the now dangling amino group can H-bond the

incoming H₂O molecule. Moreover, in the alkyne hydration with **2** or **22**, it is expected that the complex reacts with the terminal alkyne to give, via tautomerization, the vinylidene species. H-bond-mediated hydration of terminal alkyne might proceed via the mechanism depicted in **Scheme 3.5**.

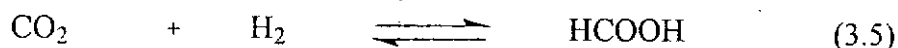


Scheme 3.5 Proposed mechanism of 2- & 22-catalyzed hydration of alkynes

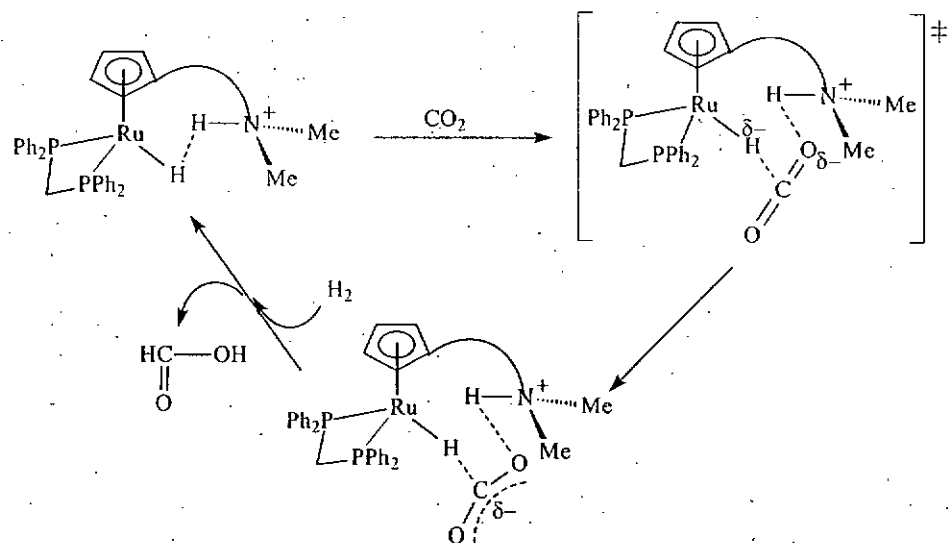
Complexes **2** & **22** were however found to be inactive in alkene and alkyne hydration. After heating the complex in a mixture of 50 equivalents each of phenylacetylene and water, and in a mixture of 50 equivalents each of methyl acrylate and water for 72 h, no hydration product was observed in either case. We then monitored the reactions of **2** with a solution of 10 equivalents each of phenylacetylene and water, and with a solution of 10 equivalents each of methyl acrylate and water in THF-*d*₈ at 80°C by ¹H and ³¹P{¹H} NMR spectroscopies at 2 and 4 h intervals for a period of 48 h; it is observed that complex **2** remained unchanged and no coordination of methyl acrylate or phenylacetylene was observed in either case. Same results were obtained when **22** was used in place of **2**. This is probably due to the fact that the coordination power of the amino side arms of **2** and **22** are strong, the substrates are therefore not able to displace them.

3.3.9 Reactivity of $[(\eta^5:\eta^1\text{-C}_3\text{H}_4\text{CH}_2\text{CH}_2\text{NMe}_2)\text{Ru}(\text{dppm})]\text{BF}_4$ (2**) and $[(\eta^5:\eta^1\text{-C}_9\text{H}_6\text{CH}_2\text{CH}_2\text{NMe}_2)\text{Ru}(\text{dppm})]\text{BF}_4$ (**22**) towards H₂/CO₂; formic acid and sodium formate.**

Catalytic hydrogenation of CO₂ to formic acid by transition-metal complexes has attracted much interest in recent years.[212-223] (eq. 3.5)



Our research group has previously learned that $[(\eta^5:\eta^1\text{-C}_5\text{H}_4\text{CH}_2\text{CH}_2\text{NMe}_2)\text{Ru}(\text{dppm})]\text{BF}_4$ (**2**) is able to catalyze CO_2 hydrogenation to formic acid in THF solution at 80°C under $\text{H}_2/\text{CO}_2(40\text{atm}/40\text{atm})$ for 16 h, albeit in low yield (Turnover number = 6). An intramolecular dihydrogen-bonded complex $[(\eta^5\text{-C}_5\text{H}_4\text{CH}_2\text{CH}_2\text{NMe}_2\text{H}^+)\text{Ru}(\text{dppm})\text{H}]\text{BF}_4$ formed by the action of H_2 on **2** is proposed to be the key species in catalytic hydrogenation of CO_2 to yield formic acid.[20] Theoretical study, employing hybrid density functional (B3LYP) calculation on this catalytic process shows that formation of the formate intermediate proceeds via the path in which the incoming CO_2 abstracts the hydrido ligand, without directly coordinating to the Ru atom.(Scheme 3.6) That this path is possible in this system is due to the promotion effect of the protonated amine side arm; the promoting effect originates from enhancement of the electrophilicity at the carbon of CO_2 by H-bonding interaction of the proton of the amine side arm with one of the oxygens of CO_2 . [21]



Scheme 3.6

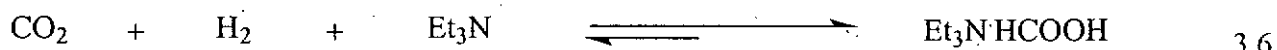
It is therefore interesting to compare the activity of $[(\eta^5\text{-}\eta^1\text{-C}_9\text{H}_6\text{CH}_2\text{CH}_2\text{NMe}_2)\text{Ru}(\text{dppm})]\text{BF}_4$ (22) with $[(\eta^5\text{-}\eta^1\text{-C}_5\text{H}_4\text{CH}_2\text{CH}_2\text{NMe}_2)\text{Ru}(\text{dppm})]\text{BF}_4$ (2) in the hydrogenation of CO_2 . It was found that stirring a DMSO solution of 2 or 22 at 80°C under H_2/CO_2 (30 atm / 30 atm) for 16 h led to the production of formic acid. The results of CO_2 hydrogenation with 2 & 22 are as shown in Table 3.1.

Table 3.1 CO₂ reduction with **2** & **22**^a

Complex used	Additives	Turnover no. ^b
InNRu(dppm)BF ₄ (22)	Triethylamine ^c	142
	Nil	10
CpNRu(dppm)BF ₄ (2)	Triethylamine ^c	25
	Nil	3

^aTypical conditions: catalyst, 0.014 mmol; solvent, DMSO (10 mL); H₂, 30 atm; CO₂, 30 atm; reaction time, 16 h; temperature, 80°C, ^bTurnover no. = mol of product/mol of catalyst. ^ctriethylamine, 1 mL.

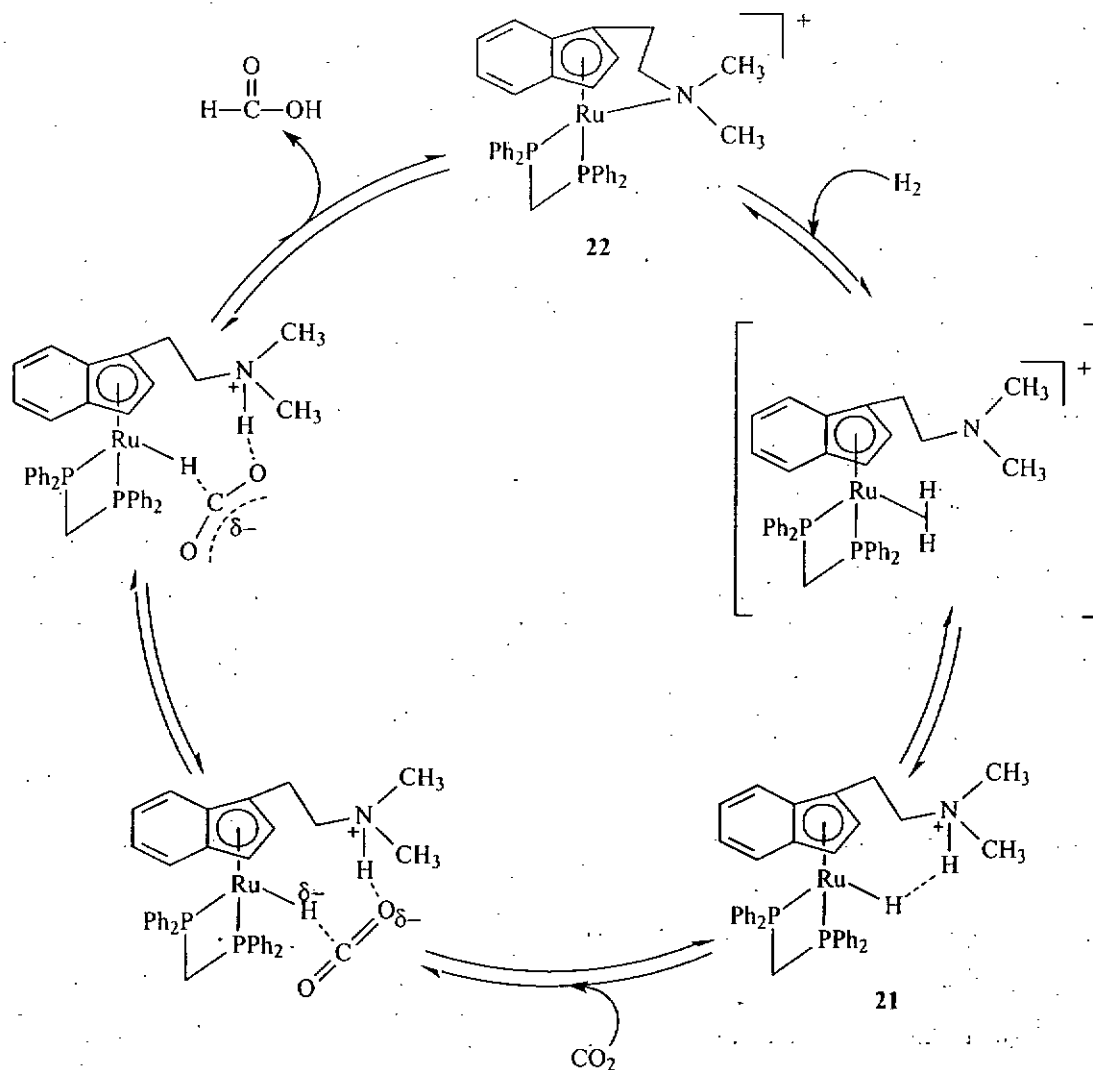
The turnover numbers of the CO₂ hydrogenation reactions were found to be higher in the presence of a base (triethylamine). The enhanced activity might be due to the formation of a thermodynamically stable adduct between the base and formic acid, thus shifting the equilibrium to the side of the product. (eq. 3.6)



In previous studies, our research group had monitored the reaction of [(η^5 : η^1 -C₅H₄CH₂CH₂NMe₂)Ru(dppm)]BF₄ (**2**) with H₂/CO₂ by high pressure ³¹P {¹H} NMR spectroscopy, and had found that **2** was completely converted to



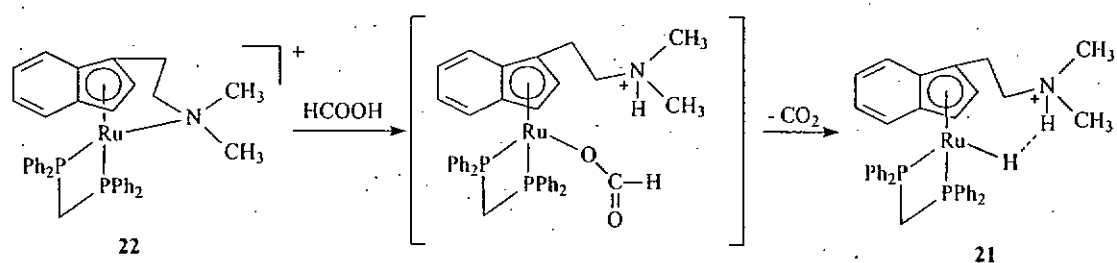
$[(\eta^5\text{-}\eta^1\text{-C}_5\text{H}_4\text{CH}_2\text{CH}_2\text{NMe}_2\text{H}^+)\text{Ru}(\text{dppm})\text{H}]\text{BF}_4$ (**1**), which remained the only detectable metal complex in the system after 24 h. Similarly, a high pressure $^{31}\text{P}\{^1\text{H}\}$ NMR study of the H_2/CO_2 reaction with **22** showed that $[(\eta^5\text{-C}_9\text{H}_6\text{CH}_2\text{CH}_2\text{NMe}_2\text{H}^+)\text{Ru}(\text{dppm})\text{H}]\text{BF}_4$ (**21**) was the only detectable metal complex throughout the experiment. **21** was probably formed by the reaction of **22** with H_2 . A mechanism for the hydrogenation of CO_2 to formic acid with **22** is shown in **Scheme 3.7**. The crucial step in the catalysis is proposed to be the heterolytic cleavage of H_2 to generate **21**. We suggested that H-bonding of the amine-bound proton in **21** to the oxygen atom of an incoming CO_2 , which is not coordinate to the metal center, enhances the electrophilicity at the carbon of the molecule, enabling it to abstract the hydride from the metal to form the transient metal-formate intermediate.



Scheme 3.7 Proposed mechanism of 22-catalyzed CO₂ hydrogenation

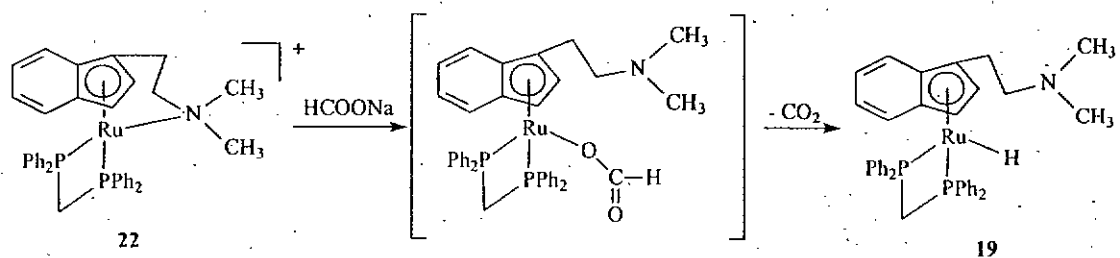
It is usually true that the metal complexes that can effect the CO₂ hydrogenation to formic acid, can effect the reverse reaction as well, i.e. decomposition of formic acid to CO₂ and H₂. It was found that reaction of 22 with formic acid in refluxing DMSO for 16 h led to the formation 21. (Scheme 3.8) Probably, HCOOH was first added across the Ru-N bond to form the transient metal formate $[(\eta^5\text{-C}_9\text{H}_6(\text{CH}_2)_2\text{NH}^+\text{Me}_2)\text{Ru}(\text{HCOO})(\text{dppm})]\text{BF}_4$, which then extruded a

CO₂ molecule to give 21.



Scheme 3.8

Moreover, reaction of 22 with sodium formate gave (η^5 -C₉H₇(CH₂)₂NMe₂)Ru(dppm)H (19). Apparently, 19 was formed by elimination of the CO₂ molecule from the metal formate intermediates. (Scheme 3.9) In fact, elimination of a CO₂ from a formate species is one of the common methods to prepare transition-metal hydride.



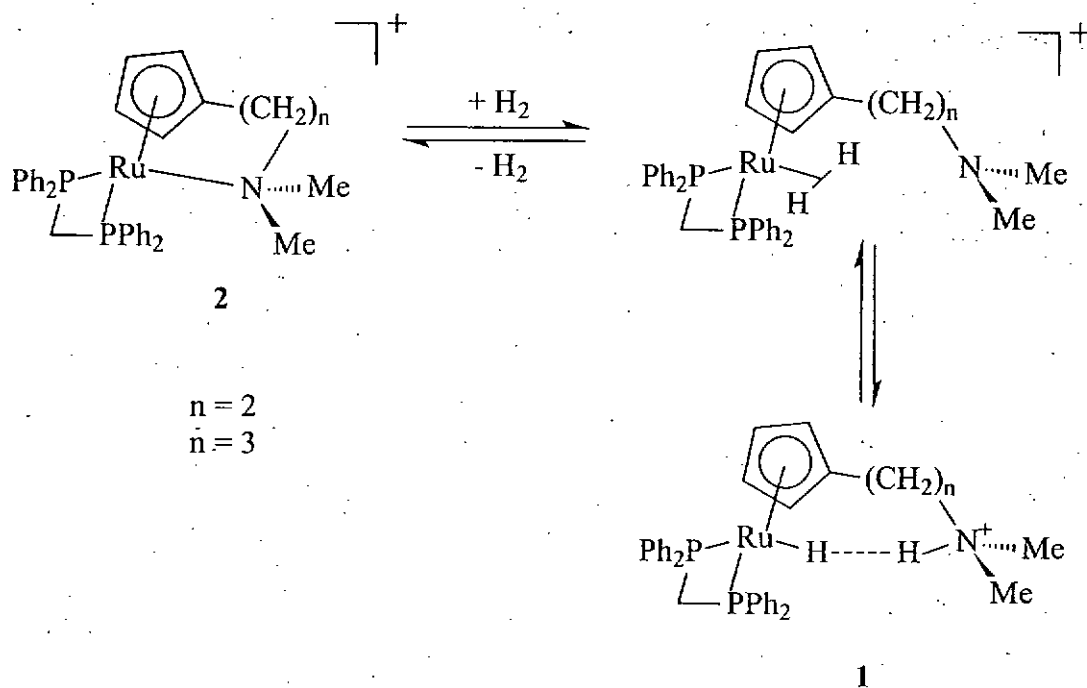
Scheme 3.9

Chapter 4 Dihydrogen-Bond-Promoted Catalysis: Catalytic Hydration of Nitriles and Hydrogenation of Unsaturated Hydrocarbon with the Aminoindenyl Ruthenium Complexes

4.1 Introduction

Our research group has studied the reactivity of the aminocyclopentadienyl complex $[(\eta^5\text{-}\eta^1\text{-C}_5\text{H}_4(\text{CH}_2)_n\text{NMe}_2)\text{Ru}(\text{dppm})]^+\text{BF}_4^-$ (**2**) and has learned that the amino side arm is able to function as an internal base to heterolytically cleave the $\eta^2\text{-H}_2$ ligand to generate the Ru-H \cdots H-N intramolecularly dihydrogen-bonded species **1** (Scheme 4.1).^[20]

1 (Scheme 4.1).^[20]



Scheme 4.1 Intramolecular N-H \cdots H-Ru Dihydrogen-Bond-Mediated Proton

Transfer

To further our investigation on the dihydrogen-bond-promoted catalytic hydration of nitriles with indenylruthenium hydride complexes described in Chapter 2, the aminoindenyl complex $(\eta^5\text{-C}_9\text{H}_6(\text{CH}_2)_2\text{NMe}_2)\text{Ru}(\text{dppm})\text{H}$ (**19**) was synthesized; this complex has an amino side arm attached to the indenyl ligand. The catalytic activity of **19** in nitriles hydration is compared with that of $(\eta^5\text{-C}_9\text{H}_7)\text{Ru}(\text{dppm})\text{H}$ (**3**). It is anticipated that the amino side arm of the indenyl ligand might play a role in the catalysis.

Reports on Hydrogenation of unsaturated hydrocarbons catalyzed by indenyl complexes are scarce; [224] not surprisingly, there is no report of aminoindenyl complex-catalyzed hydrogenation reactions. It is therefore interesting to study the activity of the aminoindenyl ruthenium and indenylruthenium complexes in catalytic hydrogenation of unsaturated hydrocarbons, and to understand the mechanisms of the reactions, especially the one catalyzed by the aminoindenyl complex.

4.2 Experimental

4.2.1 Materials and instrumentation

All reactions were carried out under a dry nitrogen atmosphere using the standard Schlenk techniques. Ruthenium trichloride, $\text{RuCl}_3 \cdot 3\text{H}_2\text{O}$, indene, bis(diphenylphosphino)methane (dppm), 4-chlorobenzonitrile, 4-nitrobenzonitrile and 4-methoxybenzonitrile were purchased from Aldrich and were used as received. The complex $\text{IndRu}(\text{PPh}_3)_2\text{H}$ (**23**)[166] was synthesized according to literature method. Solvents were distilled under a dry nitrogen atmosphere with appropriate drying agents (solvent/drying agent): methanol/ Mg-I_2 , acetonitrile/ CaH_2 , tetrahydrofuran/ Na -benzophenone, diethyl ether/ Na , n-hexane/ Na , 1-pentanol/ K_2CO_3 , benzonitrile/ K_2CO_3 . Substrates used for hydrogenation studies were obtained from Aldrich, Fluka, and Acros. Their purities were checked by NMR spectroscopy, and where necessary, the reagents were distilled under nitrogen prior to use.

Proton NMR spectra were obtained from a Bruker DPX 400 spectrometer. Chemical shifts were reported relative to the residual protons of the deuterated solvents. $^{31}\text{P}\{^1\text{H}\}$ NMR spectra were recorded on a Bruker DPX 400 spectrometer at

162 MHz; chemical shifts were externally referenced to 85% H₃PO₄ in D₂O.

4.2.2 Reactions

4.2.2.1 Catalytic hydration of neat nitriles with InNRu(dppm)H (19).

In a typical run, a sample of **19** (0.010 g, 0.017 mmol) was dissolved in a 1:1 mixture of nitrile (0.017 mol) and water (0.30 mL, 0.017 mol). The solution was heated at reflux for 72 h, after which the solution was cooled to room temperature, and the amide formed was dissolved by addition of 1 mL of acetone. An 0.1 mL aliquot of the solution was removed and analyzed by ¹H NMR spectroscopy (in CDCl₃). Comparison of the integrations of the characteristic peaks of the amide and the unreacted nitrile gave the turnover number of the reaction.

4.2.2.2 Catalytic hydration of nitriles with InNRu(dppm)H (19) in 1-pentanol.

To a sample of **19** (0.010 g, 0.017 mmol) in 2 mL of 1-pentanol were added nitrile (0.017 mol) and water (0.31 mL, 0.017 mol). The resulting solution was heated at 120 °C for 72 h. At the end of the reaction time, the solution was cooled to room temperature, an 0.1 mL aliquot of it was removed and analyzed by ¹H NMR spectroscopy (in CDCl₃). Comparison of the integrations of the characteristic peaks of

the amide product and the unreacted nitrile yielded the turnover number of the reaction.

4.2.2.3 NMR study of hydration of acetonitrile with 19

A sample of complex 19 (0.010 g, 0.017 mmol) was loaded into a 5 mm NMR tube which was then capped with a rubber septum. The tube was evacuated and filled with nitrogen gas for three cycles. Degassed THF- d_8 (0.4 mL) was added, via a syringe, to dissolve the sample. Ten equivalents of H₂O and acetonitrile each were added through microsyringes. The tube was loaded into the NMR probe preheated to 80°C, and the sample was analyzed at 80°C by ¹H and ³¹P{¹H} NMR spectroscopies in 15 min intervals for the first 4 h. After refluxing the solution at 80°C overnight, the sample was analyzed at 80°C by ¹H and ³¹P{¹H} NMR spectroscopies in 4 h intervals for 48 h. It was found that the catalyst remained unchanged throughout the reaction. The yield of the hydration product was measured by ¹H NMR spectroscopy.

4.2.2.4 H/D exchange experiment between complex 19 and D₂O.

A sample of complex 19 (0.010 g, 0.017 mmol) was loaded into a 5 mm NMR tube which was then capped with a rubber septum. The tube was purged and filled with nitrogen for three cycles. Degassed THF- d_8 (0.4 mL) was syringed in to dissolve

the sample. D₂O (20 μL) was then added to the solution by using a micro-syringe. The ¹H NMR spectrum of the mixture was recorded immediately at room temperature. The sample was then refluxed at 120°C (oil bath temperature). The H/D exchange between Ru-H of **19** and D₂O was analyzed at room temperature by ¹H NMR and ³¹P{¹H} NMR spectroscopies in 1 h intervals for the first 12 h. After refluxing the solution at 120°C overnight, the sample was analyzed at room temperature by ¹H NMR and ³¹P{¹H} NMR spectroscopies in 24 h intervals for 72 h. The percentage of deuteration of the Ru-H signal was measured by ¹H NMR spectroscopy.

4.2.2.5 Typical procedure for the catalytic hydrogenation reactions with **3 and **19****

The reactions were carried out in a 250 mL stainless steel autoclave. In a typical run, a sample of complex **3** or **19** (0.015 mmol) was loaded into a 50 mL flat bottom flask. Ten mL of freshly distilled tetrahydrofuran and 0.015 mol of the substrate were added, and the flask was placed inside the autoclave. After flushing the autoclave five times with H₂, the system was heated with stirring at 80°C under 30 bar H₂. At the end of the reaction, the autoclave was cooled rapidly and vented carefully. The products were analyzed by ¹H NMR spectroscopy.

4.2.2.6 Recovery of catalyst (hydration of nitriles).

Upon the conclusion of the catalytic hydration of nitriles, the solvent of the resulting solution was removed by vacuum. The residue was extracted with toluene (2 x 2 mL), and after removal of the solvent of the combined extracts under vacuum, the recovered catalyst obtained was washed with hexane (2 x 1 mL). It was found by ^1H and $^{31}\text{P}\{^1\text{H}\}$ NMR spectroscopies that the catalyst remained unchanged after the catalysis.

4.2.2.7 Recovery of catalyst (hydrogenation of unsaturated hydrocarbons).

At the end of the hydrogenation of unsaturated hydrocarbons, the solvent of the resulting solution was removed by vacuum. The recovered catalyst obtained was washed with hexane (5 x 2 mL). It was found by ^1H and $^{31}\text{P}\{^1\text{H}\}$ NMR spectroscopies that the catalyst remained unchanged after the catalysis.

4.3 Results and discussion

4.3.1 Catalytic hydration of nitriles with indenyl and aminoindenyl ruthenium complexes.

The complex $(\eta^5\text{-C}_9\text{H}_6(\text{CH}_2)_2\text{NMe}_2)\text{Ru}(\text{dppm})\text{H}$ (**19**), which is a derivative of $\text{IndRu}(\text{dppm})\text{H}$ (**3**), has an amino side arm attached to the indenyl ligand. In the catalytic hydration of nitriles with **19**, it is anticipated that the nitrogen atom of the amino side arm would be a potential site to hydrogen-bond the water molecule. (Chart 4.1) Such hydrogen bonding interaction can enhance the nucleophilicity of the oxygen atom of H_2O and guide the course of nucleophilic attack at the carbon atom of cyano group of the attached nitrile, therefore rendering the attack more facile.

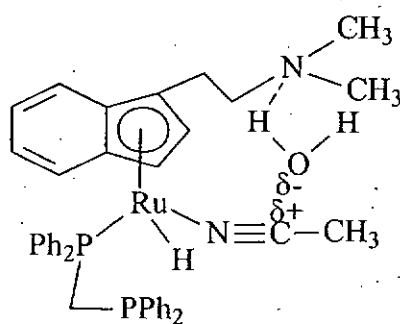


Chart 4.1

Studying the catalytic activity of **19** in the hydration of nitriles and comparing it with that of **3** is one of the means to demonstrate the promoting effect of the amino

side arm of **19**. It is found that **19** is, in general, more active than IndRu(dppm)H (**3**), which does not include an amino side arm on the indenyl ligand, in catalyzing the hydration of nitriles, as indicated by the experimental turnover numbers for **3** & **19** shown in Table 4.1.

Table 4.1. Hydration of nitriles with **3** & **19**^a

Entry	Substrate	Turnover no. ^b (time)	
		InNRu(dppm)H (19)	IndRu(dppm)H (3)
1	CH ₃ CN	1000(72h)	865(72h)
2	CH ₃ CN	1000(60h)	585(60h)
3	CH ₃ CN	700(48h)	370(48h)
4	Benzonitrile	1000(72h)	800(72h)
5	Benzonitrile	960(60h)	522(60h)
6	Benzonitrile	580(48h)	300(48h)
7 ^c	Benzonitrile	560(72h)	300(72h)
8 ^c	4-nitrobenzonitrile	500(72h)	210(72h)
9 ^c	4-chlorobenzonitrile	360(72h)	110(72h)
10 ^c	4-methoxybenzonitrile	250(72h)	40(72h)

^aTypical reaction condition: catalyst, 0.015mmole; substrate : H₂O : catalyst = 1000 : 1000 : 1; temperature for entries 1-3, reflux temperature, for the others, 120°C. ^bTurnover no. (TON) = mol of product/mol of catalyst. ^csolvent, 1-pentanol(2mL).

The turnover numbers of the **19**-catalyzed hydration reactions of nitriles were found to be considerably higher than those of the **3**-catalyzed reactions (Table 4.1). We propose that the presence of hydrogen-bonding-interaction between the nitrogen atom of the amino side arm and the water molecule in the transition state lowers the reaction barrier, and that such interaction is lacking in the case of **3**, therefore the energy barrier is higher than that of the **19**-catalyzed reaction. This proposition is substantiated with the help of theoretical calculations shown in section 4.3.5.

In the hydration of nitrobenzonitrile in 1-pentanol (entry 8, Table 4.1), the turnover number was found to be slightly lower than that of the hydration of benzonitrile (entry 7, Table 4.1). This is probably due to the fact that the nitro group of the substrate might compete with the nitrogen atom of the amino side arm for H-bonding with H₂O.

From the entries 8-10, it is found that the 4-nitrobenzonitrile and the 4-chlorobenzonitrile, which contain the electron-withdrawing nitro and chloro substituents, respectively, show higher rates of hydration than the 4-methoxybenzonitrile, which contains the electron donating methoxy substituent. These results are similar to those obtained by Kaminskaia and Kostic,[45] i.e. the

rates of hydration of derivatives of benzonitrile increase with increasing electron withdrawing ability of the substituents on the benzene rings. This is presumably due to the fact that an electron withdrawing substituent increases the electrophilicity of the carbon atom of the cyano group, rendering it more susceptible to nucleophilic attack by the water molecule.

4.3.2 Effects of acid on the rates of nitrile hydration by complex 19

To gain additional support to our proposition that the enhanced catalytic reactivity of the aminoindenyl ruthenium complex **19** in nitrile hydration over than that of the indenyl ruthenium complex might be due to the hydrogen-bonding interaction between the nitrogen atom of the amino side arm and water, we study the effect of acid on the activity of **19** in the hydration of acetonitrile; it is anticipated that protonation of the amino side arm will significantly attenuate its ability of hydrogen-bonding with the water molecule and therefore lower the overall catalytic activity of **19**. Table 4.2 shows the results of the **19**-catalyzed hydration of acetonitrile in the absence and presence of $\text{HBF}_4 \cdot \text{Et}_2\text{O}$.

Table 4.2. **19**-catalyzed hydration of nitriles with/without acid.^a

Entry	Substrate	Acid	Turnover no. ^b
1	CH ₃ CN	Nil	1000
2 ^c	CH ₃ CN	HBF ₄ ·Et ₂ O	420

^aTypical reaction condition: catalyst, 0.015mmole; substrate : H₂O : catalyst = 1000 : 1000 : 1; reaction time, 72h; temperature, 120°C. ^bTurnover no, (TON) = mol of product/mol of catalyst. ^cHBF₄·Et₂O, 0.017mmol.

It can be seen that addition of acid significantly lowered the turnover number of the **19**-catalyzed hydration reaction of CH₃CN. The attenuated activity is probably due to the nitrogen atom of amino side arm being partially protonated, therefore lowering the degree of the hydrogen-bonding interaction between the amino side arm and the water molecule. Enhancement of nucleophilicity of the oxygen atom of the H₂O by this kind of interacting is thus circumvented, rendering it less capable of attacking the cyano group of the attached nitrile.

It could be argued that the acid could protonate the ruthenium hydride rather than the nitrogen atom of amino side arm of **19** and that the decrease in turnover number of nitrile hydration is due to interruption of the function of ruthenium hydride. This hypothesis, however, seems unlikely in our case, because in monitoring the reaction

of **19** with 1.1 equivalent of $\text{HBF}_4 \cdot \text{Et}_2\text{O}$ in $\text{THF-}d_8$ at room temperature by ^1H and $^{31}\text{P}\{^1\text{H}\}$ NMR spectroscopies, it was observed that the methyl groups attached to nitrogen (δ 2.71 ppm) was downfield-shifted compared to the analogous signals of complex **19** (δ 2.18 ppm) and the hydride signal is slightly upfield (by 26 ppb) relative to that of **19**. Similar downfield shift of the N-methyl protons has been observed in $(\eta^5\text{-C}_5\text{H}_4(\text{CH}_2)_2\text{NMe}_2\text{H}^+)\text{Ru}(\text{dppm})\text{H}$, [20] as well as molybdenum [140, 141] and rhodium [206] complexes containing similar ligands. On the other hand, upfield shift of the hydride signal of $\text{WH}(\text{CO})_2(\text{NO})(\text{PMe}_3)_2$ was observed upon addition of acidic alcohol, due to the formation of intermolecular $\text{M-H}\cdots\text{H-OR}$ hydrogen bonding. Thus, the **19**/ $\text{HBF}_4 \cdot \text{Et}_2\text{O}$ experiment unequivocally demonstrates that the acid protonates the amino side arm and the resulting ammonium group forms $\text{Ru-H}\cdots\text{H-N}$ dihydrogen bond with Ru-H. It is therefore conceivable that the nitrogen atom of the amino side arm was protonated when the catalytic hydration of nitrile with **19** carried out in the presence of acid; the protonated amino side arm was no longer capable of hydrogen-bonding with the water molecule.

4.3.3 Reaction of $\text{InNRu}(\text{dppm})\text{H}$ and $\text{IndRu}(\text{dppm})\text{H}$ with D_2O .

In the nitrile hydration reactions with **19**, other than interacting with the amino

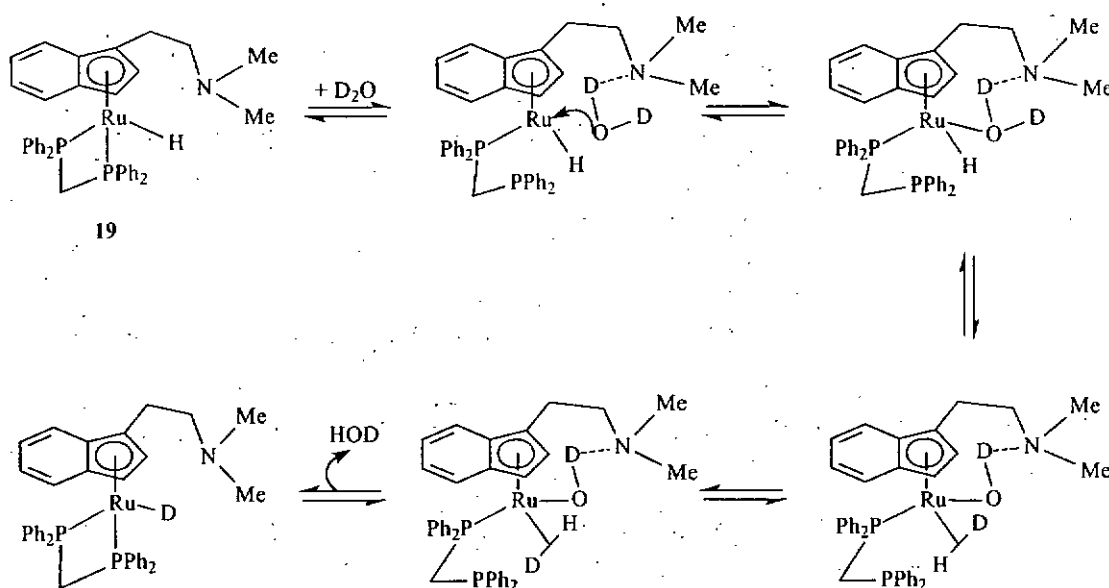
side arm of the InN ligand, the attacking water molecule has the option of interacting with the hydride ligand. To confirm this, we studied the reactions of **19** and **3** with D₂O and compared the rates of H/D exchange between Ru-H of the two complexes with D₂O. Table 4.3 shows the results of H/D exchange between Ru-H of **19** and **3** and D₂O.

Table 4.3. Percentage of deuteration of Ru-H of **3** and **19** by D₂O^a

Time / h	Percentage of deuteration of Ru-H ^b	
	InNRu(dppm)H (19)	IndRu(dppm)H (3)
1	54%	1%
2	80%	4%
6	93%	9%
12	91%	16%
24	90%	30%
48	89%	45%
72	91%	66%

^aReaction condition: catalyst **3** or **19**, 0.017 mmol; D₂O, 20 μL; solvent, THF-*d*₈ (0.4 mL); reaction temperature: 120°C. ^bdetermined by ¹H NMR spectroscopy using H² of indenyl ligand as internal reference.

It can be seen from Table 4.3 that the Ru-H of **19** undergoes H/D exchange with D_2O much faster than that of **3**. The enhancement of the H/D exchange process in **19** relative to that **3** can be explained in terms of the sequence depicted in Scheme 4.2.



Scheme 4.2 Proposed mechanism for H/D exchange of the hydride of **19 with D_2O**

The hydrogen bond formed between the nitrogen atom of amino side arm can enhance the nucleophilicity of the oxygen atom of D_2O and guides the course of nucleophilic attack at the Ru metal center. The acidity of the D_2O is enhanced after coordination to the Ru metal center and thus making it more capable of deuterating the Ru-H via the formation of η^2 -HD intermediate. The N...D-OD hydrogen-bonding

interaction can stabilize the intermediates of H/D exchange reaction with D₂O while it is not possible in **3**. Therefore, we propose that a hydrogen bond existing between the nitrogen atom of amino side arm and water in nitriles hydration might be important in promoting the catalytic reaction.

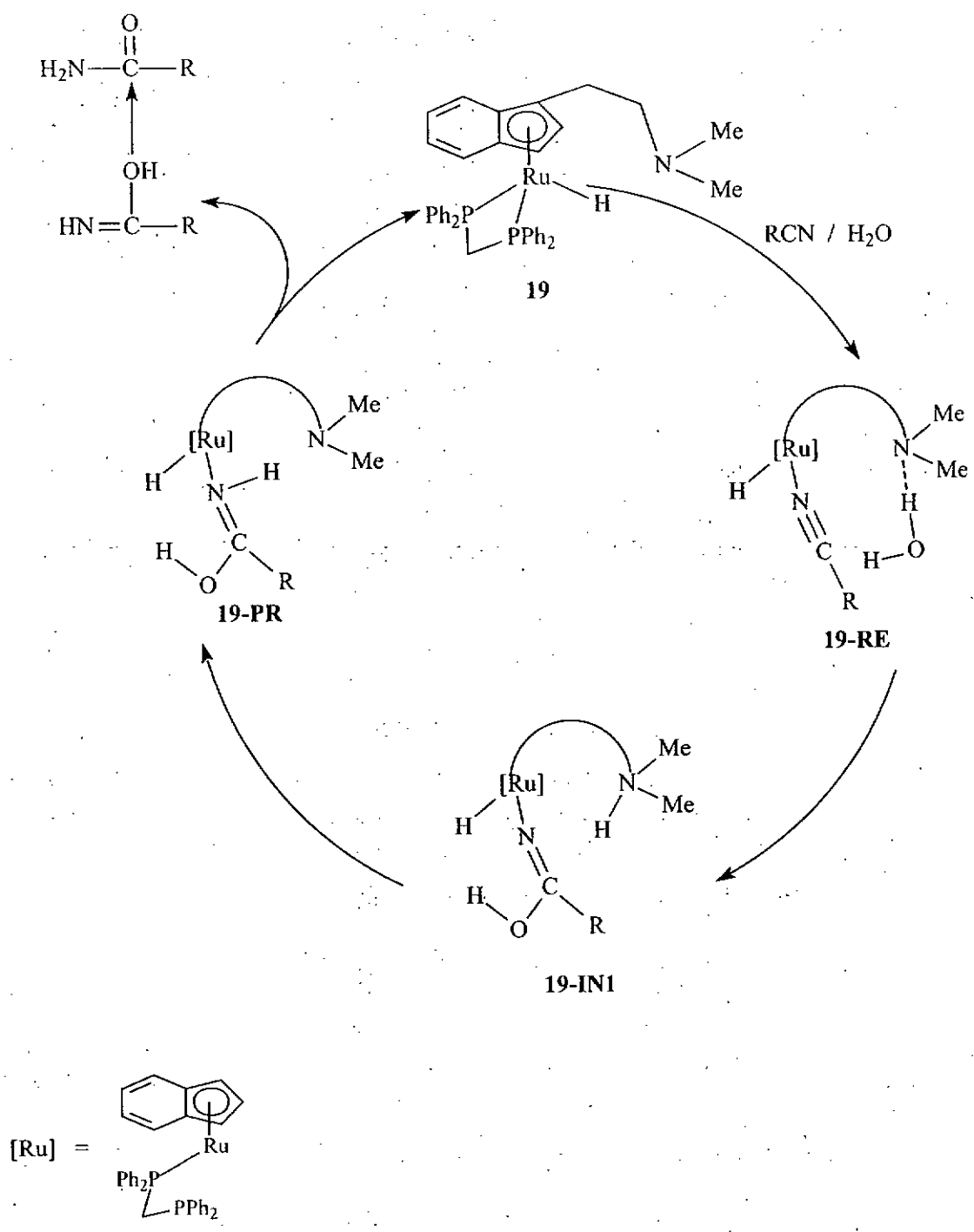
4.3.4 Possible mechanism for hydration of nitriles catalyzed by **19**

To provide a rationale for the difference in catalytic activity of **19** and **3** in nitrile hydration, we propose that the presence of an amino side arm in **19** facilitates the catalytic process in the hydration of nitriles. We have shown that **19** is consistently more active than **3** and this is likely due to the activation of the attacking water molecule through hydrogen bonding interactions. Further indirect evidence for the role of the amino side arm in the catalytic function of **19** is obtained from the decrease of activity of the catalyst in the presence of acid; resulting from the protonation of the amino side arm rendering it less available for hydrogen bonding with the water molecule.

To study the mechanism of hydration of nitriles with **19** in more detail, we have monitored the reaction of **19** with 10 equivalents each of acetonitrile and water in

THF-*d*₈ at 80°C by ¹H and ³¹P{¹H} NMR spectroscopies at 4 and 8 hour intervals for a period of 48 h. However, it was observed that while the nitrile was gradually converted to the amide, complex **19** remained unchanged throughout the experiment. Furthermore, it was learned that after heating at 80°C a THF-*d*₈ solution of **19** containing 20 equivalents of H₂O for 4 days, ¹H and ³¹P{¹H} NMR spectroscopies showed no sign of new complex, **19** remained intact.

Based on our experimental observations, we propose a mechanism to account for the enhanced catalytic activity of **19** versus **3** (Scheme 4.3). The dissociation of one arm of the dppm ligand from the metal center followed by coordination of CH₃CN is the initial step. The proposed generation of vacant site by dppm unarming is based on the result of our previous study on **3**-catalyzed hydration of nitrile. (see Chapter 2). We suggest the N···H-OH hydrogen-bonding interaction enhances the nucleophilicity of the oxygen atom of H₂O and guides the course of nucleophilic attack at the carbon atom of cyano group of the attached nitrile to form **19-IN1**. The proton attached to the amino side arm is then transferred to the nitrogen of acetonitrile to give **19-PR**. Finally, the dangling phosphine moiety of the arm-off dppm drives out the product and re-attach to the metal center.



Scheme 4.3 Proposed mechanism of 19-catalyzed hydration of nitriles

4.3.5 Theoretical study on the possible mechanism for the hydration of nitrile catalyzed by **19**

Since we have not been able to observe experimentally the intermediates of the proposed mechanism of the **19**-catalyzed nitrile hydration reaction; theoretical calculations at the B3LYP level of density function theory to study a more detailed catalytic pathway (using acetonitrile as the substrate) were carried out.

The model catalyst (η^5 -C₉H₆CH₂CH₂NMe₂)Ru(H₂PCH₂PH₂)H, in which the phenyl group of the dppm ligand were replaced by H atoms, was used. Our earlier work[225] demonstrated that the dissociation of one arm of the diphosphine ligand from the metal center followed by the coordination of a CH₃CN molecule was the initial event for the **3**-catalyzed hydration of nitriles because the diphosphine unarming requires only 15.2 kcal/mol in energy. We expect that the initial event for the **19**-catalyzed hydration is similar to the **3**-catalyzed reaction. Figure 4.1 shows the possible reaction pathways together with the calculated free energies (kcal/mol in parentheses) for species involved in the **19**-catalyzed reaction. Figure 4.2 gives the optimized structures for species involved in the reaction paths shown in Figure 4.1.

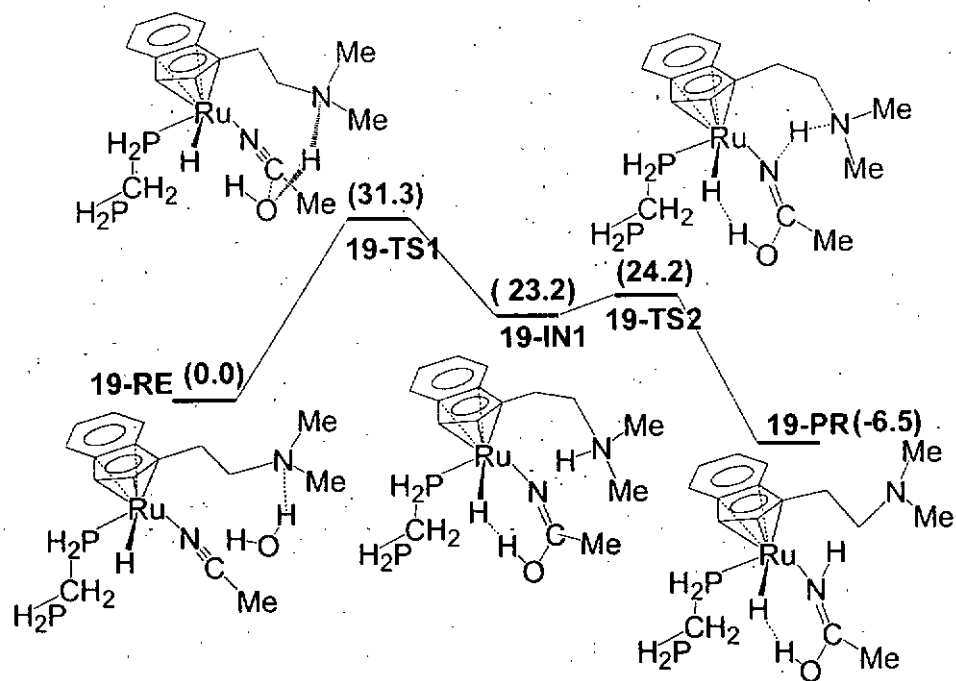


Figure 4.1 Calculated free energy profile of 19-catalyzed hydration of acetonitriles.

The energies are in kcal/mol

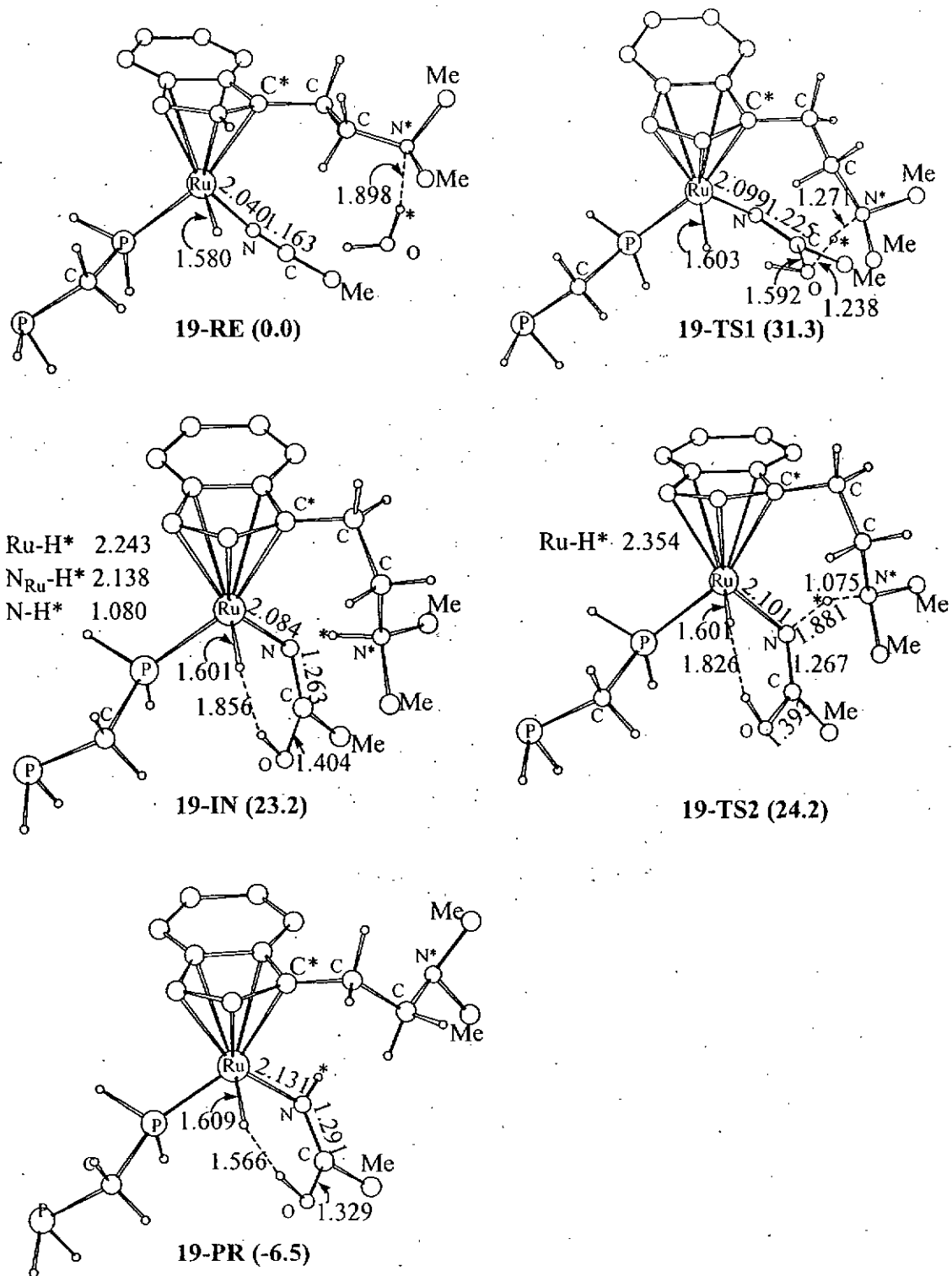
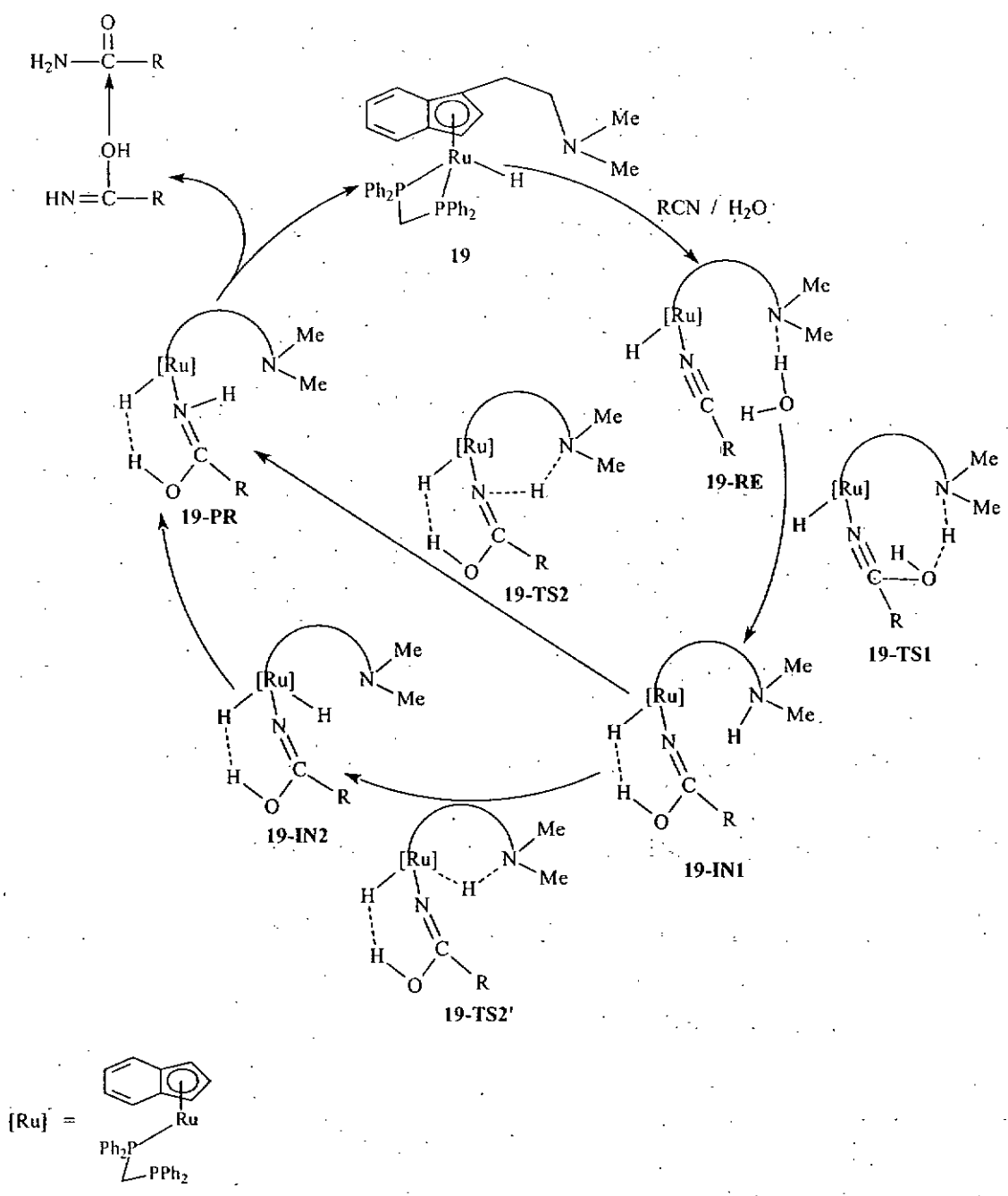


Figure 4.2. B3LYP optimized structures for those species shown in Figure 4.1.

The amino sidearm of the acetonitrile-coordinated species **19-RE** interacts with a water molecule with a N...H distance of 1.898 Å (Figure 4.2). The C*-C-C-N* dihedral angle is about 161°. The amino moiety and the indenyl ligand are therefore almost trans-disposed. From **19-RE**, the reaction proceeds by having a barrier of 31.3 kcal/mol through **19-TS1**, which is the rate-determining step, to give the intermediate **19-IN1**. In this process, the C*-C-C-N* dihedral angle changes from 161° (**19-RE**) to 60° (**19-IN1**). The rotation of the amino sidearm brings the H₂O molecule closer to the CH₃CN ligand, enabling the nucleophilic attack at the carbon atom of the coordinated nitrile molecule. The calculations show that a dihydrogen-bonding interaction is present in **19-IN1**. The selected structural parameters shown in Figure 4.2 indicate the Ru-H...H-O (1.856 Å) interaction in the intermediate. From **19-IN1**, the reaction can proceed via two possible pathways. (Scheme 4.4)



Scheme 4.4 Proposed mechanism of 19-catalyzed hydration of nitriles (derived by theoretical calculations)

In the one-step pathway, the proton attached to the amine sidearm migrates directly to the nitrogen atom of the iminol ligand, giving **19-PR**, a precursor complex having the hydroxo imine as a ligand (Figure 4.1). In the stepwise pathway, the proton migrates to the metal center, giving a four-legged piano-stool dihydride intermediate followed by a reductive elimination to generate **19-PR**. Our calculations show that the stepwise pathway has a substantially higher barrier than the one-step pathway. The one-step proton migration via **19-TS2** has a barrier of only 1 kcal/mol. The stepwise pathway requires a barrier of 12 kcal/mol. It should be pointed out that the dihydrogen-bonding interaction between the hydride ligand and the iminol hydrogen is evident throughout the proton-transfer process (**19-IN1** to **19-PR** via **19-TS2**). In addition to the Ru-H...H-O (1.826 Å) dihydrogen-bonding interaction, a strong hydrogen bond N...H-N* (1.881 Å) is also present in the transition state **19-TS2**. Clearly, the dihydrogen bond together with the strong hydrogen bond makes **19-TS2** an early transition state and lowers the reaction barrier. **19-PR** also contains a strong Ru-H...H-O (1.560 Å) dihydrogen bonding interaction. The dissociation of the hydroxo imine (HN=C(OH)Me) requires only about 12 kcal/mol in energy, similar to that reported previously,[225] making the catalytic cycle feasible.

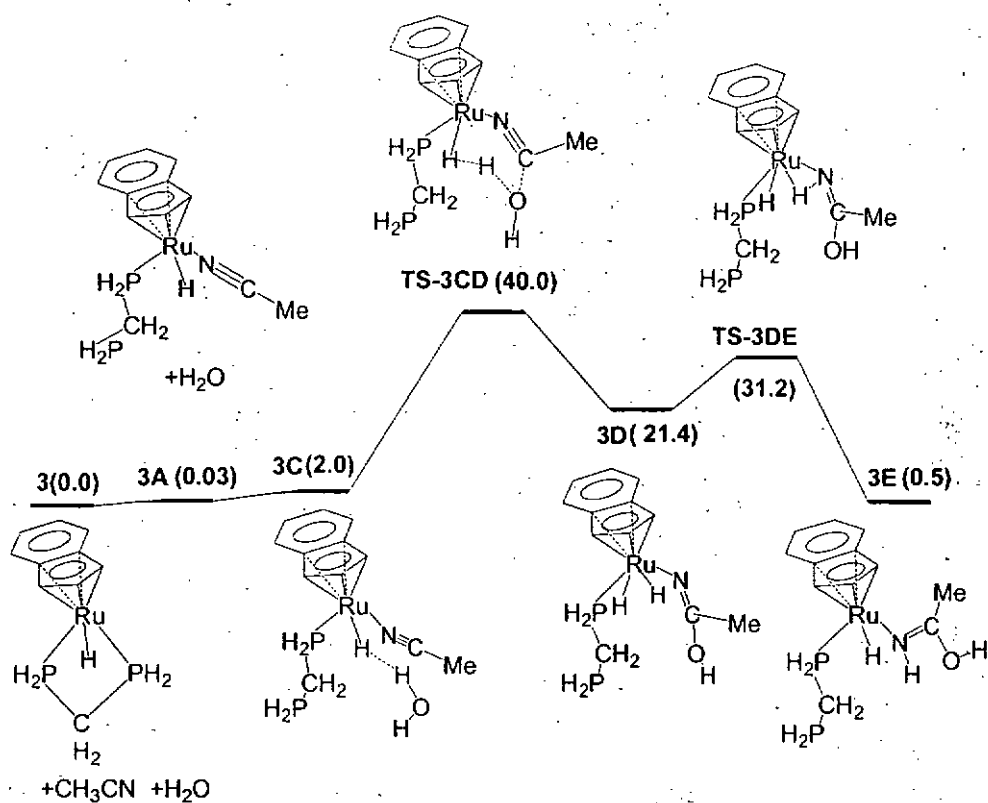


Figure 4.3 Calculated free energy profile of 3-catalyzed hydration of acetonitriles. The energies are in kcal/mol

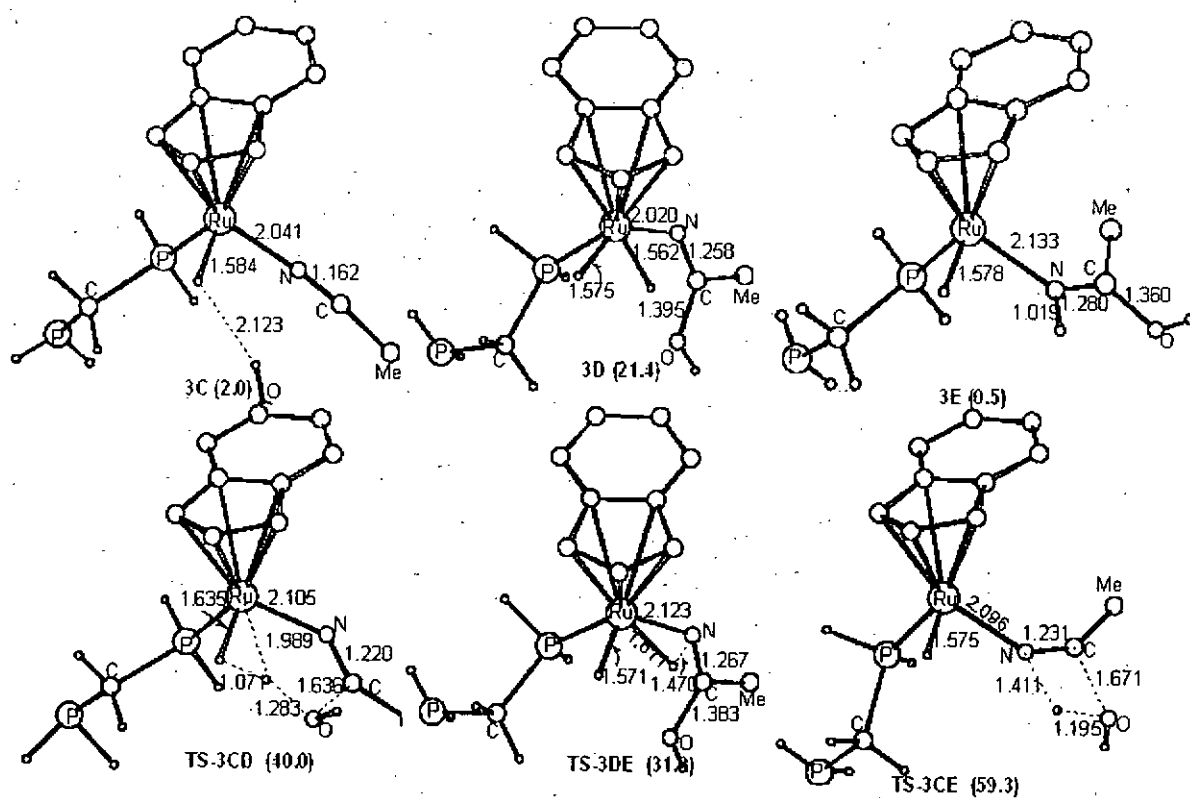


Figure 4.4 B3LYP optimized structures for those species shown in Figure 4.3.

Comparing the two multi-step process of the **19**-catalyzed nitrile hydration reaction (Fig. 4.1) with that of the **3**-catalyzed reaction (Fig. 4.3), we can see that the InN system has smaller reaction barrier. A 6.7 kcal/mol energy difference (38 kcal/mol in Fig. 4.3 vs 31.3 kcal/mol in Fig. 4.1) in the O-H bond breaking steps between the two systems is expected to give significant difference in their reaction rates.[225] These results are consistent with the experimental observation that rate acceleration was observed in the **19**-catalyzed nitrile hydration reactions. Examination of the calculated structures for the stationary points in the reaction profiles (Figures

4.2 & 4.4) reveals that the transition state **19-TS2** for the InN system has a strong hydrogen-bonding interaction $N\cdots H-N^*$, but the corresponding transition state **TS-3DE** for the IN system (Fig. 4.3) does not contain such interaction. The dihydrogen-bonding interaction and additional hydrogen bonding interaction make **19-TS2** an early transition and lowers the reaction barrier. This work is thus a good example demonstrating that with a suitably designed structure, we can make use of hydrogen bonding interactions (conventional and unconventional) to promote catalysis.

4.3.6 Effect of the monodentate ligands on the rates of nitriles hydration

To investigate the effect of the phosphine ligands on the catalytic activity of **3** and **19**, we studied the catalytic nitrile hydration with the PPh_3 analogues of **3** and **19**. It was found that the PPh_3 analogues of **3** and **19**, $IndRu(PPh_3)_2H$ (**23**) and $InNRu(PPh_3)_2H$ (**20**), respectively are also active in catalyzing the nitrile hydration reactions. However, comparison of the results depicted in Table 4.4 and Table 4.1 indicates that **20** and **23** are less active than their dpmm counterparts.

Table 4.4. Hydration of nitriles with **20** & **23**^a

Entry	Substrate	Turnover no. ^b	
		InNRu(PPh ₃) ₂ H(20)	IndRu(PPh ₃) ₂ H(23)
1	CH ₃ CN	600	140
2	Benzonitrile	450	50
3 ^c	Benzonitrile	300	20
4 ^c	4-nitrobenzonitrile	400	250
5 ^c	4-chlorobenzonitrile	290	130
6 ^c	4-methoxybenzonitrile	200	100

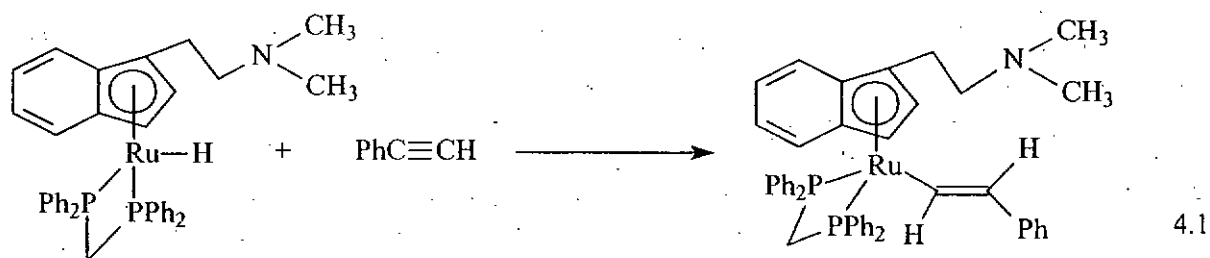
^aTypical reaction condition: catalyst, 0.015 mmol; substrate : H₂O : catalyst = 1000 : 1000 : 1; reaction time, 72h; temperature for entry 1, reflux temperature, for the others, 120°C. ^bTurnover no, (TON) = mol of product/mol of catalyst. ^csolvent, 1-pentanol(2 mL).

The results in Table 4.4 show that like its dppm analogue, the complex with the amino side arm (**20**) is more active than **23**, which contains the non-functionalized indenyl ligand, in the nitrile hydration. Similar to the hydration reactions catalyzed by **3** and **19**, the electronic effects of the substituents on the benzonitriles also have substantial effects on the yields of the hydration products. At this stage, we do not have an explanation for the higher catalytic activities of the **3** and **19** relative to those of **20** and **23**, respectively. It might be due to the dppm ligand undergoing arm-off readily (because of angle strain) to provide a vacant site for the nitrile, or due to the

fact that the dangling phosphine moiety of the arm-off dppm is more capable of driving out the product from the metal center after the hydration steps, i.e. to lower the barrier of the product dissociation step.

4.3.7 Reactivity of InNRu(dppm)H (19) towards alkene and alkyne hydration

Apart from the nitrile hydration reactions with **19**, the catalytic activity of complex **19** in the hydration reactions of alkynes and alkenes were studied. It was found that complex **19** did not promote the catalytic hydration of alkenes and alkynes. For instance, in the attempted hydration of phenylacetylene, the reaction came to a stop after the insertion of the alkyne into the Ru-H bond giving the metal-vinyl species. (eq. 4.1)



On the other hand, ^1H and $^{31}\text{P}\{^1\text{H}\}$ NMR spectroscopic studies showed that complex **19** remained unchanged after it was allowed to react with methyl acrylate

and water at 100°C for 48 h. Failure of this electron deficient alkene to react with **19** might be attributable to its poor coordination ability. In view of the failure of the hydration reaction with methyl acrylate, which is an activated alkene, the hydration reactions of the non-activated alkenes would be non-productive. Experiment on this is probably not significant and therefore unnecessary.

4.3.8 Hydrogenation of unsaturated hydrocarbons

It is well-known that many Ru(II)-hydride complexes are good catalysts for the hydrogenation of unsaturated hydrocarbons. In view of the enhanced activity of **19** relative to **3** in nitrile hydration, it is interesting to see if **19** also shows higher activity than **3** in catalytic hydrogenation of unsaturated hydrocarbons.

The results of the **3**- and **19**-catalyzed hydrogenation of alkenes are shown in Table 4.5.

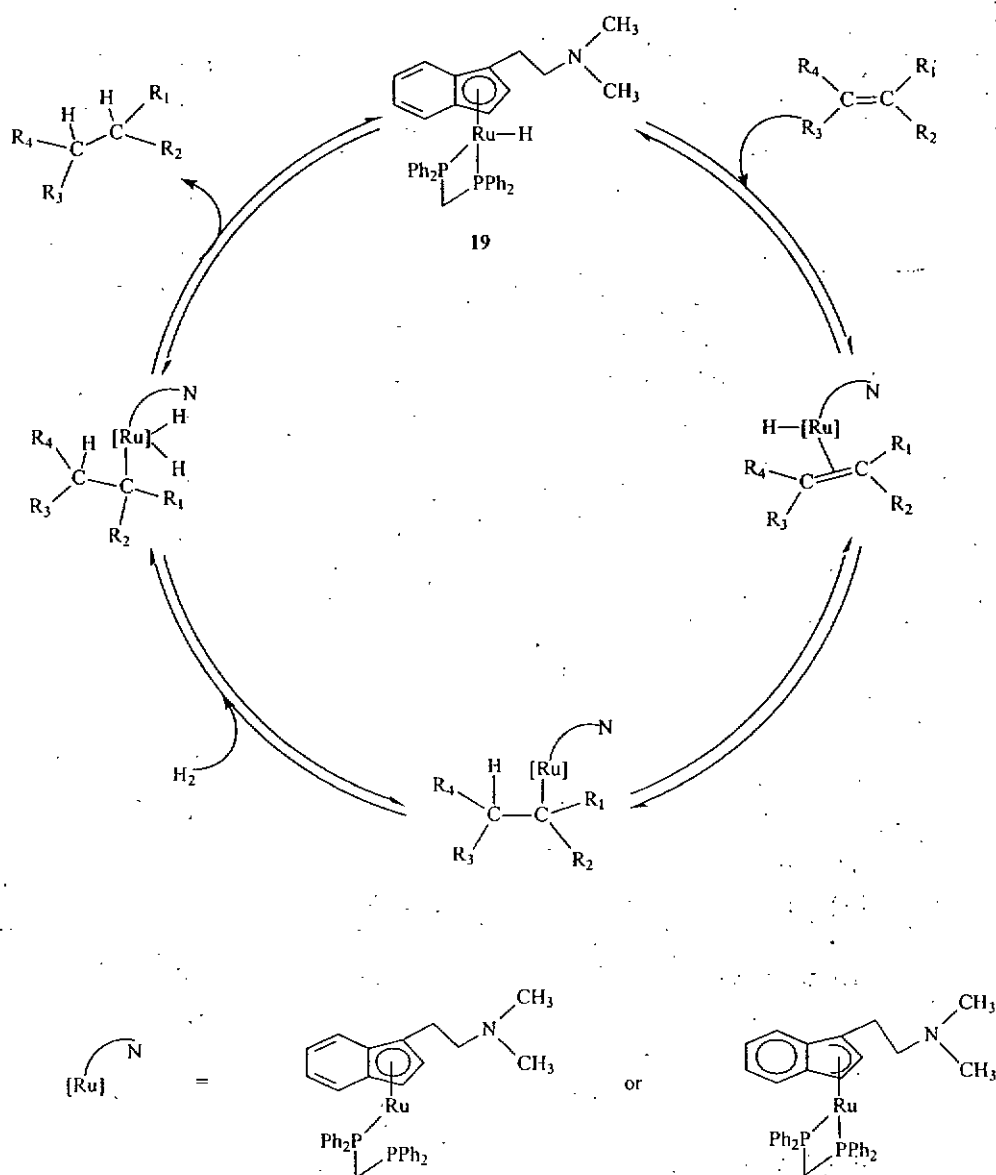
Table 4.5. Catalytic hydrogenation of alkenes with **3** and **19**.^a

Entry	Substrate	Product	Turnover no. ^b	
			IndRu(dppm)H (3)	InNRu(dppm)H (19)
1	Cyclohexene	Cyclohexane	320	350
2	1-octene	Octane	1340	1330
3	Styrene	Ethylbenzene	100	110

^aTypical conditions: catalyst, 0.015 mmol; substrate, 0.045 mol; solvent, THF (10 mL); H₂, 30 atm; temperature, 80°C; reaction time, 3h. ^bTurnover no. = mol of product/mol of catalyst.

Perusal of Table 4.5 shows that there is no obvious difference in the turnover numbers between the **3**- and **19**-catalyzed hydrogenation of alkenes, indicating that the amino side arm of **19** probably does not play a role in the reaction. This is probably due to the fact that the involvement of the amino side arm is not necessary during the catalysis of hydrogenation of alkenes. (Scheme 4.5) It is probably true that no hydrogen-bonding interaction is formed between the nitrogen atom of amino side arm and the carbon atom of alkenes, thus the energy barrier for **3**- and **19**-catalyzed hydrogenation of alkene should be the same. Moreover, the activation of molecular hydrogen process would probably take place via dihydride intermediate but not the η^2 -dihydrogen intermediate. It is believed that, if the η^2 -dihydrogen complex is

formed, the basic amino side arm would probably deprotonate the $\eta^2\text{-H}_2$ ligand and the rate enhancement would be observed in **19**-catalyzed hydrogenation reactions. However, the results show that the turnover number of **19**-catalyzed hydrogenation of alkenes is similar to that of the **3**-catalyzed reaction. And therefore, the η^2 -dihydrogen intermediate is unlikely in our cases.



Scheme 4.5 Proposed mechanism of 19-catalyzed hydrogenation of alkene

Hydrogenation of α,β -unsaturated ketones with **3** and **19** were also studied. The results of the reactions are shown in Table 4.6.

Table 4.6. Catalytic hydrogenation of α,β -unsaturated ketones with **3** and **19**.^a

Entry	Substrate	Product	Turnover no. ^b	
			IndRu(dppm)H (3)	InNRu(dppm)H (19)
1	Trans-Chalcone $\begin{array}{c} \text{Ph} \quad \text{H} \quad \text{O} \\ \quad \quad \\ \text{H}-\text{C}=\text{C}-\text{C}-\text{Ph} \end{array}$	1,3-diphenyl-1-propanone $\begin{array}{c} \text{Ph} \quad \text{H} \quad \text{O} \\ \quad \quad \\ \text{H}-\text{C}-\text{C}-\text{C}-\text{Ph} \\ \quad \\ \text{H} \quad \text{H} \end{array}$	22	60
2	Benzylidene acetone $\begin{array}{c} \text{Ph} \quad \text{H} \quad \text{O} \\ \quad \quad \\ \text{H}-\text{C}=\text{C}-\text{C}-\text{CH}_3 \end{array}$	4-phenylbutan-2-one $\begin{array}{c} \text{Ph} \quad \text{H} \quad \text{O} \\ \quad \quad \\ \text{H}-\text{C}-\text{C}-\text{C}-\text{CH}_3 \\ \quad \\ \text{H} \quad \text{H} \end{array}$	40	85
3	Methyl vinyl ketone $\begin{array}{c} \text{H} \quad \text{H} \quad \text{O} \\ \quad \quad \\ \text{H}-\text{C}=\text{C}-\text{C}-\text{CH}_3 \end{array}$	2-butanone $\begin{array}{c} \text{H} \quad \text{H} \quad \text{O} \\ \quad \quad \\ \text{H}-\text{C}-\text{C}-\text{C}-\text{CH}_3 \\ \quad \\ \text{H} \quad \text{H} \end{array}$	250	875

^aTypical conditions: catalyst, 0.015 mmol; substrate, 0.015 mol; solvent, THF (10 mL); H₂, 30 atm; temperature, 80°C; reaction time, 3h. ^bTurnover no. = mol of product/mol of catalyst.

We learned that **3** and **19** both regioselectively catalyze the reduction of the C=C bonds of the α,β -unsaturated ketones; however, in general **19** was found to be more

active than 3 in the reactions. We suspect that there might be interaction between the nitrogen atom, which is relatively nucleophilic, of the amino side arm in the complex and the electrophilic carbon atom of the carbonyl group of the α,β -unsaturated ketone. This interaction probably lowers the barrier of the hydrogenation reaction.

The results depicted in Table 4.6 show that the electronic properties of the olefins have substantial effects on the yields of the hydrogenation products. The substrates with more electron withdrawing substituents (eg. Ph group) attach to the C=C or next to the keto group, give lower turnover number for the reduction of the C=C bond of the α,β -unsaturated ketones. It is envisaged that the electron withdrawing substituents decrease the nucleophilicity of the C=C bond of the α,β -unsaturated ketone, rendering its insertion into Ru-H less facile, therefore, lowering the overall rate of C=C bond reduction.

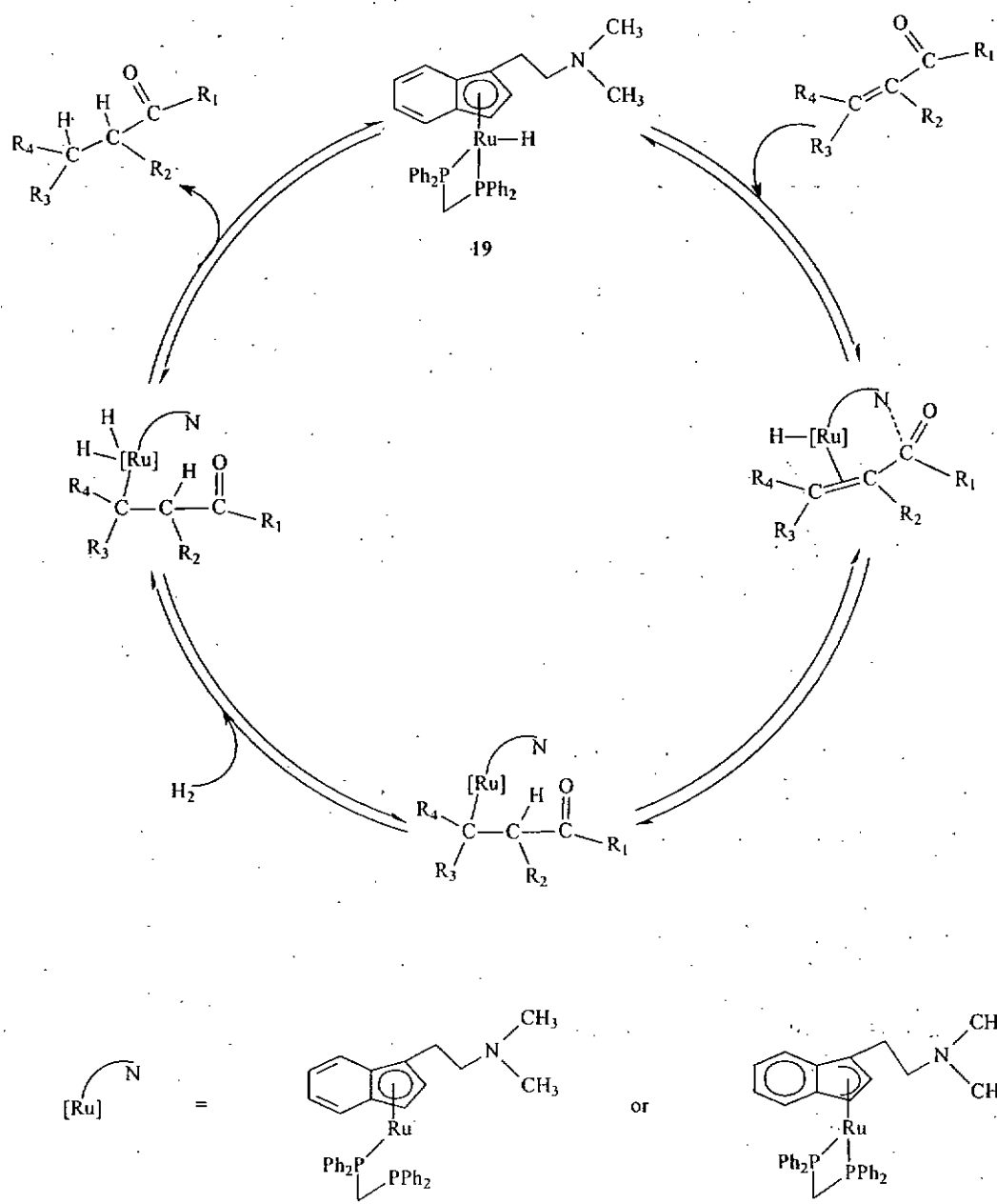
In addition, the results of Table 4.5 and 4.6 show that steric effect is an important factor affecting the yields of hydrogenation products, the conversions of bulkier olefins and ketones are in general lower. Thus, styrene and trans-chalcone gave the lowest turnover numbers among the olefins and unsaturated ketones, respectively.

4.3.9 Possible mechanism for hydrogenation of α,β -unsaturated ketone catalyzed by **19**

Based on our experimental results, we propose that the presence of an amino side arm facilitates the catalytic process in the reduction of C=C bond of α,β -unsaturated ketone. In order to substantiate this proposition and study the mechanism in more detail, we monitored the reaction of **19** with 10 equivalents of benzylidene acetone under pressurized H₂ (30 bar) in THF-*d*₈ by high pressure NMR spectroscopy. The solution was heated at 80°C, and the ¹H and ³¹P{¹H} NMR spectra were taken at 80°C in 1 h intervals for a period of 12 h. It was observed that while the benzylidene acetone was gradually converted to 4-phenylbutan-2-one, complex **19** remained unchanged throughout the experiment. We believed that the hydrogen-bonded intermediate was a transient species in the catalysis, and eluded observation by NMR spectroscopy.

A proposed reaction mechanism to account for the preponderance of the catalytic activity of **19** in reducing C=C of α,β -unsaturated ketone over that of **3** is depicted in **Scheme 4.6**. We suggest that the hydrogen bonding interaction between the nitrogen atom of amino side arm of **19** with the carbon atom of carbonyl group of ketone might

play a role in lowering the activation energy of the insertion step. That the complex 3 is less active is probably attributable to the fact that no hydrogen bond can be formed between the complex and the ketone, therefore, the energy barrier for the insertion process is relatively higher.



Scheme 4.6 Proposed mechanism of 19-catalyzed hydrogenation of α,β -unsaturated ketone

Chapter 5 Conclusion

Ruthenium hydride complexes are found to be active in the catalytic hydration of nitriles while the chloro analogues are not. Among those ruthenium hydride complexes, the $\text{IndRu}(\text{dppm})\text{H}$ (**3**) is found to be the most active in catalyzing the hydration of nitriles. The important role of the hydride in the catalytic cycle with complex **3** is to form the hydrogen bond with the water molecule thus lowering the reaction barrier of the nucleophilic attack of its attack at the carbon center of the coordinated nitrile. Our work provides a clear example demonstrating the principle of promoting a catalytic reaction by the use of $\text{M-H}\cdots\text{H-X}$ dihydrogen-bonding interaction in an indenylruthenium hydride system.

Ruthenium complexes containing functionalized indenyl ligands with N-donor sidearms are synthesized and characterized. The ruthenium complex $[(\eta^5:\eta^1\text{-C}_9\text{H}_6\text{CH}_2\text{CH}_2\text{NH}^+\text{Me}_2)\text{Ru}(\text{dppm})\text{H}]\text{BF}_4$ (**21**) has been shown to display intramolecular $\text{Ru-H}\cdots\text{H-N}$ proton-hydride interaction. This intramolecular hydrogen bonding is evidenced by relaxation time T_1 measurements. The complex $[(\eta^5:\eta^1\text{-C}_9\text{H}_6\text{CH}_2\text{CH}_2\text{NMe}_2)\text{Ru}(\text{dppm})]\text{BF}_4$ (**22**) reversibly add H_2 to give **21**, which are most likely formed by the displacement of the bound H_2 with the help of amino

side arm.

In addition, the complex **22** are used to compare the reactivity towards hydrogenation of CO₂ and hydration of nitriles with the CpN complex ($\eta^5:\eta^1$ -C₅H₄CH₂CH₂NMe₂)Ru(dppm)]BF₄ (**2**). Heating the solution of **22** under H₂/CO₂ (30atm/30atm) at 80°C for 16 h gave formic acid with yield higher than that of the reaction catalyzed by complex **2**. The formation of the formic acid can be explained by a mechanism involving intramolecular heterolytic cleavage of the bound H₂ by the amino side arm to generate **21** following by CO₂ insertion into Ru-H and then N-H protonation of the formate ligand.

Furthermore, the aminoindenyl ruthenium hydride complex is found to be active in catalyzing the nitriles hydration. The activity of this complex is higher than that of the corresponding indenyl ruthenium hydride complex without the amino side arm. The important role of the amino side arm in the catalytic nitrile hydration with InNRu(dppm)H (**19**) is to lower the reaction barrier, owing to the presence of Ru-H...H-OH dihydrogen bonding interaction and additional InN...H-N=(OH)Me hydrogen bonding in the transition state. No such additional InN...H-N=(OH)Me hydrogen-bonding interaction is present in the **3**-catalyzed hydration reaction.

In addition to the hydration reaction, the indenyl and aminoindenyl ruthenium hydride complex is also capable of catalyzing the hydrogenation of alkenes and selectively reducing the C=C bonds of α,β -unsaturated ketones. However, the aminoindenyl complex **19** is found to give similar results for the hydrogenation of alkenes in comparison with those of complex **3**, implying that there is no promoting effect due to the amino side arm during the hydrogenation of alkenes. Interestingly, the complex **19** is found to be more active than **3** in catalyzing the hydrogenation of α,β -unsaturated ketones. We suggest that the hydrogen bonding interaction between the nitrogen atom of amino side arm of **19** with the carbon atom of carbonyl group of ketone might play a role in lowering the activation energy of the insertion step.

References

1. Shubina, E. S., Belkova, N. V., Krylov, A. N., Vorontsov, E. V., Epstein, L. M., Gusev, D. G., Niedermann, M., and Berke, H., Spectroscopic evidence for intermolecular M-H...H-OR hydrogen bonding: Interaction of $\text{WH}(\text{CO})_2(\text{NO})\text{L}_2$ hydrides with acidic alcohols. *Journal of the American Chemical Society*, 1996, 118(5), 1105-1112.
2. Bennett, M. A. and Yoshida, T., Homogeneously Catalyzed Hydration of Nitriles to Carboxamides. *Journal of the American Chemical Society*, 1973, 95(9), 3030-3031.
3. Shubina, E. S., Belkova, N. V., and Epstein, L. M., Novel types of hydrogen bonding with transition metal π -complexes and hydrides. *Journal of Organometallic Chemistry*, 1997, 536(1-2), 17-29.
4. Crabtree, R. H., Siegbahn, P. E. M., Eisenstein, O., and Rheingold, A. L., A new intermolecular interaction: Unconventional hydrogen bonds with element-hydride bonds as proton acceptor. *Accounts of Chemical Research*, 1996, 29(7), 348-354.
5. Crabtree, R. H., Recent advances in hydrogen bonding studies involving metal hydrides. *Journal of Organometallic Chemistry*, 1998, 557(1), 111-115.

6. Alkorta, I., Rozas, I., and Elguero, J., Non-conventional hydrogen bonds. *Chemical Society Reviews*, 1998, 27(2), 163-170.
7. Crabtree, R. H., Chemistry - A new type of hydrogen bond. *Science*, 1998, 282(5396), 2000-2001.
8. Crabtree, R. H., Eisenstein, O., Sini, G., and Peris, E., New types of hydrogen bonds. *Journal of Organometallic Chemistry*, 1998, 567(1-2), 7-11.
9. Kelly, P. and Loza, M., A special bond. *Chemistry in Britain*, 1999, 35(11), 26-28.
10. Ayllon, J. A., Gervaux, C., SaboEtienne, S., and Chaudret, B., First NMR observation of the intermolecular dynamic proton transfer equilibrium between a hydride and coordinated dihydrogen: $(\text{dppm})_2\text{HRuH}\cdots\text{H-OR}=[(\text{dppm})_2\text{HRu}(\text{H}_2)]^+(\text{OR})^-$. *Organometallics*, 1997, 16(10), 2000-2002.
11. Shubina, E. S., Belkova, N. V., Bakhmutova, E. V., Vorontsov, E. V., Bakhmutov, V. I., Ionidis, A. V., Bianchini, C., Marvelli, L., Peruzzini, M., and Epstein, L. M., In situ IR and NMR study of the interactions between proton donors and the Re(I) hydride complex $[\{\text{MeC}(\text{CH}_2\text{PPh}_2)_3\}\text{Re}(\text{CO})_2\text{H}]$. $\text{ReH}\cdots\text{H}$ bonding and proton-transfer pathways. *Inorganica Chimica Acta*, 1998, 280(1-2), 302-307.

12. Messmer, A., Jacobsen, H., and Berke, H., Probing regioselective intermolecular hydrogen bonding to $[\text{Re}(\text{CO})\text{H}_2(\text{NO})(\text{PR}_3)_2]$ complexes by NMR titration and equilibrium NMR methodologies. *Chemistry, a European Journal*, 1999, 5(11), 3341-3349.
13. Custelcean, R. and Jackson, J. E., Dihydrogen bonding: Structures, energetics, and dynamics. *Chemical Reviews*, 2001, 101(7), 1963-1980.
14. Abad, M. M., Atheaux, I., Maisonnat, A., and Chaudret, B., Control of proton transfer by hydrogen bonding in the protonated forms of the binucleophilic complex $[\{\eta^5\text{-C}_5\text{H}_4\text{CH}(\text{CH}_2)_4\text{NMe}\}\text{Ir}(\text{PPh}_3)\text{H}_2]$. *Chemical Communications*, 1999, (4), 381-382.
15. Guari, Y., Ayllon, J. A., Sabo-Etienne, S., Chaudret, B., and Hessen, B., Influence of hydrogen bonding on the spectroscopic properties and on the reactivity of ruthenium hydride dihydrogen complexes. *Inorganic Chemistry*, 1998, 37(4), 640-644.
16. Aime, S., Ferriz, M., Gobetto, R., and Valls, E., Coordination of an imine ligand on an Os_3 cluster stabilized by intramolecular $\text{Os-H}\cdots\text{H-N}$ hydrogen bonding. *Organometallics*, 1999, 18(10), 2030-2032.
17. Aime, S., Gobetto, R., and Valls, E., Role of $\text{Os-H}\cdots\text{H-N}$ interactions in directing the stereochemistry of carbonyl cluster hydride derivatives.

- Organometallics*, 1997, 16(24), 5140-5141.
18. Yao, W. B. and Crabtree, R. H., An η^1 -aldehyde complex and the role of hydrogen bonding in its conversion to an η^1 -imine complex. *Inorganic Chemistry*, 1996, 35(10), 3007-3011.
 19. Lee, J. C., Rheingold, A. L., Muller, B., Pregosin, P. S., and Crabtree, R. H., Complexation of an Amide to Iridium Via an Iminol Tautomer and Evidence for an Ir-H \cdots H-O Hydrogen-Bond. *Journal of the Chemical Society-Chemical Communications*, 1994, (8), 1021-1022.
 20. Chu, H. S., Lau, C. P., Wong, K. Y., and Wong, W. T., Intramolecular N-H \cdots H-Ru proton-hydride interaction in ruthenium complexes with (2-(dimethylamino)ethyl)cyclopentadienyl and (3-(dimethylamino)propyl)cyclopentadienyl ligands. Hydrogenation of CO₂ to formic acid via the N-H \cdots H-Ru hydrogen-bonded complexes. *Organometallics*, 1998, 17(13), 2768-2777.
 21. Matsubara, T., Promotion effect of the protonated amine arm of a ruthenium complex on hydride migration to CO₂: A density functional study. *Organometallics*, 2001, 20(1), 19-24.
 22. Matsubara, T. and Hirao, K., Density functional study on the hydride migration to CO₂ and CS₂ of the (η^5 -C₅H₄(CH₂)₃NH₃⁺)MH(H₂PCH₂PH₂) (M =

- Fe, Ru, and Os) complexes promoted by the protonated amine arm. Which path does the reaction take, abstraction or insertion? *Organometallics*, 2001, 20(26), 5759-5768.
23. Gatling, S. C. and Jackson, J. E., Reactivity control via dihydrogen bonding: Diastereoselection in borohydride reductions of α -hydroxyketones. *Journal of the American Chemical Society*, 1999, 121(37), 8655-8656.
24. Caballero, A., Jalon, F. A., and Manzano, B. R., Three-centre dihydrogen bond with fast interchange between proton and hydride: a very active catalyst for D^+ - H_2 exchange. *Chemical Communications*, 1998, (17), 1879-1880.
25. Abdur-Rashid, K., Gusev, D. G., Lough, A. J., and Morris, R. H., Intermolecular proton-hydride bonding in ion pairs: Synthesis and structural properties of $[K(Q)][MH_5((P^iPr_3)_2)]$ (M = Os, Ru; Q=18-crown-6, 1-aza-18-crown-6, 1,10-diaza-18-crown-6). *Organometallics*, 2000, 19(5), 834-843.
26. Patel, B. P., Kavallieratos, K., and Crabtree, R. H., Effects of dihydrogen bonding on fluxionality in $ReH_5(PPh_3)_2L$. *Journal of Organometallic Chemistry*, 1997, 528(1-2), 205-207.
27. Kavallieratos, K. and Crabtree, R. H., Catalysis of aldehyde imination by hydrogen bonding with a simple organic disulfonamide receptor. *Chemical*

- Communications*, 1999, (20), 2109-2110.
28. Tominaga, M., Konishi, K., and Aida, T., Catalysis of nucleobase via multiple hydrogen-bonding interactions: Acceleration of aminolysis of 6-chloropurine derivatives by uracils. *Journal of the American Chemical Society*, 1999, 121(33), 7704-7705.
 29. Rankin, K. N., Gauld, J. W., and Boyd, R. J., Catalysis mediated by hydrogen bonding: A computational study of the aminolysis of 6-chloropyrimidine. *Journal of the American Chemical Society*, 2000, 122(22), 5384-5386.
 30. Rankin, K. N., Gauld, J. W., and Boyd, R. J., Hydrogen-bond mediated catalysis: The aminolysis of 6-chloropyrimidine as catalyzed by derivatives of uracil. *Journal of the American Chemical Society*, 2001, 123(9), 2047-2052.
 31. Collman, J. P., Hegedus, L. S., Norton, J. R., and Finke, R. G., *Principles and Applications of organotransition Metal Chemistry*. Mill Vally, CA: University Science Books, 1987.
 32. Spencer, A., *Comprehensive Coordination Chemistry*. Vol. 6. New York: Pergamon, 1987.
 33. Parshall, G. W. and Ittel, S. D., *Homogeneous Catalysis*. 2nd ed. New York: Wiley, 1992.
 34. Chalonger, P. A., Esteruelas, M. A., Joo, F., and Oro, L. A., *Homogeneous*

Hydrogenation. Boston: Kluwer, 1994.

35. Bruner, H., *Applied Homogeneous Catalysis with Organometallic Compounds*. Vol. 1. New York, 1996.
36. Noyori, R., *Asymmetric Catalysis in Organic Synthesis*. New York: Wiley, 1994.
37. Takaya, H. and Noyori, R., *Comprehensive Organic Synthesis*. Vol. 8. New York: Pergamon, 1990.
38. Noyori, R. and Hashiguchi, S., Asymmetric transfer hydrogenation catalyzed by chiral ruthenium complexes. *Accounts of Chemical Research*, 1997, 30(2), 97-102.
39. Giardello, M. A., Conticello, V. P., Brard, L., Gagne, M. R., and Marks, T. J., Chiral Organolanthanides Designed for Asymmetric Catalysis - a Kinetic and Mechanistic Study of Enantioselective Olefin Hydroamination/Cyclization and Hydrogenation by C1-Symmetrical $\text{Me}_2\text{Si}(\text{Me}_4)\text{C}_5(\text{C}_5\text{H}_3\text{R}^*)\text{Ln}$ Complexes Where R^* =Chiral Auxiliary. *Journal of the American Chemical Society*, 1994, 116(22), 10241-10254.
40. Ohkuma, T., Ooka, H., Ikariya, T., and Noyori, R., Preferential Hydrogenation of Aldehydes and Ketones. *Journal of the American Chemical Society*, 1995, 117(41), 10417-10418.

41. Wiles, J. A., Bergens, S. H., and Young, V. G., The first structure determination of a possible intermediate in ruthenium 2,2'-bis(diphenylphosphino)-1,1'-binaphthyl catalyzed hydrogenation with a prochiral group bound to ruthenium. Stoichiometric reaction of a chiral ruthenium-carbon bond with dihydrogen gas. *Journal of the American Chemical Society*, 1997, 119(12), 2940-2941.
42. Fehring, V. and Selke, R., Highly enantioselective complex-catalyzed reduction of ketones - Now with purely aliphatic derivatives too. *Angewandte Chemie-International Edition*, 1998, 37(13-14), 1827-1830.
43. Troutman, M. V., Appella, D. H., and Buchwald, S. L., Asymmetric hydrogenation of unfunctionalized tetrasubstituted olefins with a cationic zirconocene catalyst. *Journal of the American Chemical Society*, 1999, 121(20), 4916-4917.
44. Burk, M. J., Harper, T. G. P., and Kalberg, C. S., Highly Enantioselective Hydrogenation of Beta-Keto-Esters under Mild Conditions. *Journal of the American Chemical Society*, 1995, 117(15), 4423-4424.
45. Kaminskaia, N. V. and Kostic, N. M., Nitrile hydration catalysed by palladium(II) complexes. *Journal of the Chemical Society-Dalton Transactions*, 1996, (18), 3677-3686.

46. Hegedus, L. S. and Nade, L. G., *Compendium of Organic Synthetic methods*. New York: Wiley, 1977.
47. Izzo, B., Harrell, C. L., and Klein, M. T., Nitrile reaction in high-temperature water: Kinetics and mechanism. *Aiche Journal*, 1997, 43(8), 2048-2058.
48. Kim, J. H., Britten, J., and Chin, J., Kinetics and Mechanism of a Co(III) Complex Catalyzed Hydration of Nitriles. *Journal of the American Chemical Society*, 1993, 115(9), 3618-3622.
49. Curtis, N. J., Hagen, K. S., and Sargeson, A. M., Intramolecular Hydrolysis of Coordinated Acetonitrile in a Binuclear μ -Amido-Octaamminedicobalt(III) Complex. *Journal of the Chemical Society-Chemical Communications*, 1984, (23), 1571-1573.
50. Curtis, N. J. and Sargeson, A. M., Synthesis and Base Hydrolysis of Pentaammine N,N-Dimethylformamide and Acetonitrile Complexes of Rh(III) and Ir(III). *Journal of the American Chemical Society*, 1984, 106(3), 625-630.
51. Zanella, A. W. and Ford, P. C., Base Hydrolyses of Penta-Ammineruthenium(III) Complexes of Organonitriles. *Journal of the Chemical Society-Chemical Communications*, 1974, (19), 795-796.
52. Chin, C. S., Chong, D., Lee, B., Jeong, H., Won, G., Do, Y., and Park, Y. J., Activation of acetonitrile in $[\text{Cp}^*\text{Ir}(\eta^3\text{-CH}_2\text{CHCHPh})(\text{NCMe})]^+$: Crystal

- structures of iridium-amidine, imino-ether, amido, and amide complexes. *Organometallics*, 2000, 19(4), 638-648.
53. Rouschias, G. and Wilkinson, G., The Chemistry of Rhenium-Nitrile Complexes. *J. Chem. Soc., A*, 1968, 489-495.
54. Bokach, N. A., Kukushkin, V. Y., Kuznetsov, M. L., Garnovskii, D. A., Natile, G., and Pombeiro, A. J. L., Direct addition of alcohols to organonitriles activated by ligation to a platinum(IV) center. *Inorganic Chemistry*, 2002, 41(8), 2041-2053.
55. Khan, M. M. T. and Martell, A. E., *Homogeneous Catalysis by Metal Complexes*. Vol. II. New York: Academic Press, 1974. 91.
56. Khan, M. M. T., Halligudi, S. B., and Shukla, S., Hydration of Acetylene to Acetaldehyde Using $K[Ru^{III}(EDTA-H)Cl]2H_2O$. *Journal of Molecular Catalysis*, 1990, 58(3), 299-305.
57. Harman, W. D., Dobson, J. C., and Taube, H., Alkyne Addition-Reactions on Pentaammineosmium(II) - the Formation of π -Enol and π -Vinyl Ether Complexes. *Journal of the American Chemical Society*, 1989, 111(8), 3061-3062.
58. Blum, J., Huminer, H., and Alper, H., Alkyne Hydration Promoted by $RhCl_3$ and Quaternary Ammonium-Salts. *Journal of Molecular Catalysis*, 1992,

- 75(2), 153-160.
59. Imai, K., Imai, K., and Utimoto, K., Regioselective Hydration of Alkynones by Palladium Catalysis. *Tetrahedron Letters*, 1987, 28(27), 3127-3130.
 60. Badrieh, Y., Kayyal, A., and Blum, J., Rearrangement, Hydrochlorination and Hydration of Conjugated Alkynones by Platinum(IV) Compounds under Homogeneous and under Biphasic Conditions. *Journal of Molecular Catalysis*, 1992, 75(2), 161-167.
 61. Hiscox, W. and Jennings, P. W., Catalytic Hydration of Alkynes with Zeise Dimer. *Organometallics*, 1990, 9(7), 1997-1999.
 62. Baidossi, W., Lahav, M., and Blum, J., Hydration of alkynes by a PtCl₄-CO catalyst. *Journal of Organic Chemistry*, 1997, 62(3), 669-672.
 63. Haak, E., Bytschkov, I., and Doye, S., Intermolecular hydroamination of alkynes catalyzed by dimethyltitanocene. *Angewandte Chemie-International Edition*, 1999, 38(22), 3389-3391.
 64. Haak, E., Siebeneicher, H., and Doye, S., An ammonia equivalent for the dimethyltitanocene-catalyzed intermolecular hydroamination of alkynes. *Organic Letters*, 2000, 2(13), 1935-1937.
 65. Pohlki, F. and Doye, S., The mechanism of the [Cp₂TiMe₂]-catalyzed intermolecular hydroamination of alkynes. *Angewandte Chemie-International*

- Edition*, 2001, 40(12), 2305-2308.
66. Johnson, J. S. and Bergman, R. G., Imidotitanium complexes as hydroamination catalysts: Substantially enhanced reactivity from an unexpected cyclopentadienide/amide ligand exchange. *Journal of the American Chemical Society*, 2001, 123(12), 2923-2924.
 67. Straub, B. F. and Hofmann, P., Copper(I) carbenes: The synthesis of active intermediates in copper-catalyzed CS cyclopropanation. *Angewandte Chemie-International Edition*, 2001, 40(7), 1288-1290.
 68. Shi, Y. H., Ciszewski, J. T., and Odom, A. L., $\text{Ti}(\text{NMe}_2)_4$ as a precatalyst for hydroamination of alkynes with primary amines. *Organometallics*, 2001, 20(19), 3967-3969.
 69. Cao, C. S., Ciszewski, J. T., and Odom, A. L., Hydroamination of alkynes catalyzed by a titanium pyrrolyl complex. *Organometallics*, 2001, 20(24), 5011-5013.
 70. Cao, C. S., Shi, Y. H., and Odom, A. L., Intermolecular alkyne hydroaminations involving 1,1-disubstituted hydrazines. *Organic Letters*, 2002, 4(17), 2853-2856.
 71. Tillack, A., Castro, I. G., Hartung, C. G., and Beller, M., Anti-Markovnikov hydroamination of terminal alkynes. *Angewandte Chemie-International*

Edition, 2002, 41(14), 2541-2543.

72. Bytschkov, I. and Doye, S., Group-IV metal complexes as hydroamination catalysts. *European Journal of Organic Chemistry*, 2003, (6), 935-946.
73. Uchimaru, Y., N-H activation vs. C-H activation: ruthenium-catalysed regioselective hydroamination of alkynes and hydroarylation of an alkene with N-methylaniline. *Chemical Communications*, 1999, (12), 1133-1134.
74. Tokunaga, M., Eckert, M., and Wakatsuki, Y., Ruthenium-catalyzed intermolecular hydroamination of terminal alkynes with anilines: A practical synthesis of aromatic ketimines. *Angewandte Chemie-International Edition*, 1999, 38(21), 3222-3225.
75. Tokunaga, M., Ota, M., Haga, M. A., and Wakatsuki, Y., A practical one-pot synthesis of 2,3-disubstituted indoles from unactivated anilines. *Tetrahedron Letters*, 2001, 42(23), 3865-3868.
76. Kadota, I., Shibuya, A., Lutete, L. M., and Yamamoto, Y., Palladium benzoic acid catalyzed hydroamination of alkynes. *Journal of Organic Chemistry*, 1999, 64(13), 4570-4571.
77. Shimada, T. and Yamamoto, Y., Palladium-catalyzed intermolecular hydroamination of alkynes: A dramatic rate-enhancement effect of o-aminophenol. *Journal of the American Chemical Society*, 2002, 124(43),

12670-12671.

78. Ohkuma, T., Takeno, H., Honda, Y., and Noyori, R., Asymmetric hydrogenation of ketones with polymer-bound BINAP/diamine ruthenium catalysts. *Advanced Synthesis & Catalysis*, 2001, 343(4), 369-375.
79. Noyori, R., Yamakawa, M., and Hashiguchi, S.; Metal-ligand bifunctional catalysis: A nonclassical mechanism for asymmetric hydrogen transfer between alcohols and carbonyl compounds. *Journal of Organic Chemistry*, 2001, 66(24), 7931-7944.
80. Alonso, D. A., Brandt, P., Nordin, S. J. M., and Andersson, P. G., Ru(arene)(amino alcohol)-catalyzed transfer hydrogenation of ketones: Mechanism and origin of enantioselectivity. *Journal of the American Chemical Society*, 1999, 121(41), 9580-9588.
81. Yamakawa, M., Ito, H., and Noyori, R., The metal-ligand bifunctional catalysis: A theoretical study on the ruthenium(II)-catalyzed hydrogen transfer between alcohols and carbonyl compounds. *Journal of the American Chemical Society*, 2000, 122(7), 1466-1478.
82. Abdur-Rashid, K., Lough, A. J., and Morris, R. H., Ruthenium dihydride $\text{RuH}_2(\text{PPh}_3)_2((\text{R,R})\text{-cyclohexyldiamine})$ and ruthenium monohydride $\text{RuHCl}(\text{PPh}_3)_2((\text{R,R})\text{-cyclohexyldiamine})$: Active catalyst and catalyst

- precursor for the hydrogenation of ketones and imines. *Organometallics*, 2000, 19(14), 2655-2657.
83. Abdur-Rashid, K., Faatz, M., Lough, A. J., and Morris, R. H., Catalytic cycle for the asymmetric hydrogenation of prochiral ketones to chiral alcohols: Direct hydride and proton transfer from chiral catalysts trans-Ru(H)₂(diphosphine)(diamine) to ketones and direct addition of dihydrogen to the resulting hydridoamido complexes. *Journal of the American Chemical Society*, 2001, 123(30), 7473-7474.
84. Morris, R. H., Abdur-Rashid, K., Clapham, S. E., Hadzovic, A., Lough, A., and Harvey, J. N., Mechanism of the hydrogenation of ketones catalyzed by dihydrido(diamine)ruthenium(II) complexes. *Abstracts of Papers of the American Chemical Society*, 2002, 224, U733-U733.
85. Ohkuma, T., Ooka, H., Hashiguchi, S., Ikariya, T., and Noyori, R., Practical Enantioselective Hydrogenation of Aromatic Ketones. *Journal of the American Chemical Society*, 1995, 117(9), 2675-2676.
86. Doucet, H., Ohkuma, T., Murata, K., Yokozawa, T., Kozawa, M., Katayama, E., England, A. F., Ikariya, T., and Noyori, R., trans-[RuCl₂(phosphane)₂(1,2-diamine)] and chiral trans-[RuCl₂(diphosphane)(1,2-diamine)]: Shelf-stable precatalysts for the

- rapid, productive, and stereoselective hydrogenation of ketones. *Angewandte Chemie-International Edition*, 1998, 37(12), 1703-1707.
87. Hashiguchi, S., Fujii, A., Takehara, J., Ikariya, T., and Noyori, R., Asymmetric Transfer Hydrogenation of Aromatic Ketones Catalyzed by Chiral Ruthenium(II) Complexes. *Journal of the American Chemical Society*, 1995, 117(28), 7562-7563.
88. Uematsu, N., Fujii, A., Hashiguchi, S., Ikariya, T., and Noyori, R., Asymmetric transfer hydrogenation of imines. *Journal of the American Chemical Society*, 1996, 118(20), 4916-4917.
89. Haack, K. J., Hashiguchi, S., Fujii, A., Ikariya, T., and Noyori, R., The catalyst precursor, catalyst, and intermediate in the Ru-II-promoted asymmetric hydrogen transfer between alcohols and ketones. *Angewandte Chemie-International Edition in English*, 1997, 36(3), 285-288.
90. Palmer, M. J. and Wills, M., Asymmetric transfer hydrogenation of C=O and C=N bonds. *Tetrahedron-Asymmetry*, 1999, 10(11), 2045-2061.
91. Noyori, R. and Ohkuma, T., Asymmetric catalysis by architectural and functional molecular engineering: Practical chemo- and stereoselective hydrogenation of ketones. *Angewandte Chemie-International Edition*, 2001, 40(1), 40-73.

92. Ito, M., Hirakawa, M., Murata, K., and Ikariya, T., Hydrogenation of aromatic ketones catalyzed by $(\eta^5\text{-C}_5\text{(CH}_3)_5\text{)Ru}$ complexes bearing primary amines. *Organometallics*, 2001, 20(3), 379-381.
93. Kubas, G. J., Molecular-Hydrogen Complexes - Coordination of a Sigma-Bond to Transition-Metals. *Accounts of Chemical Research*, 1988, 21(3), 120-128.
94. Crabtree, R. H., Dihydrogen Complexes - Some Structural and Chemical Studies. *Accounts of Chemical Research*, 1990, 23(4), 95-101.
95. Jessop, P. G. and Morris, R. H., Reactions of Transition-Metal Dihydrogen Complexes. *Coordination Chemistry Reviews*, 1992, 121, 155-284.
96. Heinekey, D. M. and Oldham, W. J., Coordination Chemistry of Dihydrogen. *Chemical Reviews*, 1993, 93(3), 913-926.
97. Crabtree, R. H., Transition-Metal Complexation of Sigma-Bonds. *Angewandte Chemie-International Edition in English*, 1993, 32(6), 789-805.
98. Esteruelas, M. A. and Ore, L. A., Dihydrogen complexes as homogeneous reduction catalysts. *Chemical Reviews*, 1998, 98(2), 577-588.
99. Grundemann, S., Ulrich, S., Limbach, H. H., Golubev, N. S., Denisov, G. S., Epstein, L. M., Sabo-Etienne, S., and Chaudret, B., Solvent-assisted reversible proton transfer within an intermolecular dihydrogen bond and characterization

- of an unstable dihydrogen complex. *Inorganic Chemistry*, 1999, 38(11), 2550-2551.
100. Casey, C. P., Singer, S. W., Powell, D. R., Hayashi, R. K., and Kavana, M., Hydrogen transfer to carbonyls and imines from a hydroxycyclopentadienyl ruthenium hydride: Evidence for concerted hydride and proton transfer. *Journal of the American Chemical Society*, 2001, 123(6), 1090-1100.
101. Wilkinson, G., Stone, F. G. A., and Abel, E. W., *Comprehensive Organometallics Chemistry*. Vol. 3-7: Oxford, 1982.
102. *Adv. Organomet. Chem.* Vol. 1-34, 1964-1992.
103. Okuda, J., *Nachr. Chem. Tech. Lab.* Vol. 41, 1993.
104. Okuda, J., *Top. Curr. Chem.* Vol. 160, 1991.
105. Janiak, J. and Schumann, H., *Adv. Organomet. Chem.* Vol. 33, 1991.
106. Caddy, P., Green, M., O'Brien, E., Smart, L. E., and Woodward, P., Reactivity of η^5 -Indenylrhodium(I) Complexes - Cyclocotrimerization of Alkynes with Alkenes. *Angewandte Chemie-International Edition in English*, 1977, 16(9), 648-649.
107. Caddy, P., Green, M., O'Brien, E., Smart, L. E., and Woodward, P., Reactions of Coordinated Ligands .22. The Reactivity of "Bis(Ethylene)(η^5 -Indenyl)Rhodium in Displacement-Reactions with Olefins,

- Dienes, and Acetylenes - Crystal-Structure of η^5 -Indenyl(1-2-3-4- η^4 -[6-Endo-Propen-2-yl-1,2,3,4-Tetrakis(Trifluoromethyl)Cyclohexa-1,3-Diene])Rhodium Formed in a Cyclo-Cotrimerization Reactions. *Journal of the Chemical Society-Dalton Transactions*, 1980, (6), 962-972.
108. Rerek, M. E., Ji, L. N., and Basolo, F., The Indenyl Ligand Effect on the Rate of Substitution-Reactions of $\text{Rh}(\eta\text{-C}_9\text{H}_7)(\text{CO})_2$ and $\text{Mn}(\eta\text{-C}_9\text{H}_7)(\text{CO})_3$. *Journal of the Chemical Society-Chemical Communications*, 1983, (21), 1208-1209.
109. Rerek, M. E. and Basolo, F., Kinetics and Mechanism of Substitution-Reactions of η^5 -Cyclopentadienyldicarbonylrhodium(I) Derivatives - Rate Enhancement of Associative Substitution in Cyclopentadienylmetal Compounds. *Journal of the American Chemical Society*, 1984, 106(20), 5908-5912.
110. Kakkar, A. K., Taylor, N. J., Calabrese, J. C., Nugent, W. A., Roe, D. C., Connaway, E. A., and Marder, T. B., An Unusual Rotational Distortion in an $[(\eta\text{-Indenyl})\text{RhI}_2]$ Complex - Molecular-Structures of $[(\eta\text{-1,2,3-Me}_3\text{C}_9\text{H}_4)\text{Rh}(\eta\text{-C}_2\text{H}_4)_2]$ and $[(\eta\text{-C}_9\text{H}_7)\text{Rh}(\text{CO})_2]$. *Journal of the Chemical Society-Chemical Communications*, 1989, (15), 990-992.
111. Merola, J. S. and Kacmarcik, R. T., Synthesis and Reaction Chemistry of

- (η^5 -Indenyl)(Cyclooctadiene)Iridium - Migration of Indenyl from Iridium to Cyclooctadiene. *Organometallics*, 1989, 8(3), 778-784.
112. Kakkar, A. K., Jones, S. F., Taylor, N. J., Collins, S., and Marder, T. B., The Hapticity of η -Indenyl Complexes - Molecular-Structures of $[(\eta^5\text{-C}_9\text{R}_7)\text{Rh}(\eta^4\text{-COD})]$ (R = H, Me) (COD = Cyclo-Octa-5-Diene). *Journal of the Chemical Society-Chemical Communications*, 1989, (19), 1454-1456.
113. Marder, T. B. and Williams, I. D., Facile Displacement of an η^5 -Indenyl Ligand - Crystal-Structure of the $[\text{Rh}(\text{Me}_2\text{PCH}_2\text{CH}_2\text{PMe}_2)_2]^+$ Salt of the Naked Indenyl Anion. *Journal of the Chemical Society-Chemical Communications*, 1987, (19), 1478-1480.
114. Huffman, M. A. and Liebeskind, L. S., Insertion of (η^5 -Indenyl)Cobalt(I) into Cyclobutenones - the 1st Synthesis of Phenols from Isolated Vinylketene Complexes. *Journal of the American Chemical Society*, 1990, 112(23), 8617-8618.
115. Marder, T. B., Calabrese, J. C., Roe, D. C., and Tulip, T. H., The Slip-Fold Distortion of π -Bound Indenyl Ligands - Dynamic NMR and X-Ray Crystallographic Studies of (η -Indenyl) RhL_2 Complexes. *Organometallics*, 1987, 6(9), 2012-2014.
116. Merola, J. S., Kacmarcik, R. T., and Vanengen, D., η^5 to η^3 Conversion in

- Indenyliridium Complexes. *Journal of the American Chemical Society*, 1986, 108(2), 329-331.
117. Kakkar, A. K., Taylor, N. J., and Marder, T. B., Synthesis and Structure of the $[\text{Rh}_2(\text{dmpe})_4(\mu\text{-dmpe})]^{2+}$ Salt of the Naked Cyclopentadienyl Anion - a Comparison of the Reactivity of $[(\eta\text{-Indenyl})\text{Rh}(\eta\text{-C}_2\text{H}_4)_2]$ and $[(\eta\text{-C}_5\text{H}_5)\text{Rh}(\eta\text{-C}_2\text{H}_4)_2]$. *Organometallics*, 1989, 8(7), 1765-1768.
118. Hart-Davis, A. J. and Mawby, R. J., Reaction of π -Indenyl Complexes of Transition Metals. Part I. Kinetics and Mechanisms of Reactions of Tricarbonyl- π -indenylmethylmolybdenum with Phosphorus(III) Ligands. *J. Chem. Soc., A*, 1969, 2403-2407.
119. Oconnor, J. M. and Casey, C. P., Ring-Slippage Chemistry of Transition-Metal Cyclopentadienyl and Indenyl Complexes. *Chemical Reviews*, 1987, 87(2), 307-318.
120. Kubas, G. J., Kiss, G., and Hoff, C. D., Solution Calorimetric, Equilibrium, and Synthetic Studies of Oxidative Addition Reductive Elimination of $\text{C}_5\text{R}_3\text{H}$ (R = H, Me, Indenyl) to/from the Complexes $\text{M}(\text{CO})_3(\text{RCN})_3/(\eta^5\text{-C}_5\text{R}_3)\text{M}(\text{CO})_3\text{H}$ (M = Cr, Mo, W). *Organometallics*, 1991, 10(8), 2870-2876.
121. Calhorda, M. J., Gamelas, C. A., Romao, C. C., and Veiros, L. F., Compared reductive chemistry of molybdenocene and indenyl-substituted complexes.

- European Journal of Inorganic Chemistry*, 2000, (2), 331-340.
122. Veiros, L. F., The role of haptotropic shifts in phosphine addition to tricarbonylmanganese organometallic complexes: The indenyl effect revisited. *Organometallics*, 2000, 19(16), 3127-3136.
123. Calhorda, M. J. and Veiros, L. F., Ring slippage in indenyl complexes: structure and bonding. *Coordination Chemistry Reviews*, 1999, 186, 37-51.
124. Ascenso, J. R., Goncalves, I. S., Herdtweck, E., and Romão, C. C., Ring slippage in indenyl derivatives of molybdenum and tungsten. *Journal of Organometallic Chemistry*, 1996, 508(1-2), 169-181.
125. Garrett, C. E. and Fu, G. C., Exploiting η^5 - to η^3 -indenyl ring slippage to access a directed reaction: Ether-directed, rhodium-catalyzed olefin hydroboration. *Journal of Organic Chemistry*, 1998, 63(5), 1370-1371.
126. Muller, C., Vos, D., and Jutzi, P., Results and perspectives in the chemistry of side-chain-functionalized cyclopentadienyl compounds. *Journal of Organometallic Chemistry*, 2000, 600(1-2), 127-143.
127. Jutzi, P. and Redeker, T., Aminoethyl-functionalized cyclopentadienyl complexes of d-block elements. *European Journal of Inorganic Chemistry*, 1998, (6), 663-674.
128. Jutzi, P. and Siemeling, U., Cyclopentadienyl Compounds with Nitrogen

- Donors in the Side-Chain. *Journal of Organometallic Chemistry*, 1995, 500(1-2), 175-185.
129. Jutzi, P. and Dahlhaus, J., (Dimethylaminoethyl)Cyclopentadienyl Ligands in Compounds of S-Block and P-Block Elements. *Coordination Chemistry Reviews*, 1994, 137, 179-199.
130. Pearson, R. G. and Scott, A., *Survey of Progress in Chemistry*. New York: Academic Press, 1969.
131. Jeffrey, J. C. and Rauchfuss, T. B., Metal-Complexes of Hemilabile Ligands - Reactivity and Structure of Dichlorobis(Ortho-(Diphenylphosphino)Anisole)Ruthenium(II). *Inorganic Chemistry*, 1979, 18(10), 2658-2666.
132. Slone, C. S., Weinberger, D. A., and Mirkin, C. A., The transition metal coordination chemistry of hemilabile ligands. *Progress in Inorganic Chemistry*, Vol 48, 1999, 48, 233-350.
133. Williams, R. A., Hanusa, T. P., and Huffman, J. C., Structures of Ionic Decamethylmetallocenes - Crystallographic Characterization of $(\text{Me}_5\text{C}_5)_2\text{Ca}$ and $(\text{Me}_5\text{C}_5)_2\text{Ba}$ and a Comparison with Related Organolanthanide Species. *Organometallics*, 1990, 9(4), 1128-1134.
134. Anwander, R., Herrmann, W. A., Scherer, W., and Munck, F. C., Lanthanoid

- Complexes .6. Monomeric Homoleptic $\text{Ln}(\text{R}^{\text{D}_0}\text{Cp})_3$ Complexes ($\text{Ln}=\text{La}, \text{Nd}$) with Amino-Functionalized Cyclopentadienyl Ligands. *Journal of Organometallic Chemistry*, 1993, 462(1-2), 163-174.
135. Flores, J. C., Chien, J. C. W., and Rausch, M. D., ([2-(Dimethylamino)Ethyl]Cyclopentadienyl)Trichlorotitanium - a New-Type of Olefin Polymerization Catalyst. *Organometallics*, 1994, 13(11), 4140-4142.
136. Engelhardt, L. M., Papasergio, R. I., Raston, C. L., and White, A. H., Crystal-Structures of Trichloro (η^5 -Cyclopentadienyl)Titanium(IV) and Zirconium(IV). *Organometallics*, 1984, 3(1), 18-20.
137. Jutzi, P., Kristen, M. O., Dahlhaus, J., Neumann, B., and Stammer, H. G., Cobalt Complexes with the 1-[2-(N,N-Dimethylamino)Ethyl]-2,3,4,5-Tetramethylcyclopentadienyl Ligand. *Organometallics*, 1993, 12(8), 2980-2985.
138. Jutzi, P., Kristen, M. O., Neumann, B., and Stammer, H. G., Rhodium and Iridium Complexes with the 1-(2-(Dimethylamino)Ethyl)-2,3,4,5-Tetramethylcyclopentadienyl Ligand. *Organometallics*, 1994, 13(10), 3854-3861.
139. Nlate, S., Herdtweck, E., and Fischer, R. A., An intermolecularly donor-stabilized silanediyl(silyl)nickel complex: Combined Si-Si bond

- cleavage and methyl migration between silicon centers. *Angewandte Chemie-International Edition in English*, 1996, 35(16), 1861-1863.
140. Wang, T. F., Lee, T. Y., Chou, J. W., and Ong, C. W., Half-Sandwich Complex with Intramolecular Amino Group Coordination - Synthesis of Molybdenum Iodide Complexes. *Journal of Organometallic Chemistry*, 1992, 423(1), 31-38.
141. Wang, T. F. and Wen, Y. S., Half-Sandwich Complexes with Intramolecular Amino Group Coordination - Synthesis and Structure of Cationic Molybdenum Dienyl Complexes. *Journal of Organometallic Chemistry*, 1992, 439(2), 155-162.
142. Wang, T. F., Lai, C. Y., and Wen, Y. S., Preparation and reactions of half-sandwich rhenium nitrosyl complexes containing a tethered amino ligand. *Journal of Organometallic Chemistry*, 1996, 523(2), 187-195.
143. Wang, T. F., Hwu, C. C., Tsai, C. W., and Lin, K. J., Formation of a carbon dioxide complex of rhenium via formal oxidation of a carbon monoxide ligand. *Organometallics*, 1997, 16(14), 3089-3090.
144. Wang, T. F., Lai, C. Y., Hwu, C. C., and Wen, Y. S., Half-sandwich aminorhenium complexes: Preparation and regioselective N-versus Re-alkylations. *Organometallics*, 1997, 16(6), 1218-1223.
145. Wang, T. F., Lee, T. Y., Wen, Y. S., and Liu, L. K., Synthesis of a Novel

- Bidentate Complex of $\eta^5\text{-C}_5\text{H}_4\text{CH}_2\text{CH}(\text{CH}_3)\text{N}(\text{CH}_3)(\text{C}_3\text{H}_5)\text{Mn}(\text{CO})_2$. *Journal of Organometallic Chemistry*, 1991, 403(3), 353-358.
146. Frankcom, T. M., Green, J. C., Nagy, A., Kakkar, A. K., and Marder, T. B., Electronic-Structure and Photoelectron-Spectroscopy of D(8) Rhodium Indenyl Complexes. *Organometallics*, 1993, 12(9), 3688-3697.
147. Trost, B. M. and Kulawiec, R. J., Chemoselectivity in the Ruthenium-Catalyzed Redox Isomerization of Allyl Alcohols. *Journal of the American Chemical Society*, 1993, 115(5), 2027-2036.
148. Halterman, R. L., Synthesis and Applications of Chiral Cyclopentadienylmetal Complexes. *Chemical Reviews*, 1992, 92(5), 965-994.
149. Razavi, A. and Atwood, J. L., Isospecific Propylene Polymerization with Unbridged Group-4 Metallocenes. *Journal of the American Chemical Society*, 1993, 115(16), 7529-7530.
150. Hauptman, E., Saboetienne, S., White, P. S., Brookhart, M., Garner, J. M., Fagan, P. J., and Calabrese, J. C., Design and Study of Rh(III) Catalysts for the Selective Tail-to-Tail Dimerization of Methyl Acrylate. *Journal of the American Chemical Society*, 1994, 116(18), 8038-8060.
151. Bonifaci, C., Ceccon, A., Gambaro, A., Ganis, P., Mantovani, L., Santi, S., and Venzo, A., Heterobimetallic Heptamethylindenyl Complexes of Cr^0 and

- Rh^I: Trans-[Cr(CO)₃-Indenyl-Asterisk-RhL₂] (L₂=COD, L=CO). *Journal of Organometallic Chemistry*, 1994, 475(1-2), 267-276.
152. Deboer, H. J. R. and Royan, B. W., Electronic Effects in Alkene Polymerization Catalyzed by Substituted Bis(Indenyl) Zirconium Complexes and Methylalumoxane. *Journal of Molecular Catalysis*, 1994, 90(1-2), 171-175.
153. Lewis, J., Raithby, P. R., and Ward, G. N., Polynuclear Clusters of Fused-Ring Hydrocarbons - the Synthesis and X-Ray Structure of [Os₄H(CO)₉(μ₃-η²-η²-η⁵-C₁₃H₁₅)] (C₁₃H₁₅=1,3-Diethylindenyl). *Journal of the Chemical Society-Chemical Communications*, 1995, (7), 755-756.
154. Ohare, D., Murphy, V., Diamond, G. M., Arnold, P., and Mountford, P., Synthesis of Permethylindenyl Complexes of the Early Transition-Metals - Crystal-Structures of Ti(η⁵-C₉Me₇)Cl₃ and Zr(η⁵-C₉Me₇)₂Cl₂. *Organometallics*, 1994, 13(12), 4689-4694.
155. Ceccon, A., Elsevier, C. J., Ernsting, J. M., Gambaro, A., Santi, S., and Venzo, A., Indenyl Hapticity in (η-Indenyl-RhL₂) and Cr(CO)₃(μ-η-η-Indenyl-RhL₂) Complexes - a H¹, C¹³ and Rh¹⁰³ NMR Spectroscopic Study. *Inorganica Chimica Acta*, 1993, 204(1), 15-26.
156. Erker, G., Aulbach, M., Knickmeier, M., Wingbermhle, D., Kruger, C., Nolte,

- M., and Werner, S., The Role of Torsional Isomers of Planarly Chiral Nonbridged Bis(Indenyl)Metal Type Complexes in Stereoselective Propene Polymerization. *Journal of the American Chemical Society*, 1993, 115(11), 4590-4601.
157. Honan, M. B., Atwood, J. L., Bernal, I., and Herrmann, W. A., Crystal and Molecular-Structure of 1-Bromobenzocymantrene, $(\eta^5\text{-C}_9\text{H}_6\text{Br})\text{Mn}(\text{CO})_3$. *Journal of Organometallic Chemistry*, 1979, 179(4), 403-410.
158. Han, Y. H., Heeg, M. J., and Winter, C. H., Permercuration of Ferrocenes and Ruthenocenes - New Approaches to Complexes Bearing Perhalogenated Cyclopentadienyl Ligands. *Organometallics*, 1994, 13(8), 3009-3019.
159. Scott, P., Rief, U., Diebold, J., and Brintzinger, H. H., Homobimetallic and Heterobimetallic Bis(Fulvalene) Complexes from Bis(Cyclopentadienyl)-Substituted and Bis(Indenyl)-Substituted Ferrocenes. *Organometallics*, 1993, 12(8), 3094-3101.
160. Grotjahn, D. B., Incarvito, C. D., and Rheingold, A. L., Combined effects of metal and ligand capable of accepting a proton or hydrogen bond catalyze anti-Markovnikov hydration of terminal alkynes. *Angewandte Chemie-International Edition*, 2001, 40(20), 3884.
161. Tokunaga, M., Suzuki, T., Koga, N., Fukushima, T., Horiuchi, A., and

- Wakatsuki, Y., Ruthenium-catalyzed hydration of 1-alkynes to give aldehydes: Insight into anti-Markovnikov regiochemistry. *Journal of the American Chemical Society*, 2001, 123(48), 11917-11924.
162. Suzuki, T., Tokunaga, M., and Wakatsuki, Y., Ruthenium complex-catalyzed anti-Markovnikov hydration of terminal alkynes. *Organic Letters*, 2001, 3(5), 735-737.
163. Basallote, M. G., Duran, J., Fernandez-Trujillo, M. J., Manez, M. A., and de la Torre, J. R., Kinetics of formation of dihydrogen complexes: protonation of cis-[FeH₂{P(CH₂CH₂PPh₂)₃} with acids in tetrahydrofuran. *Journal of the Chemical Society-Dalton Transactions*, 1998, (5), 745-750.
164. Schlaf, M. and Morris, R. H., A Dihydrogen Complex, [Os(η^2 -H₂)(CO)(quS)(PPh₃)₂]⁺, in Equilibrium with Its Coordinated Thiol Tautomer (quS=Quinoline-8-Thiolate). *Journal of the Chemical Society-Chemical Communications*, 1995, (6), 625-626.
165. Lee, J. C., Peris, E., Rheingold, A. L., and Crabtree, R. H., An Unusual Type of H...H Interaction - Ir-H...H-O and Ir-H...H-N Hydrogen-Bonding and Its Involvement in Sigma-Bond Metathesis. *Journal of the American Chemical Society*, 1994, 116(24), 11014-11019.
166. Oro, L. A., Ciriano, M. A., Campo, M., Focesfoces, C., and Cano, F. H.,

- Indenyl Complexes of Ruthenium(II) - Crystal-Structure of $[\text{Ru}(\text{CO})(\text{PPh}_3)_2(\eta^5\text{-C}_9\text{H}_7)]\text{ClO}_4 \cdot 1/2\text{CH}_2\text{Cl}_2$. *Journal of Organometallic Chemistry*, 1985; 289(1), 117-131.
167. Chan, W. C., Lau, C. P., Chen, Y. Z., Fang, Y. Q., Ng, S. M., and Jia, G. C., Syntheses and characterization of hydrotris(1-pyrazolyl)borate dihydrogen complexes of ruthenium and their roles in catalytic hydrogenation reactions. *Organometallics*, 1997, 16(1), 34-44.
168. Ng, S. M., Fang, Y. Q., Lau, C. P., Wong, W. T., and Jia, G. C., Synthesis, characterization, and acidity of ruthenium dihydrogen complexes with 1,4,7-triazacyclononane, 1,4,7-trimethyl-1,4,7-triazacyclononane, and hydrotris(pyrazolyl)borato ligands. *Organometallics*, 1998, 17(10), 2052-2059.
169. Alcock, N. W., Burns, I. D., Claire, K. S., and Hill, A. F., Ruthenatetaboranes - Synthesis of $[\text{Ru}(\text{B}_3\text{H}_8)(\text{PPh}_3)(\text{HB}(\text{pz})_3)]$ and Crystal-Structure of $[\text{RuCl}(\text{PPh}_3)_2(\text{HB}(\text{pz})_3)]$ (pz = Pyrazol-1-yl). *Inorganic Chemistry*, 1992, 31(13), 2906-2908.
170. Bruce, M. I., Humphrey, M. G., Swincer, A. G., and Wallis, R. C., Cyclopentadienyl-Ruthenium and Cyclopentadienyl-Osmium Chemistry .23. Synthesis and Reactions of Some Hydrido Complexes Containing Ruthenium

- or Osmium, and Related Chemistry. *Australian Journal of Chemistry*, 1984, 37(8), 1747-1755.
171. Gamasa, M. P., Gimeno, J., GonzalezBernardo, C., MartinVaca, B. M., Monti, D., and Bassetti, M., Phosphine substitution in indenyl- and cyclopentadienylruthenium complexes. Effect of the η^5 ligand in a dissociative pathway. *Organometallics*, 1996, 15(1), 302-308.
172. Kakkar, A. K., Taylor, N. J., Marder, T. B., Shen, J. K., Hallinan, N., and Basolo, F., Kinetics and Mechanism of CO Ligand Substitution in the Ring-Substituted Indenyl Rhodium Complexes $[(\eta^5\text{-C}_9\text{R}_n\text{H}_{7-n})\text{Rh}(\text{CO})_2]$. *Inorganica Chimica Acta*, 1992, 200, 219-231.
173. Calhorda, M. J., Romao, C. C., and Veiros, L. F., The nature of the indenyl effect. *Chemistry-a European Journal*, 2002, 8(4), 868-875.
174. Milet, A., Dedieu, A., Kapteijn, G., and vanKoten, G., sigma-bond metathesis reactions involving palladium(II) hydride and methyl complexes: A theoretical assessment. *Inorganic Chemistry*, 1997, 36(15), 3223-3231.
175. Yin, C. Q., Xu, Z. T., Yang, S. Y., Ng, S. M., Wong, K. Y., Lin, Z. Y., and Lau, C. P., Promoting effect of water in ruthenium-catalyzed hydrogenation of carbon dioxide to formic acid. *Organometallics*, 2001, 20(6), 1216-1222.
176. Crabtree, R. H., Lavin, M., and Bonneviot, L., Some Molecular-Hydrogen

- Complexes of Iridium: *Journal of the American Chemical Society*, 1986, 108(14), 4032-4037.
177. Jazzar, R. F. R., Bhatia, P. H., Mahon, M. F., and Whittlesey, M. K., N-heterocyclic carbene stabilized trans-dihydrido aqua and ethanol complexes of ruthenium: Precursors to complexes with Ru-heteroatom bonds. *Organometallics*, 2003, 22(4), 670-683.
178. Rachidi, I. E., Eisenstein, O., and Jean, Y., A Theoretical-Study of the Possible Structures of D₆ M₁₅ Complexes. *New Journal of Chemistry*, 1990, 14(8-9), 671-677.
179. Huang, D. J., Heyn, R. H., Bollinger, J. C., and Caulton, K. G., Oxidative addition of a Si-C(sp) bond to ruthenium: Synthesis and reactivity of Ru(SiMe₃)(C≡CSiMe₃)(CO)(P^tBu₂Me)₂. *Organometallics*, 1997, 16(3), 292-293.
180. Kubacek, P. and Hoffmann, R., Deformations from Octahedral Geometry in d⁴ Transition-Metal Complexes. *Journal of the American Chemical Society*, 1981, 103(15), 4320-4332.
181. Kamata, M., Hirotsu, K., Higuchi, T., Tatsumi, K., Hoffmann, R., Yoshida, T., and Otsuka, S., A Highly Distorted Octohedral d⁴ Compound, cis-Mo(Trans-BuS)₂(Trans-BuNC)₄. *Journal of the American Chemical*

- Society*, 1981, 103(19), 5772-5778.
182. Gusev, D. G., Kuhlman, R., Rambo, J. R., Berke, H., Eisenstein, O., and Caulton, K. G., Structural and Dynamic Properties of $\text{OsH}_2\text{X}_2\text{L}_2$ ($\text{X}=\text{Cl}, \text{Br}, \text{I}$, $\text{L}=(\text{P}^i\text{Pr}_3)$) Complexes - Interconversion between Remarkable Nonoctahedral Isomers. *Journal of the American Chemical Society*, 1995, 117(1), 281-292.
183. Yang, S. Y., Leung, W. H., and Lin, Z. Y., Geometric features and electronic structures of six-coordinated dialkyl and dithiolate complexes of osmium(IV) porphyrins. *Organometallics*, 2001, 20(14), 3198-3201.
184. Damiano, J. P. and Postel, M., $\text{FeCl}_3\text{-H}_2\text{O}$: A specific system for arylacetylene hydration. *Journal of Organometallic Chemistry*, 1996, 522(2), 303-305.
185. Ganguly, S. and Roundhill, D. M., Hydration of Diethyl Maleate in the Presence of Bimetallic Hydroxy Palladium(II) Complexes of 1,2-Bis(Diphenylphosphino)Ethane(dppe) as Catalysts. *Journal of the Chemical Society-Chemical Communications*, 1991, (9), 639-640.
186. Ganguly, S. and Roundhill, D. M., Catalytic Hydration of Diethyl Maleate to Diethyl Malate Using Divalent Complexes of Palladium(II) as Catalysts. *Organometallics*, 1993, 12(12), 4825-4832.
187. Kumar, K. S. R., Baskaran, S., and Chandrasekaran, S., An Unusual Antimarkovnikov Hydration of Alkenes with Titanium(III) Tetrahydroborates.

- Tetrahedron Letters*, 1993, 34(1), 171-174.
188. Gasc, M. B., Lattes, A., and Perie, J. J., Amination of Alkenes. *Tetrahedron*, 1983, 39(5), 703-731.
189. Muller, T. E. and Beller, M., Metal-initiated amination of alkenes and alkynes. *Chemical Reviews*, 1998, 98(2), 675-703.
190. Nobis, M. and Driessen-Holscher, B., Recent developments in transition metal catalyzed intermolecular hydroamination reactions - A breakthrough? *Angewandte Chemie-International Edition*, 2001, 40(21), 3983-3985.
191. Laryer, R. W., The Chemistry of Imines. *Chem. Rev.*, 1963, 489(63), 489-510.
192. Viehe, H. G., *Chemistry of Actylenes*. New York: Marcel Dekker, 1969. 286.
193. Hudrlik, P. F. and Hudrlik, A. M., *The Chemistry of the Carbon-Carbon Triple Bond*. New York: Wiley, 1978. 244.
194. Larock, R. C. and Leong, W. W., *Comprehensive Organic Synthesis*. Oxford: Pergamon Press, 1991. 290.
195. March, J., *Advanced Organic Chemistry*. New York: Wiley, 1992. 769.
196. Muller, T. E., Grosche, M., Herdtweck, E., Pleier, A. K., Walter, E., and Yan, Y. K., Developing transition-metal catalysts for the intramolecular hydroamination of alkynes. *Organometallics*, 2000, 19(2), 170-183.
197. Brunet, J. J. and Neibecker, D., *Catalytic Heterofunctionalization*. Weinheim,

- Germany: Wiley-VCH, 2001. 91.
198. Abel, E. W., Stone, F. G. A., and Wilkinson, G., *Comprehensive Organometallic Chemistry II*: Vol. 7: Pergamon, 1995.
199. Qian, C. T., Li, H. F., Sun, J., and Nie, W. L., Synthesis and crystal structure of bis(2-dimethylaminoethylindenyl) divalent organolanthanides (Ln = Sm, Yb). *Journal of Organometallic Chemistry*, 1999, 585(1), 59-62.
200. Hallman, P. S., Stephenson, T. A., and Wilkinson, G., *Inorg. Synth.*, 1970. 237.
201. Groux, L. F., Belanger-Gariepy, F., Zargarian, D., and Vollmerhaus, R., Preparation and characterization of nickel complexes with eta-indenyl ligands bearing a pendant aminoalkyl chain. *Organometallics*, 2000, 19(8), 1507-1513.
202. Garrou, P. E., Delta-R Ring Contributions to P-31 NMR Parameters of Transition-Metal-Phosphorus Chelate Complexes. *Chemical Reviews*, 1981, 81(3), 229-266.
203. Bianchini, C., Perez, P. J., Peruzzini, M., Zanobini, F., and Vacca, A., Classical and Nonclassical Polyhydride Ruthenium(II) Complexes Stabilized by the Tetrphosphine $P(CH_2CH_2PPh_2)_3$. *Inorganic Chemistry*, 1991, 30(2), 279-287.
204. Chinn, M. S. and Heinekey, D. M., Dihydrogen Complexes of Ruthenium .2. Kinetic and Thermodynamic Considerations Affecting Product Distribution.

- Journal of the American Chemical Society*, 1990, 112(13), 5166-5175.
205. vanderZejden, A. A. H., Novel chiral Lewis acids based on a new asymmetric cyclopentadienyl ligand. *Journal of Organometallic Chemistry*, 1996, 518(1-2), 147-153.
206. Philippopoulos, A. I., Hadjiliadis, N., Hart, C. E., Donnadieu, B., Gowan, P. C., and Poilblanc, R., Transition-metal derivatives of a functionalized cyclopentadienyl ligand. 15. Synthesis and structures of amino cyclopentadienyl derivatives of rhodium(I) and rhodium(III) including water-soluble compounds. *Inorganic Chemistry*, 1997, 36(9), 1842-1849.
207. Park, S. H., Ramachandran, R., Lough, A. J., and Morris, R. H., A New-Type of Intramolecular H...H...H Interaction Involving N-H...H(Ir)...H-N Atoms - Crystal and Molecular-Structure of $[\text{IrH}(\eta^1\text{-SC}_5\text{H}_4\text{NH})_2(\eta^2\text{-SC}_5\text{H}_4\text{N})(\text{PCy}_3)]\text{BF}_4 \cdot 0.72\text{CH}_2\text{Cl}_2$. *Journal of the Chemical Society-Chemical Communications*, 1994, (19), 2201-2202.
208. Park, S. H., Lough, A. J., and Morris, R. H., Iridium(III) complex containing a unique bifurcated hydrogen bond interaction involving Ir-H...H(N)...F-B atoms. Crystal and molecular structure of $[\text{IrH}(\eta^1\text{-SC}_5\text{H}_4\text{NH})(\eta^2\text{-SC}_5\text{H}_4\text{N})(\text{PPh}_3)_2](\text{BF}_4) \cdot 0.5\text{C}_6\text{H}_6$. *Inorganic Chemistry*, 1996, 35(10), 3001-3006.

209. Santi, S. and Broccardo, L., Bond activation by electron transfer in indenyl ruthenium(II) complexes. The electrochemical reduction of $[\text{Ru}(\eta^5\text{-C}_9\text{H}_7)\text{ClL}_2]$ and $[\text{Ru}(\eta^5\text{-C}_9\text{H}_7)(\text{L})_2]^+ \text{L}_2^- = \text{COD}$, $\text{L} = \text{PPh}_3$. *Organometallics*, 2003, 22(17), 3478-3484.
210. Cadierno, V., Gamasa, M. P., Gimeno, J., and Martin-Vaca, B. M., Intramolecular carbon-carbon coupling reactions of a $\kappa^2(\text{P,P})$ -bis(diphenylphosphino)methanide ligand with unsaturated carbene moieties in indenyl-ruthenium(II) complexes. *Journal of Organometallic Chemistry*, 2001, 617(1), 261-268.
211. Fryzuk, M. D., Montgomery, C. D., and Rettig, S. J., Synthesis and Reactivity of Ruthenium Amide Phosphine Complexes - Facile Conversion of a Ruthenium Amide to a Ruthenium Amine Via Dihydrogen Activation and Ortho Metalation - X-Ray Structure of $\text{RuCl}(\text{C}_6\text{H}_4\text{PPh}_2)[\text{NH}(\text{SiMe}_2\text{CH}_2\text{PPh}_2)_2]$. *Organometallics*, 1991, 10(2), 467-473.
212. Khan, M. M. T., Halligudi, S. B., and Shukla, S., Stoichiometric Reduction of Carbon-Dioxide to HCHO and HCOOH by $\text{K}[\text{Ru}^{\text{III}}(\eta\text{-H})\text{Cl}]\cdot 2\text{H}_2\text{O}$. *Journal of Molecular Catalysis*, 1989, 53(3), 305-313.
213. Tsai, J. C. and Nicholas, K. M., Rhodium-Catalyzed Hydrogenation of Carbon-Dioxide to Formic-Acid. *Journal of the American Chemical Society*,

- 1992, 114(13), 5117-5124.
214. Gassner, F. and Leitner, W., CO₂-Activation .3. Hydrogenation of Carbon-Dioxide to Formic-Acid Using Water-Soluble Rhodium Catalysts. *Journal of the Chemical Society-Chemical Communications*, 1993, (19), 1465-1466.
215. Leitner, W., Dinjus, E., and Gassner, F., Activation of Carbon-Dioxide .4. Rhodium-Catalyzes Hydrogenation of Carbon-Dioxide to Formic-Acid. *Journal of Organometallic Chemistry*, 1994, 475(1-2), 257-266.
216. Jessop, P. G., Ikariya, T., and Noyori, R., Homogeneous Catalytic-Hydrogenation of Supercritical Carbon-Dioxide. *Nature*, 1994, 368(6468), 231-233.
217. Fornika, R., Górls, H., Seemann, B., and Leitner, W., Complexes [(P₂)Rh(hfacac)] (P₂=Bidentate Chelating Phosphane, hfacac=Hexafluoroacetylacetonate) as Catalysts for CO₂ Hydrogenation - Correlations between Solid-State Structures, ¹⁰³Rh NMR Shifts and Catalytic Activities. *Journal of the Chemical Society-Chemical Communications*, 1995, (14), 1479-1481.
218. Lau, C. P. and Chen, Y. Z., Hydrogenation of Carbon-Dioxide to Formic-Acid Using a 6,6'-dichloro-2,2'-bipyridine Complex of Ruthenium,

- cis*-[Ru(6,6'-Cl₂bpy)₂(H₂O)₂](CF₃SO₃)₂. *Journal of Molecular Catalysis a-Chemical*, 1995, 101(1), 33-36.
219. Jessop, P. G., Hsiao, Y., Ikariya, T., and Noyori, R., Methyl Formate Synthesis by Hydrogenation of Supercritical Carbon-Dioxide in the Presence of Methanol. *Journal of the Chemical Society-Chemical Communications*, 1995, (6), 707-708.
220. Jessop, P. G., Ikariya, T., and Noyori, R., Homogeneous Hydrogenation of Carbon-Dioxide. *Chemical Reviews*, 1995, 95(2), 259-272.
221. Leitner, W., Carbon-Dioxide as a Raw-Material - the Synthesis of Formic-Acid and Its Derivatives from CO₂. *Angewandte Chemie-International Edition in English*, 1995, 34(20), 2207-2221.
222. Jessop, P. G., Hsiao, Y., Ikariya, T., and Noyori, R., Homogeneous catalysis in supercritical fluids: Hydrogenation of supercritical carbon dioxide to formic acid, alkyl formates, and formamides. *Journal of the American Chemical Society*, 1996, 118(2), 344-355.
223. Hutschka, F., Dedieu, A., Eichberger, M., Fornika, R., and Leitner, W., Mechanistic aspects of the rhodium-catalyzed hydrogenation of CO₂ to formic acid - A theoretical and kinetic study. *Journal of the American Chemical Society*, 1997, 119(19), 4432-4443.

224. Brunner, H. and Fisch, K., Optically-Active Transition-Metal Complexes .101.
Catalytic Hydrosilylation or Hydrogenation at One Coordination Site of
[Cp'Fe(Co)(X)] Fragments. *Angewandte Chemie-International Edition in
English*, 1990, 29(10), 1131-1132.
225. Fung, W. K., Huang, X., Man, M. L., Ng, S. M., Hung, M. Y., Lin, Z. Y., and
Lau, C. P., Dihydrogen-bond-promoted catalysis: Catalytic hydration of
nitriles with the indenylruthenium hydride complex $(\eta^5\text{-C}_9\text{H}_7)\text{Ru}(\text{dppm})\text{H}$
(dppm = bis(diphenylphosphino)methane). *Journal of the American Chemical
Society*, 2003, 125(38), 11539-11544.

Appendix

1H NMR (PPH3)2Cl 17 00:13 2:25 PM 8/20/03

Current Data Parameters
 NAME 1HMR (PPH3) C
 EXPNO 52
 PROCNO 1

F2 - Acquisition Parameters
 Date_ 20030820
 Time 14 26
 INSTRUM spect
 PROBHD 5 mm QNP 1H
 PULPROG zgpg30
 TD 65536
 SOLVENT CDCl3
 NS 16
 DS 4
 SWH 16025.641 MHz
 FIDRES 0.488964 MHz
 AQ 1.0224115 sec
 RG 400.1
 CH 31 200 usec
 DE 4.50 usec
 TE 300.2 K
 D1 2.00000000 sec

===== CHANNEL f1 =====
 NUC1 1H
 P1 9.50 usec
 PL1 -6.00 dB
 SFO1 400.1278883 MHz

F2 - Processing parameters
 SF 400.1300855 MHz
 EQ 16.284
 EM
 SSB 0
 LB 0.30 MHz
 GB 0
 PC 1.00

ID NMR plot parameters
 SI 20.00 cm
 F1 P 9.000 ppm
 F1 360.17 Hz
 F2 P -1.000 ppm
 F2 -400.13 Hz
 PRIN 0.00000000
 WZ 200.05000 MHz

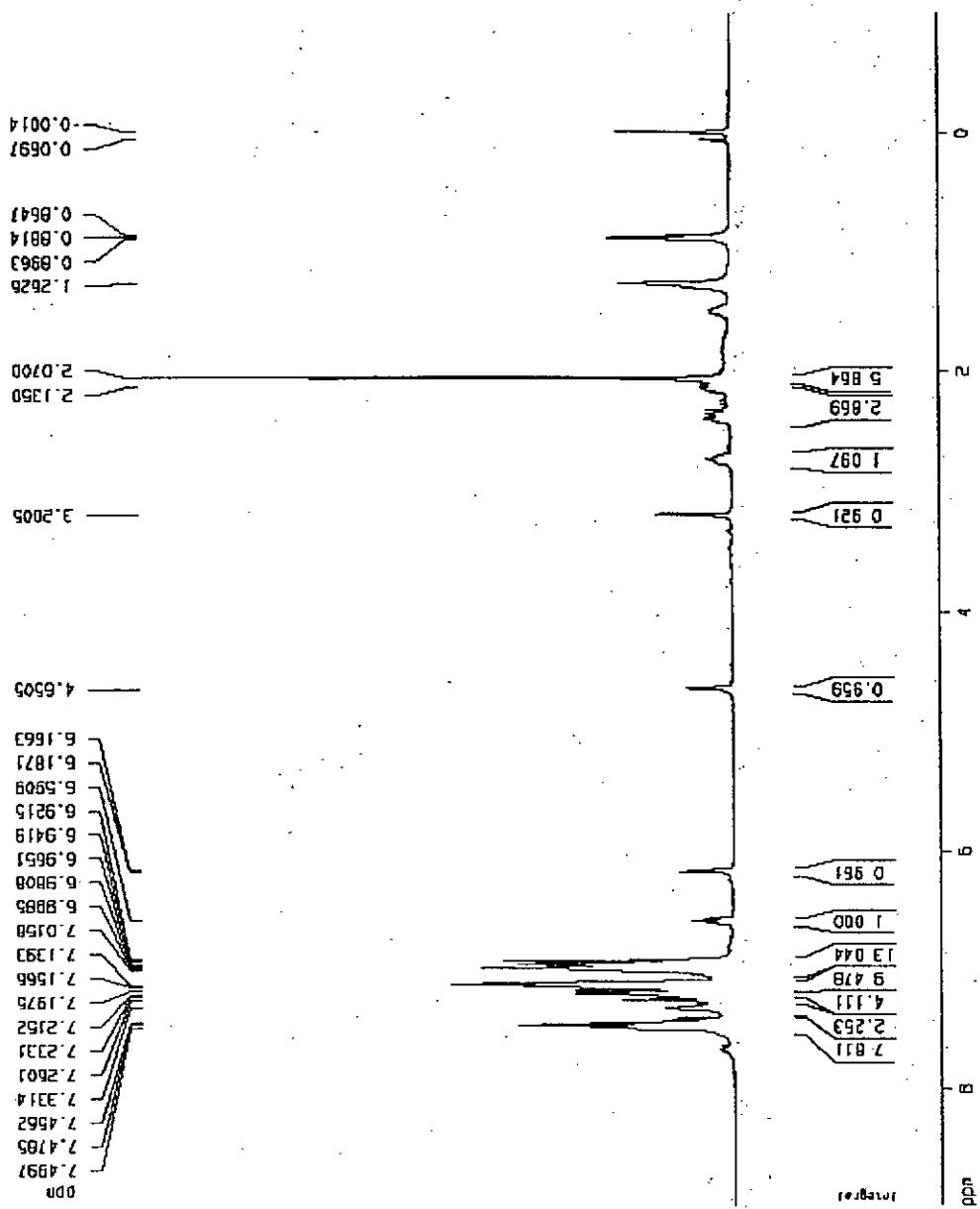


Figure 3.1 400 MHz ¹H-NMR spectrum of (η⁵-C₉H₆CH₂CH₂NMe₂)Ru(PPh₃)₂Cl (17)

13C NMR (PPH3)2Cl in CDCl3 2:24 PM 8/20/03

```

Current Data Parameters
NAME  P1NRU (PPH3)2Cl
EXPNO  61
PROCNO  1

F2 - Acquisition Parameters
Date_  20030820
Time  14 24
INSTRUM  spect
PROBHD  5 mm QNP 1H
PULPROG  zgpg30
TD  32768
SOLVENT  CDCl3
NS  64
DS  0
SWH  64830.065 MHz
FIDRES  1.981651 Hz
AQ  0.2521636 sec
RG  11085.2
DM  7.700 usec
DE  4.80 usec
TE  300.2 K
D1  1.0000000 sec

===== CHANNEL f1 =====
NUC1  31P
P1  7.20 usec
PL1  -6.00 dB
SFO1  161.876300 MHz

F2 - Processing parameters
SI  16384
SF  161.876300 MHz
XQ1  EM
SFO  0
LB  0.00 Hz
GB  0
PC  1.00

10 NMR PLOT PARAMETERS
SI  20.00 cm
F1  66.050 ppm
F2  10706.06 Hz
P2P  -2.008 ppm
FZ  -323.20 Hz
PPh3M  3.40450 ppm/cm
N2DM  6.6161261 Hz/cm
  
```

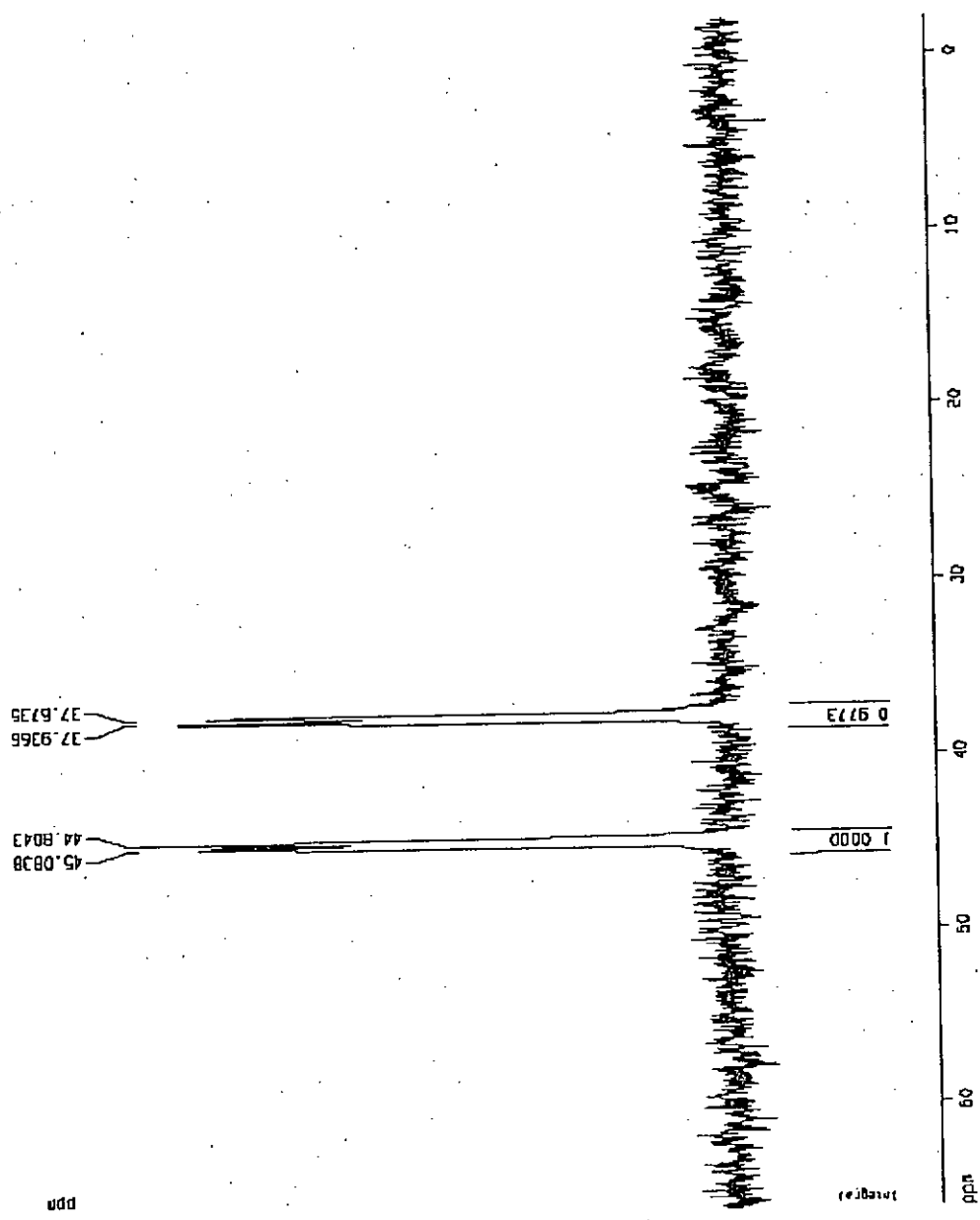


Figure 3.2 162 MHz ³¹P{¹H}-NMR spectrum of (η⁵-C₆H₆CH₂CH₂NMe₂)Ru(PPh₃)₂Cl (17)

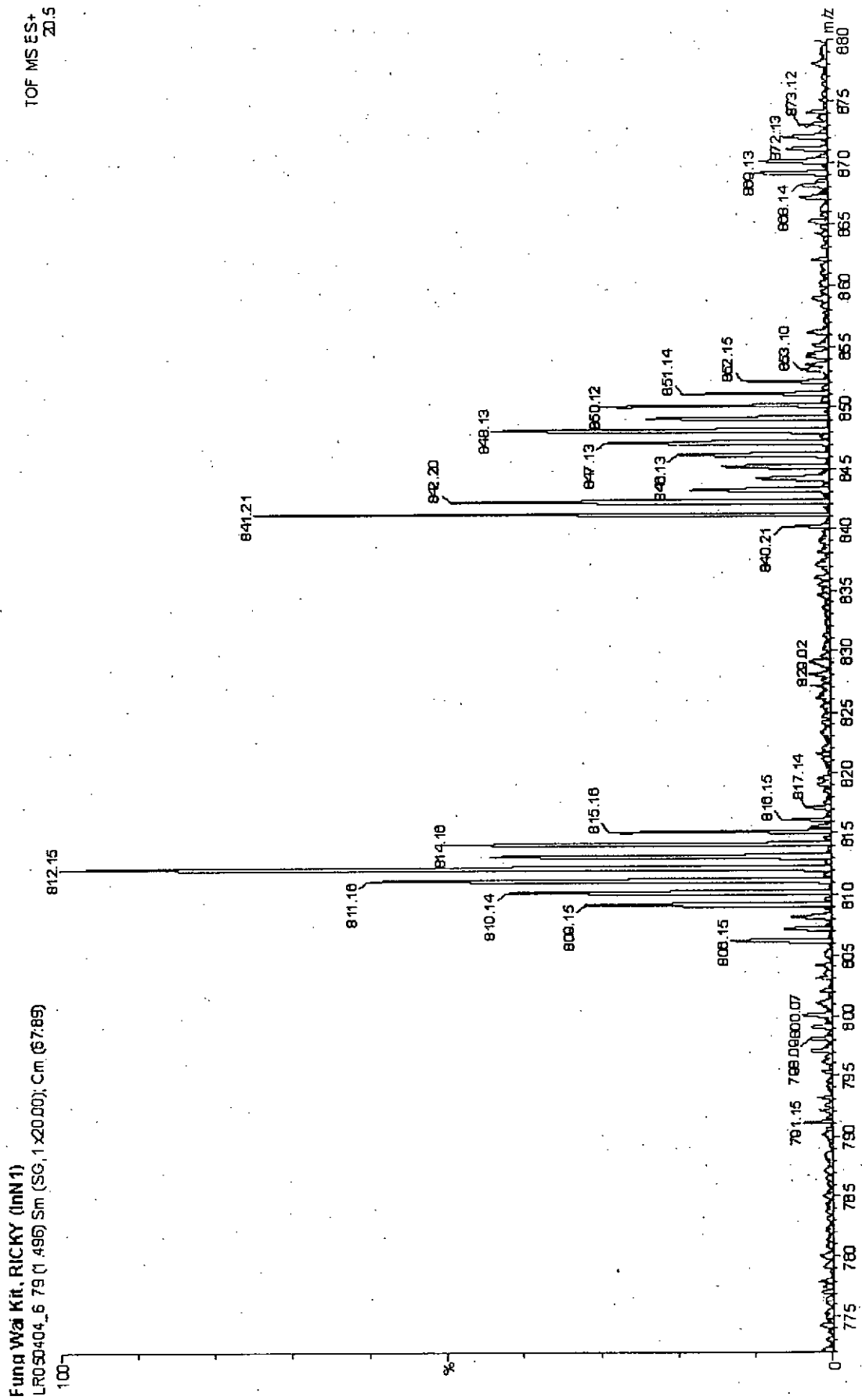


Figure 3.3 Mass spectrum of $(\eta^5\text{-C}_9\text{H}_6\text{CH}_2\text{CH}_2\text{NMe}_2)\text{Ru}(\text{PPh}_3)_2\text{Cl}$ (17)

1H NMR (dppm) Cl, in CDCl3 2:06 PM 4/5/04

Current Data Parameters
 NAME: 1H NMR (dppm) Cl
 EXPNO: 116
 PROCNO: 1
 F2 - Acquisition Parameters
 Date_: 20040605
 Time: 14:07
 INSTRUM: gpc400
 PROBHD: 5 mm QNP 1H
 PULPROG: zgpg30
 TD: 32768
 SOLVENT: CDCl3
 NS: 16
 DS: 0
 SWH: 16020.641 MHz
 FIDRES: 0.488064 MHz
 AQ: 1.0244116 sec
 RG: 0/1.7
 DM: 31 200 uS/SEC
 DE: 4.60 uS/SEC
 TE: 300.2 K
 D1: 2.0000000 sec
 CHANNEL: 13
 NUC1: 1H
 P1: 9.50 uS/SEC
 PL1: -6.00 dB
 SF01: 400.1476833 MHz
 F2 - Processing parameters
 SI: 16384
 SF: 400.130085 MHz
 MDW: EM
 SSB: 0
 LB: 0.30 Hz
 GB: 0
 PC: 1.00
 1D NMR files parameters
 C: 20.00 cm
 F1P: 9.000 GHz
 F1: 3601.17 Hz
 F2P: -1.000 GHz
 F2: -400.13 Hz
 AFMCH: 0 65000 000/00
 HZM4: 200 00502 HZ/CM

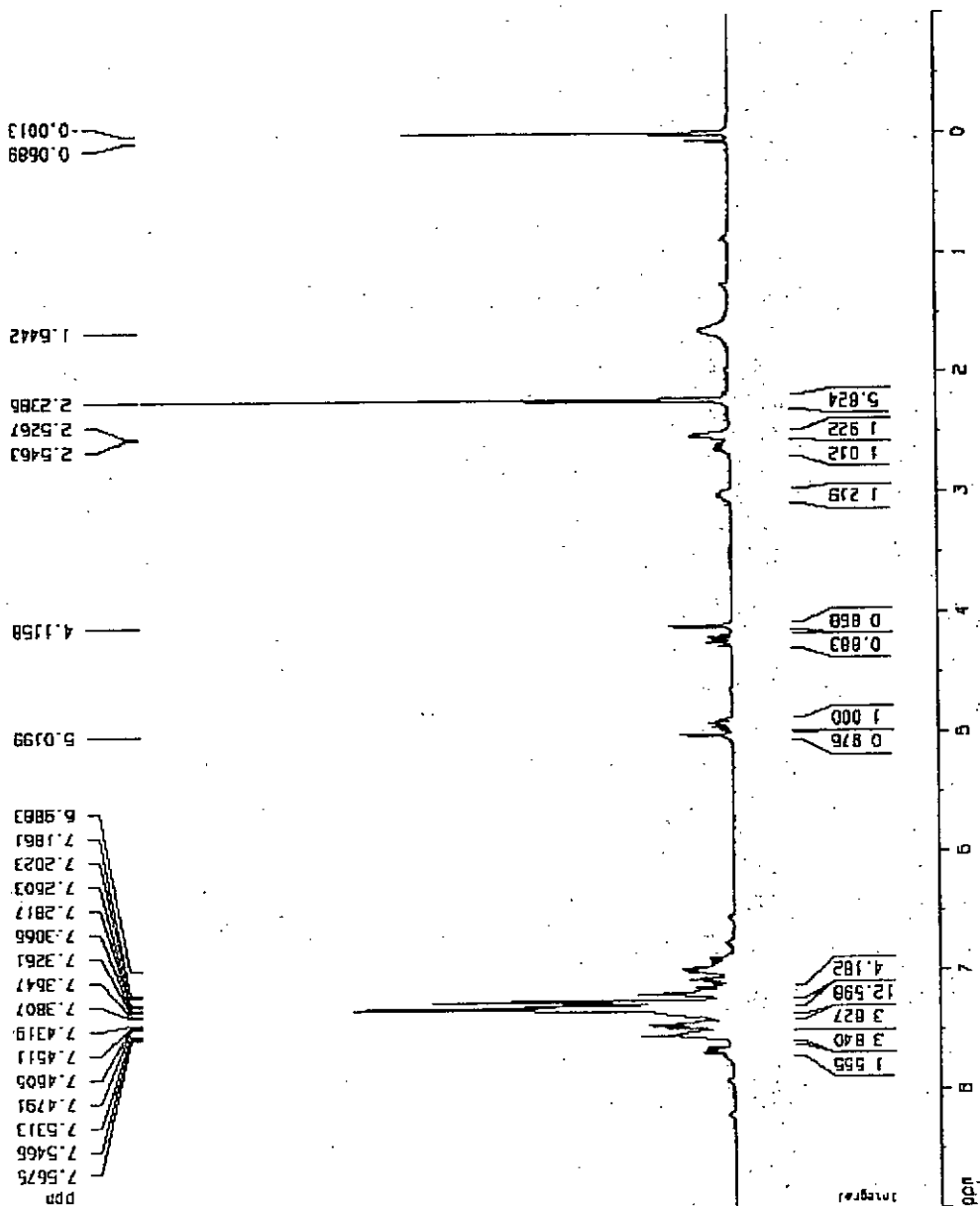


Figure 3.4 400 MHz ¹H-NMR spectrum of (η⁵-C₉H₆CH₂CH₂NMe₂)Ru(dppm)Cl (18)

10NRU (ppm) [] IN CDCl3 2:03 PM 4/5/04

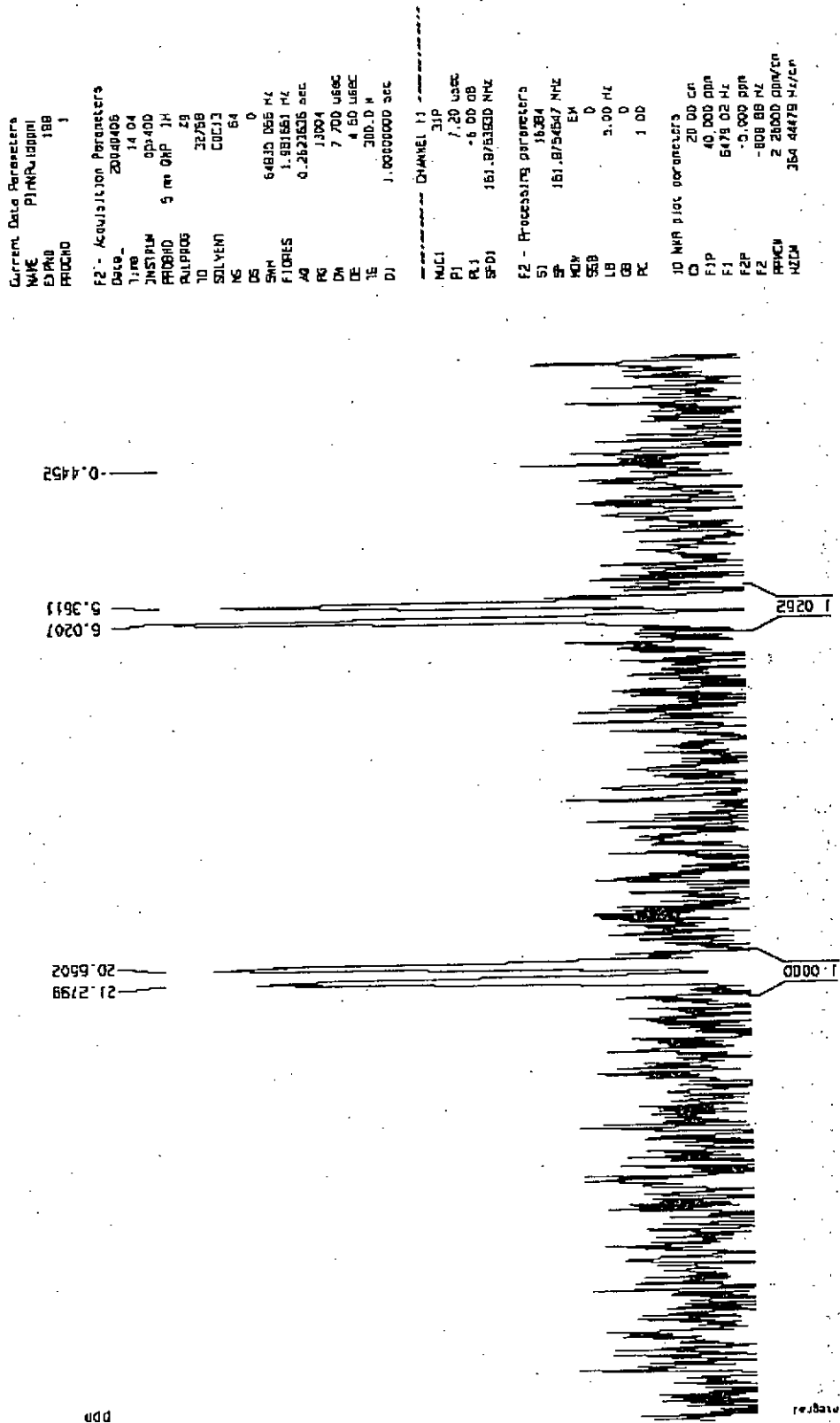


Figure 3.5 162 MHz $^{31}\text{P}\{^1\text{H}\}$ -NMR spectrum of $(\eta^5\text{-C}_9\text{H}_6\text{CH}_2\text{CH}_2\text{NMe}_2)\text{Ru}(\text{dppm})\text{Cl}$ (18)

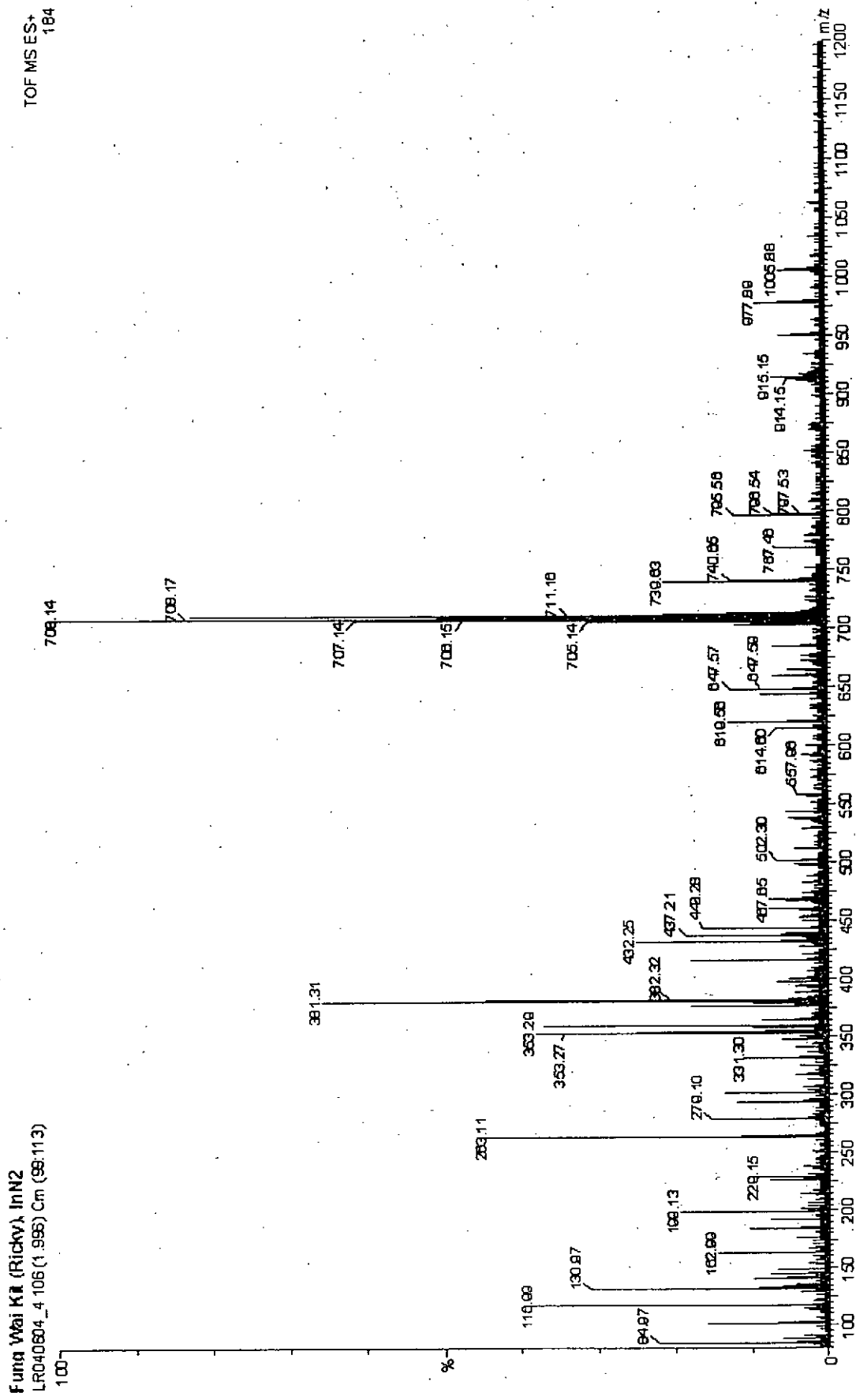


Figure 3.6 Mass spectrum of $(\eta^5\text{-C}_9\text{H}_6\text{CH}_2\text{CH}_2\text{NMe}_2)\text{Ru}(\text{dppm})\text{Cl}$ (18)

1H NMR (400 MHz) in CDCl3, 4:33 PM 3/13/04

```

Current Data Parameters
NAME      1hNMR(dppm)H
EXPNO    31
PROCNO   1

F2 - Acquisition Parameters
Date_    20021021
Time     16:34
INSTRUM  gpc400
PROBHD   5 mm QNP 1H
PULPROG zg30
TD        32768
SOLVENT  CDCl3
NS        15
DS        4
SWH       15020.841 MHz
FIDRES    0.489064 MHz
AQ        1.0824115 sec
RG        812.7
Dw        31.200 usec
DE        4.50 usec
TE        300.2 K
D1        2.00000000 sec

===== CHANNEL f1 =====
NUC1      1H
P1        9.50 usec
PL1       -6.00 dB
SFO1      400.1278603 MHz

F2 - Processing parameters
SI        16384
SF        400.1300445 MHz
WDW       EM
SSB       0
LB        0.30 Hz
GB        0
PC        1.00

3D NMR plot parameters
D1        20.00 sec
F1P       10.000 dB
F2        400.130 Hz
P2P       -10.000 dB
F2        -600.00 Hz
PRICM     1 25000 dBV/cm
HZCM     500 16384 Hz/cm
  
```

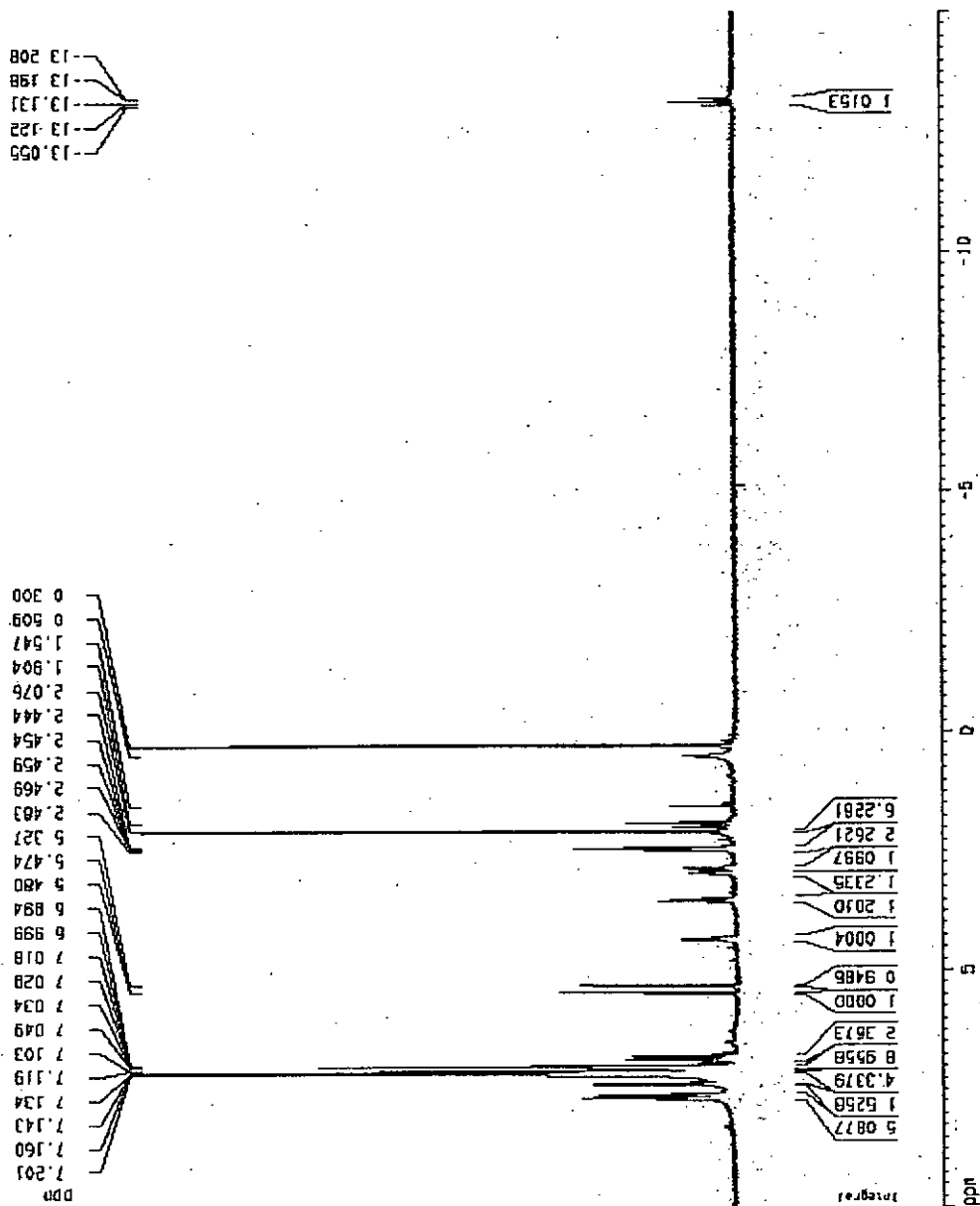


Figure 3.7 400 MHz ¹H-NMR spectrum of (η⁵-C₆H₆CH₂CH₂NMe₂)Ru(dppm)H (19)

31P NMR (dppm) H 10 1606 4' 30 PM 3/3/04

Current Data Parameters
 NAME P10NRU10ppmH
 EXPNO 6
 PROCNO 1

F2 - Acquisition Parameters
 Date_ 20021021
 Time 16 32
 INSTRUM dpp400
 PROBHD 5 mm QNP 1H
 PULPROG zg
 TD 32768
 SOLVENT CDCl3
 NS 64
 DS 4
 SWH 64833.065 Hz
 FIDRES 1.981561 Hz
 AQ 0.2823635 sec
 RG 13004
 OR 7.700 usec
 DE 4.50 usec
 TE 300.2 K
 D1 1.00000000 sec

----- CHANNEL f1 -----
 NUC1 31P
 P1 7.20 usec
 PL1 -8.00 dB
 SF01 161.8753603 MHz

F2 - Processing parameters
 SI 161.8782828 MHz
 EQN EM
 LB 0
 GB 0
 PC 1.00

30 NMR plots parameters
 CD 20 DD CN
 F1P 35.075 ppm
 F1 6843.68 Hz
 F2P -8243.55 Hz
 F2 -8243.55 Hz
 PRGCM 3 73110 ppm/Hz
 NUCM 604 76683 Hz/Hz

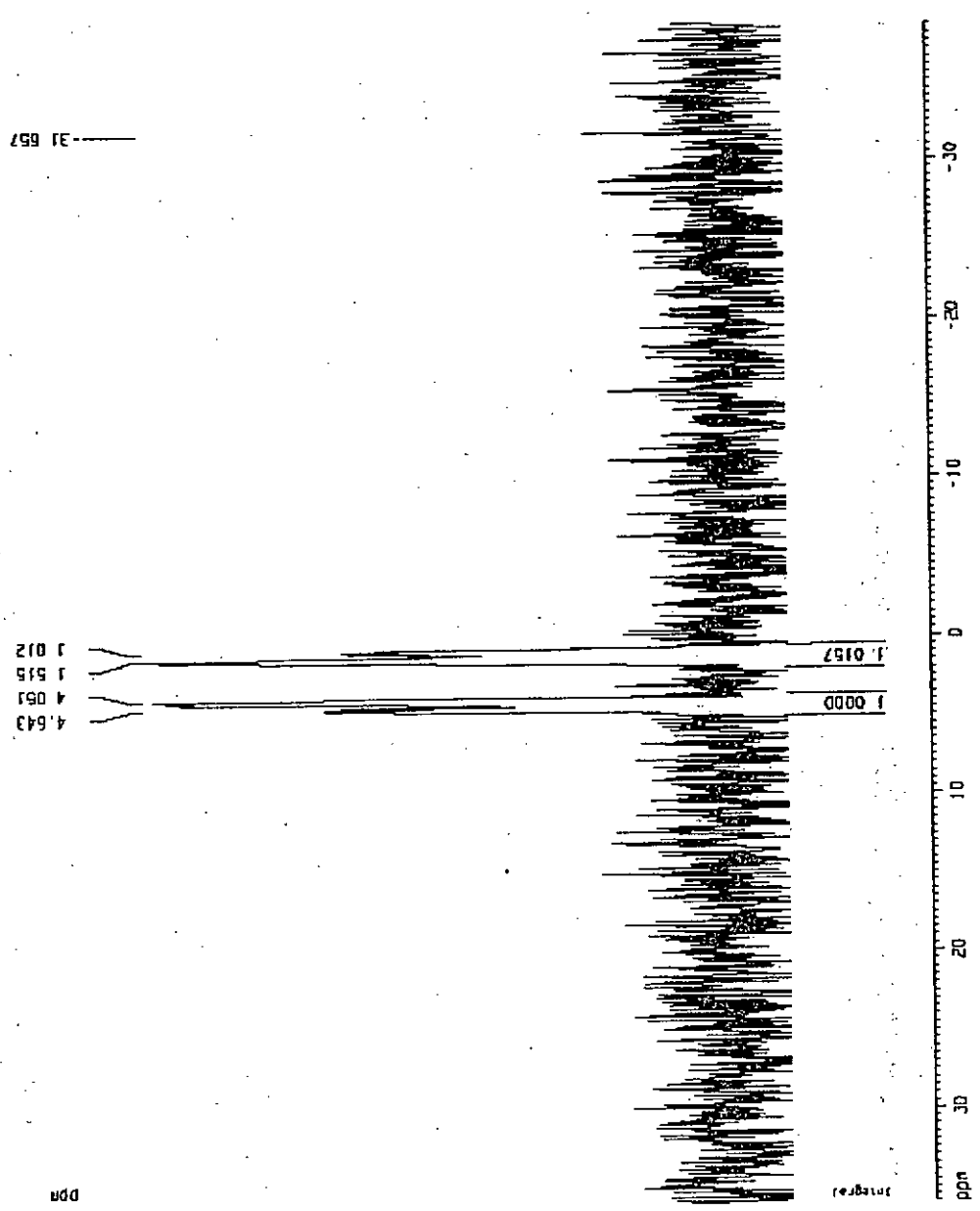


Figure 3.8 162 MHz ³¹P{¹H}-NMR spectrum of (η⁵-C₉H₆CH₂CH₂NMe₂)Ru(dppm)H (19)

Fung Wai Kit (Rickw), InN3
LR040604_5_42 (0.799) Cm (40:48)

TOF MS ES+
164

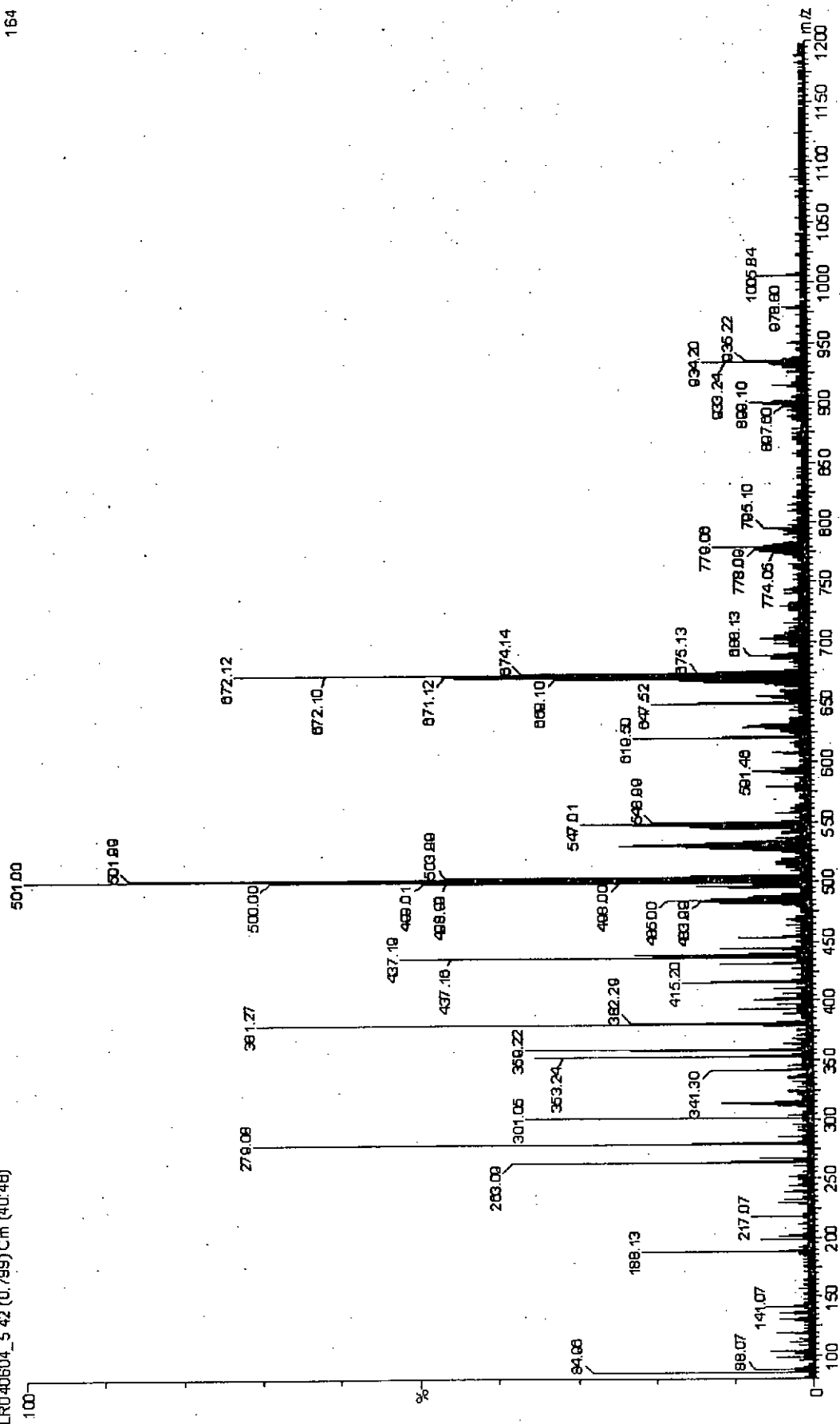


Figure 3.9 Mass spectrum of $(\eta^5\text{-C}_9\text{H}_6\text{CH}_2\text{CH}_2\text{NMe}_2)\text{Ru}(\text{dppm})\text{H}$ (19)

1H NMR (PPH3)2H IN C6D6 3:10 PM 4/25/02

Current Data Parameters
 NAME 1H NMR (PPH3)2H
 EXPNO 16
 PROCNO 1

F2 - Acquisition Parameters
 Date_ 20020426
 Time 15 11
 INSTRUM spect
 PROBHD 5 mm QNP 1H
 PULPROG zgpg30
 TD 4930
 SOLVENT CDCl3
 NS 16
 DS 0
 SWH 16025.641 MHz
 FIDRES 0.489064 MHz
 AQ 1.0234116 sec
 RG 287.4
 DM 31 200 usec
 DE 4 50 usec
 TE 300.2 K
 D1 2.0000000 sec

----- CHANNEL f1 -----
 NUC1 1H
 P1 9.50 usec
 PL1 -6.00 dB
 SF01 400.1278853 MHz

F2 - Processing parameters
 SI 16384
 SF 400.1300445 MHz
 MD 64
 LB 0
 GB 0
 PC 1.00

3D NMR plot parameters
 D 20.00 cm
 F1P 8.062 cm
 F1 3326.816 MHz
 F2P -19.044 ppm
 F2 -6218.72 MHz
 PPRM 1 16031.000 Hz
 MZCM 472.2/681.1 Hz/cm

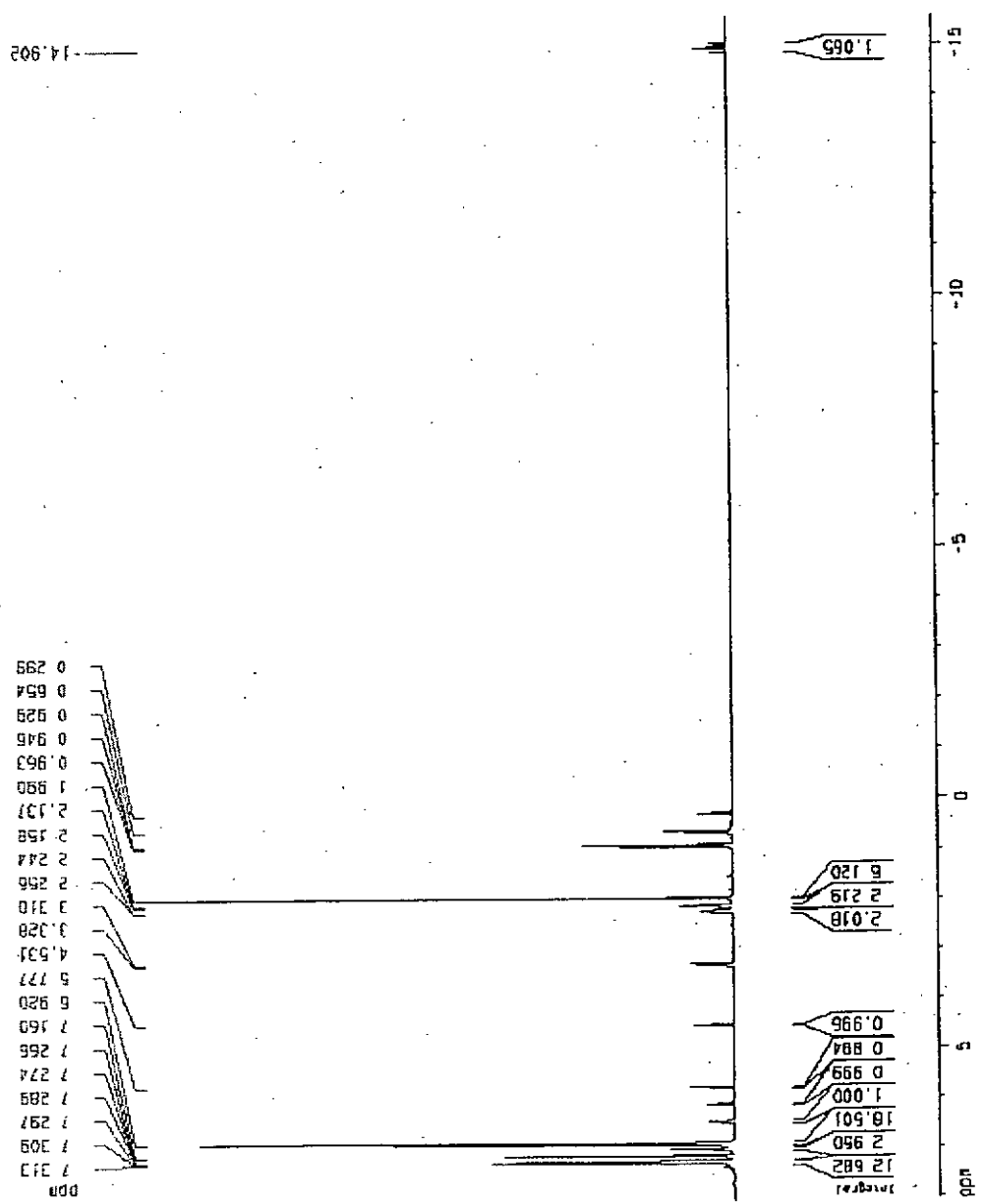


Figure 3.10 400 MHz ¹H-NMR spectrum of (η⁵-C₉H₆CH₂CH₂NMe₂)Ru(PPh₃)₂H (20)

14NRU (PPH3)2H v1 C606 3:08 PM 4/26/02

```

Current Data Parameters
NAME      P1NRU (PPH3)H
EXPNO    17
PROCNO   1

F2 - Acquisition Parameters
Date_    20020426
Time     15:08
INSTRUM  dp400
PROBHD   5 mm QNP 1H
PULPROG  zg
TD        32768
SOLVENT  CDCl3
NS        54
DS        0
SWH       64810.866 MHz
FIDRES   1.381561 MHz
AQ        0.2523535 sec
RG        13004
ON        7.700 usec
DE        4.50 usec
TE        300.2 K
D1        1.00000000 sec

===== CHANNEL f1 =====
NUC1      31P
P1        7.20 usec
PL1       -8.00 dB
SFO1     161.876800 MHz

F2 - Processing parameters
SI        16384
SF        161.876800 MHz
AQ        0.2523535 sec
RG        13004
ON        7.700 usec
DE        4.50 usec
TE        300.2 K
D1        1.00000000 sec

===== CHANNEL f2 =====
NUC2      31P
P2        7.20 usec
PL2       -8.00 dB
SFO2     161.876800 MHz

===== CHANNEL f3 =====
NUC3      31P
P3        7.20 usec
PL3       -8.00 dB
SFO3     161.876800 MHz

===== CHANNEL f4 =====
NUC4      31P
P4        7.20 usec
PL4       -8.00 dB
SFO4     161.876800 MHz

===== CHANNEL f5 =====
NUC5      31P
P5        7.20 usec
PL5       -8.00 dB
SFO5     161.876800 MHz

===== CHANNEL f6 =====
NUC6      31P
P6        7.20 usec
PL6       -8.00 dB
SFO6     161.876800 MHz

===== CHANNEL f7 =====
NUC7      31P
P7        7.20 usec
PL7       -8.00 dB
SFO7     161.876800 MHz

===== CHANNEL f8 =====
NUC8      31P
P8        7.20 usec
PL8       -8.00 dB
SFO8     161.876800 MHz

===== CHANNEL f9 =====
NUC9      31P
P9        7.20 usec
PL9       -8.00 dB
SFO9     161.876800 MHz

===== CHANNEL f10 =====
NUC10     31P
P10       7.20 usec
PL10      -8.00 dB
SFO10    161.876800 MHz

===== CHANNEL f11 =====
NUC11     31P
P11       7.20 usec
PL11      -8.00 dB
SFO11    161.876800 MHz

===== CHANNEL f12 =====
NUC12     31P
P12       7.20 usec
PL12      -8.00 dB
SFO12    161.876800 MHz

===== CHANNEL f13 =====
NUC13     31P
P13       7.20 usec
PL13      -8.00 dB
SFO13    161.876800 MHz

===== CHANNEL f14 =====
NUC14     31P
P14       7.20 usec
PL14      -8.00 dB
SFO14    161.876800 MHz

===== CHANNEL f15 =====
NUC15     31P
P15       7.20 usec
PL15      -8.00 dB
SFO15    161.876800 MHz

===== CHANNEL f16 =====
NUC16     31P
P16       7.20 usec
PL16      -8.00 dB
SFO16    161.876800 MHz

===== CHANNEL f17 =====
NUC17     31P
P17       7.20 usec
PL17      -8.00 dB
SFO17    161.876800 MHz

===== CHANNEL f18 =====
NUC18     31P
P18       7.20 usec
PL18      -8.00 dB
SFO18    161.876800 MHz

===== CHANNEL f19 =====
NUC19     31P
P19       7.20 usec
PL19      -8.00 dB
SFO19    161.876800 MHz

===== CHANNEL f20 =====
NUC20     31P
P20       7.20 usec
PL20      -8.00 dB
SFO20    161.876800 MHz

===== CHANNEL f21 =====
NUC21     31P
P21       7.20 usec
PL21      -8.00 dB
SFO21    161.876800 MHz

===== CHANNEL f22 =====
NUC22     31P
P22       7.20 usec
PL22      -8.00 dB
SFO22    161.876800 MHz

===== CHANNEL f23 =====
NUC23     31P
P23       7.20 usec
PL23      -8.00 dB
SFO23    161.876800 MHz

===== CHANNEL f24 =====
NUC24     31P
P24       7.20 usec
PL24      -8.00 dB
SFO24    161.876800 MHz

===== CHANNEL f25 =====
NUC25     31P
P25       7.20 usec
PL25      -8.00 dB
SFO25    161.876800 MHz

===== CHANNEL f26 =====
NUC26     31P
P26       7.20 usec
PL26      -8.00 dB
SFO26    161.876800 MHz

===== CHANNEL f27 =====
NUC27     31P
P27       7.20 usec
PL27      -8.00 dB
SFO27    161.876800 MHz

===== CHANNEL f28 =====
NUC28     31P
P28       7.20 usec
PL28      -8.00 dB
SFO28    161.876800 MHz

===== CHANNEL f29 =====
NUC29     31P
P29       7.20 usec
PL29      -8.00 dB
SFO29    161.876800 MHz

===== CHANNEL f30 =====
NUC30     31P
P30       7.20 usec
PL30      -8.00 dB
SFO30    161.876800 MHz

===== CHANNEL f31 =====
NUC31     31P
P31       7.20 usec
PL31      -8.00 dB
SFO31    161.876800 MHz

===== CHANNEL f32 =====
NUC32     31P
P32       7.20 usec
PL32      -8.00 dB
SFO32    161.876800 MHz

===== CHANNEL f33 =====
NUC33     31P
P33       7.20 usec
PL33      -8.00 dB
SFO33    161.876800 MHz

===== CHANNEL f34 =====
NUC34     31P
P34       7.20 usec
PL34      -8.00 dB
SFO34    161.876800 MHz

===== CHANNEL f35 =====
NUC35     31P
P35       7.20 usec
PL35      -8.00 dB
SFO35    161.876800 MHz

===== CHANNEL f36 =====
NUC36     31P
P36       7.20 usec
PL36      -8.00 dB
SFO36    161.876800 MHz

===== CHANNEL f37 =====
NUC37     31P
P37       7.20 usec
PL37      -8.00 dB
SFO37    161.876800 MHz

===== CHANNEL f38 =====
NUC38     31P
P38       7.20 usec
PL38      -8.00 dB
SFO38    161.876800 MHz

===== CHANNEL f39 =====
NUC39     31P
P39       7.20 usec
PL39      -8.00 dB
SFO39    161.876800 MHz

===== CHANNEL f40 =====
NUC40     31P
P40       7.20 usec
PL40      -8.00 dB
SFO40    161.876800 MHz

===== CHANNEL f41 =====
NUC41     31P
P41       7.20 usec
PL41      -8.00 dB
SFO41    161.876800 MHz

===== CHANNEL f42 =====
NUC42     31P
P42       7.20 usec
PL42      -8.00 dB
SFO42    161.876800 MHz

===== CHANNEL f43 =====
NUC43     31P
P43       7.20 usec
PL43      -8.00 dB
SFO43    161.876800 MHz

===== CHANNEL f44 =====
NUC44     31P
P44       7.20 usec
PL44      -8.00 dB
SFO44    161.876800 MHz

===== CHANNEL f45 =====
NUC45     31P
P45       7.20 usec
PL45      -8.00 dB
SFO45    161.876800 MHz

===== CHANNEL f46 =====
NUC46     31P
P46       7.20 usec
PL46      -8.00 dB
SFO46    161.876800 MHz

===== CHANNEL f47 =====
NUC47     31P
P47       7.20 usec
PL47      -8.00 dB
SFO47    161.876800 MHz

===== CHANNEL f48 =====
NUC48     31P
P48       7.20 usec
PL48      -8.00 dB
SFO48    161.876800 MHz

===== CHANNEL f49 =====
NUC49     31P
P49       7.20 usec
PL49      -8.00 dB
SFO49    161.876800 MHz

===== CHANNEL f50 =====
NUC50     31P
P50       7.20 usec
PL50      -8.00 dB
SFO50    161.876800 MHz

===== CHANNEL f51 =====
NUC51     31P
P51       7.20 usec
PL51      -8.00 dB
SFO51    161.876800 MHz

===== CHANNEL f52 =====
NUC52     31P
P52       7.20 usec
PL52      -8.00 dB
SFO52    161.876800 MHz

===== CHANNEL f53 =====
NUC53     31P
P53       7.20 usec
PL53      -8.00 dB
SFO53    161.876800 MHz

===== CHANNEL f54 =====
NUC54     31P
P54       7.20 usec
PL54      -8.00 dB
SFO54    161.876800 MHz

===== CHANNEL f55 =====
NUC55     31P
P55       7.20 usec
PL55      -8.00 dB
SFO55    161.876800 MHz

===== CHANNEL f56 =====
NUC56     31P
P56       7.20 usec
PL56      -8.00 dB
SFO56    161.876800 MHz

===== CHANNEL f57 =====
NUC57     31P
P57       7.20 usec
PL57      -8.00 dB
SFO57    161.876800 MHz

===== CHANNEL f58 =====
NUC58     31P
P58       7.20 usec
PL58      -8.00 dB
SFO58    161.876800 MHz

===== CHANNEL f59 =====
NUC59     31P
P59       7.20 usec
PL59      -8.00 dB
SFO59    161.876800 MHz

===== CHANNEL f60 =====
NUC60     31P
P60       7.20 usec
PL60      -8.00 dB
SFO60    161.876800 MHz

===== CHANNEL f61 =====
NUC61     31P
P61       7.20 usec
PL61      -8.00 dB
SFO61    161.876800 MHz

===== CHANNEL f62 =====
NUC62     31P
P62       7.20 usec
PL62      -8.00 dB
SFO62    161.876800 MHz

===== CHANNEL f63 =====
NUC63     31P
P63       7.20 usec
PL63      -8.00 dB
SFO63    161.876800 MHz

===== CHANNEL f64 =====
NUC64     31P
P64       7.20 usec
PL64      -8.00 dB
SFO64    161.876800 MHz

===== CHANNEL f65 =====
NUC65     31P
P65       7.20 usec
PL65      -8.00 dB
SFO65    161.876800 MHz

===== CHANNEL f66 =====
NUC66     31P
P66       7.20 usec
PL66      -8.00 dB
SFO66    161.876800 MHz

===== CHANNEL f67 =====
NUC67     31P
P67       7.20 usec
PL67      -8.00 dB
SFO67    161.876800 MHz

===== CHANNEL f68 =====
NUC68     31P
P68       7.20 usec
PL68      -8.00 dB
SFO68    161.876800 MHz

===== CHANNEL f69 =====
NUC69     31P
P69       7.20 usec
PL69      -8.00 dB
SFO69    161.876800 MHz

===== CHANNEL f70 =====
NUC70     31P
P70       7.20 usec
PL70      -8.00 dB
SFO70    161.876800 MHz

===== CHANNEL f71 =====
NUC71     31P
P71       7.20 usec
PL71      -8.00 dB
SFO71    161.876800 MHz

===== CHANNEL f72 =====
NUC72     31P
P72       7.20 usec
PL72      -8.00 dB
SFO72    161.876800 MHz

===== CHANNEL f73 =====
NUC73     31P
P73       7.20 usec
PL73      -8.00 dB
SFO73    161.876800 MHz

===== CHANNEL f74 =====
NUC74     31P
P74       7.20 usec
PL74      -8.00 dB
SFO74    161.876800 MHz

===== CHANNEL f75 =====
NUC75     31P
P75       7.20 usec
PL75      -8.00 dB
SFO75    161.876800 MHz

===== CHANNEL f76 =====
NUC76     31P
P76       7.20 usec
PL76      -8.00 dB
SFO76    161.876800 MHz

===== CHANNEL f77 =====
NUC77     31P
P77       7.20 usec
PL77      -8.00 dB
SFO77    161.876800 MHz

===== CHANNEL f78 =====
NUC78     31P
P78       7.20 usec
PL78      -8.00 dB
SFO78    161.876800 MHz

===== CHANNEL f79 =====
NUC79     31P
P79       7.20 usec
PL79      -8.00 dB
SFO79    161.876800 MHz

===== CHANNEL f80 =====
NUC80     31P
P80       7.20 usec
PL80      -8.00 dB
SFO80    161.876800 MHz

===== CHANNEL f81 =====
NUC81     31P
P81       7.20 usec
PL81      -8.00 dB
SFO81    161.876800 MHz

===== CHANNEL f82 =====
NUC82     31P
P82       7.20 usec
PL82      -8.00 dB
SFO82    161.876800 MHz

===== CHANNEL f83 =====
NUC83     31P
P83       7.20 usec
PL83      -8.00 dB
SFO83    161.876800 MHz

===== CHANNEL f84 =====
NUC84     31P
P84       7.20 usec
PL84      -8.00 dB
SFO84    161.876800 MHz

===== CHANNEL f85 =====
NUC85     31P
P85       7.20 usec
PL85      -8.00 dB
SFO85    161.876800 MHz

===== CHANNEL f86 =====
NUC86     31P
P86       7.20 usec
PL86      -8.00 dB
SFO86    161.876800 MHz

===== CHANNEL f87 =====
NUC87     31P
P87       7.20 usec
PL87      -8.00 dB
SFO87    161.876800 MHz

===== CHANNEL f88 =====
NUC88     31P
P88       7.20 usec
PL88      -8.00 dB
SFO88    161.876800 MHz

===== CHANNEL f89 =====
NUC89     31P
P89       7.20 usec
PL89      -8.00 dB
SFO89    161.876800 MHz

===== CHANNEL f90 =====
NUC90     31P
P90       7.20 usec
PL90      -8.00 dB
SFO90    161.876800 MHz

===== CHANNEL f91 =====
NUC91     31P
P91       7.20 usec
PL91      -8.00 dB
SFO91    161.876800 MHz

===== CHANNEL f92 =====
NUC92     31P
P92       7.20 usec
PL92      -8.00 dB
SFO92    161.876800 MHz

===== CHANNEL f93 =====
NUC93     31P
P93       7.20 usec
PL93      -8.00 dB
SFO93    161.876800 MHz

===== CHANNEL f94 =====
NUC94     31P
P94       7.20 usec
PL94      -8.00 dB
SFO94    161.876800 MHz

===== CHANNEL f95 =====
NUC95     31P
P95       7.20 usec
PL95      -8.00 dB
SFO95    161.876800 MHz

===== CHANNEL f96 =====
NUC96     31P
P96       7.20 usec
PL96      -8.00 dB
SFO96    161.876800 MHz

===== CHANNEL f97 =====
NUC97     31P
P97       7.20 usec
PL97      -8.00 dB
SFO97    161.876800 MHz

===== CHANNEL f98 =====
NUC98     31P
P98       7.20 usec
PL98      -8.00 dB
SFO98    161.876800 MHz

===== CHANNEL f99 =====
NUC99     31P
P99       7.20 usec
PL99      -8.00 dB
SFO99    161.876800 MHz

===== CHANNEL f100 =====
NUC100    31P
P100      7.20 usec
PL100     -8.00 dB
SFO100    161.876800 MHz
    
```

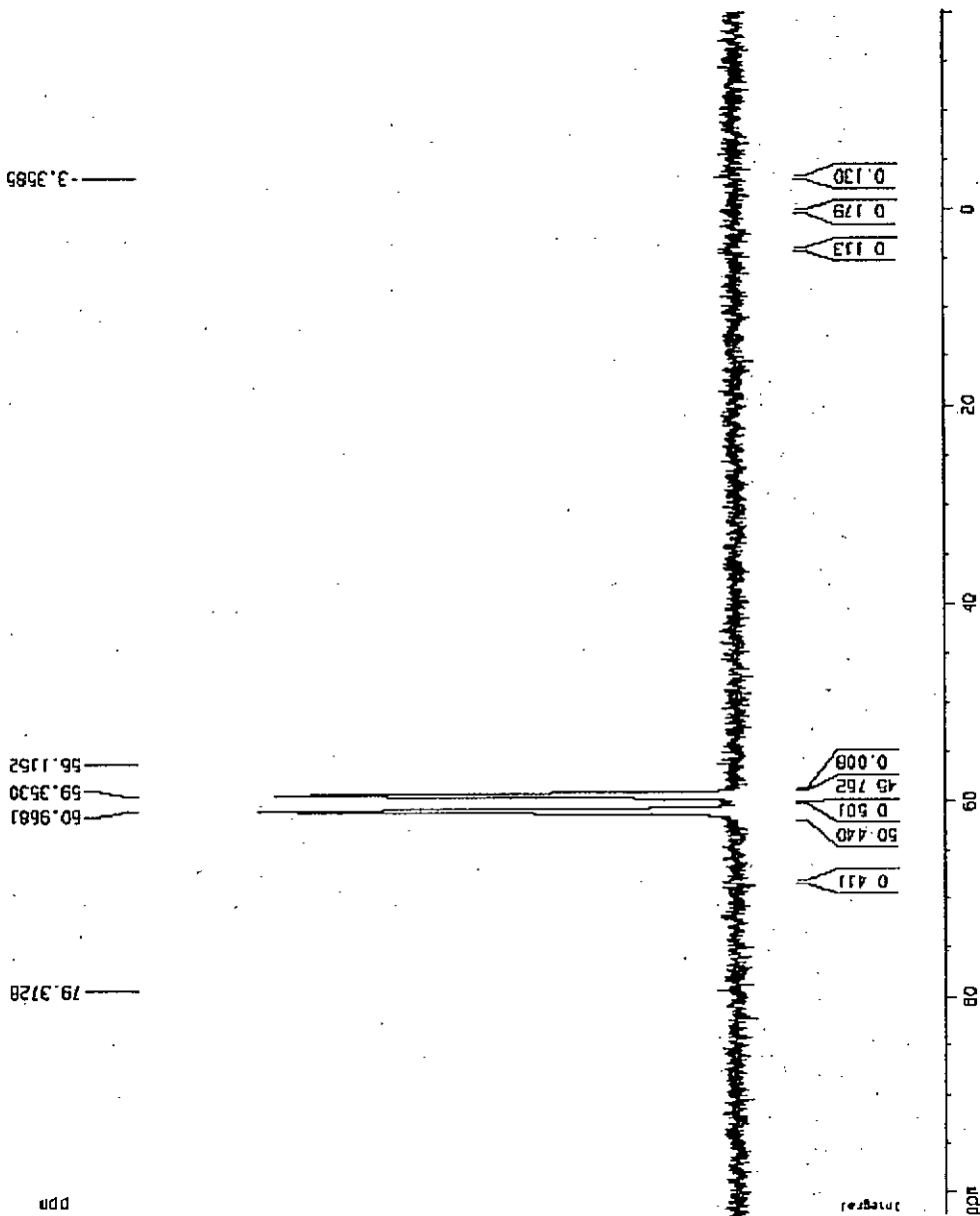


Figure 3.11 162 MHz $^{31}\text{P}\{^1\text{H}\}$ -NMR spectrum of $(\eta^5\text{-C}_9\text{H}_6\text{CH}_2\text{CH}_2\text{NMe}_2)\text{Ru}(\text{PPh}_3)_2\text{H}$ (20)

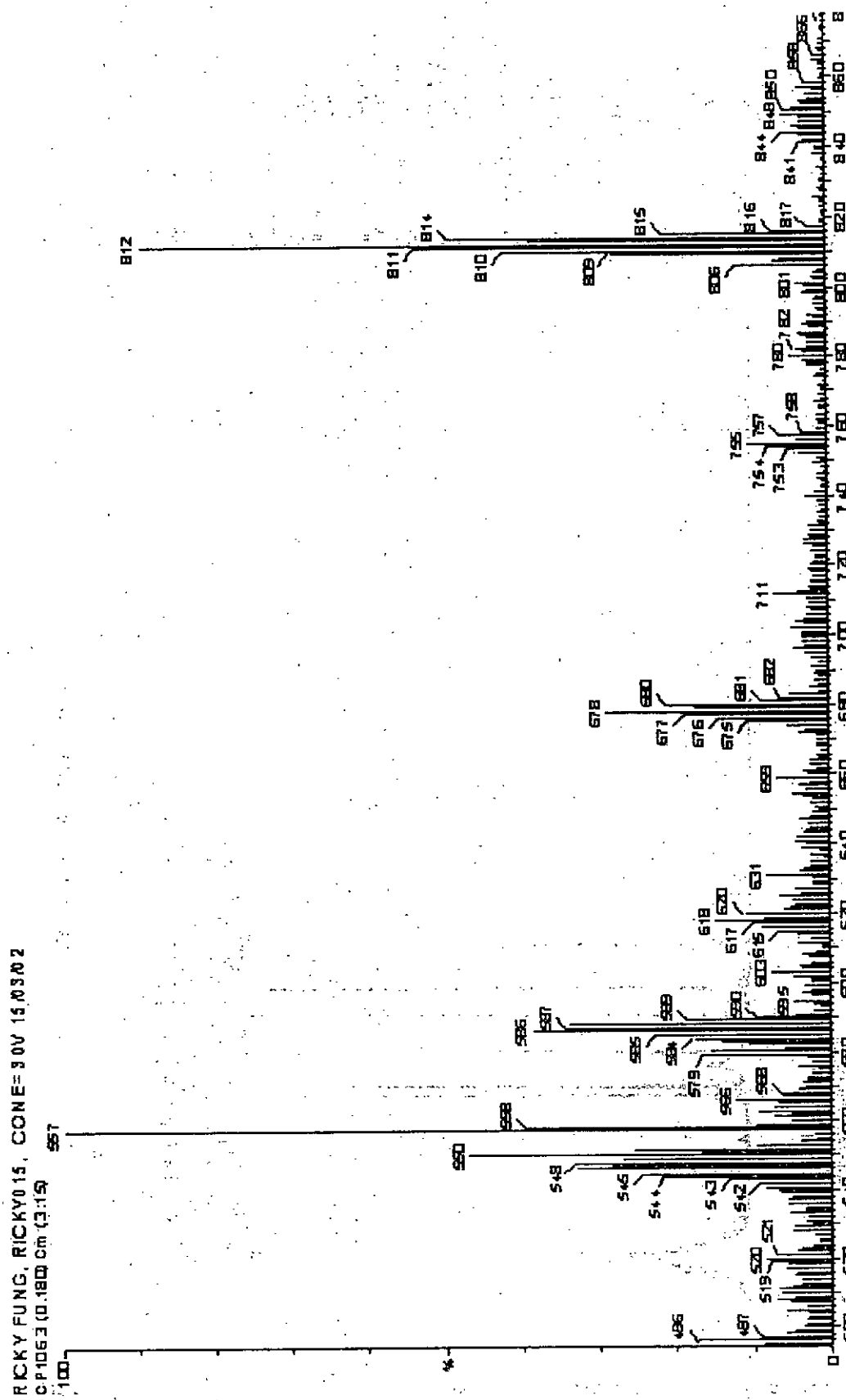


Figure 3.12 Mass spectrum of $(\eta^5\text{-C}_9\text{H}_6\text{CH}_2\text{CH}_2\text{NMe}_2)\text{Ru}(\text{PPh}_3)_2\text{H}$ (20)

100MHz (ppm) H-1 HBF4 .E12D .in 0-1HF

Current Data Parameters
 NAME 100MHz (ppm) H-1
 EX PNO 24
 PRICHO 1

F2 - Acquisition Parameters
 Date_ 20031215
 Time_ 13 14
 INSTRUM DPX400
 PROBNM 5 mm QNP 1H
 PULPROG zgpg
 TD 32768
 SOLVENT THF
 NS 32
 DS 4
 SWH 16023.641 Hz
 FIDRES 0.489064 Hz
 AQ 1.0224016 sec
 RG 181
 DR 31 2DD UBBC
 DE 4 6D UBBC
 TE 300.2 K
 D1 2.0000000 sec

CHANNEL F1
 NUC1 1H
 P1 9.50 usec
 PL -5.00 dB
 SFO1 400.1276833 MHz

F2 - Processing parameters
 S1 11.364
 SF 400.1282222 MHz
 WDN EK
 SSB 0
 LB 0.30 Hz
 GB 0
 PC 1.00

3D NMR plot parameters
 D 20 DD CN
 E1P 8 614 DD
 E1 3446 95 Hz
 F2P -13.975 ppm
 F2 -5981.88 Hz
 PRICH 1 12948 DD/CN
 MZCM 461 93728 Hz/CN

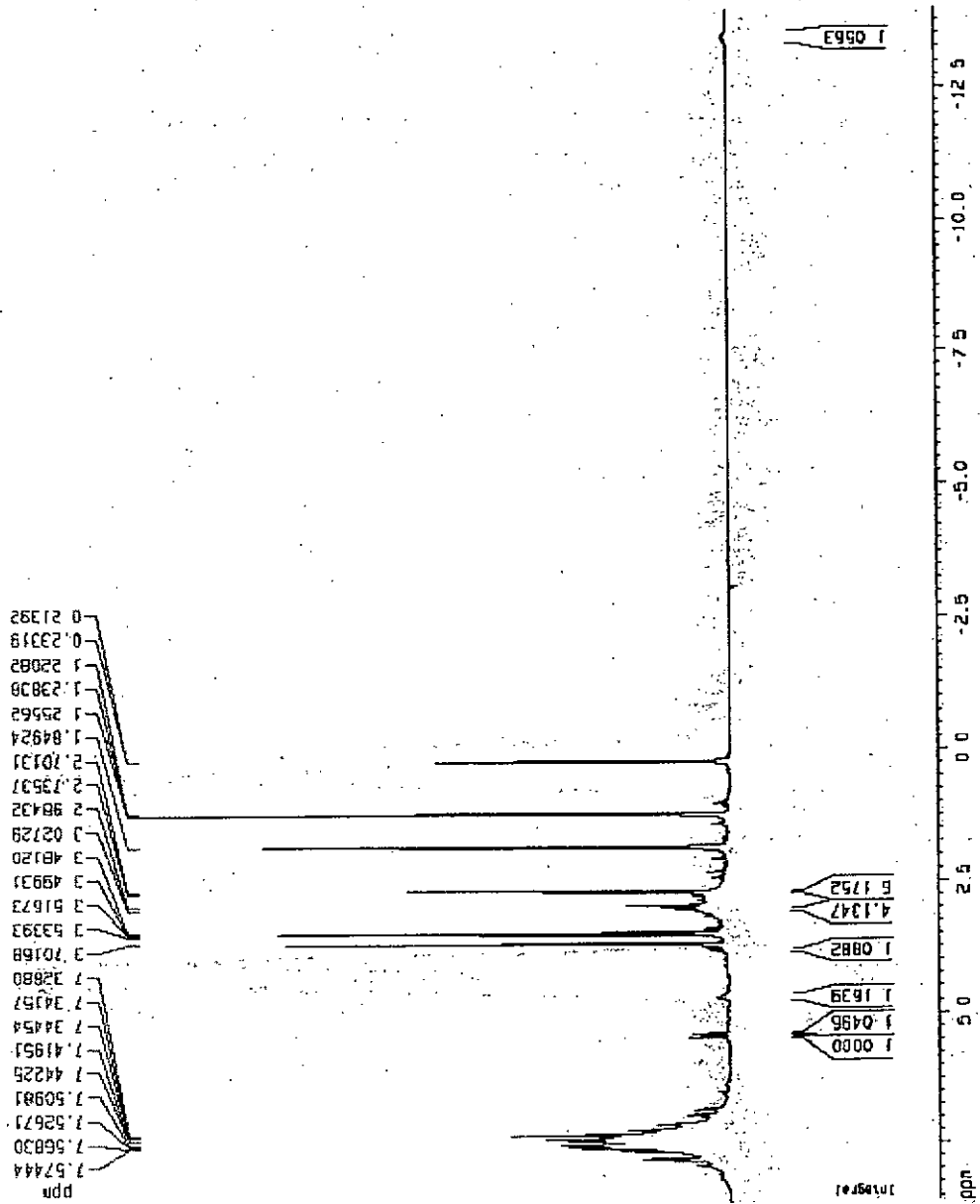


Figure 3.13 400 MHz ¹H-NMR spectrum of [(η⁵-C₆H₆CH₂CH₂NMe₂H⁺)Ru(dppm)H]BF₄ (21)

1H NMR (dppm) H + HBEF4.E120 in D-THF

```

Current Data Parameters
NAME: P1NMR (dppm) H
EXPNO: 3
PROCNO: 1
F2 - Acquisition Parameters
Date_: 20040603
Time: 15:53
INSTRUM: gpc400
PROBHD: 5 mm QNP 1H
PULPROG: zgpg30
TD: 32768
SOLVENT: THF
NS: 64
DS: 0
SWH: 64830.055 Hz
FIDRES: 1.981651 Hz
AQ: 0.2623526 sec
RG: 11098.0
DM: 7.700 usec
DE: 4.60 usec
TE: 300.2 K
D1: 1.0000000 sec
----- CHANNEL f1 -----
NUC1: 31P
P1: 7.20 usec
PR1: -6.00 dB
SFO1: 161.875000 MHz
F2 - Processing parameters
SI: 16384
SF: 161.875000 MHz
WDW: EM
SSB: 0
LB: 0
GB: 0
PC: 1.00
ID: NMR plot parameters
CQ: 20.00 CP
F1P: 13.403 dB
F2: 2171.05 Hz
F3: -13.717 dB
F4: -2221.84 Hz
RGY: 3.38602 dB/CP
HZDN: 218.64161 Hz/CP
  
```

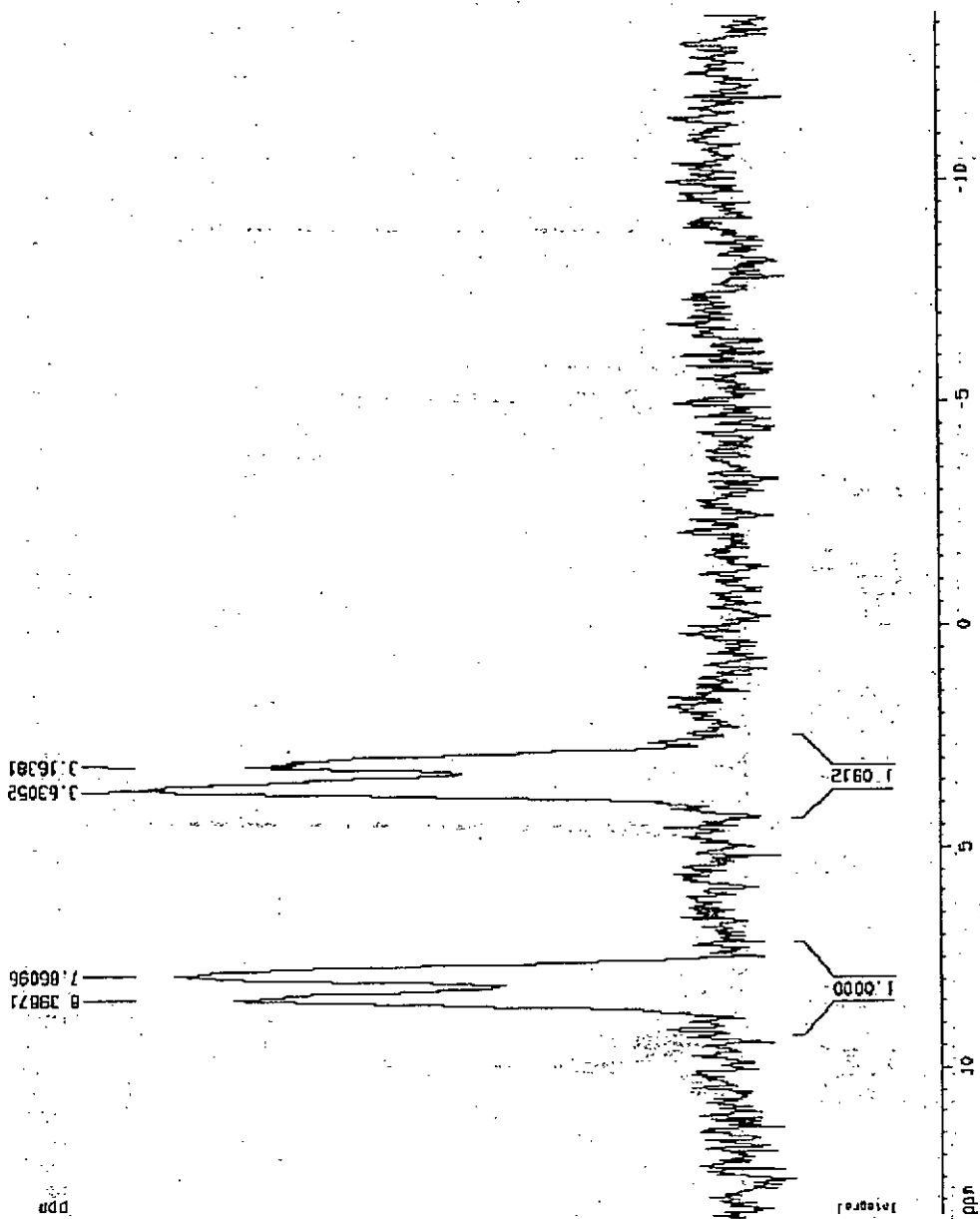


Figure 3.14 162 MHz ^1H -NMR spectrum of $[(\eta^5\text{-C}_9\text{H}_6\text{CH}_2\text{CH}_2\text{NMe}_2\text{H}^+)\text{Ru}(\text{dppm})\text{H}]\text{BF}_4$ (21)

¹H-NMR (ppm) BF₄ in CDCl₂

Current Data Parameters
 NAME 10MR.dppmCl
 EXPNO 117
 PROCNO 1

F2 - Acquisition Parameters
 Date_ 20040503
 Time 11:52
 INSTRUM spect
 PROBHD 5 mm QNP 1H
 PULPROG zgpg30
 TO 32758
 SOLVENT CDCl₃
 NS 54
 DS 0
 SWH 16025.841 MHz
 FIDRES 0.483064 MHz
 AQ 1.0324815 sec
 RG 514.7
 PC 31.230 usec
 DM 4.60 usec
 DE 300.0 H
 TE 300.2 K
 D1 2.0000000 sec

===== CHANNEL f1 =====
 NUC1 1H
 P1 9.50 usec
 PL1 -6.00 dB
 SFO1 400.1278800 MHz

F2 - Processing parameters
 SI 16384
 SF 400.1300150 MHz
 MDX EA
 SSB 0
 LB 0.30 MHz
 GB 0
 PC 1.00

3D NMR plot parameters
 CD 20.00 cm
 FIP 8.910 cm
 F1 3664.98 MHz
 F2 -1.711 ppm
 PRACH 0.63104 ppm/cm
 RZCH 213.48853 MHz/cm

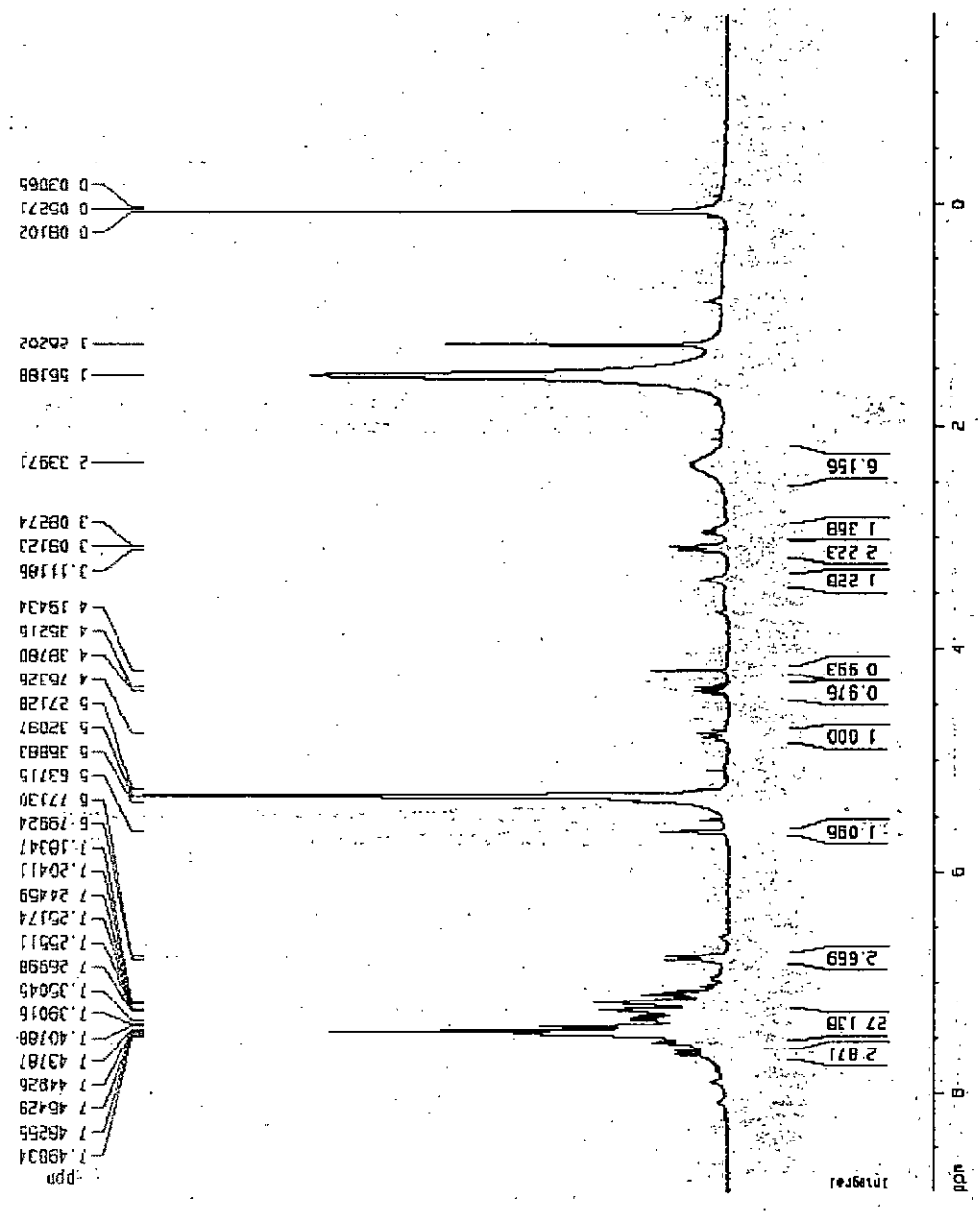


Figure 3.15 400 MHz ¹H-NMR spectrum of [(η⁵:η¹-C₆H₉CH₂CH₂NMe₂)Ru(dppm)]BF₄ (22)

101MRU (ppm) BF4 in CDCl2

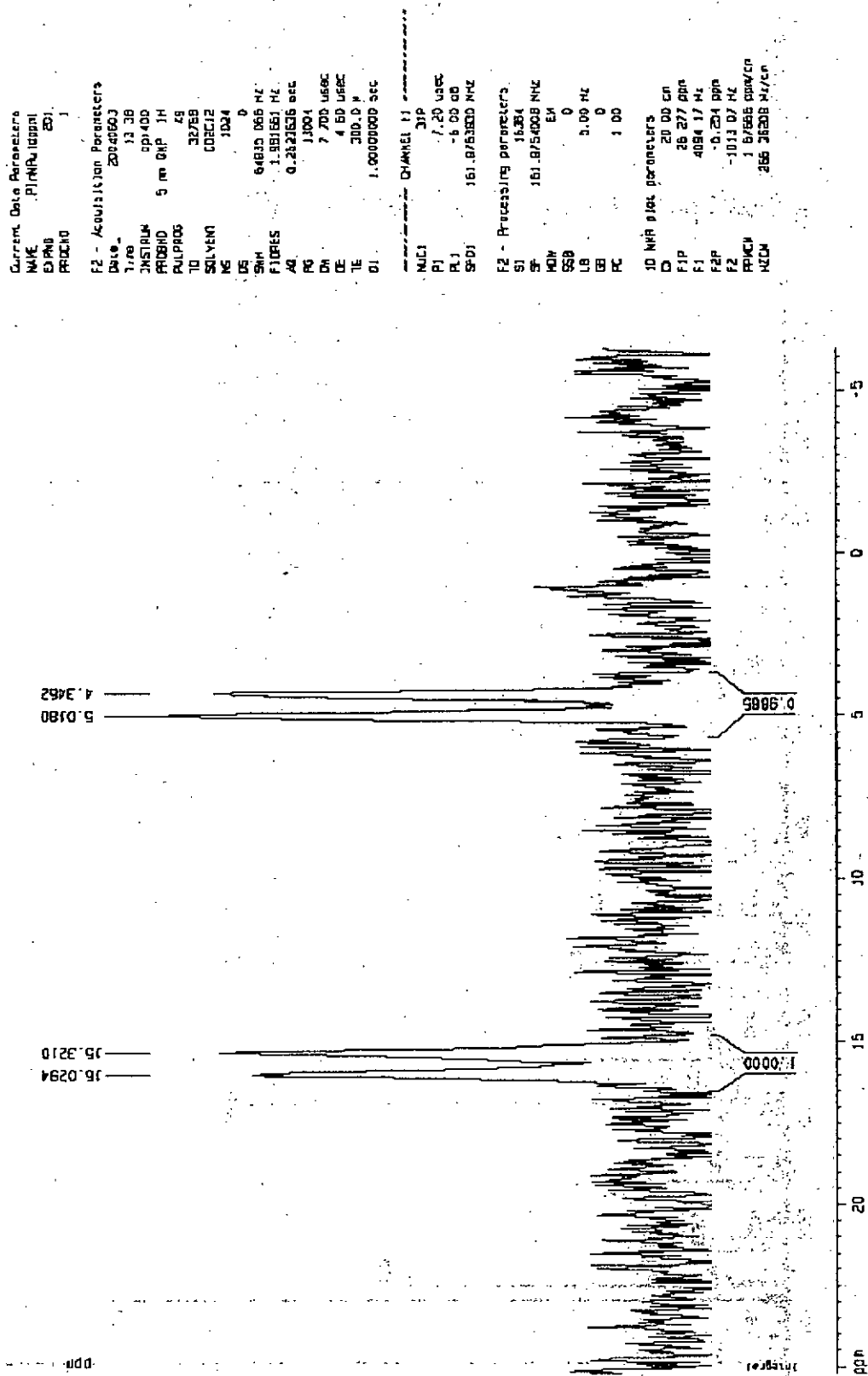


Figure 3.16 162 MHz $^{31}\text{P}\{^1\text{H}\}$ -NMR spectrum of $[(\eta^5\text{-}\eta^1\text{-C}_9\text{H}_6\text{CH}_2\text{CH}_2\text{NMe}_2)\text{Ru}(\text{dppm})]\text{BF}_4$ (22)

RICKY FUNG, RICKY016, CONE=20V 15.03.02
 CP10829 (1523) cm (19.31)

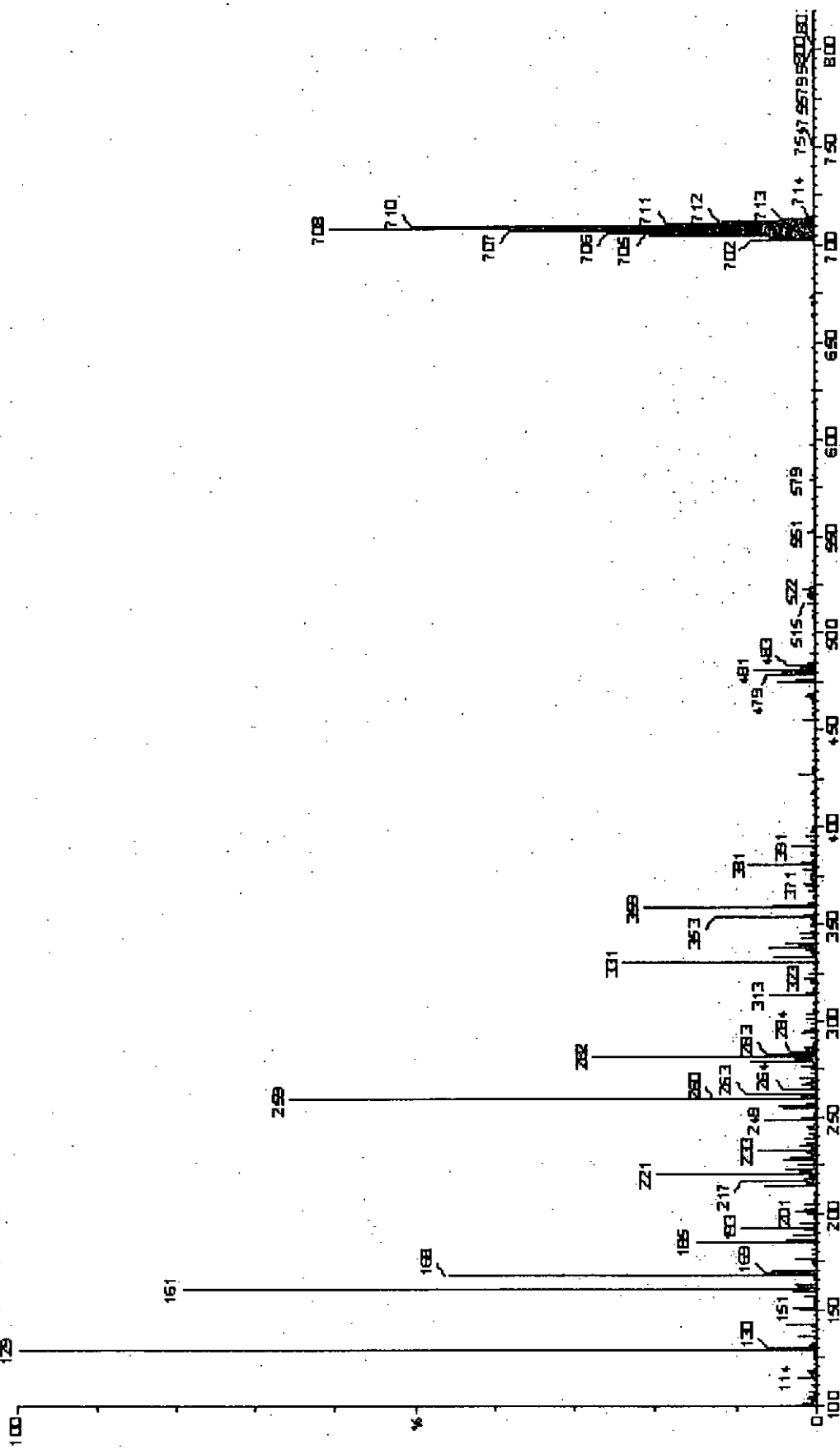


Figure 3.17 Mass spectrum of $[(\eta^5\text{-}\eta^1\text{-C}_9\text{H}_6\text{CH}_2\text{CH}_2\text{NMe}_2)\text{Ru}(\text{dppm})]\text{BF}_4$ (22)